



UNIVERSITY OF  

---

LIVERPOOL

*Enantioselective Chemo-Enzymatic  
Synthesis of Triaryl Phosphine oxides  
and Phosphines*

*Thesis submitted in accordance with the requirements of the  
University of Liverpool for the degree of Doctor in Philosophy by:*

**Harry Hatton**

*February 2021*

## Acknowledgements

I would firstly like to thank Dr. Andrew Carnell for allowing me to join his research group and for the guidance during my PhD, especially towards the latter stages of my projects. I would also like to thank the past and present members of the Carnell and Cosstick group including Dr. Christopher Riley, Dr. Daniele Parisi and Lucy Ward for their continuing moral support and aid with any challenges, scientific or otherwise, throughout my time in the group.

I would like to extend a huge thanks to Dr. Neil Kershaw for aiding me throughout my PhD, not just in chemistry but for keeping me going through the difficult times faced during my PhD.

Finally, I would like to thank my Mum, Dad and girlfriend, Laura who have given me immense support throughout my time at university. Their support has pushed me to achieve my goals when I did not think it would be possible and for that I cannot thank them enough.

## Abstract

The chemo-enzymatic synthesis of triaryl P-chiral ligands was achieved from readily available starting materials using the metallo-induced 1,4-rearrangement of phosphonates to produce pro-chiral phosphine oxides which could be enzymatically desymmetrized in good yield and high enantiomeric excess using CAL-A. The chiral phosphine oxide could then be derivatized further to produce ligand like structures. A chiral phosphine oxide could be selectively reduced to give an oxidatively stable P-chiral phosphine, with minimal loss in enantiomeric excess. Although the synthesised P-chiral ligand displayed configurational instability, slight alterations to the structure predicted by our molecular modelling results could potentially give both oxidatively and configurationally stable P-chiral phosphine ligands. Furthermore, based on unpublished results using an achiral monodentate ligand we believe that our P-chiral ligands would find application in copper-catalysed asymmetric 1,6-boration reactions with high *cis* selectivity.

## Abbreviations

2,6-DHBD	2,6-Dihydroxybenzoic acid decarboxylase
AIBN	Azobisisobutyronitrile
BINAP	2,2'-bis(diphenylphosphino)-1,1'-binaphthyl
BREP-	Butanol rinsed enzyme preparation
CAL-A	<i>Candida antarctica</i> Lipase A
CAL-B	<i>Candida antarctica</i> Lipase B
CAMP	Cyclohexylanisylmethyl phosphine
CMCR	<i>Candida magnoliae</i> carbonyl reductase
Cod	Cyclooctadiene
Cy	Cyclohexyl
DCM	Dichloromethane
DFT	Density functional theory
DHP	3,4-Dihydropyran
DIPAMP	Di-Phenylanisylmethylphosphine
DIPEA	Diisopropylethyl amine
DKR	Dynamic kinetic resolution
DMAP	Dimethyl aminopyridine
DMSO	Dimethyl sulfoxide
EA	Ethyl acetate
e.e.	Enantiomeric excess
Eqv	Equivalents
FAD	Flavin adenine dinucleotide
GOase	Galactose Oxidase
HPLC	High performance liquid chromatography
HOMO	Highest occupied molecular orbital
HRP	Horse radish peroxidase
ISPA	Isopropenyl Acetate
IR	Infra-red Spectroscopy
Imid	Imidazole
LDA	Lithium diisopropylamide
LAS	Lipase AS Amano

LUMO	Lowest unoccupied molecular orbital
<i>m</i> -CPBA	<i>meta</i> -Chloroperbenzoic acid
MS	Mass Spectrometry
Ms-Cl	Mesyl Chloride
NAD	Nicotinamide adenine dinucleotide
NADP	Nicotinamide adenine dinucleotide phosphate
NMR	Nuclear magnetic resonance
NR	No reaction
PAMP	Phenylanisylmethylphosphine
PCC	Pyridinium Chlorochromate
Pin	Pinacol
PMHS	Polymethyl hydrogen siloxane
PPL	Pancreatic Porcine Lipase
PTE	Phosphotriesterase
<i>p</i> -TSA	<i>p</i> -Toluene sulfonic acid
Pyr	Pyridine
R.F.	Retention Factor
RT	Room temperature
RPM	Revolutions per minute
TBAF	Tetrabutyl ammonium fluoride
TBAI	Tetrabutyl ammonium iodide
TBDPS-Cl	<sup>t</sup> Butyl diphenyl silyl chloride
TEP	Tolmans electronic parameter
THF	Tetrahydrofuran
THP	Tetrahydropyranyl ether
TLC	Thin layer Chromatography
TMDS	Tetramethyldisiloxane
TPO	Triphenylphosphine oxide
VA	Vinyl Acetate

## Table of Contents

Acknowledgements	i
Abstract	ii
Abbreviations	iii
Table of Contents	v
Introduction	1
1.1 – Phosphines in organic synthesis	1
1.2 – Phosphines structure and bonding	2
1.2.1 – Structure of phosphines	2
1.2.2 - Phosphines bonding to metals	4
1.3 – Inversion of phosphines	10
1.3.1 - Effects of electronegativity on inversion energy	11
1.3.2 - Effects of sterics on inversion energy	13
1.3.3 - Effects of conjugation on inversion energy	15
1.4 – Stability of phosphines to oxidation	16
1.5 – Chirality in phosphines	17
1.5.1 - C-2 Symmetry	18
1.5.2 – Non-P* stereogenic phosphines	19
1.5.3 - P-Chiral phosphines	21
1.6 - Synthesis of chiral phosphines and phosphine oxides	24
1.6.1 – Chemical routes to chiral phosphines	24
1.7 – Green chemistry	27
1.8 – Enzymes as biocatalysts	28
1.8.1 – Enzyme structure	30
1.8.2 – Mechanisms of enzyme activity	32
1.9 – Enantioselective enzymatic transformations	33
1.9.1 – Enzymatic kinetic resolution	33
1.9.2 – Enzymatic dynamic kinetic resolution	34
1.9.3 – Enzymatic desymmetrization	36
1.10 - Enzymatic synthesis of chiral phosphorus compounds	37
1.11 – Copper-catalysed asymmetric 1,6-boration	38
1.12 – Project aims	45
2 – Results and discussion	48
2.1 - 1 <sup>st</sup> Generation synthesis of prochiral phosphines	48
2.2 – Synthesis of the pro-chiral phosphine oxide	54

2.3 – 2 <sup>nd</sup> Generation synthesis of the pro-chiral substrate	57
2.4 - Expansion of the rearrangement reaction	64
3 – Enzymatic transformations	69
3.1 – Lipase-catalysed desymmetrization	70
3.1.2 – Immobead 150 CAL-A organic solvent screen	74
3.1.3 – Effect of temperature	76
3.1.4 – Enzyme concentration studies	77
3.2 – Immobilization of CAL-A	78
3.2.1 – Purolite BE immobilized CAL-A condition screen	83
3.2.3 – Substrate concentration with Purolite BE CAL-A	86
3.2.4 – Water concentration screen with Purolite BE CAL-A	87
3.2.5 – Purolite CAL-A scale up reaction	90
3.3 – Lipase-catalysed hydrolytic desymmetrization reactions	94
3.4 – Kinetic resolution of derivatives of 102	95
3.5 – Alcohol oxidase catalysed desymmetrization and kinetic resolution reactions	98
3.6 – Conclusion	101
4 – Synthetic route to 'ligand' Structures	102
5 – Stereoselective reduction of phosphine oxides	114
6 – DFT Modelling of the inversion barrier of tertiary phosphines	130
7 – Synthesis of phenolic derivatives	139
7.1 – Synthesis of phenolic derivatives from benzylic compound 129	139
7.2 – Direct synthesis of phenolic derivatives	142
8 – Enzymatic desymmetrization and kinetic resolutions of phenolic containing phosphine oxide derivatives	146
8.1 – Desymmetrization reactions	146
8.2 - Kinetic resolution reactions	152
9 - Conclusion	154
10 - Experimental	157
10.1 - General experimental	157
10.2 - Chapter 2 synthesis of phosphines and phosphine oxides experimental	158
10.3 - Chapter 2.3 phosphonate synthesis and rearrangement experimental	165
10.4 - Chapter 3 enzymatic desymmetrization and kinetic resolution reactions experimental	174
10.5 - Chapter 4 synthesis of ligand structures experimental	183
10.6 – Chapter 5 phosphine oxide reduction experimental	191

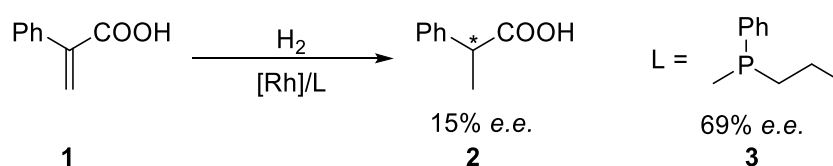
10.7 – Chapter 6 inversion barrier calculation experimental (DFT)-----	194
10.8 - Chapter 7 synthesis of phenolic structures from 147 experimental--	194
10.8.1 – Chapter 8.2 direct synthesis of phenolic phosphine oxides experimental-----	197
10.9 - Chapter 8 phenolic phosphine oxide desymmetrization and kinetic resolution experimental-----	206
11 – References-----	213



# Introduction

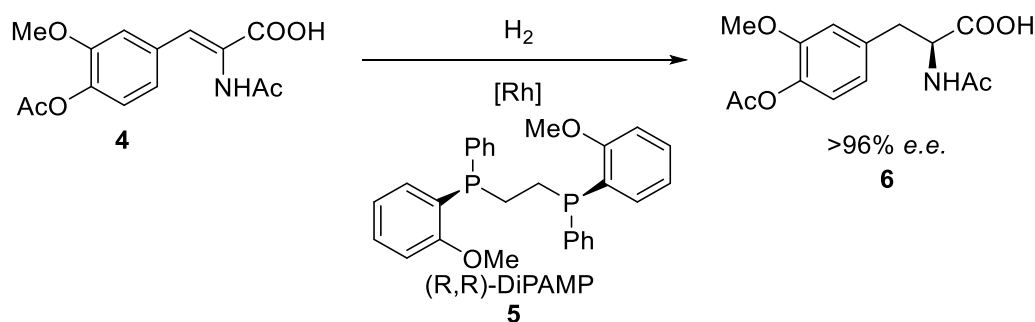
## 1.1 – Phosphines in organic synthesis

Phosphines and phosphine oxides have undeniably played a pivotal part in organic chemistry throughout the years, however, the application of chiral phosphine and phosphorus containing ligands in asymmetric catalysis has become one of the most effective routes for the construction of chiral building blocks for synthesis<sup>[1-5]</sup>. With a rise in the need for enantiomerically pure pharmaceuticals and fine chemicals, asymmetric catalysis remains at the forefront of synthetic organic chemistry to meet this demand in both, academia and industry. The first application of a chiral phosphine ligand was in the asymmetric hydrogenation of alkenes, Knowles *et al.* pioneered this work using several different tertiary phosphines for the rhodium catalysed hydrogenation. Initially, the dialkyl aryl phosphine ligand (**3**) shown in **Scheme 1**, was applied to the reduction of alkene **1** which gave the desired product with an e.e. of only 15%. However, the ligand used for the reaction was only at 69% e.e.<sup>[6]</sup>



**Scheme 1** – Rhodium-catalysed asymmetric hydrogenation of **1** using a P-chiral ligand leading the desired product **2** in 15% e.e.<sup>[6]</sup>.

The asymmetric methodology was largely improved upon in the hydrogenation of the precursor to L-DOPA, **4** to give **6**, where the chiral mono-dentate ligand, CAMP gave an e.e. of 85%.<sup>[7]</sup> In 1972, Knowles *et al.* improved on this even further with the use of the bi-dentate, di-Phenylanisylmethylphosphine (DiPAMP) ligand **5** (**Scheme 2**) which gave the same product in 96% e.e.<sup>[8]</sup> Furthermore, this process has been scaled up to produce over 250 tons per year of L-DOPA, a treatment for Parkinson's disease.



**Scheme 2** – Industrial Monsanto synthesis of L-DOPA precursor using the rhodium catalysed asymmetric hydrogenation of **4**.

## 1.2 – Phosphines structure and bonding

### 1.2.1 – Structure of phosphines

Phosphines span a broad range of structures, but they can be broadly categorized to be either, primary (PRH<sub>2</sub>), secondary (PRR'H) or tertiary (PRR'R''), which relates to the level of substitution around the phosphorus atom.<sup>[9]</sup> The simplest phosphine structure is phosphine gas with the formula

PH<sub>3</sub>, consisting of three P-H bonds with a H-P-H angle of 93.5° in the trigonal pyramidal shape with a singular lone pair which is perpendicular to the phosphorus atom, as shown in **Figure 1**. Due to the low H-P-H angle of 93.5°, PH<sub>3</sub> can be described as a Drago molecule, which states that there is no hybridization of the phosphorus orbitals (i.e. sp<sup>3</sup>) to form the P-H bonds which are therefore formed entirely of pure p orbitals which are orthogonal to the central phosphorus and the s orbital of the hydrogen atoms. Furthermore, this means that the lone pair is made almost entirely of the s orbital of the phosphorus atom. This contrasts with structures such as ammonia (NH<sub>3</sub>) which show a pyramidal or distorted tetrahedral structure due to sp<sup>3</sup> hybridization, with larger bond angles of 107°. The lone pair of ammonia, therefore, sits in the sp<sup>3</sup> orbitals and unlike PH<sub>3</sub> is not formed entirely of s orbital.<sup>[10]</sup>

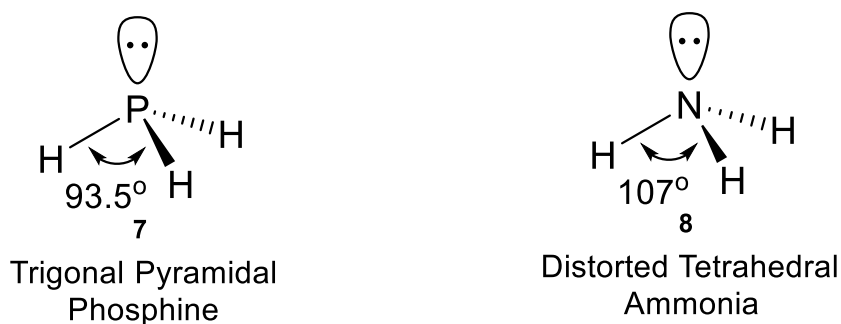


**Figure 1** – Structure of phosphine and ammonia displaying the difference in bond angle.

As we move to a tertiary phosphine such as PMe<sub>3</sub>, the C-P-C angle increases to approximately 98.6° and whilst this angle is still lower than the 109° angle approximated by sp<sup>3</sup> hybridized, tetrahedral structures, it can be argued that

$\text{PMe}_3$  has more  $\text{sp}^3$  hybridized character.<sup>[11]</sup> The use of hybridization in phosphines can also be used to better explain the mechanism of the inversion of phosphines, which will be covered in more detail.

### 1.2.2 - Phosphines bonding to metals

The properties of phosphines as ligands have been extensively studied over the last few decades<sup>[12-16]</sup>, especially tertiary phosphines, to the point where the tuning of both steric and electronic effects can be carried out with a large amount of predictability. Phosphines bind to transition metals through the contribution of two electrons from the phosphorus lone pair to an empty metallic d orbital and the level of donation depends on the substituents attached to the phosphorus atom. In alkyl phosphines, such as trimethyl phosphine **9**, the alkyl  $\text{sp}^3$  bonds tend to be better electron donors than those that possess  $\text{sp}^2$  bonds such as triphenyl phosphine **10** (**Figure 2**). This progresses further, as electron-withdrawing or releasing groups attached to the substituents can also have a remarkable effect on the electron density on the phosphorus atom.

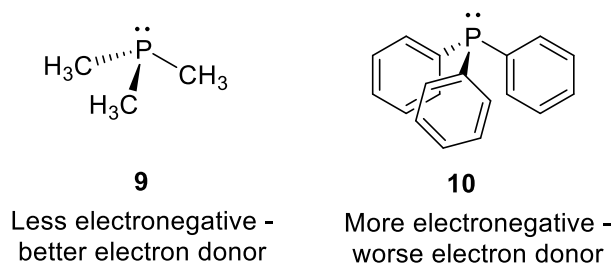
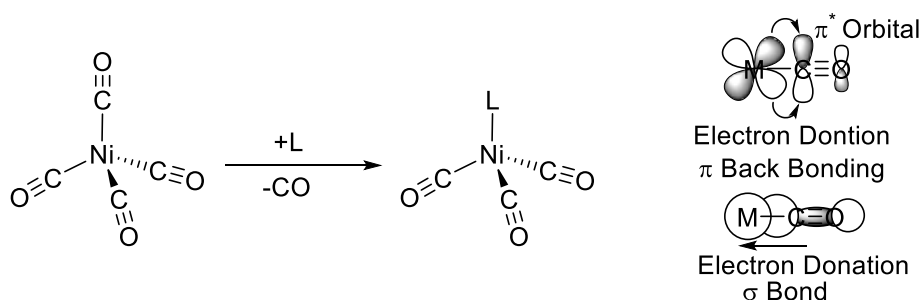


**Figure 2** – *Electron donation properties of both trimethyl phosphine (9) and triphenylphosphine (10).*

The electron-withdrawing and donating ability of a ligand can be explained further using the Tolman's electronic parameter (TEP), where the electronic effects of a ligand can be defined through the effect on the vibrational frequency of carbon monoxide in a metal species. A common metal species to measure the TEP is  $[\text{LNi}(\text{CO})_3]$  (**Scheme 3**), where L relates to the ligand of interest. The three carbonyl molecules bind to the metal causing a decrease in the vibrational frequency of free C-O at  $2143 \text{ cm}^{-1}$ .<sup>[12]</sup>

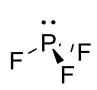
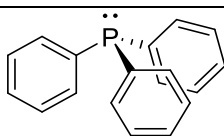
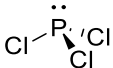
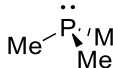
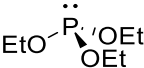
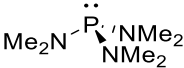
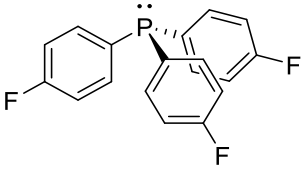
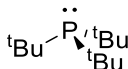


**Scheme 3** – Characterisation of the electronics of phosphine ligands by Tolman through measurement of the IR of C-O bonds.

The shift in the IR frequency of the C-O bond can be explained through the pi back bonding which occurs when the nickel atom donates electrons from its d orbitals into the empty  $\pi^*$  anti-bonding orbitals on the CO. This strengthens the metal-carbon bond but subsequently weakens the C-O bond resulting in the lower vibrational frequency observed. When a phosphine binds to the nickel which increases the density of the pi electrons on the metal, the degree of back bonding to the metal-carbon bond increases too, weakening the C-O bond even further. Tolman *et al.* used a series of phosphine ligands with varying withdrawing and donating effects to show this phenomenon; as

expected the most electronegative ligand, PF<sub>3</sub>, showed the smallest decrease in the frequency of the C-O bond as it removes electron density from the nickel atom. Inversely, the trialkyl phosphines such as PMe<sub>3</sub> and P<sup>t</sup>Bu<sub>3</sub> showed the greatest decrease in the frequency of the C-O bond (**Table 1**), due to the increased electron donation into the metal.<sup>[12,13]</sup>

**Table 1** – Tolman's electronic parameter for several different phosphine ligands and their effect on the  $\nu(\text{CO})$  of the carbonyl bond.

Ligand	$\nu(\text{CO}) \text{ cm}^{-1}$	Ligand	$\nu(\text{CO}) \text{ cm}^{-1}$
	2110.8		2068.9
	2097.0		2064.1
	2076.3		2061.9
	2071.3		2056.1

Phosphines can also participate in back bonding in metal complexes, however, the electronics of back bonding from the metals d orbitals to the phosphines orbitals is fundamentally different to molecules such as carbon monoxide, which undergoes back bonding into the pi antibonding C=O orbital as described above. Traditionally, back bonding in phosphines was attributed to the interaction between the metallic dπ orbital and the empty 3d orbital on the phosphorus atom, however this was disproved through a series of

experiments in which the bond lengths of the metal to the phosphine (P-M) and the bond lengths of the phosphorus and attached group (P-R) were measured. Oxidation of the metal centre, which decreases the ability of the metal to back bond to the phosphorus, led to the lengthening of the P-M bond due to the lesser amount of bonding between the two atoms. Oxidation of the metal centre also led to the shortening of the P-R bond of the phosphine which shows that the back bonding must involve participation from the  $\delta^*$  P-R orbitals to account for the shortening of this bond. This can be further proved through the changing of substituents on the phosphorus atom, as the inclusion of more electronegative atoms on the phosphorus atoms decreases the energy of the sigma antibonding orbital (increasing the pi acidity) allowing for greater contribution to the LUMO from the phosphorus as well as greater back bonding from the metal, a phenomenon shown in **Figure 3**. The level of pi acidity in cases such as  $\text{PF}_3$  becomes as great as that found for carbon monoxide which shows strong bonding into the pi antibonding orbital and not the sigma antibonding orbital.<sup>[10,13]</sup>

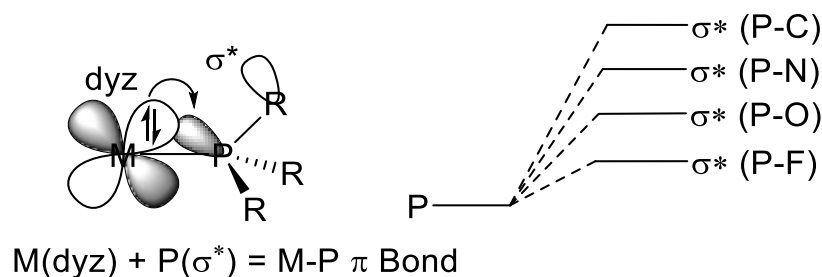


**Figure 3** – Formation of the metal-phosphine complex and pi back bonding from the metal d orbital to the  $\delta^*$  orbitals of the phosphorus atom.

Inversely, when a phosphine binds to an electron-rich metal you would expect the P-C, anti-bonding orbitals to become more populated increasing the P-C bond length however, this effect is often hidden by an opposing effect in which the donation of the lone pair into the metal also decreases the P(lone pair) – R(bonding pair) repulsion which in turn decreases P-R bond length.

The tuning of metal catalysed reactions often comes from the use of different sized phosphine ligands and in addition to the Tolman's electronic parameter, the Tolman's cone angle can be used to identify ligands which are suitable based on sterics. This parameter is particularly useful as the phosphine ligands are often what provide the asymmetric induction in metal reactions and when used correctly can control the co-ordination around the metal centre. The Tolman's cone angle is defined through measurement of the angle which encompasses the structure of the whole ligand where the apex of the cone is the metal (**Figure 4**).

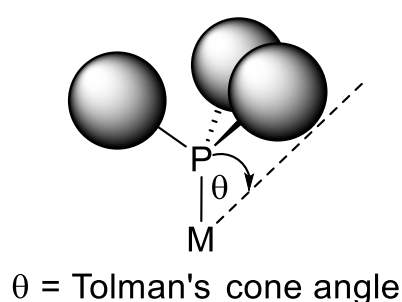


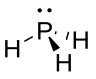
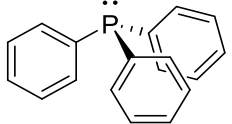
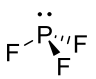
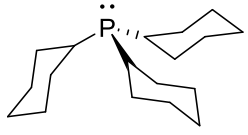
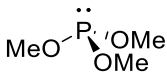
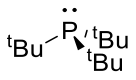
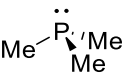
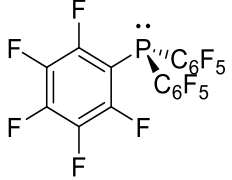
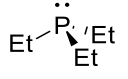
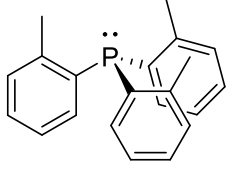
**Figure 4** – Calculation of Tolman's cone angle for metal-phosphine complexes.

Tolman *et al.* calculated the cone angle of a variety of different phosphines (**Table 2**) using a zerovalent nickel complex and as expected the smallest



ligands such as  $\text{PH}_3$ ,  $\text{PF}_3$  and  $\text{PMe}_3$  gave much smaller cone angles than the bulkier ligands such as  $\text{P}^t\text{Bu}_3$  and  $\text{PPh}_3$ .<sup>[14,15]</sup>

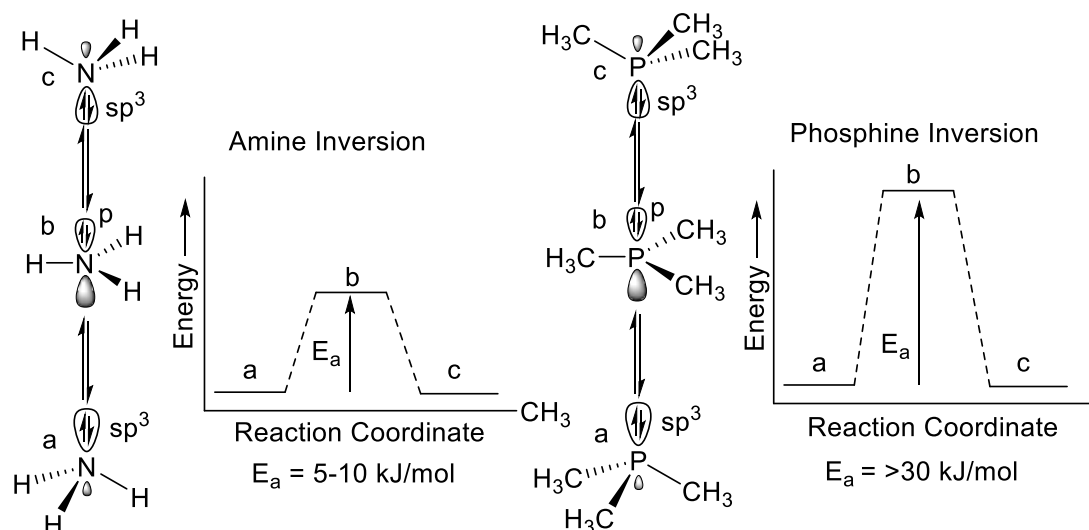
**Table 2** – Calculated Tolman's cone angle for phosphines with varying size substituents.

Ligand	Cone angle	Ligand	Cone angle
	87°		145°
	104°		179°
	107°		182°
	118°		184°
	118°		194°

Whilst the calculation of the cone angle is relatively simple with symmetrical ligands such as  $\text{PMe}_3$  and  $\text{PPh}_3$ , this calculation can still be applied to asymmetric ligands where the substituents half angles are averaged and then doubled to find the total cone angle. This allows the characterisation of the properties of chiral ligands in asymmetric catalysis to better understand the enantioselectivity of the products.<sup>[16]</sup>

### 1.3 – Inversion of phosphines

Phosphines show remarkably different inversion properties compared to their second-row amine counterparts. Amines which contain three different substituents do not show any optical activity due to the rapid inversion of the nitrogen. Whilst this rapid stereo isomerization exists in amines, phosphines do not always display this trait. The activation energy for the inversion of phosphines is typically in excess of 30 kcal/mol compared to the activation energy of 5-10 kcal/mol for amines which means that individual enantiomers of phosphines can be isolated.<sup>[17]</sup> The most general, recognised mechanism of inversion of phosphines and amines occurs through an ‘umbrella’ type or vertex mechanism (**Scheme 4**) in which the centre atom (N or P) changes from an  $sp^3$  hybridized, trigonal pyramidal shape ( $C_{3v}$ ) to the  $sp^2$  hybridized, trigonal planar ( $D_{3h}$ ) and the orbital which contains the lone pair on the central atoms changes from  $sp^3$  to a p orbital on the phosphorus atom.<sup>[18-21]</sup> Whilst this mechanism does explain the inversion of many phosphines, it does not describe the mechanism of inversion for all phosphines, as the edge inversion pathway has also been reported for trihalogenated phosphines.<sup>[17,21-23]</sup>



**Scheme 4** – Inversion pathway for both ammonia and  $\text{PMe}_3$ , showing the movement from the  $\text{sp}^3$  hybridized trigonal pyramidal structure to the trigonal planar transition state.

Whilst many phosphines display stability to inversion, this stability is determined by several factors. Most importantly, the electronegativity of the substituents, the steric demands of the substituents and conjugation of the phosphorus lone pair have the greatest effect. However, the presence of lone pairs in proximity to the phosphorus atom and the angular constraints within the molecule can also affect inversion barrier.

### 1.3.1 - Effects of electronegativity on inversion energy

Beginning with electronegativity, both DFT and *ab initio* calculations<sup>[21]</sup> have shown that moving from the simplest phosphine,  $\text{PH}_3$ , with increasing substitution with electronegative fluorine atoms ( $\text{PH}_2\text{F}$  to  $\text{PF}_3$ ) leads to an increase in the inversion barrier. This trend is also observed in the trihalide

phosphines where moving from PBr<sub>3</sub> to PCl<sub>3</sub> to the most electronegative, PF<sub>3</sub>, shows incremental increases in the inversion barrier. Creve and Nguyen used DFT calculations to find the barrier and the pathway of inversion for several substituted halogenated phosphines,<sup>[22]</sup> as shown in **Table 3**.

**Table 3** – *Inversion pathway and energies of several halogenated phosphines.*

Species	Inversion Pathway	Inversion Barrier (kJ/mol)
PH <sub>3</sub>	Vertex	141.3
PH <sub>2</sub> F	Vertex	215.3
PHF <sub>2</sub>	Edge	210.9
PF <sub>3</sub>	Edge	221.1
PH <sub>2</sub> Cl	Vertex	185.6
PHCl <sub>2</sub>	Edge	203.1
PCl <sub>3</sub>	Edge	211.5
PH <sub>2</sub> Br	Vertex	179.6
PHBr <sub>2</sub>	Edge	164.4
PBr <sub>3</sub>	Edge	165.9
PMe <sub>3</sub>	Vertex	171.0

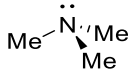
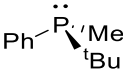
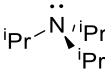
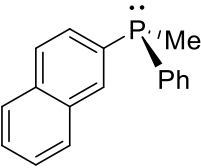
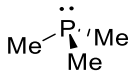
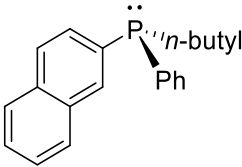
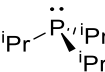
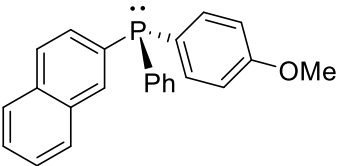
A simplistic explanation of the observed increase in inversion barrier can be attributed to the shortening of the gap between the HOMO and the LUMO orbital in the more electronegative phosphines, as shown in **Figure 3**. This depopulates the phosphines p orbital, which is required for inversion, in favour of the fluorine P-orbital which ultimately destabilizes the trigonal planer

transition state, due to the large energy gap between the HOMO and the LUMO in the planar transition state.<sup>[22]</sup>

### **1.3.2 - Effects of sterics on inversion energy**

The steric bulk of the substituents also have a profound effect on the inversion barrier of phosphines but also greatly influences the properties of the phosphines when acting as a ligand. As steric bulk of the substituents increases the repulsions between these substituents in a trigonal pyramidal structure also increases, therefore, increasing the planarity of the trigonal geometry decreasing the barrier to inversion. This is highlighted when viewing the sum of the angles around the phosphorus centre, in which the trend shows that a higher internal sum of the C-P-C bonds leads to a lower energy barrier for inversion.<sup>[23,24]</sup> Whilst this same argument could be applied to the planar trigonal transition state, the angles in this planar geometry are larger at  $120^\circ$ , compared to those of approximately  $109^\circ$  (depending on substituents) of the trigonal pyramidal configuration, meaning that the planar transition state is not influenced by sterics as greatly as the trigonal pyramidal geometry.

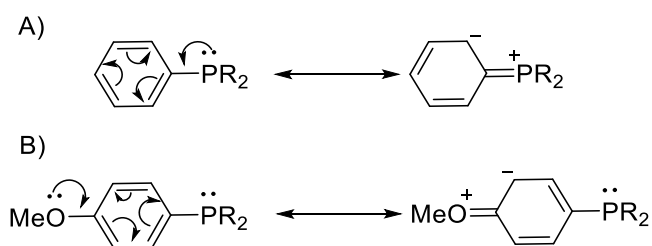
**Table 4** – Inversion barrier of tertiary phosphines highlighting the negative effects sterics have on inversion stability.

Calc. Inversion		Calc. Inversion	
Compound	Barrier	Compound	Barrier
	34.7 kJ/mol		136.8 kJ/mol
	5.9 kJ/mol		126.9 kJ/mol
	153.3 kJ/mol		126.5 kJ/mol
	139.5 kJ/mol		113.7 kJ/mol

As shown by the calculations in **Table 4**, moving from the less sterically demanding trimethyl amine/phosphine to the more sterically demanding isopropyl substituents or phenyl containing substituents there is a significant drop in the inversion barrier energy of both the amine and phosphine centered compounds.<sup>[23,25]</sup> This trend is further cemented through the work by Holz *et al.* in which triaryl phosphines were shown to have a relatively low inversion barrier, highlighted through both experimental work and DFT calculations. The inversion barrier energy and half-life were increased dramatically through the substitution of an anisyl group for a lesser sterically demanding methyl or *n*-butyl chain.<sup>[24]</sup>

### 1.3.3 - Effects of conjugation on inversion energy

Conjugation is another factor which has been shown to affect the inversion barrier as delocalization of the lone pair of the phosphorus atom would allow for stabilization of the transition state, decreasing activation energy. Aryl substituents or heteroatoms which contain available d orbitals, allow for conjugation and therefore display this trend as they show activation energies lower than that of non-conjugated phosphine such as trialkyl phosphines, as shown by Mislow *et al.*<sup>[26]</sup> Furthermore, the presence of heteroatoms which contain lone pairs adjacent to the phosphorus atom also destabilizes the planar transition state due to the repulsion between lone pairs of the heteroatom and the phosphorus. This is highlighted in the study by Holz *et al.* in which the half-life for molecules which contain groups, such as phenolic derivatives in the *ortho*- or *para*- position, disrupt the conjugation of the phosphorus lone pair (**Scheme 5**) and therefore show a greater energy barrier.<sup>[24]</sup>



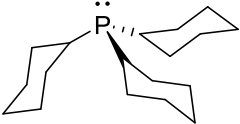
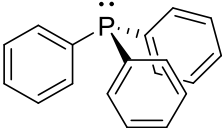
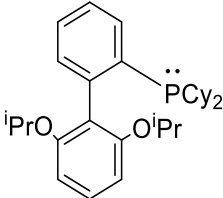
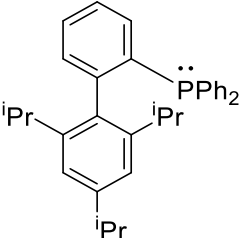
**Scheme 5** – A) Stabilization of the phosphorus lone pair through conjugation into the aromatic ring. B) Delocalization of phosphorus lone pair into the aromatic ring is prevented by electron releasing, aromatic substituents.

## 1.4 – Stability of phosphines to oxidation

In addition to configurational stability, the stability of phosphine ligands towards oxidation under atmospheric conditions depends on several factors, however and steric effects are likely to be the most important factor.<sup>[27,28]</sup> The Buchwald group reported the varying stability of phosphines to oxidation in toluene through exposing a variety of different phosphine structures to three different conditions for 65 hours; an oxygen atmosphere at room temperature, an oxygen atmosphere at 100°C and under air at 100°C. The least bulky, tricyclohexyl phosphine, showed almost complete oxidation under all three conditions, whereas the bulkier, triphenyl phosphine showed complete stability at room temperature but a large amount of oxidation in air and oxygen atmospheres at the elevated temperature of 100°C.<sup>[27]</sup> The oxidation under all three conditions could be decreased to under 8% when moving to phosphines which contain extremely bulky, biaryl substituents which also contain isopropyl groups in the 2,4,6- positions of the non-phosphorus containing aryl ring, as highlighted in **Table 5**.



**Table 5** – Observed oxidation of 4 different tertiary phosphines in 3 different oxidative conditions.

Compound	% of oxidation seen after 65 h		
	Condition A	Condition B	Condition C
	99%	99%	99%
	0%	72%	73%
	<5%	34%	69%
	0%	5%	7%

Condition A - Oxygen atmosphere at room temperature. Condition B – Air atmosphere at 100°C. Condition C – Oxygen atmosphere at 100°C<sup>[27]</sup>.

## 1.5 – Chirality in phosphines

There are two main categories of chiral phosphine ligands, those where the chirality lies on the phosphorus atoms itself and those where the chirality is located elsewhere in the phosphines structure. The latter structures include those with axial chirality. Both types of chiral phosphines have their advantages and disadvantages in catalysis as well as their ease of synthesis

and stability. Historically, P-chiral ligands have been neglected due to certain prejudices surrounding their configurational stability. However, it can be argued that for the greatest asymmetric induction from the ligands surrounding the metal it would be preferential for the chirality to lie on the phosphorus atom, due to the proximity of the phosphorus to the metal. Due to these prejudices, the number of P-chiral ligands is greatly outnumbered by chiral phosphines which contain the chirality elsewhere in the structure.

### 1.5.1 - C-2 Symmetry

C-2 symmetry can be advantageous in both P-chiral ligands and ligands such as (*R*)-BINAP and (*R,R*)-DIOP and accounts for the high enantioselectivity in a large number of catalytic asymmetric reactions. It is often thought that increased symmetry within asymmetric catalysts would be detrimental to selectivity, however, asymmetric induction only requires the ligand to be chiral. C-2 symmetry improves selectivity as it decreases the number of unique approaches and transition states (**Figure 5**) as rotation of the ligand leads to an identical transition state or intermediate.<sup>[29,30]</sup>

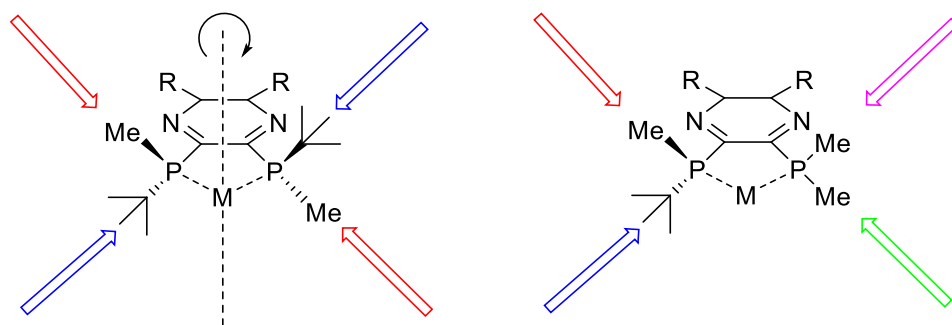


**Figure 5** – Explanation of C-2 symmetric where the C-2 symmetric structure on the left shows only 2 unique points of reaction (red + blue) where the asymmetric molecule on the right shows 4 unique points of reaction.

### 1.5.2 – Non-P\* stereogenic phosphines

As mentioned previously, the number of non-P-stereogenic ligands vastly outnumbers that of the P-stereogenic phosphine ligands. Some of these ligands have been applied to multiple areas of catalysis and are known as ‘privileged ligands’ (**Figure 6**).

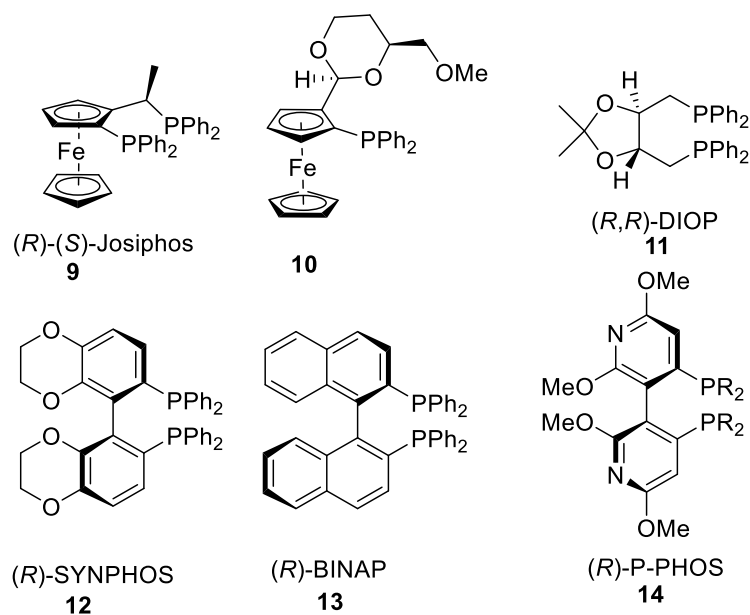
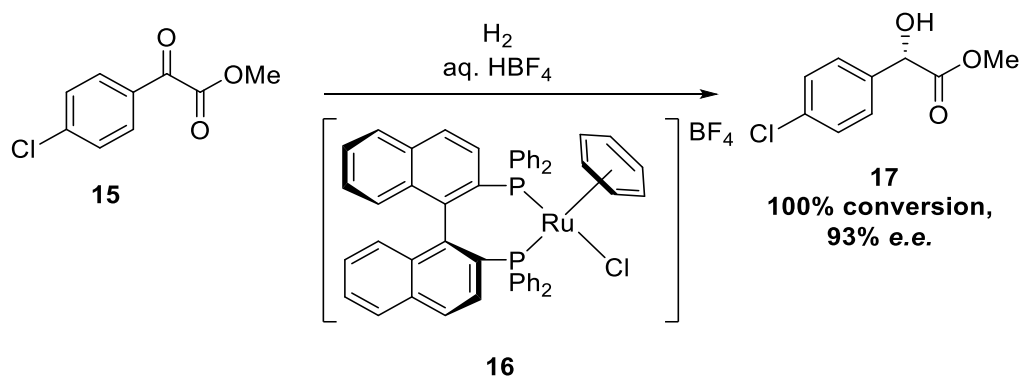


**Figure 6** – Structures of 'privileged' chiral phosphine ligands which do not contain a *P*-stereogenic centre.

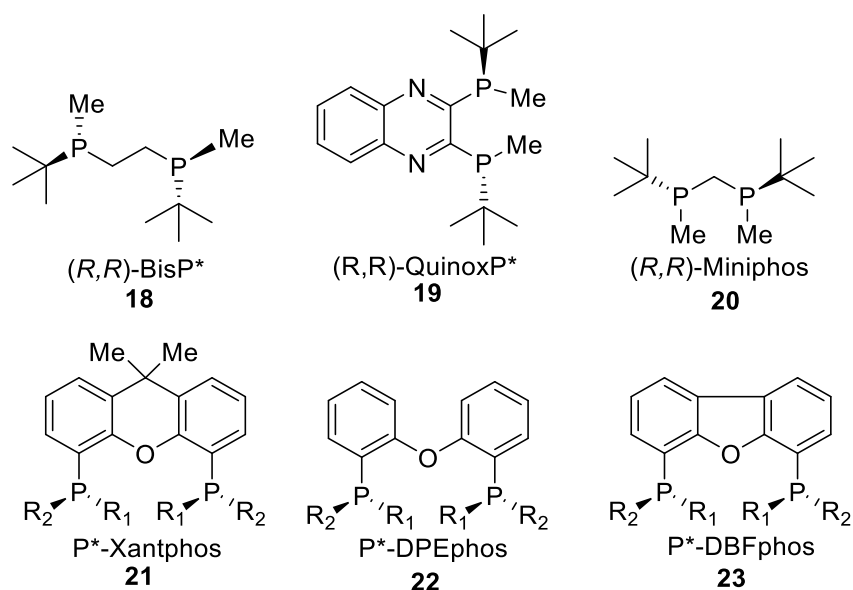
One of the most widely known and used phosphine ligands is 2,2'-bis(diphenylphosphino)-1,1'-binaphthyl (BINAP) (**13**), which unlike DIPAMP and CAMP, BINAP does not contain a stereogenic phosphorus or carbon as its chirality lies axially within the backbone of its structure. BINAP has been applied as a ligand in both rhodium<sup>[31-33]</sup> and ruthenium<sup>[34-37]</sup> catalysis. Some of the most pioneering work with BINAP was shown by Nobel prize winning chemist, Noyori, who developed the rhodium-BINAP catalysed asymmetric hydrogenation of functionalized ketones (**Scheme 6**).<sup>[38,39]</sup>



**Scheme 6** – Use of Rhodium-BINAP complex (**16**) for the asymmetric reduction of an  $\alpha$ -ketoester to give the chiral alcohol **17**.

### 1.5.3 - P-Chiral phosphines

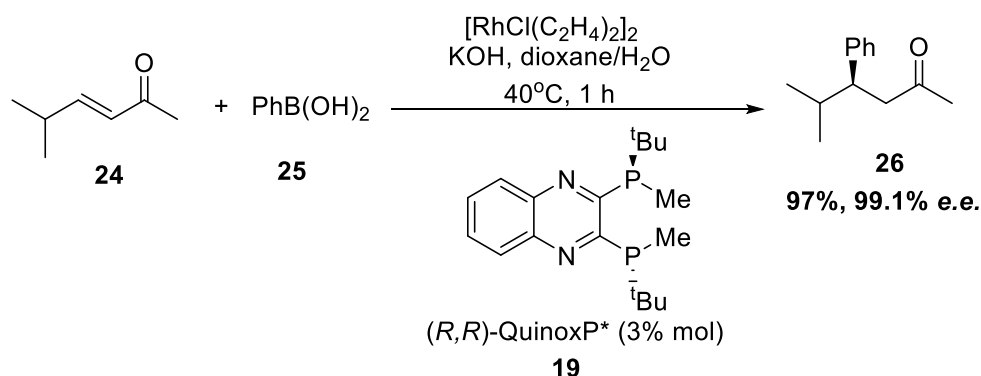
Two of the most well-known P-chiral ligands are cyclohexylanisylmethyl phosphine (CAMP) and DIPAMP, which were mentioned previously (**Section 1.1**) in the asymmetric hydrogenation of L-DOPA were inspiration for many modern P-chiral asymmetric ligands.<sup>[6-8]</sup> Since then the spectrum of P-chiral ligands has grown to include a vast range of structures (**Figure 7**) which have been applied to several different areas of metal-catalysed reactions.<sup>[40-42]</sup>



$R_1, R_2 = 2\text{-anisyl}, 3\text{-anisyl}, 4\text{-anisyl}, 2\text{-tolyl}, 3\text{-tolyl}, 4\text{-tolyl}, 2\text{-EtO-Ph}, 3\text{-EtO-Ph}, 4\text{-EtO-Ph}, 2\text{-Et-Ph}, 3\text{-Et-Ph}, 2\text{-}^i\text{PrO-Ph}, 3\text{-}^i\text{PrO-Ph}, 2\text{-}^i\text{Pr-Ph}, 3\text{-}^i\text{Pr-Ph}, 3,5\text{-MeOPh}, 1\text{-naphthyl}, 2\text{-naphthyl}$

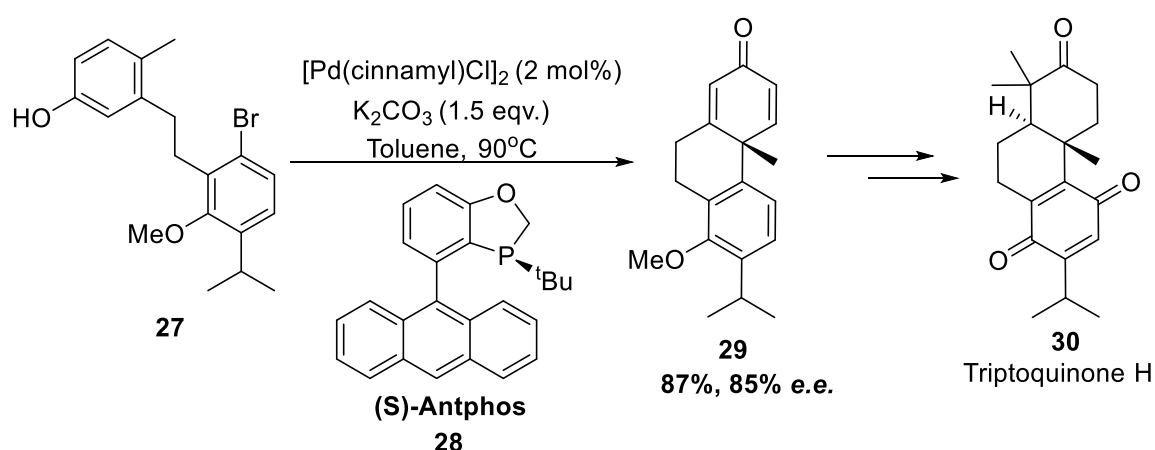
**Figure 7** – Examples of *P*-chiral ligands used in asymmetric catalysis.

Imamoto *et al.* used the air-stable, (R,R)-QuinoxP\* (**19**) ligand in the enantioselective rhodium-catalysed 1,4-addition of arylboronic acids to  $\alpha,\beta$ -unsaturated ketones (**Scheme 7**), to give the chiral product **26** in both high yield and enantiomeric excess.<sup>[40]</sup>



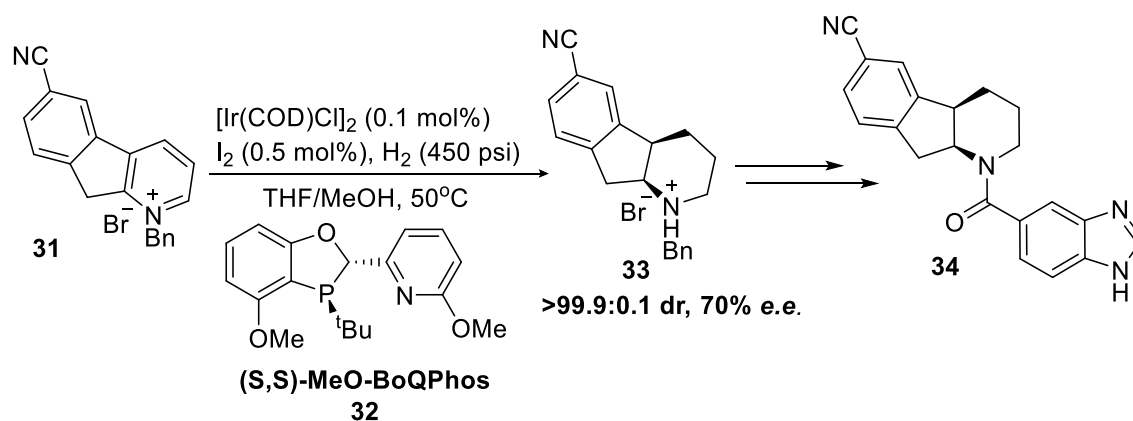
**Scheme 7** – Rhodium-catalysed 1,4-addition of arylboronic acids to  $\alpha,\beta$ -unsaturated ketones with (R,R)-QuinoxP\* ligand to give chiral products.<sup>[40]</sup>

Alternatively, Cao *et al.* demonstrated the use of the P-chiral ligand, (S)-Antphos **28**, in the total synthesis of the biologically active molecule triptoquinone H (**30**). The palladium-catalysed cyclization of intermediate **27** afforded the tricyclic, chiral molecule **29** in an e.e. of 85%, which included a carbon quaternary centre (**Scheme 8**).<sup>[43]</sup>



**Scheme 8** – Palladium-catalysed cyclization of **27** utilizing P-chiral ligand, (S)-Antphos **28**, to afford the tricyclic intermediate **29** in 85% e.e.

Similarly, the P-chiral ligand, MeO-BoqPhos (**32**) was utilized in the total synthesis of a potent 11 $\beta$ -HSD-1 inhibitor (**34**), used in the treatment of metabolic diseases such as diabetes, through the iridium-catalysed asymmetric hydrogenation of the pyridinium ring in precursor **31** (**Scheme 9**). This proceeded to give the tricyclic intermediate **33** in high diastereoselectivity and modest enantioselectivity. This was scaled up to multi kilogram reaction with consistent selectivity.<sup>[44]</sup>



**Scheme 9** – Iridium-catalysed asymmetric hydrogenation of the pyridinium ring of **31** to produce chiral intermediate **33** in 70% e.e. in high diastereomeric excess.

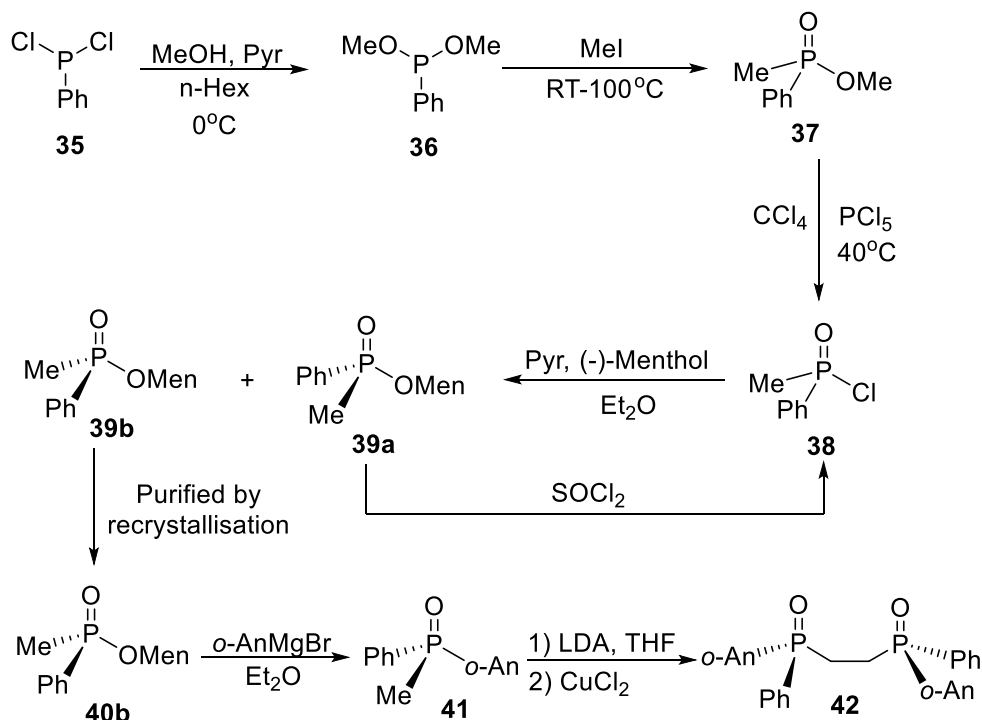
## 1.6 - Synthesis of chiral phosphines and phosphine oxides

### 1.6.1 – Chemical routes to chiral phosphines

There are several established synthetic routes to P-stereogenic phosphines, although these often require the use of chiral auxiliaries followed by crystallisation to separate the diastereomers, which can be both expensive and low yielding. In the 1960's Mislow *et al.* demonstrated the synthesis of chiral phosphinates, using (-)-menthol as a chiral auxiliary, where the separation of a single diastereomer could be achieved through crystallization in which the other remained in the mother liquor. The yield could be increased further through the reaction of the mother liquor with thionyl chloride to yield the precursor, **38** which could be reacted with (-)-menthol to re-form the diastereomeric mixture. The resulting phosphinate (**40b**) can then be reacted with a Grignard reagent to yield the tertiary phosphine oxide.<sup>[45,46]</sup> This



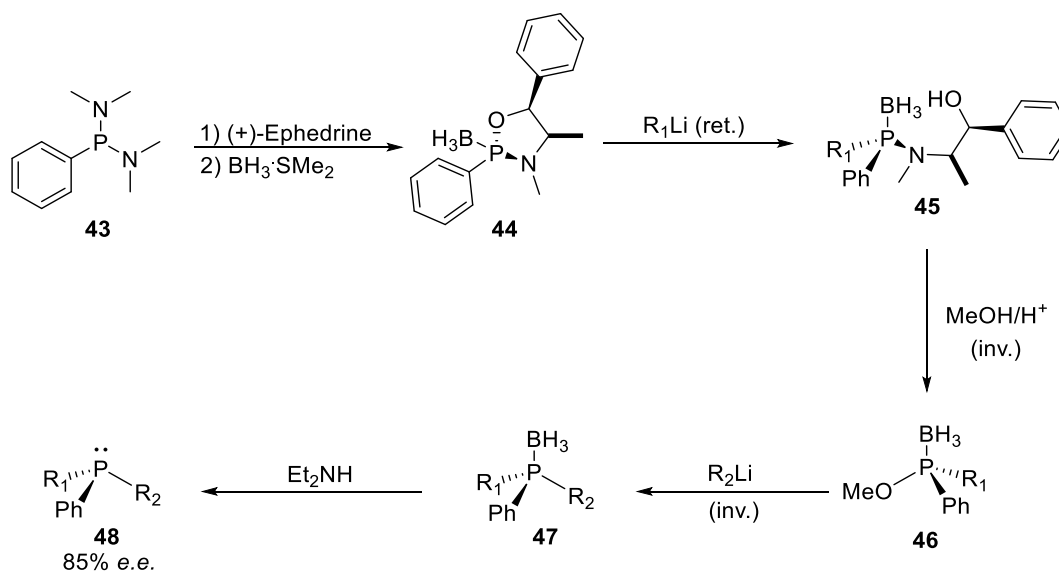
procedure has been used by Knowles *et al.* to synthesise the oxide precursor, **42**, to the chiral bidentate ligand, DIPAMP (**Scheme 10**).<sup>[47]</sup>



**Scheme 10** – Synthesis of a chiral bis-phosphine oxide **50** using (-)-menthol as a chiral auxiliary.<sup>[47]</sup>

More recent syntheses of P-chiral ligands include the use of bidentate, chiral auxiliaries such as amino alcohols or ephedrine.<sup>[48,49]</sup> Juge *et al.* used (+)-ephedrine for the synthesis of a tertiary, P-chiral phosphine ligand starting with the condensation of bis(dimethylamino)phenyl phosphine with (+)-ephedrine and then trapping of the free phosphine with  $\text{BH}_3\text{-SMe}_2$  to give the chiral oxazaphospholidine-borane complex **44** (**Scheme 11**). The alcohol group of the auxiliary can then be selectively displaced through the addition of a lithiated nucleophilic species, such as an aryl or alkyl group, with retention of the phosphorus centre. The next two steps both occur with inversion of the

phosphorus centre as the amine group of the auxiliary is then cleaved away from the phosphorus atom under acidic methanol conditions to give the phosphinite-borane, **46**, which upon addition of another lithiated, nucleophilic species yields the chiral, tertiary phosphine-borane **47**.<sup>[48,49]</sup>



**Scheme 11** – *Enantioselective synthesis of phosphines and phosphine-boranes using (+)-ephedrine as a chiral auxiliary.*

The chiral phosphine-borane **47** was then decomplexed through the addition of a secondary amine to yield the P-chiral, tertiary phosphine **48** with an e.e. of 85%.<sup>[48,49]</sup> This route, however, suffers from several shortcomings, such as the size limitation of the nucleophiles which can be used in the displacements at the phosphorus centre as large, bulky groups gave drastically reduced yields. Furthermore, this route like other P-chiral synthetic routes also requires multiple recrystallization steps to achieve homochirality, which can have negative effects on yields.

## 1.7 – Green chemistry

Green chemistry is a broad discipline which encompasses and can be applied to almost all areas of chemistry but is mainly applied to the areas of synthesis, catalysis and chemical engineering.<sup>[50-54]</sup> Green chemistry is defined as “the design of chemical product and processes which reduce or eliminate the use or generation of hazardous substances” and there are 12 main principles<sup>[55,56]</sup> which can be considered when using the green chemistry approach which are defined as:

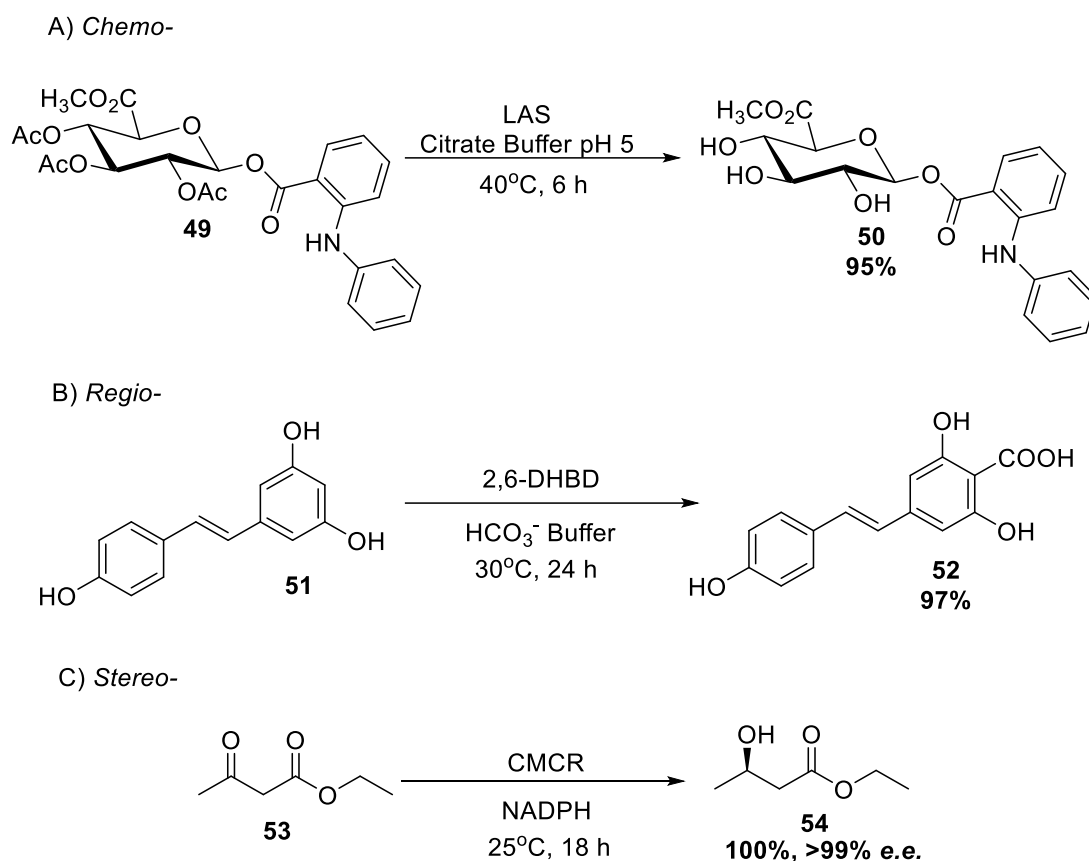
- 1) Prevention of waste preferred over the treatment of waste
- 2) Methods of synthesis should be atom efficient
- 3) Synthetic products should not possess human/environmental toxicity
- 4) Products should retain efficacy while reducing toxicity
- 5) Solvents and other auxiliaries should be unnecessary where possible
- 6) Reduction of energy requirements and use of ambient conditions
- 7) Use of renewable feedstocks
- 8) Reducing derivatives (i.e. protection/deprotection)
- 9) Moving toward catalytic reagents from stoichiometric
- 10) Design of biodegradable products
- 11) Analytical methods for real-time hazard/pollutant prevention
- 12) Use of safer reagents, which are benign in the event of an accidental spill

Since 1990, when the US pollution prevention act was passed,<sup>[57]</sup> companies have aimed to reduce the level of pollutants produced through cost-effective

modifications to existing and new processes. This has led to the formation of E(nvironmental) factor for assessing the environmental impact of chemical processes and can be defined as the kg waste/kg product, where companies now strive for low E factors where zero equates to zero waste produced.<sup>[9]</sup> Journals such as *Green Chemistry*, first published by in 1999 by the Royal Society of Chemistry, have become a repository for all aspects of green chemistry in synthesis, catalysis and chemical engineering.<sup>[53,54,56,58]</sup>

## 1.8 – Enzymes as biocatalysts

Enzymes have been utilised for hundreds of years in the production of alcohol and other food products, mostly unbeknownst to the users of them. The first reported use of enzymes in synthetic chemistry was in the isolation of pure (-)-tartaric acid, by Louis Pasteur, where the opposite enantiomer, (+)-tartaric acid, was selectively consumed by *P. glaucum* mould in a kinetic resolution.<sup>[59-61]</sup> Since then, biocatalysis using enzymes has been at the forefront of green chemistry in recent years due to the chemo-, regio- and stereoselectivity (**Scheme 12**) shown by enzymes which allows for greater atom economy, as conventional protection and deprotection methods can be made redundant due to high chemo-selectivity.<sup>[62-65]</sup>



**Scheme 12** – A) *Lipase AS Amano* catalysed chemo-selective hydrolysis of **49**. B) *2,6-dihydroxybenzoic acid decarboxylase* catalysed regio-selective carboxylation of phenol **51**. C) *Candida m. carbonyl reductase* catalysed stereo-selective reduction of **53**.

Furthermore, enzymes allow for the move from stoichiometric reagents to catalytic reactions. Biocatalysts typically operate in neutral aqueous conditions, which is environmentally benign, as well as them being biodegradable and non-hazardous.

## 1.8.1 – Enzyme structure

Enzymes are protein macromolecules which can split into a four-tier hierarchy of structure consisting of primary, secondary, tertiary and quaternary functions, which is summarised in **Figure 8**. The primary structure relates to the enzyme's amino acid sequence, consisting of combinations of the 21 key amino acids, bonded through the strong amide bonds between each amino acid. Due to the nature of the amino acids' hydrogen bonding donating and accepting ability, H-bonding between neighbouring amino acids leads to the secondary structure of enzymes which manifests most commonly as either  $\alpha$ -helixes or  $\beta$ -sheets.<sup>[66,67]</sup>

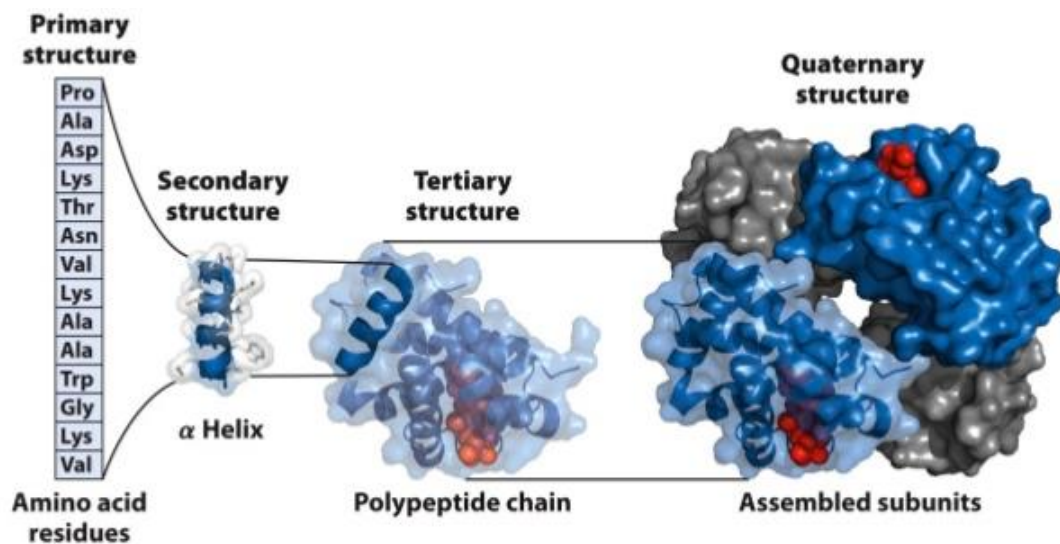
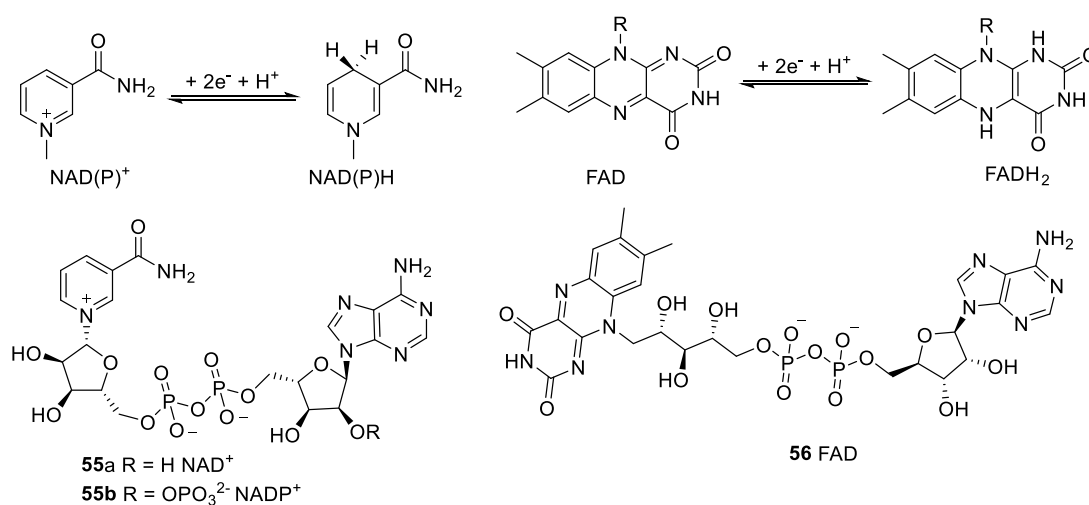


**Figure 8** – The structural formation of proteins showing the primary, secondary, tertiary and quaternary structure to give the assembled macromolecular protein.<sup>[66]</sup>

The secondary structures fold further into a more stable, tertiary structure, which is driven through the lower energy isolating alkyl and other non-polar

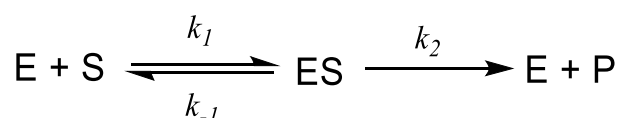
residues internally, away from the aqueous environment they are formed in. Inversely, the polar residues are situated towards the surface of the protein to interact with the aqueous environment and stabilise the structure of the protein. Furthermore, additional bonding interactions occur such as  $\pi$ - $\pi$  stacking between aromatic residues, Van der Waals forces, disulfide bonds between cysteine residues and salt bridges to enforce the 3D shape of the tertiary structure. Finally, the quaternary structure is formed when any number of the additional interactions bring together separate tertiary structures to form the final, protein structure.<sup>[66,67]</sup> Enzymes may also contain tightly bound metal ions such as iron, copper or molybdenum to aid in catalysis or use fusible co-factors such as FAD and NAD(P) (**Scheme 13**). These co-factors assist in processes such as metabolism and electron transfer, a function that an enzyme could not carry out without the aid of co-factors. More specifically, they are responsible for the delivering and occupation of reducing equivalents in oxidoreductase enzymes.



**Scheme 13** – Redox activity of both NAD(P) and FAD to NAD(P)H and FAD.

## 1.8.2 – Mechanisms of enzyme activity

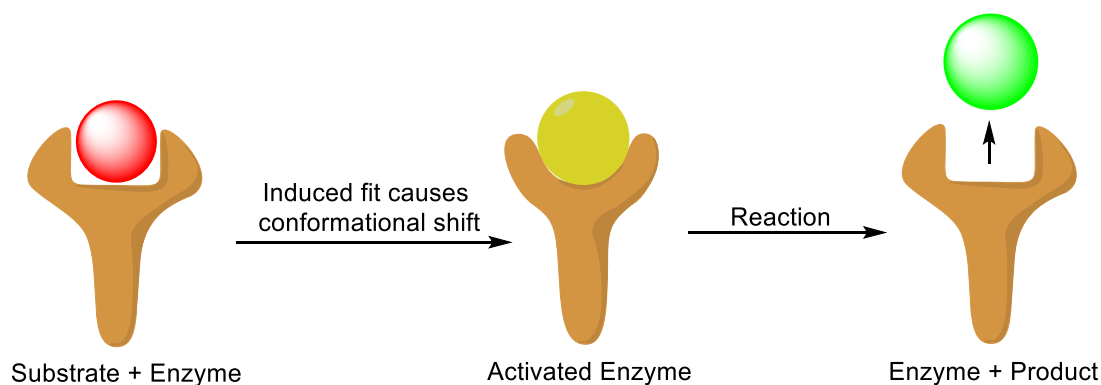
As enzymes act as nature's catalysts, they function like other chemical catalysts in that they increase the rate of the reaction without being consumed and without affecting the equilibrium of the reaction. They achieve this through reduction of the activation energy in a reaction coordinate, either through stabilisation of a transition state or through providing a lower energy pathway for the reaction. An enzyme catalysed reaction can be described through the formula shown in **Scheme 14**, in which the enzyme and the substrate form an enzyme-substrate complex, where the catalysis occurs, and the product is released. [68,69]



**Scheme 14** – Generalised reaction of an enzyme (E) and substrate (S) leading to the enzyme-substrate complex (ES) to give the enzyme and product (P).

A key feature of enzymes is that the reaction takes place inside the active site of the enzyme where certain amino acid residues bind to the substrate. Emil Fischer initially postulated that the binding of the substrate to the active site of the enzyme was entirely complementary, the so-called 'lock and key' hypothesis. [70]





**Scheme 15** – *The induced fit model postulated by Koshland in 1958.*<sup>[71,72]</sup>

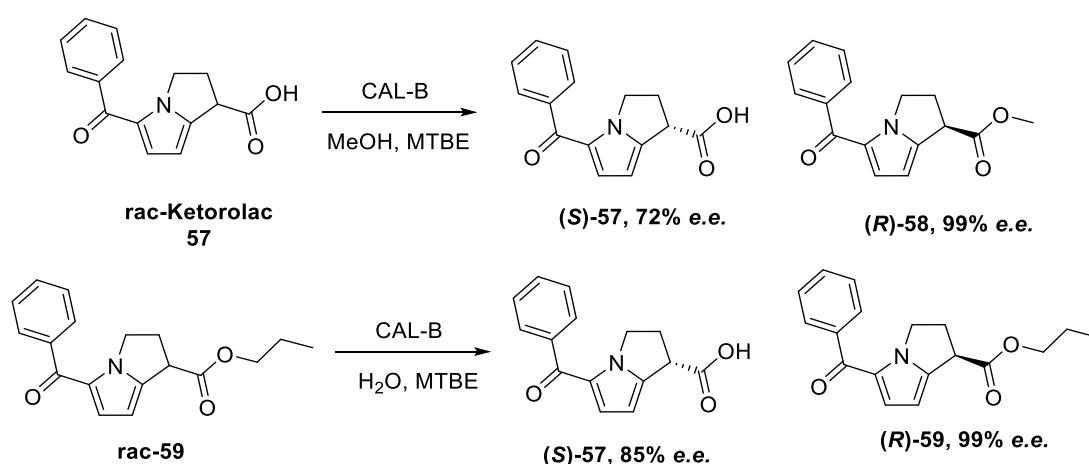
However, the ‘lock and key’ theory has been disproven in favour of the induced fit model (**Scheme 15**), as the lock and key theory would lead to a stabilised enzyme-substrate complex of such low energy that it would be difficult to overcome the energy barrier to reach the transition state. Inversely, the induced fit hypothesis describes that upon binding of the substrate to the enzyme leads to a conformational shift in the active site which can stabilise the transition state instead of the enzyme-substrate complex.<sup>[71-73]</sup>

## 1.9 – Enantioselective enzymatic transformations

### 1.9.1 – Enzymatic kinetic resolution

The space, residues, and interactions of the substrate within the active site are what give enzymes their high degree of chemo-, regio- and stereoselectivity.<sup>[66,68,69]</sup> This high selectivity shown by enzymes has been utilized in the resolution of racemates in a process called kinetic resolution, where an enzyme displays an increase in rate when acting upon a favoured enantiomer. This effectively leads to a separation of enantiomers, through

chemical modification of the more reactive enantiomer and this process has been used extensively in organic synthesis, especially where enantiopure pharmaceuticals and chiral building blocks are vital.<sup>[74-76]</sup> Juaristi *et al.* used a kinetic resolution in the separation of (*R/S*)-ketorolac, a non-steroidal anti-inflammatory, whose separate enantiomers show differing pharmacokinetics.<sup>[77,78]</sup> The kinetic resolution could be achieved via the lipase catalysed esterification of *rac*-**57** to give enantiopure (*R*)-**58** (Scheme 16) and (*S*)-**57** in high e.e. or via the lipase catalysed hydrolysis of the propyl ester *rac*-**59** to give enantiopure propyl ester (*R*)-**59** and ketorolac (*S*)-**57** in an e.e. of 85%.<sup>[78]</sup>

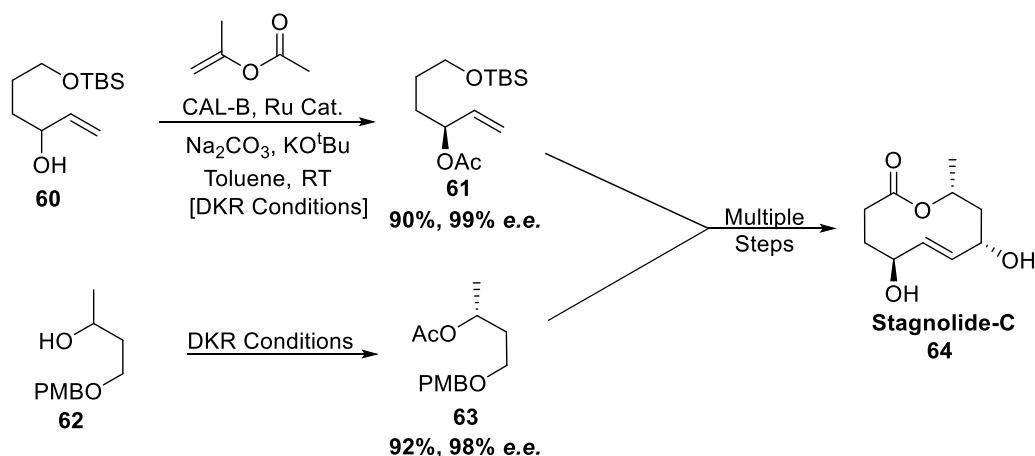


**Scheme 16** – Enzyme-catalysed kinetic resolutions of *rac*-ketorolac (*rac*-**57**) and *rac*-**59** to give enantiopure esters (*R*)-**58/59** and (*S*)-**57** in high e.e.

## 1.9.2 – Enzymatic dynamic kinetic resolution

Whilst use of enzymatic kinetic resolutions in synthetic routes provides a means to access enantiopure compounds, this is normally accompanied by a

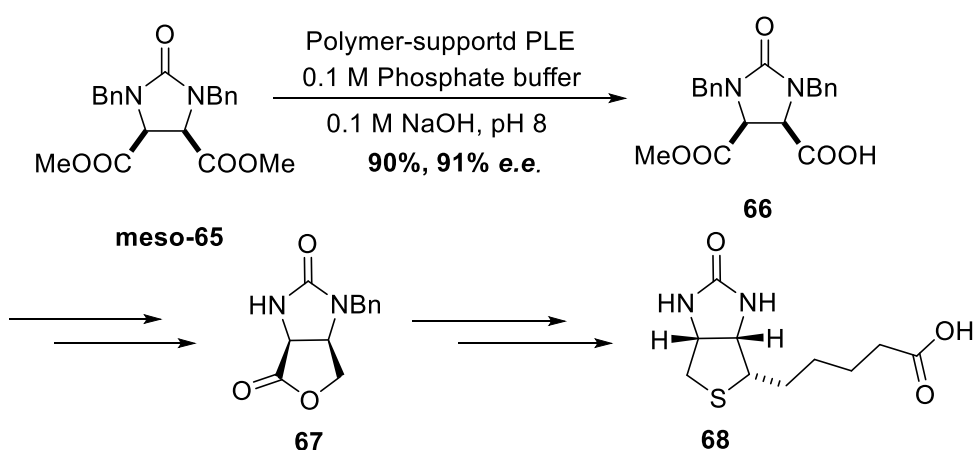
maximum 50% yield. However, this can be offset by using a dynamic kinetic resolution (DKR) in which the unreacted starting material is able to epimerize throughout the reaction to allow complete consumption of the starting material. For example, this can be achieved through the addition of a metal complex which can catalyse the epimerization of a chiral alcohol *via* a redox process.<sup>[79]</sup> The metal catalyst catalyses the reversible interconversion of the enantiomeric alcohols while the enantioselective lipase is able to selectively acylate one enantiomer. The first example of this type of chemo-enzymatic transformation was reported by Williams *et al.*, who used the rhodium catalyst [Rh<sub>2</sub>(OAc)<sub>4</sub>] and a lipase from *Pseudomonas fluorescens*.<sup>[80]</sup> This methodology has been applied in the total synthesis of the natural product stagonolide-C (**64**) in which the two chiral building acetates **61** and **63** were made by dynamic kinetic resolution using *Candida antarctica* lipase (CAL-B) (Scheme 17).<sup>[81]</sup>



**Scheme 17** – Dynamic kinetic resolutions of precursor fragments **61** and **63** which lead to the biologically active molecule **64** after several chemical steps.

### 1.9.3 – Enzymatic desymmetrization

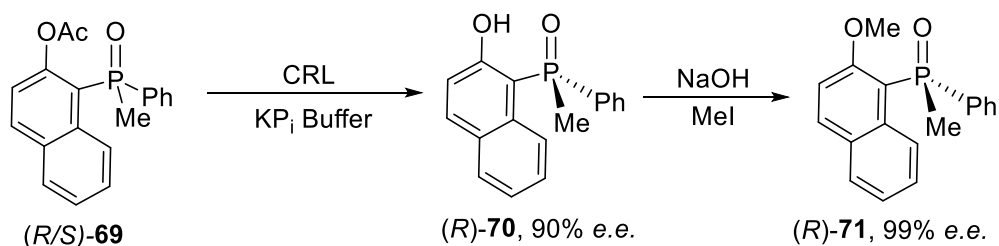
As with dynamic kinetic resolution, enzymatic desymmetrization also allows access to enantiopure molecules without the loss of yield associated with kinetic resolutions but also without the need for epimerisation of the substrate, which is not always possible. Alexander Ogston, in 1948, first highlighted the ability of enzymes to react asymmetrically on prochiral molecules with enantiotopic groups through selective interactions within the structure of the enzyme.<sup>[82-84]</sup> Although the incorporation of an enzymatic desymmetrization into a synthetic route can be challenging due to the need to incorporate a prochiral or meso molecule into the synthetic plan, this approach is often favoured over kinetic resolution due to the potential increased yield. Chen *et al.* reported the desymmetrization of the *meso* 1,4-ester **65** (**Scheme 18**) leading to an intermediate (**66**) in the synthesis of biotin **68**, utilizing vinyl acetate and pig liver esterase (PLE).<sup>[85]</sup>



**Scheme 18** – Lipase-catalysed desymmetrization of *meso* diol **65**, leading to biotin **68** after multiple steps.

## 1.10 - Enzymatic synthesis of chiral phosphorus compounds

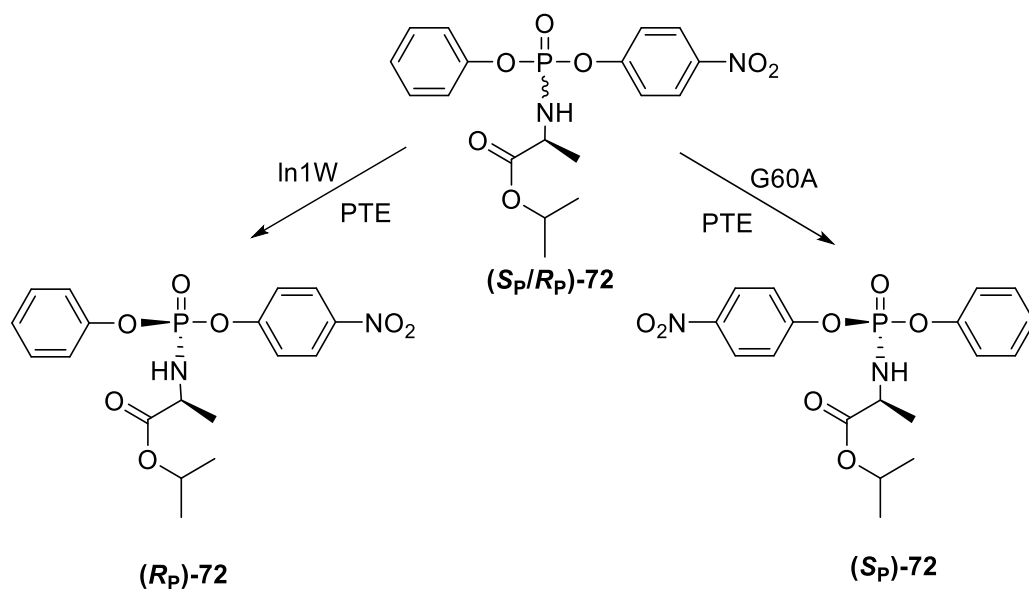
The use of enzymes in the enantioselective synthesis of phosphorus containing compounds is much less explored than that of chemical methods. However, there is literature precedent for this type of transformation. The use of enzymes has been demonstrated on P(III) compounds<sup>[86-88]</sup> and numerous groups of P(V) compounds<sup>[89-92]</sup>, highlighting the broad spectrum of enzyme substrates. The kinetic resolution of tertiary phosphine oxides containing an ester group has been reported by Kazlauskas *et al.* where a lipase from *Candida rugosa* was used to resolve the phosphine oxide **69** to give the alcohol (*R*)-**70** in 90% e.e. which could be methylated give the (*R*)-**71** in 99% e.e. after recrystallisation (**Scheme 19**).<sup>[89]</sup>



**Scheme 19** – Hydrolytic resolution of **69** to give (*R*)-**70** in 90% e.e. which was improved upon after methylation to give **71** and subsequent recrystallisation.<sup>[89]</sup>

In addition to the kinetic resolution demonstrated by Kazlauskas *et al.*, Xiang *et al.* reported complementary enzymes for the diastereoselective hydrolysis of phosphoramidate **72**, which is a precursor to several anti-viral prodrugs. Utilizing two different mutants of the enzyme phosphotriesterase (PTE), Xiang

*et al.* was able to access both diastereoisomers of the drug precursor through the selective hydrolysis of the unwanted enantiomer.<sup>[92]</sup>



**Scheme 20** – Diastereoselective hydrolysis of **72** by two mutants of PTE to give each diastereoisomer of the phosphoramidate (**(S<sub>P</sub>)-72** and **(R<sub>P</sub>)-72**).

## 1.11 – Copper-catalysed asymmetric 1,6-boration

Although phosphines and chiral phosphines have a multitude of different applications in catalysis, the asymmetric copper catalysed 1,6-boration of unsaturated compounds is one area which could benefit from the use of P-chiral monodentate phosphines. The related copper catalysed 1,4-boration is well described in the literature with both applications and mechanistic insights having been published.<sup>[93-95]</sup> However, the analogous 1,6-boration is less

researched mainly due to the difficulties with both -regio and -stereoselectivity, further complicated by limited mechanistic understanding for the 1,6-addition. The 1,6-boration of  $\alpha,\beta,\gamma,\delta$ -unsaturated esters has been reported in the literature to give allyl borates in 4 different isomeric forms, as shown in **Figure 9**, consisting of the *E/Z*- isomer of the allyl borate and the *E/Z*- isomer of the homoallylic borate.

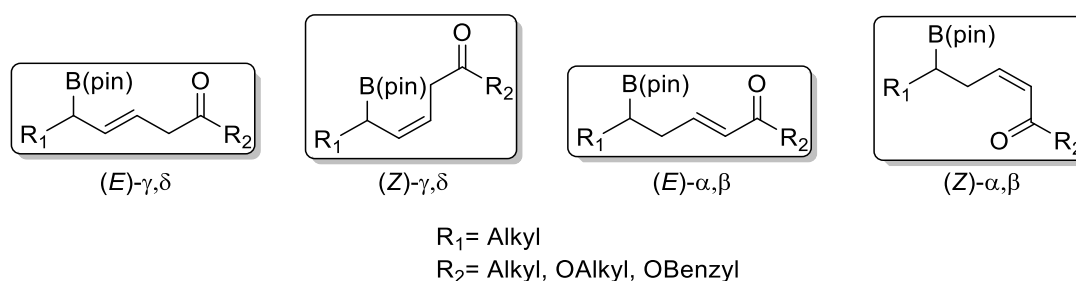
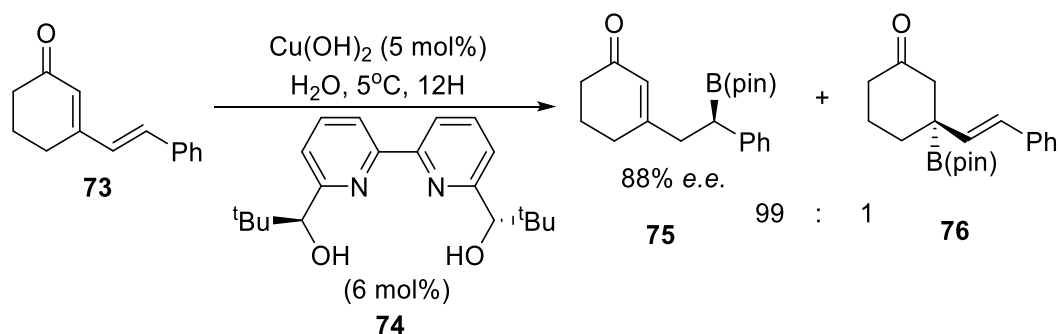


**Figure 9** – The 4 possible products from the copper catalysed 1,6-boration of  $\alpha,\beta,\gamma,\delta$ -unsaturated ester or ketones.

Kobayashi *et al.* published the 1,6-boration of cyclic diene esters such as **73** to form *E*-homoallylic allyl borates in an aqueous, copper-catalysed reaction. The reaction was done using the chiral, bidentate, pyridine-based ligand **74** (**Scheme 21**) along with several different copper (II) sources. Using these conditions, both the 1,4-boronate **75** and 1,6-boronate cyclic *E*-allyl borate **76** could be accessed depending on the addition of acetic acid or on the copper salt used, with up to 99:1 regioselectivity for the 1,6-boration over the 1,4-boration with relatively high *e.e.* Kobayashi *et al.* then went on to show that use of  $\text{Cu}(\text{OH})_2$  led to a heterogeneous system, most likely due to the formation of an insoluble polymeric  $\mu$ -hydroxide, which due to steric factors

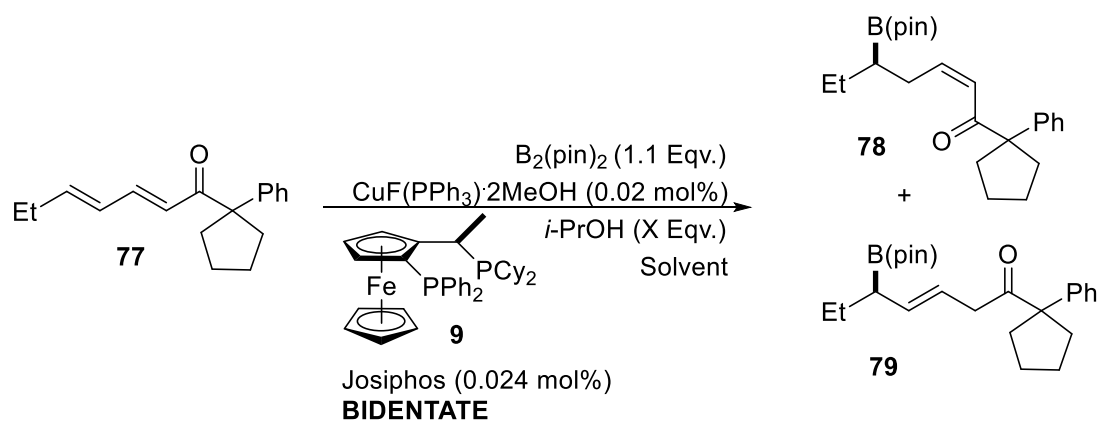
disfavours the formation of 1,4-addition. Inversely, the use of  $\text{Cu}(\text{OAc})_2$  led to a homogenous system in which the reactive species was found to be the less sterically demanding,  $(\text{pin})\text{B}-\text{Cu}(\text{OAc})-\text{Lig}$  (confirmed by ESI-MS), explaining why 1,4-addition is possible and in some examples heavily preferred.<sup>[96]</sup>



**Scheme 21** – Copper catalysed 1,6-boration of cyclic diene ketones using a bi-dentate pyridine ligand.

Lam *et al.* have shown the selective, controlled asymmetric copper catalysed 1,6-boration to acyclic  $\alpha,\beta,\gamma,\delta$ -unsaturated ketones with the use of the bi-dentate phosphine ligand, Josiphos **9** (**Scheme 22**). By switching the solvent, the concentration of the substrate, the equivalents of isopropanol and the steric bulk of the group alpha to the ketone either the chiral *Z*-homo allylic borate (**78**) or the *E*-allylic borate (**79**) can be accessed, shown in **Scheme 22** and **Table 6**.<sup>[97,98]</sup>





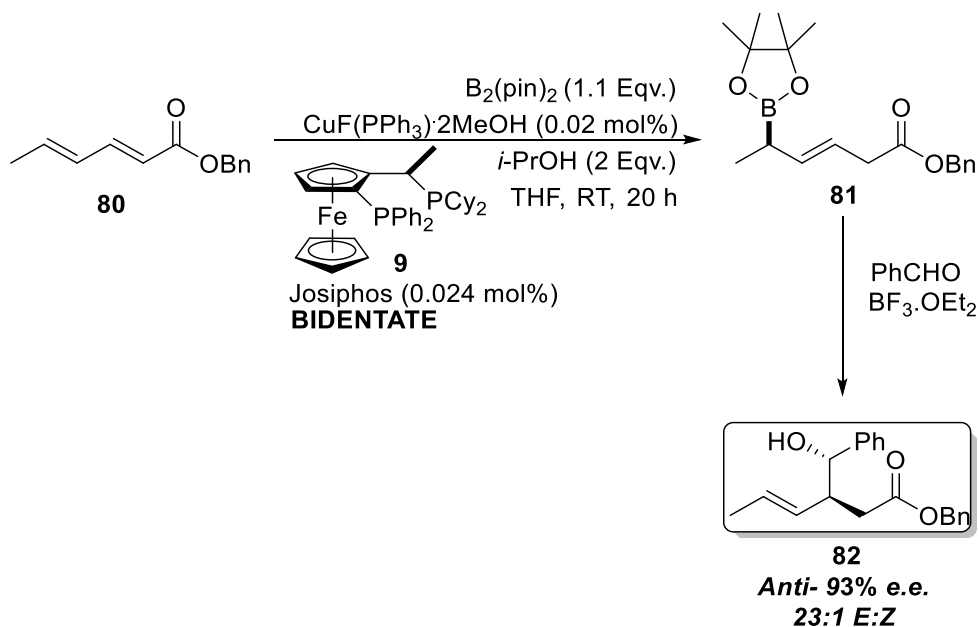
**Scheme 22** – Copper catalysed 1,6-boration of acyclic  $\alpha,\beta,\gamma,\delta$ -unsaturated ketones with bidentate Josiphos ligand to give either the  $(Z)$ - $\alpha,\beta$  or  $(E)$ - $\gamma,\delta$  product depending on addition of isopropanol and solvent.

**Table 6** – Solvent conditions and reaction conditions which give access to the allylic and homo-allylic products.

Solvents	Concentration [M]	$(Z)$ - $\alpha,\beta$ - <b>78</b> : $(E)$ - $\gamma,\delta$ - <b>79</b>
$i\text{PrOH}:\text{THF}$ (1:1)	0.1	1:14
THF	0.1	1:1
Cyclohexane/THF (4:1)	0.04	>19:1

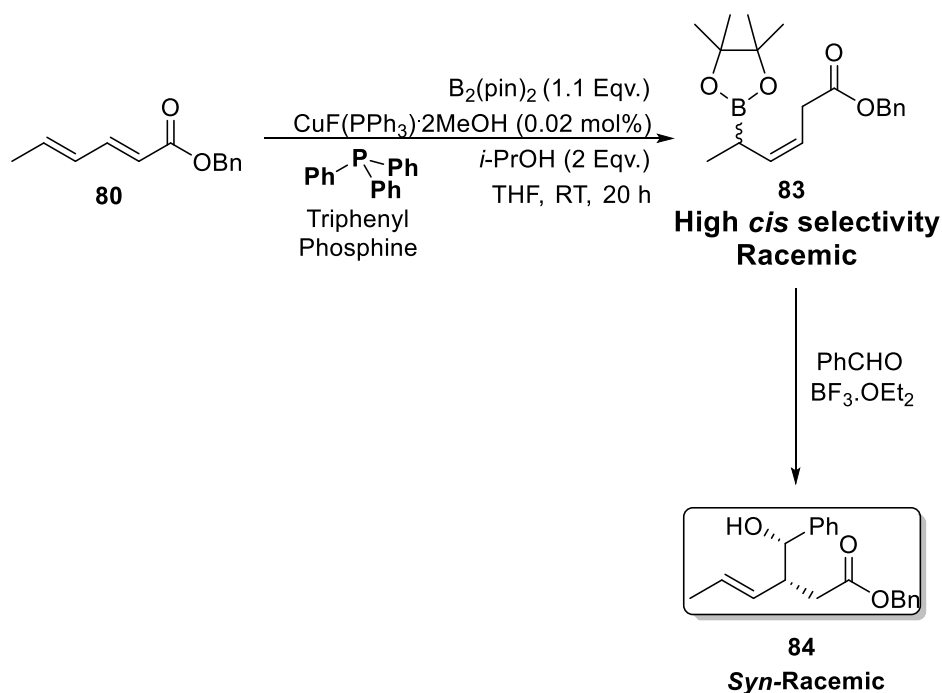
Lam *et al.* went on to apply this reaction to  $\alpha,\beta,\gamma,\delta$ -unsaturated esters using the Josiphos ligand on significant scale. This led predominately to the  $(E)$ -allyl borate with a high regioselectivity of > 19:1 for the 1,6-allyl borate over the 1,4-allyl borate and progressed in 95% e.e. (**Scheme 23**). The chiral,  $E$ -allyl borate could then be selectively oxidized with  $\text{NaBO}_3 \cdot 4\text{H}_2\text{O}$  to yield the corresponding allylic alcohol. More interestingly, Lam *et al.* showed that the 1,6-allylborate could also be used in a stereoselective allylboration with benzaldehyde and lewis acid,  $\text{BF}_3$ , as shown in **Scheme 23**, lead to an inseparable mixture of a

23:1 ratio of the (*E*)-/(*Z*)- isomers of the *anti*- adduct proceeding through a Zimmerman-Traxler transition state.<sup>[97,98]</sup>



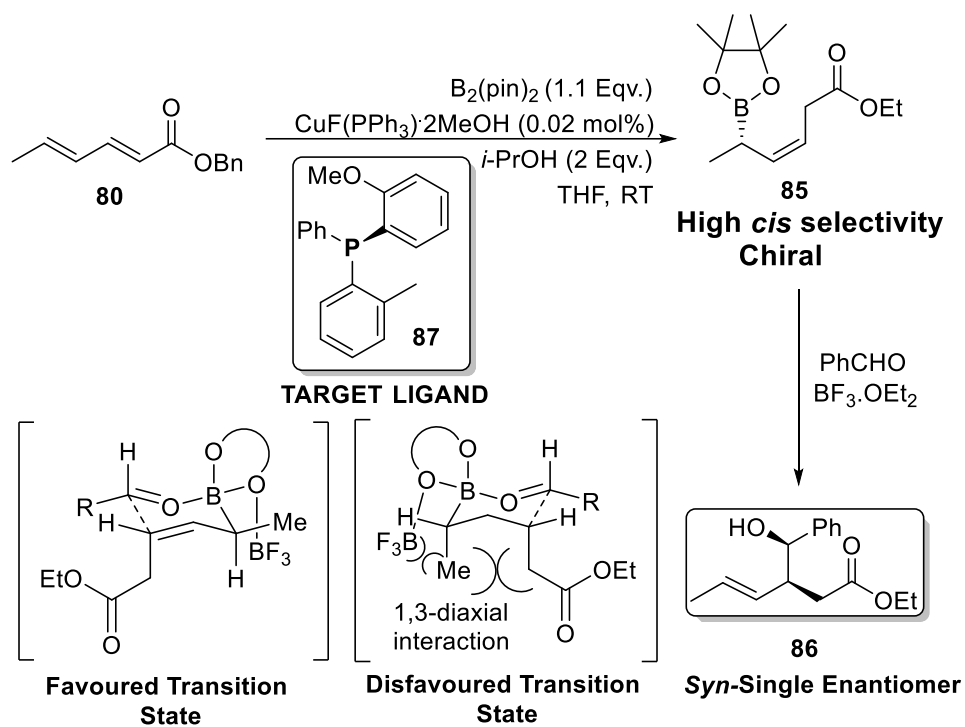
**Scheme 23** – Copper catalyzed 1,6-boration with the chiral bidentate phosphine **9** to give the (*E*)- $\gamma,\delta$  product **81** which on allyl boration with benzaldehyde and  $\text{BF}_3$  gives the *anti*- adduct **82** in a 23:1 mixture of (*E*) to (*Z*) products.

Lam *et al.* and personal communication with Prof. Luo (Co-author Ref. [97,98]) have shown that if the same copper catalyzed 1,6-boration is carried out with the use of an achiral mono-dentate, phosphine ligand, this leads to the (*Z*)-allylborate with high selectivity, albeit a racemic mixture.<sup>[99]</sup> When this (*Z*)-allylborate undergoes allylboration under the same conditions as above, this would lead to a racemic mixture of the *syn*-adduct with increased selectivity for the (*E*)-isomer as highlighted in **Scheme 24**.



**Scheme 24** - Copper catalyzed 1,6-boration with the achiral mono-dentate phosphine to give the (*Z*)- $\gamma,\delta$  product **83** which on allyl boration with benzaldehyde and  $\text{BF}_3$  gives the *syn*- adduct **84** with high (*E*)- selectivity.

Literature routes through to the acyclic, chiral 1,6-(*Z*)-allylborate are hitherto unknown, which is further complicated through the lack of mechanisms for the copper catalyzed 1,6-boration. Based on the preliminary work by Luo *et al.*, we believe a P-chiral, monodentate ligand would give access to the chiral (*Z*)- $\gamma,\delta$ -allylborate with the same high (*Z*)-selectivity. On allylboration, this would give a single enantiomer of the *syn*-adduct with high (*E*)-selectivity, which can be rationalised through the Zimmerman-Traxler transition state shown in **Scheme 25**.



**Scheme 25** – Proposed copper catalyzed 1,6-boration with the mono-dentate, *P*-chiral ligand which will allow for formation of the chiral (*Z*)- $\gamma,\delta$  allylborate **85** which on allylboration will give a single enantiomer of the syn-adduct **86**.

## 1.12 – Project aims

Based on the preliminary work by Lam *et al.* and personal communications with Professor Yunfei Luo,<sup>[97-100]</sup> we hypothesised that a P-chiral tertiary triaryl phosphine such as the target ligands, shown in **Figure 10**, would allow us to access the chiral (*Z*)- $\gamma,\delta$ -allylborate **85** (**Schemes 24** and **25**) via the copper-catalysed 1,6-boration.

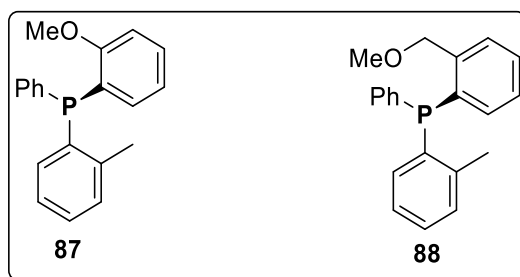
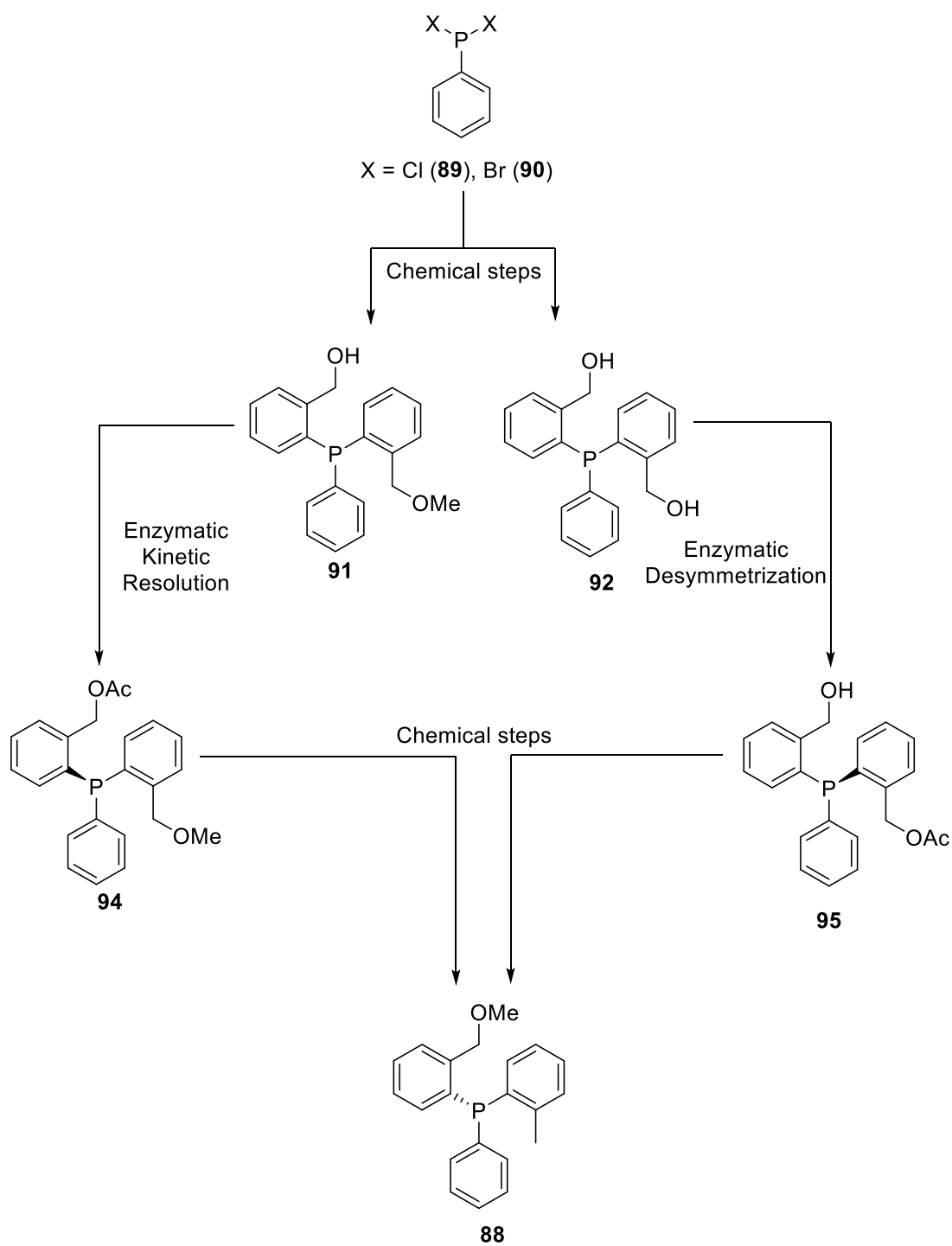


**Figure 10** – Target ligands for the copper-catalysed 1,6-boration reaction.

Furthermore, we believed that tertiary triaryl phosphines **87** and **88** would also display oxidative stability, due to high steric demands, allowing them to be stored and used under atmospheric conditions, increasing potential application.<sup>[27,28]</sup> We hypothesised that due to the large cone angle shown by tertiary triaryl phosphines, the target ligands would show good asymmetric induction during catalysis leading to high selectivity and enantiomeric excess allowing them to be applied to multiple types of metal-catalysed reactions.<sup>[14,15]</sup>

We envisaged a chemo-enzymatic synthesis of P-chiral phosphines and phosphine oxides using the enantioselectivity of enzymes to introduce chirality (Scheme 26). Starting from commercially available halophosphines (**89** and **90**), we planned to synthesise the phosphine substrates **91** and **92** which could be subjected to enzymatic kinetic resolution or desymmetrization respectively. The desymmetrization of **92** would be the quickest and most efficient route to install chirality since the substrate would require no prior derivatization. Furthermore, the implementation of a desymmetrization would give us the potential for a greater yield of over 50%, which is normally the limit of a kinetic resolution. Kinetic resolution could still give us access to P-chiral compounds albeit with a lower yield. However, access to P-chiral compounds was more important than the accompanying yield. In addition, any left-over material from a kinetic resolution could be recycled back into the enzymatic reactions. Chemical modifications of the P-chiral compounds would then allow us to fine tune the structure of the phosphine to produce stable ligands for the intended metal-catalysed asymmetric transformations.

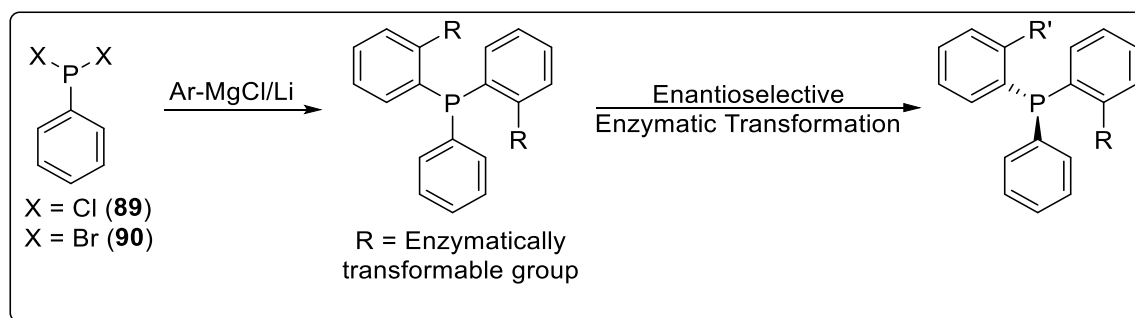


**Scheme 26** – Proposed chemo-enzymatic route utilizing either enzymatic kinetic resolution or desymmetrization and chemical modifications to give target ligand **88**.

## 2 – Results and discussion

### 2.1 - 1<sup>st</sup> Generation synthesis of prochiral phosphines

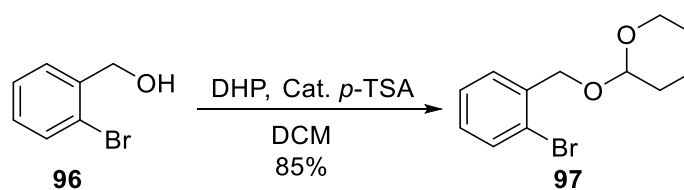
To gain access to a P-chiral monodentate ligand we first had to synthesise a racemic phosphine which could be enzymatically resolved, or a pro-chiral phosphine which could be enzymatically desymmetrized. Based on this we hypothesized that a prochiral, triaryl phosphine with *ortho*- substituents (**Scheme 27**) would allow for straight forward synthesis from simple, available halophosphines as well as options to more than one type of enzymatic transformation.



**Scheme 27** – Approach to the chemo-enzymatic synthesis of chiral phosphines.

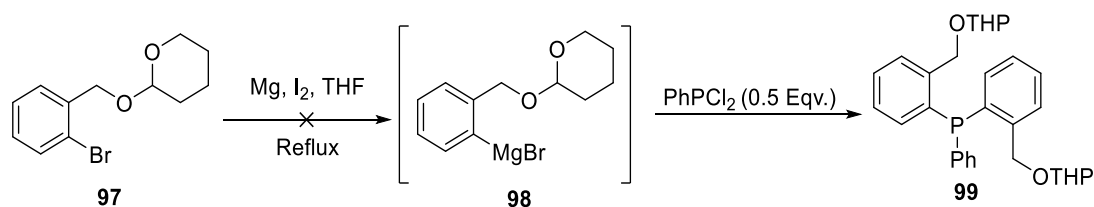
We chose a pro-chiral triarylphosphine with benzylic hydroxyl groups in the *ortho*- position, as this is a group which can be enzymatically acted upon. The hydroxyl group of 2-bromobenzyl alcohol was protected using DHP in DCM with *p*-TSA (**Scheme 28**). The choice of a THP protecting group was due to its inherent stability under basic and nucleophilic conditions, something which was needed for the upcoming steps, in addition to its straightforward removal in acidic methanol.<sup>[101]</sup>





**Scheme 28** – Protection of 2-Bromobenzyl alcohol (**96**) with DHP under acidic conditions.

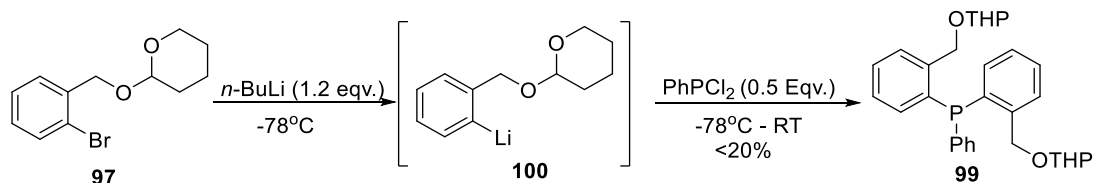
The addition of **97** to dichlorophenyl phosphine to give the tertiary phosphine was initially attempted through the formation of the Grignard reagent **98** (**Scheme 29**), a method which is prevalent in the literature for the synthesis of phosphines.<sup>[102-103]</sup> However, the initiation step in which magnesium is inserted across the C-Br bond to facilitate the formation of the Grignard reagent could not be replicated in similar conditions to that in the literature.



**Scheme 29** – Attempted synthesis of the triaryl phosphine **99** through Grignard formation and subsequent addition to dichlorophenyl phosphine which should yield the phosphine.

Due to the lack of reactivity *via* the Grignard method, the THP protected **97** was instead reacted with a slight excess (1.1 eqv.) of *n*-BuLi at -78°C in order to facilitate lithium-halogen exchange and the formation of the species **100** (**Scheme 30**). Dichlorophenyl phosphine (0.5 eqv.) was then added dropwise

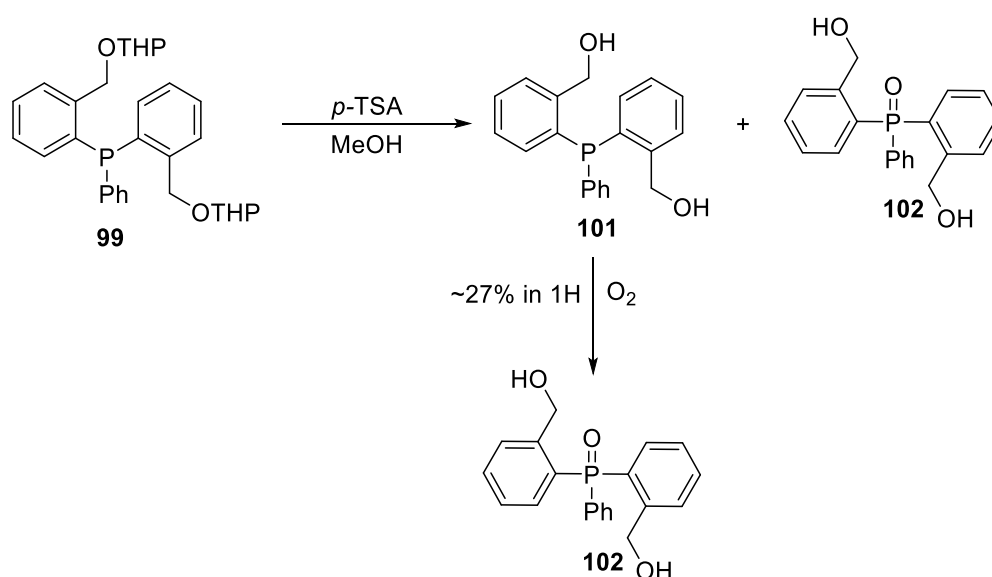
to the reaction, left to warm up to room temperature and subsequently stirred for 12 hours. After purification by column chromatography the desired phosphine **99** was obtained in quite a poor yield (<20%). The observed poor yield of the reaction may have been due to the less than optimal amount of lithium-halogen exchange occurring to form the nucleophilic species and then the competing nucleophilicity of any unreacted *n*-BuLi.



**Scheme 30** – Formation of the triaryl phosphine through lithium-halogen exchange of the -THP protected 2-bromobenzyl alcohol **97** which was subsequently added to dichlorophenyl phosphine.

Deprotection of **99** was completed in methanol and catalytic *p*-TSA proceeded with a poor yield, which was unexpected. On further analysis of the <sup>31</sup>P NMR of the product, it was shown that the phosphine **101** was spontaneously oxidizing in air to form the corresponding phosphine oxide **102** (**Scheme 31**). This oxidation was highly unexpected for a triaryl phosphine, since triphenylphosphine shows high stability to oxidation by atmospheric oxygen in air. Analysis by <sup>31</sup>P NMR identified the corresponding phosphine oxide due to the different shift compared to the phosphine, with the phosphine displaying a <sup>31</sup>P NMR shift of δ -27.1 and the phosphine oxide showing a shift of δ 40.5. It was found that the phosphine was oxidizing at a rate of just over 25% per hour which shows that the phosphine is highly unstable in atmospheric oxygen even

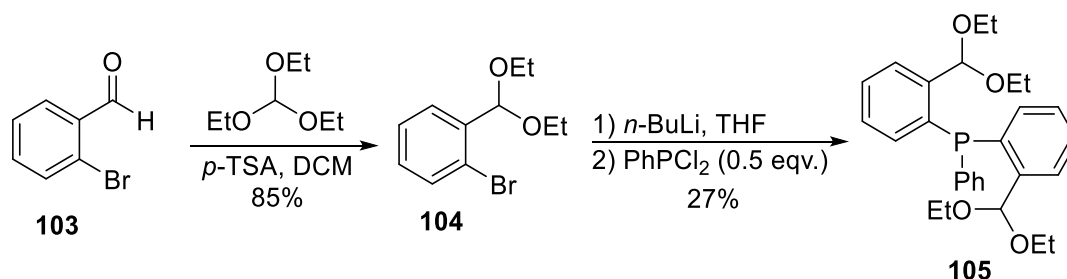
at room temperature. The observed poor oxidative stability could be due to the proximal hydroxyl group which has the potential to stabilize a radical intermediate species in the mechanism of oxidation, an effect which has been observed in phosphines containing nearby heteroatoms such as oxygen or sulfur.<sup>[28]</sup>



**Scheme 31** – Deprotection of -THP group in acidic methanol which also led to the phosphine oxide **102** through oxidation from in air at approximately 27% conversion in an hour.

In parallel, the bis-aldehyde analogue **105** was also synthesised *via* a similar route, shown in **Scheme 32**. Protection of the aldehyde derivative **103** through acetal formation was achieved through the addition of either ethylene glycol or triethyl orthoformate under acidic conditions which progressed in >85% yield and was easily characterized by the loss of the downfield aldehyde proton peak. This was then reacted in the same manner as described previously, where a slight excess of *n*-BuLi (1.1 eqv.) was added to **104** at -78°C after

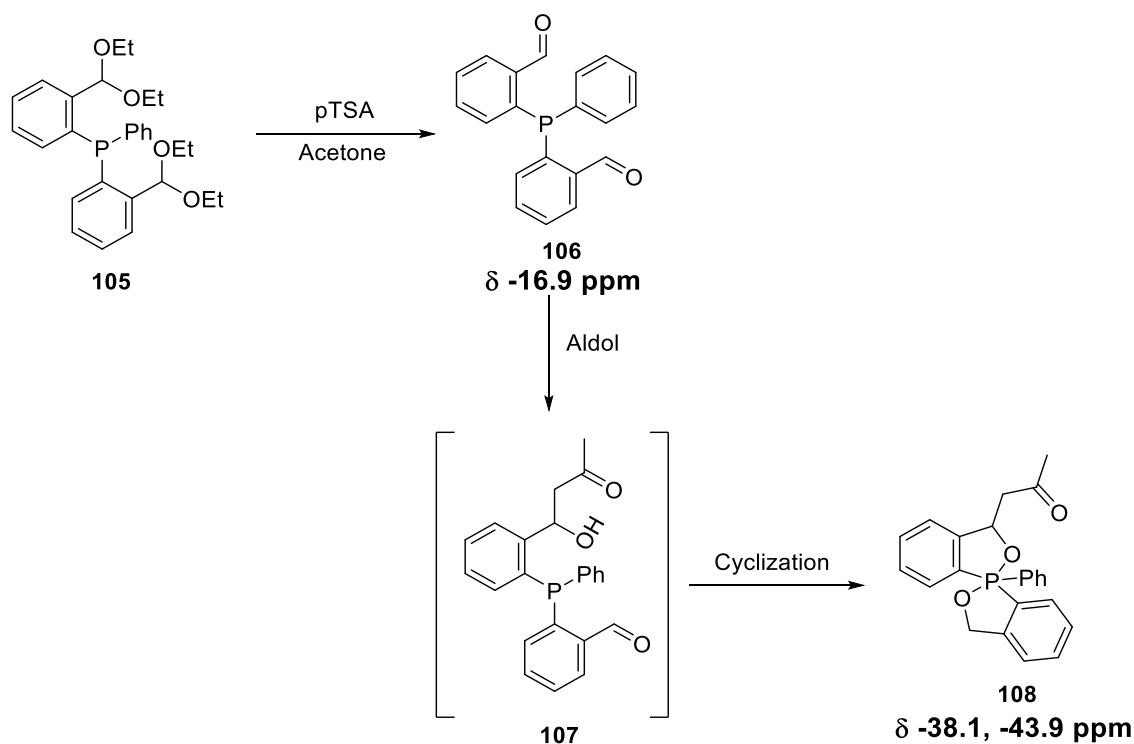
which 0.5 equivalents of dichlorophenyl phosphine was added dropwise, in half an equivalence with yields ranging from 27-40% (**Scheme 32**).



**Scheme 32** – Ethyl acetal protection of 2-bromo benzaldehyde (**103**) followed by lithium-halogen exchange, and addition of dichlorophenyl phosphine to yield the phosphine, **105**.

The removal of the acetal group was attempted in acidic acetone under reflux *via* acetal transfer to acetone. This deprotection step led to an unexpected product. Analysis of the crude material by <sup>31</sup>P NMR highlighted three main peaks at  $\delta$  -16.9, -37.1 and -42.7 and <sup>1</sup>H NMR highlighted several peaks around 5 ppm which would not have been present in the expected aldehyde product **106**. Purification of the crude material led to the identification of the phosphorus peak at  $\delta$  -16.9 belonging to the expected product **106** and the two peaks at  $\delta$  -38.1 and -43.9 belonging to a single compound. Previous literature has highlighted that the under these conditions compound **106** has been shown to undergo an aldol reaction with acetone to give the intermediate **107** which subsequently oxidised and cyclized to give the product, **108** (**Scheme 33**).<sup>[104]</sup> Similar to compound **101**, the poor oxidative stability shown by **106** under the deprotection conditions could be due to the formation of the proximal hydroxyl group in the intermediate **107**, which again may stabilize an

intermediate in the oxidation of the phosphorus centre.<sup>[28]</sup> Although we did not fully characterize the compound **108**, the <sup>1</sup>H and <sup>31</sup>P NMR support the formation of the spirophosphorane as the preliminary data was in agreement with the literature.<sup>[104,105]</sup>

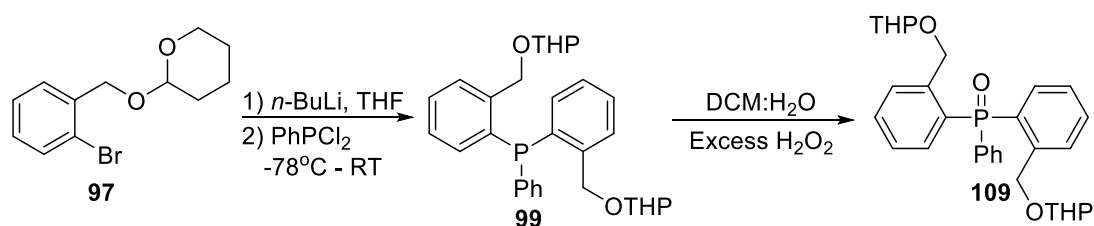


**Scheme 33** – Acetal transfer deprotection of **105** leading to the aldol reaction product **107** which subsequently cyclizes to yield **108**.

The deprotection of **105** did however proceed as expected using 1 M HCl in THF to give **106** in 83% yield without any observed cyclized product. The phosphine **106** also showed stability to oxidation. Although we did have a route to both phosphines, stability to oxidation was an issue for the phosphine **101** and therefore any means to bypass the potential loss of yield through oxidation would be beneficial for further reactions, enzymatic or chemical.

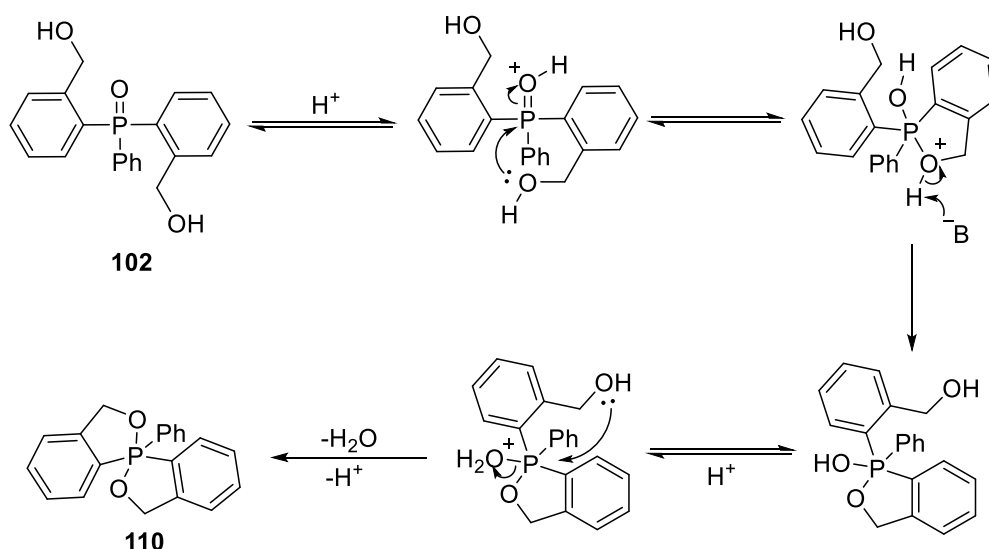
## 2.2 – Synthesis of the pro-chiral phosphine oxide

In order to by-pass the problem of oxidation seen with phosphine **101**, we hypothesised that the synthesis of the phosphine oxide **102** directly would simplify matters. The problem of oxidation stability could potentially be addressed later through the addition of groups that might increase stability. We could produce the chiral phosphine oxides through enzymatic reactions and then reduce the phosphine oxide to the phosphine prior to use in an oxygen-free atmosphere. However, bench top stability would be preferable for further application of any ligands synthesised. The phosphine oxide **102**, was synthesised, initially following the same route as shown in **Scheme 30**. However, prior to purification the crude material **99** was dissolved in a 2:1 mixture of DCM and water and excess hydrogen peroxide (**Scheme 34**) was added and left to stir at room temperature until the phosphine had been oxidised to **109**. Crude <sup>1</sup>H NMR of the reaction mixture showed that there was the possible presence of atropoisomers as the crude analysis contained an extra set of identical peaks and so the product was not fully characterized. The THP deprotection step was performed without purification of **109** and did not seem to affect the yield of the reaction.



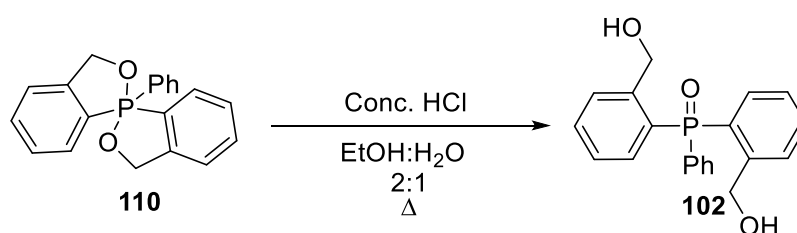
**Scheme 34** – Synthesis of phosphine, **99**, and subsequent oxidation to the corresponding phosphine oxide **109** with hydrogen peroxide in a DCM:water solution.

The removal of the THP groups was attempted in methanol with 10% *p*-TSA. However, this reaction also gave an unexpected product as  $^{31}\text{P}$  NMR analysis showed a peak at  $\delta$  -36.9 which was a phosphine-like shift, which did not correspond to the phosphine oxide product. A literature search showed that under acidic conditions, the pro-chiral phosphine oxide **102** undergoes spontaneous cyclization to form the spirophosphorane **110**, via the mechanism shown in **Scheme 35**,<sup>[104,105]</sup> and was present in our reaction in 73% yield compared to the 23% yield of the expected un-cyclized product, **102**.



**Scheme 35** – Acid catalysed cyclisation of **102** to give the spirophosphorane, **110**.

Fortunately, the spirophosphorane was much less polar and could be easily separated away from the product by column chromatography. Spirophosphorane **110** was then hydrolysed back to the desired product **102** through refluxing in a mixture of 2:1 ethanol and water along with concentrated hydrochloric acid (**Scheme 36**).<sup>[105]</sup>



**Scheme 36** – Hydrolysis of **110** back to the diol **102** through refluxing in an acidic solution of ethanol and water.

The spirophosphorane **110** showed an interesting splitting pattern in its <sup>1</sup>H NMR spectrum as it displayed extensive splitting of the -CH<sub>2</sub> groups adjacent to the P,O-phosphoether bond. These diastereotopic CH<sub>2</sub> protons displayed



different small  $J_3^{\text{HP}}$  couplings of 5.7 and 2.2 Hz and then a larger,  $J_2^{\text{HH}}$  geminal coupling of 14.2 Hz (**Figure 11**).

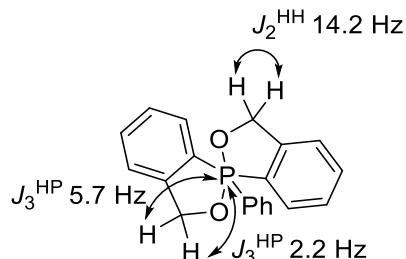


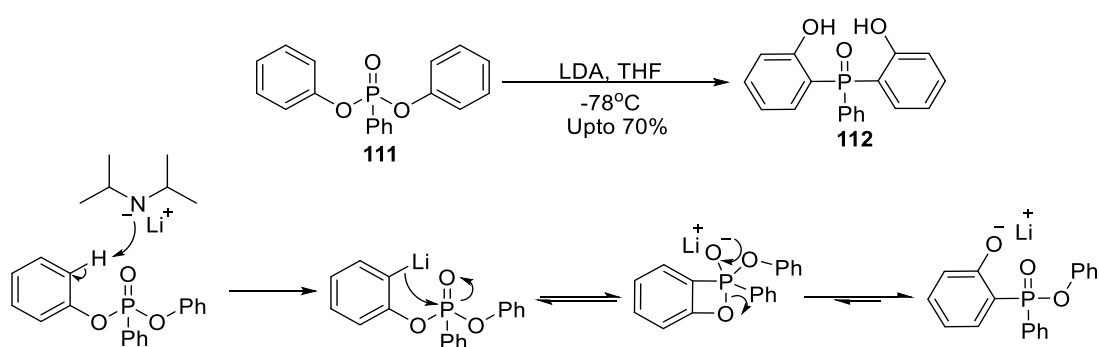
**Figure 11** –  $^1\text{H}$  NMR splitting of methylene protons of the spirophosphorane, **110**.

The prochiral diol **102**, was characterised by  $^1\text{H}$  NMR showing 4 methylene protons which resolved to two separate doublets at  $\delta$  4.67 and 4.58 ( $J = 12\text{Hz}$ ), again due to them being diastereotopic, a broad peak for the -OH, which would sometimes resolve into a triplet depending on sample concentration, and an aromatic region containing 13 protons. Analysis by  $^{31}\text{P}$  NMR showed a single peak at  $\delta$  40.4 and HRMS identified a mass of 361.0964 m/z corresponding to the  $[\text{M}+\text{Na}]^+$  ion, all of which was in agreement with literature.<sup>[102]</sup>

### 2.3 – 2<sup>nd</sup> Generation synthesis of the pro-chiral substrate

Whilst the 5-step route to **102** was successful, the overall yield was modest (<20%). Therefore, any possible optimization of the route to produce the enzymatic substrate would allow for much higher throughput for the project. Literature searching revealed a route for the synthesis of a similar, phenolic tri-aryl phosphine from the corresponding phosphonate (**111**) via a lithium

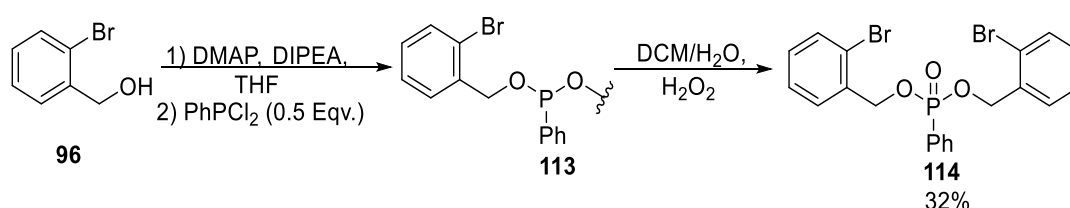
mediated 1,3-rearrangement (**Scheme 37**).<sup>[106,107]</sup> This reaction proceeds through the deprotonation of the aromatic proton, *-ortho* to the phenoxy group by LDA, to form the carbanion which undergoes the intramolecular rearrangement to form a more stable phenoxide anion. This method would also allow us to synthesise the pro-chiral phenolic derivative **112**, which could potentially be enzymatically desymmetrized to give a chiral phosphine oxide.



**Scheme 37** – LDA-induced 1,3-rearrangement of the phosphonate to the phosphine oxide.

We hypothesised that the same rearrangement could be achieved on a benzylic phosphonate to form **102**. Literature searching of this reaction showed that it had not previously been attempted on a benzylic phosphonate derivative and so conditions for the analogous 1,4-rearrangement reaction were unknown. In order to test the viability of this rearrangement, we attempted to synthesise the 2-bromoaryl phosphonate **114**, which was achieved by two different methods.<sup>[108-111]</sup> The first method attempted to synthesise the phosphonate was the use of 2-bromobenzyl alcohol (**96**), with DIPEA and a catalytic amount of DMAP (**Scheme 38**). The mixture was stirred for an hour after which dichlorophenyl phosphine was added dropwise and the

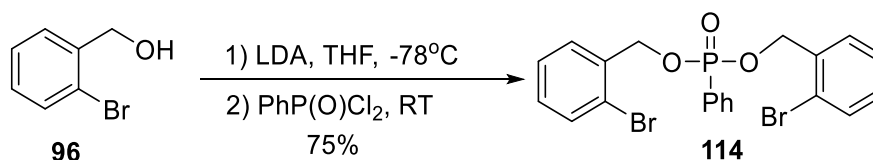
reaction was left to stir for 18 hours at room temperature. After work up the resulting residue was dissolved in a 2:1 solution of DCM and water and an excess of hydrogen peroxide was added to oxidise the phosphorus from P(III) to the P(V), phosphonate. This led to the formation of the phosphonate **114** in a modest 32% yield. We then attempted a second approach for the synthesis of the phosphonate **114**.



**Scheme 38** – Initial synthesis of the phosphonate **114** through the addition of DIPEA to the benzyl alcohol and then the addition of dichlorophosphine followed by oxidation to the phosphine oxide.

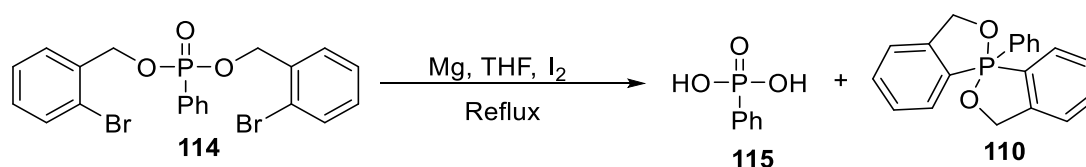
Lithium diisopropyl amide (LDA) was added to 2-bromobenzyl alcohol **96** at -78°C to form an alkoxide after which phenyl phosphinic dichloride was added to the reaction dropwise at room temperature to form the phosphonate (**Scheme 39**). This method ensured the deprotonation of the hydroxyl group and disposed of the need for a separate oxidation step, resulting in higher yields (75%) than the previously described method in **Scheme 37**. As with the spirophosphorane **110**, the benzylic phosphonates displayed a similar <sup>1</sup>H NMR -CH<sub>2</sub> splitting pattern, but with a small, identical, J<sub>3</sub><sup>HP</sup> coupling constant of 7.2 Hz due to the proximity of the phosphorus atom and a large J<sub>2</sub><sup>HH</sup> coupling constant of 12.7 Hz due to them being diastereotopic protons. The <sup>31</sup>P NMR

also showed a single peak with a shift of  $\delta$  19.79 which is also in agreement with similar phosphonates shown in the literature.<sup>[109-111]</sup>



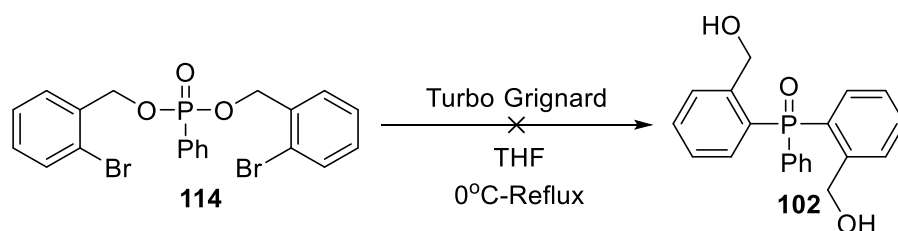
**Scheme 39** – Synthesis of the phosphonate **114** through the addition of LDA to **96** and then addition of phenyl phosphinic dichloride.

Now that we had access to the phosphonate **114**, we probed conditions which would initiate the 1,4-rearrangement through metallo-exchange of the aryl halide bond creating the nucleophilic species. The first method attempted utilised Mg and I<sub>2</sub>, to form a Grignard reagent (**Scheme 40**). Unfortunately, initiation *via* this method did not occur at room temperature but only when the reaction was refluxed for an extended period, which ultimately led to degradation of the phosphonate. Interestingly, analysis of the crude material from the reaction by <sup>31</sup>P NMR showed a small amount of spirophosphorane, **110**, at  $\delta$  -36.8. For **110** to be present in the reaction mixture, there must have been the formation of a P-C bond, showing that there is some scope for 1,4-rearrangement through initiation of the C-Br bond.



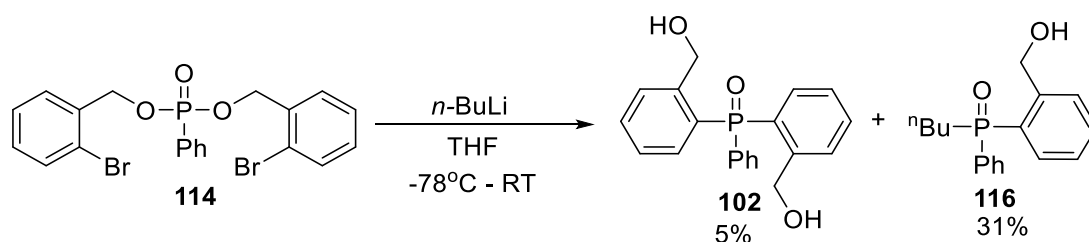
**Scheme 40** – Failed Grignard reaction leading to phosphoric acid and a small amount of **110**.

To further probe the initiation of the C-Br bond we attempted the use of  $i\text{PrMgCl}\cdot\text{LiCl}$  (Turbo Grignard), which is commonly used to facilitate the metallo-exchange group from the isopropyl group to the carbon-halogen bond of another molecule.<sup>[112,113]</sup> Turbo Grignard was added at  $0^\circ\text{C}$  to the phosphonate and the reaction heated by  $10^\circ\text{C}$  every hour but no activation occurred. The reaction was again heated to reflux for 24 hours but, no reaction was observed, and the starting material was fully recovered (**Scheme 41**).



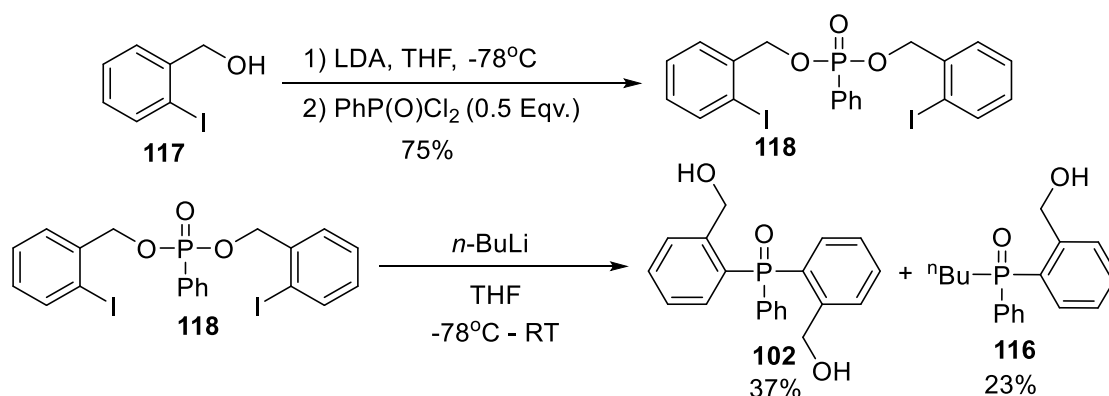
**Scheme 41** – A failed attempt of the rearrangement of the bromo-containing phosphonate **114** using Turbo Grignard reagent.

Due to the lack of reactivity shown by the Grignard-based reactions,  $n\text{-BuLi}$  was used to facilitate lithium-halogen exchange, as with the initial attempts at the synthesis of the phosphines and phosphine oxides. A slight excess of  $n\text{-BuLi}$  was added at  $-78^\circ\text{C}$  to the phosphonate in THF and left to warm up to room temperature overnight which lead to the formation of the pro-chiral phosphine oxide diol **102**, in 5% yield as well as the product (**116**) resulting from one aryl rearrangement and one displacement from  $n\text{-BuLi}$  (**Scheme 42**).



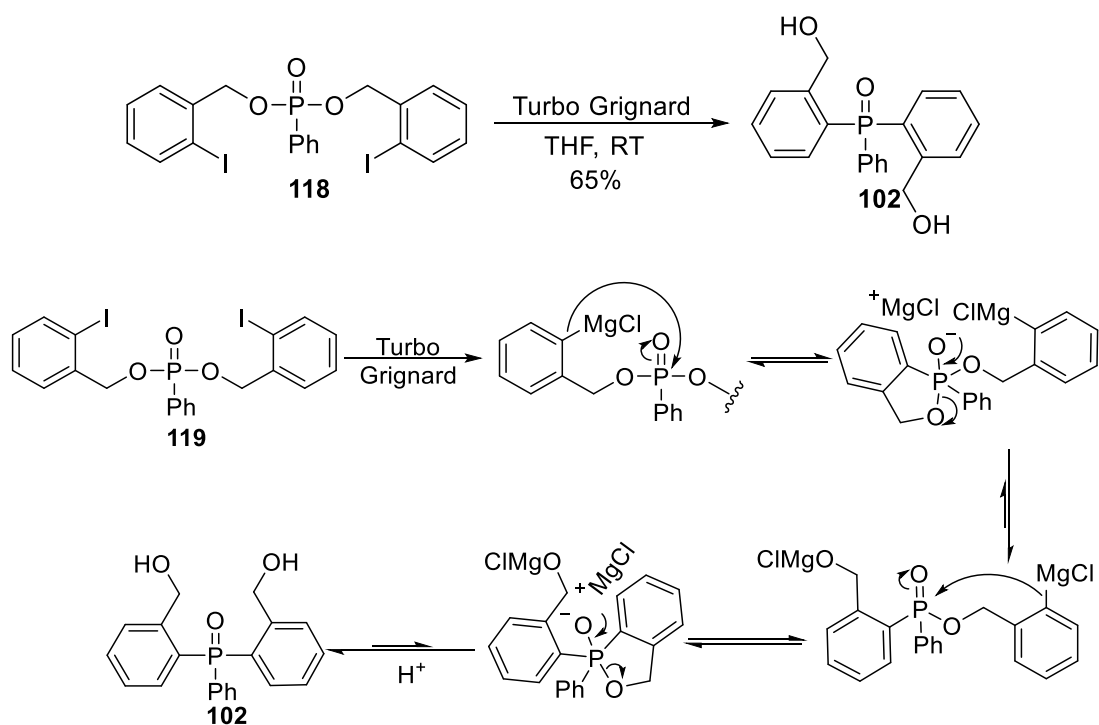
**Scheme 42** – An *n*-BuLi initiated rearrangement of **114** leading to a small amount of the product, **102** and the by-product **116**.

It was thought that the yield of **102** could be further improved by moving to the more facile exchanging 2-iodoaryl phosphonate derivative to increase the chance of the subsequent intramolecular 1,4-rearrangement. The 2-iodoaryl phosphonate **118**, was synthesised identically to **114** and progressed in a similar yield of around 75%. A slight excess of *n*-BuLi was then added to a solution of **118** in THF at -78°C over 15 minutes and the reaction was subsequently warmed up to room temperature and stirred overnight which lead to an increased yield of **102** to 37% but a large amount of **116** (23%), remained (**Scheme 43**).



**Scheme 43** - Synthesis of the iodo-phosphonate **118** and subsequent *n*-BuLi initiated rearrangement to give **102** and **116**.

To increase the yield of **102** further, the less nucleophilic, Turbo Grignard reagent was attempted again. Turbo Grignard (2.4 Eqv.) was added to **118** in THF at room temperature and the reaction was then left to stir for 24 hours leading to increased yields of **102** in up to 65%. A mechanism for this reaction is shown in **Scheme 44**. The initiation of the C-I bond at room temperature with Turbo-Grignard clearly shows improved reactivity of **118** compared to **114** and validates our move to the iodo-containing compounds. Furthermore, the throughput of the material was increased as **102** could be purified from the crude material by crystallisation from an ethyl acetate: hexane mixture in high purity, eliminating the need for difficult separation by column chromatography. The remaining 35% yield was typically split between unreacted phosphonate or the displacement of benzyl alcohol from isopropyl group of Turbo Grignard. This increased the overall yield of the bis-diol to 50% over the two steps, up from ~25% over the 4 steps of the previous methods and now that a reliable method to the main pro-chiral substrate existed, the enzymatic de-symmetrisation reactions on **102** could be attempted on greater scales.



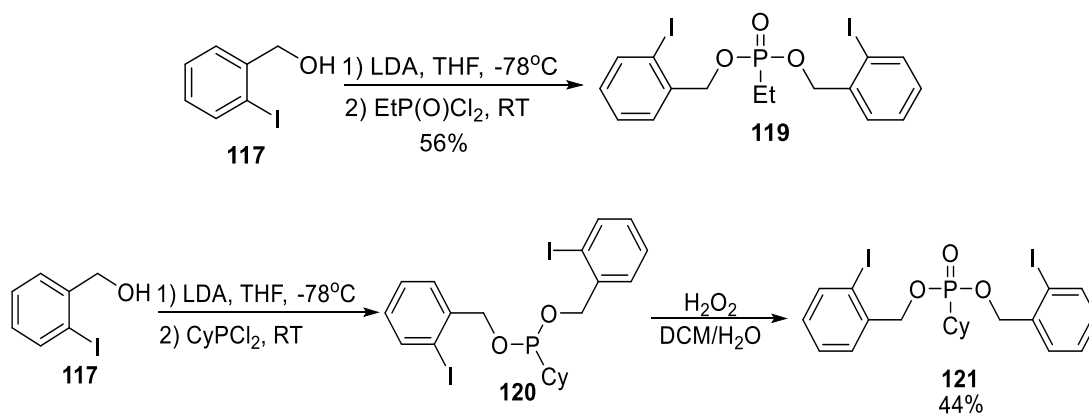
**Scheme 44** – Turbo Grignard induced metallo-rearrangement of **118**, to form the prochiral substrate, **102**, for the enzymatic desymmetrization.

## 2.4 - Expansion of the rearrangement reaction

To further test the scope of the metallo-induced phosphonate rearrangement we attempted the reaction on two different alkyl containing phosphonates. In addition to this, we also attempted a possible 1,5-rearrangement of a triaryl, benzylic phosphonate, where the C-X bond was *-meta* to the phosphonate. We hypothesised that ethyl and cyclohexyl containing phosphonate derivatives would be good candidates to test the scope of the rearrangement and so the required phosphonates were synthesised. Both the ethyl, and cyclohexyl phosphonate derivatives were synthesised *via* the same route as the triaryl phosphonates **114** and **118**. 2-iodobenzyl alcohol was deprotonated



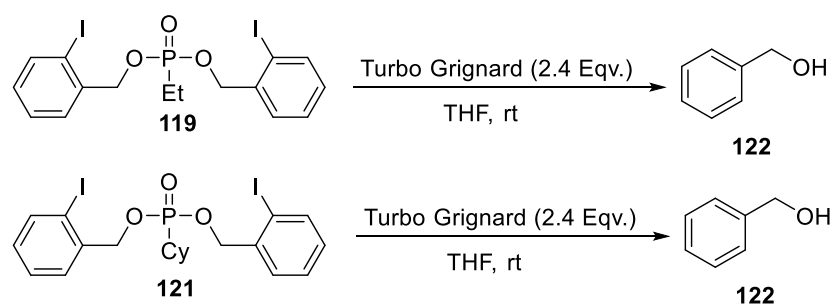
with LDA and added to the corresponding alkyl phosphinic dichloride, or alkyl dichlorophosphine in the case of the cyclohexyl derivative. As the cyclohexyl dichlorophosphine could not be purchased as the oxide it was oxidized to the phosphonate prior to purification with hydrogen peroxide. The ethyl phosphonate derivative **119** proceeded in a yield of 56% whereas the cyclohexyl derivative **121** proceeded in 44% yield over the two steps, which included the oxidation (**Scheme 45**).



**Scheme 45** – Synthesis of the two alkyl diphenyl phosphonates, **119** and **121**, through the addition of LDA to **117** and then through the addition of ethyl phosphinic dichloride or cyclohexyl dichlorophosphine.

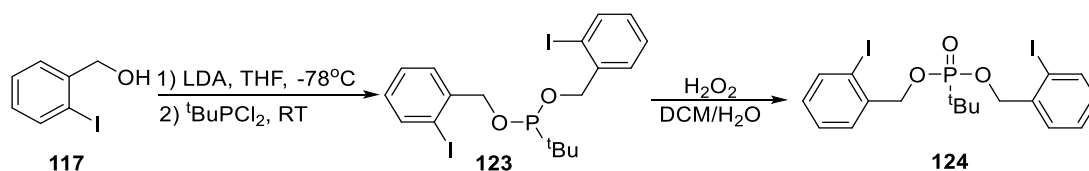
Turbo Grignard (2.4 Eqv.) was then added to the diphenyl alkyl phosphonates in THF at room temperature and monitored by TLC. The reaction with the ethyl derivative **98** led to several different products by TLC including cleavage of the phosphonate to yield benzyl alcohol (**Scheme 46**) as well as two different products which did not resemble the phosphine oxide product expected. The rearrangement of the cyclohexyl derivative **121** also led to cleavage of the phosphonate to yield benzyl alcohol and another product by TLC (**Scheme**

**46).** The second product, unfortunately, showed heavy degradation during purification by column chromatography and gave an extremely complicated  $^{31}\text{P}$  NMR and TLC, which was not evident in the crude analysis. We hypothesised that the presence of an alpha acidic proton on the alkyl groups may cause issues due to the proximity of the carbanion formed after the metallo-halide exchange which could deprotonate the alkyl proton and subsequently halt the intramolecular rearrangement.



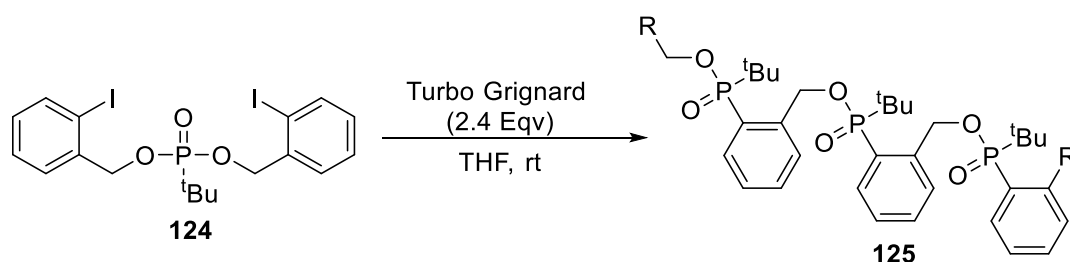
**Scheme 46** – Failed rearrangements of **119** and **121** with turbo Grignard both leading to **122**.

Therefore, to test this idea we attempted the rearrangement of a  $t$ butyl phosphonate derivative. The phosphonate **124** was synthesised by addition of LDA to 2-iodobenzyl alcohol and then subsequent addition of  $t$ butyl dichlorophosphine, as the corresponding oxide was not available. This meant that, like the cyclohexyl derivative, an extra oxidation step was needed to form the phosphonate, which was done through the addition of excess hydrogen peroxide to the crude material prior to the purification (**Scheme 47**).



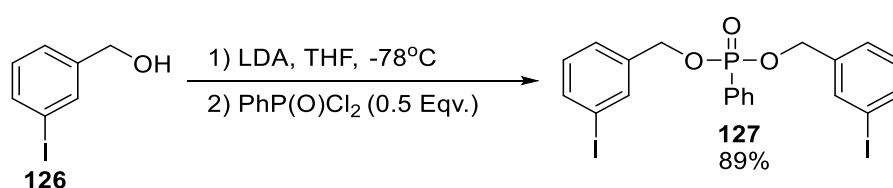
**Scheme 47** – Synthesis of the dibenzyl *t*-butyl phosphonate **124** from 2-iodobenzyl alcohol.

Turbo-Grignard (2.4 eqv.) was then added to **124** in THF at room temperature and left to stir for 24 hours after which the reaction was worked up to give a very viscous, polymeric substance which was not soluble in organic or aqueous solvents. We hypothesised that this polymeric structure could be the result of an intermolecular reaction where subsequent units of phosphonate react instead of the intramolecular rearrangement, however we could not characterise the product that was synthesised (**Scheme 48**). This change in reactivity could be due to the increased steric hinderance at the phosphorus atom associated with the *t*-butyl group which could prevent formation of the cyclic intermediate. Further work could be done to establish conditions which allow for 1,4-rearrangement of alkyl containing phosphonates.



**Scheme 48** – Proposed polymeric, phosphorus-containing structure **125** from the metallo-induced rearrangement of **124**.

Moving to the 1,5-rearrangement, the bis-3-iodobenzyl phenyl phosphonate **127**, was synthesised identically to **118** but proceeded in higher yields (89% vs 75%) than that of the *ortho*-substituted phosphonates (**Scheme 49**). This increased yield is most likely due to the lower percentage of lithium-halogen exchange occurring in the *meta*-position compared to the *ortho*-position of 2-iodobenzyl alcohol.



**Scheme 49** – Synthesis of the phosphonate **127** from **126** following the same method for previous phosphonates.

The Turbo-Grignard reagent was then added to **127** and the reaction was stirred for 18 hours, after which no rearrangement to the diol product was observed. The phosphonate, however, had undergone activation by the Turbo Grignard and was subsequently protonated upon workup leading to **128** (**Scheme 50**), which was seen through the appearance of two new protons in the aromatic region of the <sup>1</sup>H NMR. This highlights that the *-meta* lithiated species is not capable of undergoing the 1,5-rearrangement under analogous conditions to **118**, most likely due to the increased distance from the phosphorus atom. This reaction could be probed further through various temperatures however, this was not the focus of this piece of work.

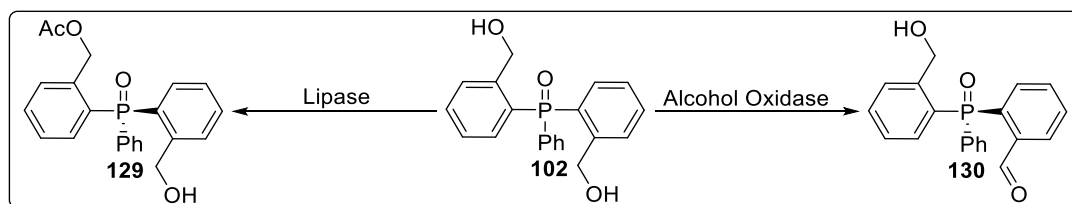


**Scheme 50** – Failed metallo-induced 1,5-rearrangement of the bis 3-iodobenzyl phenyl phosphonate which led to the protonation of the carbanion on workup giving

**128.**

### 3 – Enzymatic transformations

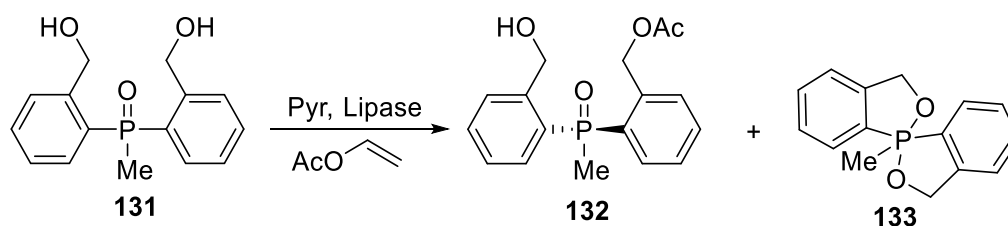
Now that we had produced the pro-chiral phosphine oxide 95, we could attempt the enantioselective enzymatic transformations to give P-chiral phosphine oxides. Due to the structure of **102**, containing a benzyl alcohol, we hypothesised that both lipases and alcohol oxidases could show activity towards this group to give a chiral product (**Scheme 51**). On this basis, and the fact that lipases typically operate in organic solvents<sup>[114]</sup>, we hypothesised that this would be an ideal starting point for the desymmetrization of **102**, due to its high lipophilicity.



**Scheme 51** – Potential enzymatic transformations for the desymmetrization of **102**.

### 3.1 – Lipase-catalysed desymmetrization

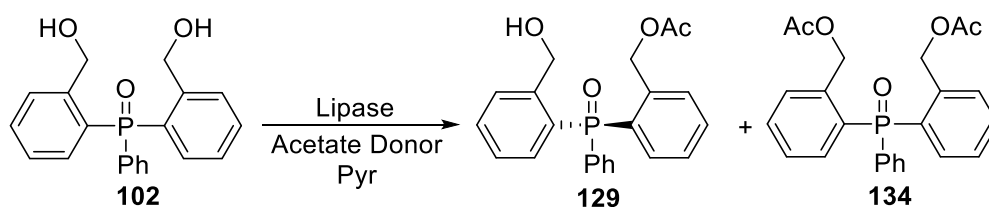
Initial screening for the enzymatic desymmetrisation of **102** to give a chiral phosphine oxide was attempted utilizing three different lipases, commonly used in the catalytic esterification's. The three lipases which were all commercially available, included porcine pancreatic lipase (PPL), *Candida antarctica* lipase A (CAL-A) and *Candida antarctica* lipase B (CAL-B), both of which were immobilized on the imobead 150 support from Sigma Aldrich. Although both CAL-A and CAL-B lipases have been used extensively in the literature for the esterification of a variety of different substrates<sup>[115-117]</sup>, neither of these enzymes have been shown to catalyse the desymmetrisation of triaryl phosphine oxides. A similar desymmetrisation (**Scheme 52**) and kinetic resolution had been performed on the diaryl alkyl phosphine oxide **131**, but it was reported that no activity was seen on the triaryl phosphine oxide **102**, due to steric factors in triaryl phosphine oxides.<sup>[102]</sup>



**Scheme 52** – Literature desymmetrization of a diaryl methyl phosphine oxide **131** leading to the chiral mono-acetate, but also the spirophosphorane, **133**.

The initial screening reactions were attempted using two acetate donors which were also readily available; isopropenyl acetate (ISPA) and vinyl acetate (VA)

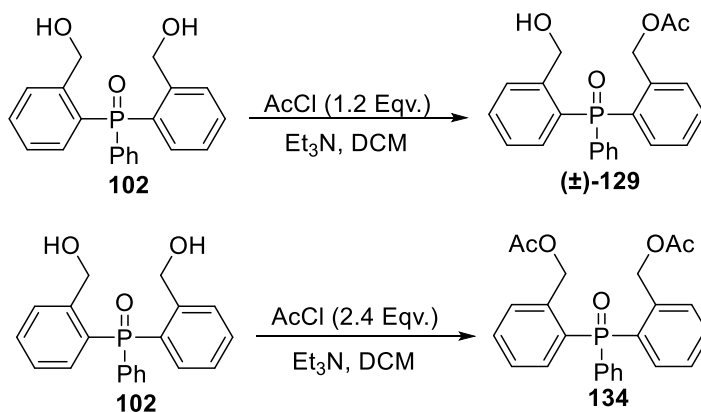
as these are commonly used in lipase catalysed reactions. Both these vinyl acetate donors are key due to the ability of the leaving group to tautomerize to acetone and acetaldehyde, respectively, and subsequently prevent the reversible reaction from occurring. In order to maximise reactivity, the reaction was attempted with the acetate donor as both the reactant and the reaction solvent. Fortunately, **102** was soluble in both vinyl acetate and isopropenyl acetate.



**Scheme 53** – Initial screening of the desymmetrization of **102**, with pyridine, a lipase and an acetate donor.

We began with 25 mM of **95**, 5 mg of either immobilized or lyophilized enzyme made up to 1 mL with either VA or ISPA (**Scheme 53**). A small amount of pyridine (2  $\mu$ L) was also added to the reaction to suppress the cyclization of **102** to **110** which can occur due to the small amounts of water present in the enzyme which could potentially hydrolyse the acetate donor releasing acetic acid which would promote the cyclisation. The reactions were shaken at 37°C for 96 hours after which an aliquot was taken and analysed by chiral HPLC against a racemic standard of the mono-acetate **129**, and the bis-acetate **134** of which both were synthesised by addition of AcCl and Et<sub>3</sub>N to **102** in DCM (**Scheme 54**). Strangely, the mono-acetate **129** and the bis-acetate **134**, both had the same R<sub>f</sub> by TLC which made purification of the separate compounds

difficult. However, they could be separated by chiral HPLC column <sup>[Footnote1]</sup> which was sufficient for the condition screening reactions on an analytical scale, without the need for purification.



**Scheme 54** – Synthesis of the racemic standard **(±)-129** and the bis-acetate standard **134**.

A control reaction was also performed in parallel which contained all the reagents, but the enzyme was omitted to measure whether any background esterification was occurring from the presence of pyridine and vinyl acetate. However, it was shown that no product was formed in the absence of the lipase. Results of the initial reactions (**Table 7**) with the three lipases were varied, as PPL showed almost no activity on **102**, whereas CAL-B showed some activity but an extremely low *e.e.* of less than 10%. CAL-A showed extremely promising activity for the first attempt as it displayed a conversion of 53% to the mono-acetate **129** with an *e.e.* of 81% with isopropenyl acetate and a conversion of 73% to the mono-acetate **129** with an *e.e.* of 91% when

Footnote<sup>1</sup>: A chromatogram for the standard of the racemic monoacetate **129** could not be provided due to the corona-virus pandemic.



vinyl acetate was used as the acetate donor, which was surprising for the initial reactivity testing of the lipases.

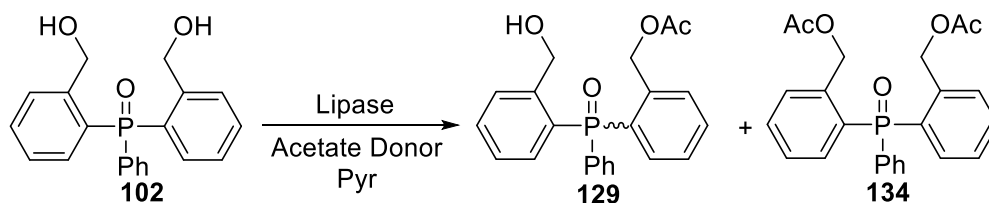


**Table 7** – Initial lipase screening of **102** for conversion to chiral monoester **129** and diester **127**.

Enzyme	Acetate Donor	Conversion to <b>129</b>	Conversion to <b>134</b>	e.e. ( <b>129</b> )
PPL	IPSA	2%	0%	5%
Lyophilized	VA	<1%	0%	N/A
CAL-B	ISPA	21%	0%	1%
Immobead 150	VA	21%	0%	7%
CAL-A	ISPA	53%	3%	<b>81%</b>
Immobead 150	VA	73%	22%	<b>91%</b>
Control	ISPA	0%	0%	0%
	VA	0%	0%	0%

Reaction Conditions: Incubated at 37°C at 180 RPM for 96 hours. Total volume 1 mL, 25 mM substrate, vinyl acetate/isopropenyl acetate as solvent, 5 mg of lyophilized/immobilized enzyme, 75 mM pyridine. HPLC Conditions: Daicel AD column, 1.2 mL/min, 83% Hexane/IPA at 210 nm.

### 3.1.2 – Immobead 150 CAL-A organic solvent screen

As CAL-A gave the best result for the initial testing we subjected the lipase to several different conditions to see if both conversion and e.e. could be improved. Firstly, we screened desymmetrization of **102** in 5 different organic solvents. The use of organic solvents in enzyme catalysed reactions has been shown in the literature to drastically change the activity and selectivity of enzymes.<sup>[118-120]</sup> The chosen organic solvents included ethyl acetate, DCM, toluene, diethyl ether and THF alongside the two different acetate donors, vinyl acetate and isopropenyl acetate which were added in 3 equivalents (75 mM) compared to the substrate.

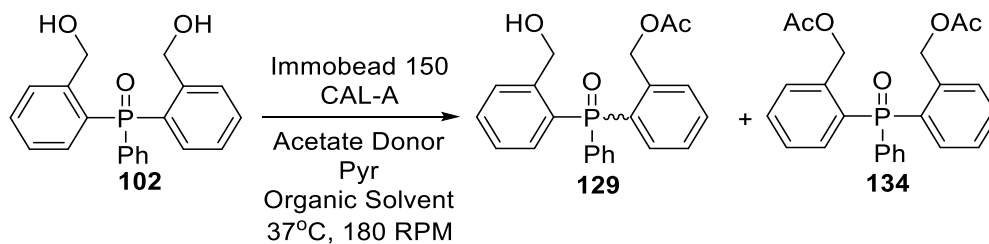


**Table 8** – Solvent screening for the immobead 150 CAL-A catalysed desymmetrization of **102**.

Solvent	Acetate Donor	Conversion to <b>129</b>	e.e. ( <b>129</b> )
Ethyl acetate	ISPA	0%	N/A
	VA	0%	N/A
DCM	ISPA	0%	N/A
	VA	0%	N/A
Toluene	ISPA	26%	84%
	VA	53%	85%
Et <sub>2</sub> O	ISPA	46%	90%
	VA	47%	87%
THF	ISPA	0%	N/A
	VA	0%	N/A

Reaction Conditions: Incubated at 37°C at 180 RPM for 24 hours. Total volume 1 mL, organic solvent to volume, 25 mM substrate, 75 mM vinyl acetate/isopropenyl acetate, 5 mg immobead 150 CAL-A, 75 mM pyridine. HPLC Conditions: Daicel AD column, 1.2 mL/min, 83% Hexane/IPA at 210 nm.

Activity was only seen in toluene and diethyl ether after 18 hours. In toluene a conversion to **129** of 26% with ISPA and 53% with VA was found. Whereas diethyl ether showed a more consistent conversion to **129** of 46% in ISPA and 47% in VA after 24 hours. Both solvents resulted in relatively high e.e. but diethyl ether gave better enantioselectivity of up to 90% e.e. despite the

substrate being much less soluble in diethyl ether than toluene. Although the use of diethyl ether as the reaction solvent gave favourable results, they did not outperform the use of VA as both solvent and acetate donor.

### 3.1.3 – Effect of temperature

The effect of temperature was also probed to see if this had any effect on both conversion and subsequent e.e. of the reaction. Due to the stability of the *Candida antarctica* lipase family,<sup>[121,122]</sup> we could increase the temperature beyond 37°C to 50°C without denaturing the protein, which is beyond the working range of most enzymes. In addition to the high temperature, we also attempted reaction with a decreased temperature of 20°C to see if a slower reaction would give better selectivity. Both reactions were attempted in vinyl acetate as solvent and donor, with the same concentrations of enzyme and substrate as used in previous screening reactions.

**Table 9** – Temperature screening for the Immobead 150 CAL-A catalysed desymmetrization of **102**.

Temperature	Acetate Donor	Conversion to <b>129</b>	Conversion to <b>134</b>	e.e. ( <b>129</b> )
20°C	VA	36%	2%	77%
37°C	VA	67%	22%	91%
50°C	VA	41%	5%	64%

Reaction Conditions: Incubated at 20-50°C at 180 RPM for 24 hours. Total volume 1 mL, 25 mM substrate, vinyl acetate/isopropenyl acetate as solvent, 5 mg enzyme, 75 mM pyridine. HPLC Conditions: Daicel AD column, 1.2 mL/min, 83% Hexane/IPA at 210 nm.

Both the lower and higher temperatures showed a significant decrease in *e.e.* with 50°C giving an *e.e.* of 64% and 20°C giving an *e.e.* of 77% after 24 hours which when compared to 37°C (**Table 9**).

### 3.1.4 – Enzyme concentration studies

We then probed the concentration of the enzyme in the reaction and so increased the amount of enzyme three-fold, from 5 mg to 15 mg, to see how this would affect *e.e.* and the conversion. The reaction was left for 24 hours at 37°C using vinyl acetate, as both the donor and the solvent. This led to a conversion of 72% and an *e.e.* of 92.7% which was the highest *e.e.* seen to this point in the project and was a promising step forward to potentially producing enantiopure compounds. In order to understand the dynamics of the desymmetrization reaction and how the *e.e.* changed over the course of a 24-hour reaction, an aliquot from the reaction was taken at regular intervals and measured by chiral HPLC to gauge both the *e.e.* and conversion. The time plot in **Figure 12** shows that over the 24-hour period, the *e.e.* began at 87.7% and then slowly increased to the final *e.e.* of 92.7% after 24 hours with a consumption of 94.6% of the substrate to **129** (72.7%) and **134** (21.9%).

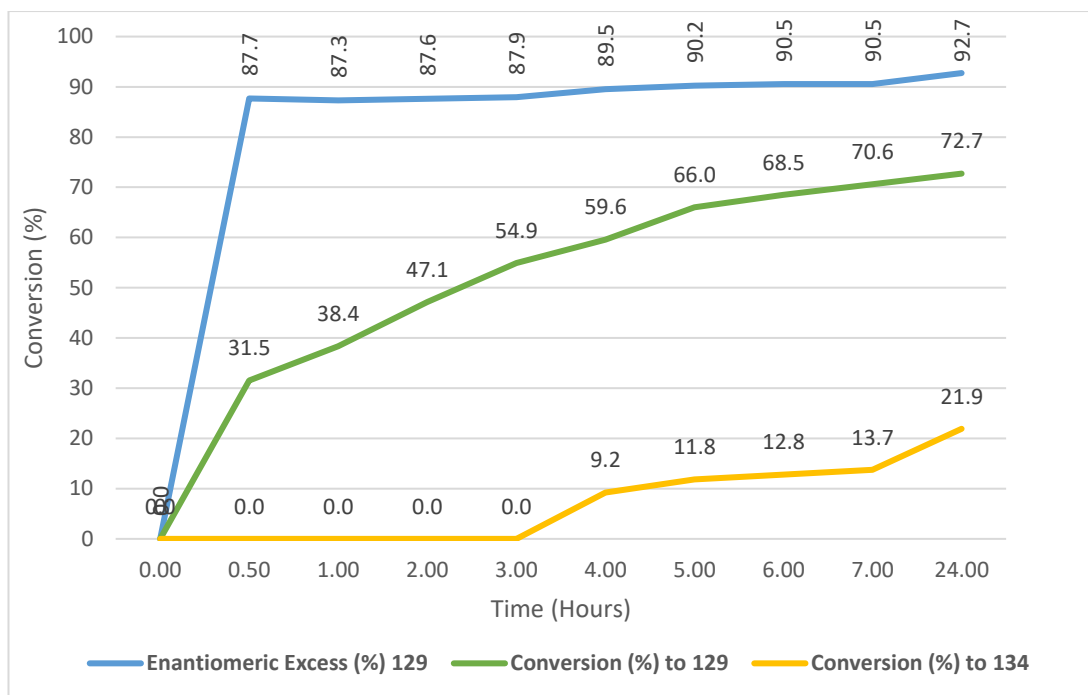
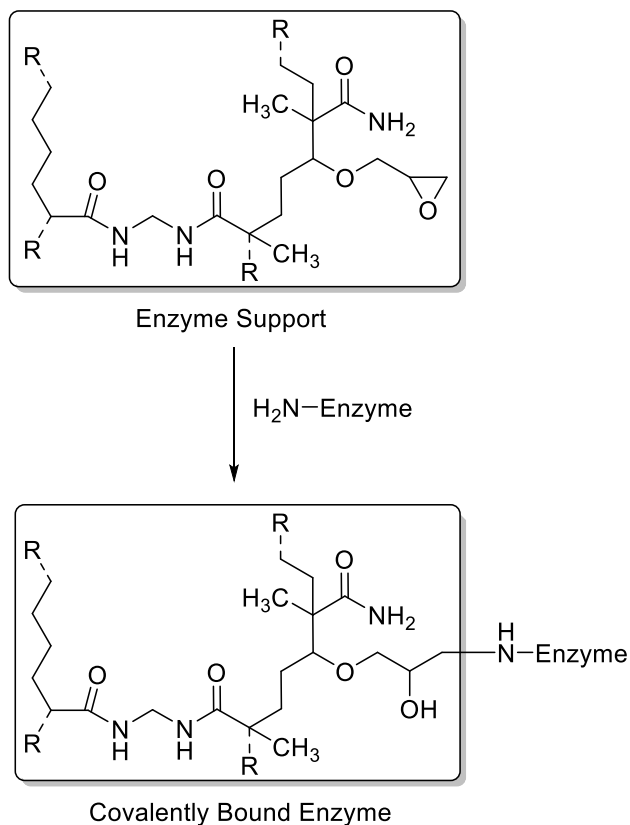


**Figure 12** – 24 Hour time plot of Immobead 150 CAL-A catalysed desymmetrization of **102**. Reaction Conditions: Incubated at 37°C at 180 RPM for 24 hours. Total volume 1 mL, 25 mM substrate, vinyl acetate as solvent, 15 mg of immobead 150 CAL-A, 75 mM pyridine. HPLC Conditions: Daicel AD column, 1.2 mL/min, 83% Hexane/IPA at 210 nm.

### 3.2 – Immobilization of CAL-A

In another bid to improve the e.e. we hypothesised that the use of a different enzyme immobilisation support could give higher selectivity. The use of different supports has previously been shown in the literature to improve both the conversion and e.e. of lipase catalysed reactions.<sup>[123,124]</sup> We used three different enzyme supports which were available to us including, Eupergit CM, Purolite ECR8215 epoxy and Purolite ECR8285 butyl epoxy, all of which are based on covalent bonding of the enzyme to the support which is achieved via

the opening of an epoxide ring on the support by the  $\text{-NH}_2$  of lysine residues in the structure of the enzyme (**Scheme 55**).



**Scheme 55** – Covalent attachment of the enzyme to the support through opening of an epoxide ring from the lysine residues of the protein.

Immobilization of crude CAL-A to the enzyme supports was achieved through the addition of the immobilization support to a solution of the enzyme in pH 7, 0.1 M potassium phosphate buffer. A concentration reading of the solution was taken at 0 hours and then the mixture was then left to shake at room temperature for 24 hours. After the allotted time, a second concentration reading of the solution was taken and the difference between the two values should equate to the enzyme loading. The three different supports showed varying degree of loading of CAL-A.

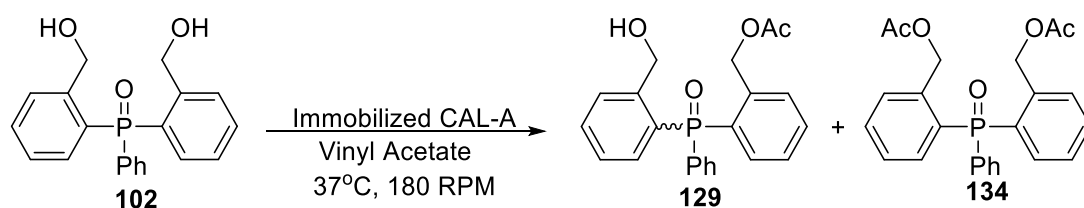


**Table 10** – Enzyme support screening for the CAL-A catalysed desymmetrization of **102**.

Support	Acetate Donor	Conversion to <b>129</b>	Conversion to <b>134</b>	e.e. ( <b>129</b> )
Eupergit CM	VA	22%	0%	75%
Purolite				
ECR8215	VA	0%	0%	0%
Epoxy				
Purolite	VA	67%	29%	<b>94%<sup>a</sup></b>
ECR8285	VA	49%	50%	<b>95%<sup>b</sup></b>
BE				

Reaction Conditions: Incubated at 37°C at 180 RPM. Total volume 1 mL, 25 mM substrate, vinyl acetate to volume, 15 mg of supported enzyme. HPLC Conditions: Daicel AD column, 1.2 mL/min, 83% Hexane/IPA at 210 nm. a) After 24 h b) After 48 h.

The Purolite butyl epoxy resin showed the greatest degree of loading at 3.4 mg/mL followed by the Purolite epoxy resin at 2.4 mg/mL and lastly, the Eupergit resin showed the lowest enzyme loading at 2 mg/mL. Of the three supports the Purolite BE performance was far superior to both Eupergit and the Purolite epoxy resin giving a conversion to **129** of 67% and e.e. of over 94% after just 24 hours (**Table 10 & Figure 13**). The Purolite butyl epoxy



reaction was left to shake for another 24 hours hour to see if any of the minor enantiomers was consumed via a double filter effect but unfortunately, this only led to an increase in e.e. of <1% but led to the consumption of 18% of mono-acetate. This shows that there is no selectivity for the second esterification between the minor and major enantiomers by CAL-A.

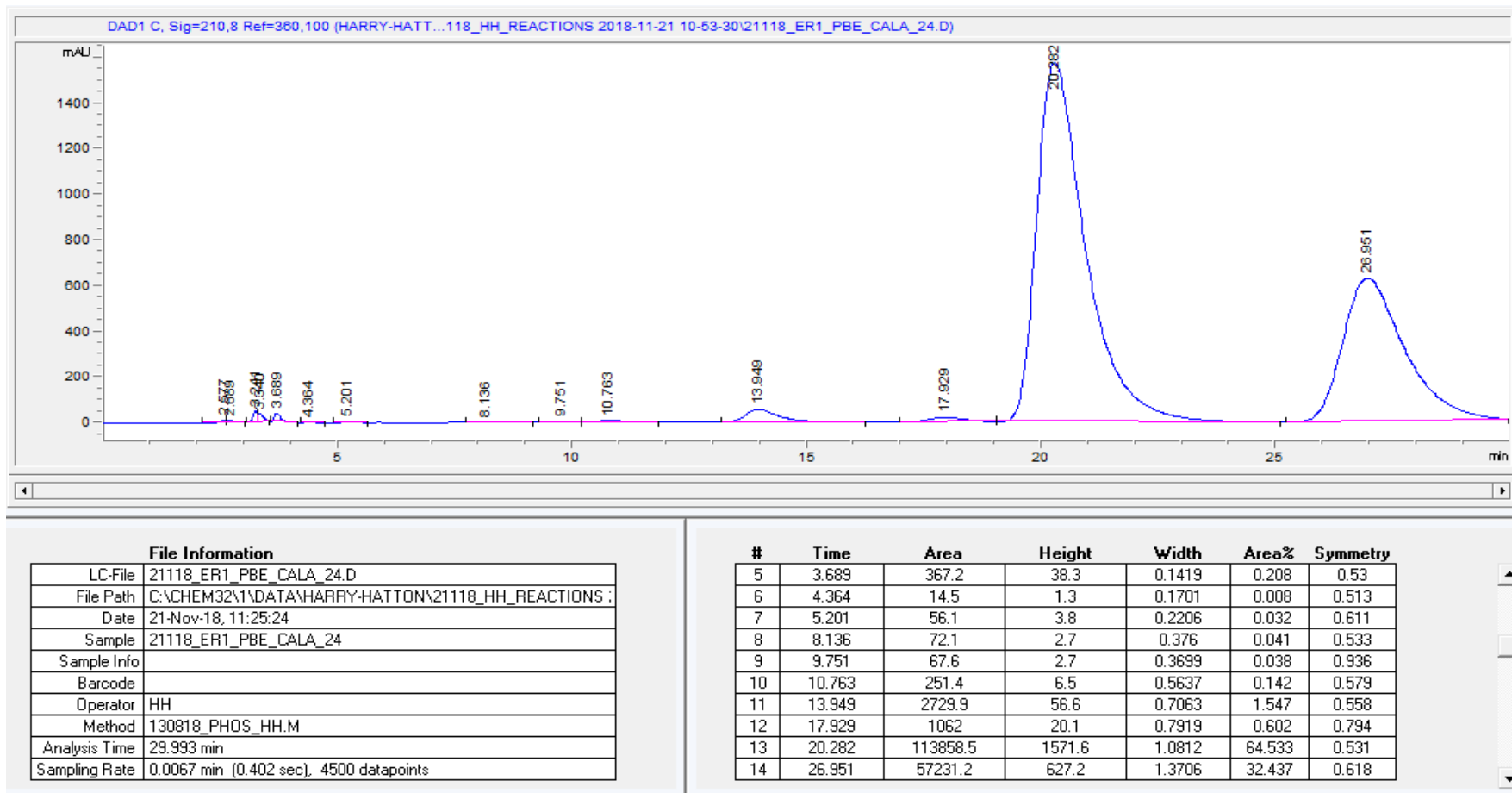


**Figure 13** - Purolite butyl epoxy immobilized CAL-A catalysed desymmetrization of **102** (17.9 min) to give **129** (13.9 min and 20.2 min) in 95% e.e and **134** (26.9 min). HPLC Conditions: Daicel AD column, 1.2 mL/min, 83% Hexane/IPA at 210 nm.

### 3.2.1 – Purolite BE immobilized CAL-A condition screen

To fully explore the reactivity of CAL-A supported on Purolite BE, we screened the range of conditions used with the Sigma Aldrich Immobead 150 CAL-A. We first tested whether VA or ISPA was superior as the solvent/donor. Purolite BE immobilized CAL-A only showed activity when vinyl acetate was used, which was surprising as both acetate donors had shown some sort of activity thus far under most conditions. We then attempted an organic solvent screen to gauge whether the Purolite BE support would show drastically different reactivity in various solvents. The same 5 solvents were used as in the previous solvent screen (with Immobead 150 CAL-A) which included a mix of polar and non-polar solvents. The reactions were attempted on a 25 mM scale along with 3 equivalents of vinyl acetate (75 mM) and were left to shake at 37°C for 18 hours. As with the previous solvent screen, activity was only seen in 2 of the solvents (**Table 11**), with vinyl acetate as both the acetate donor and solvent showing far superior activity when used alongside the Purolite BE immobilized CAL-A.

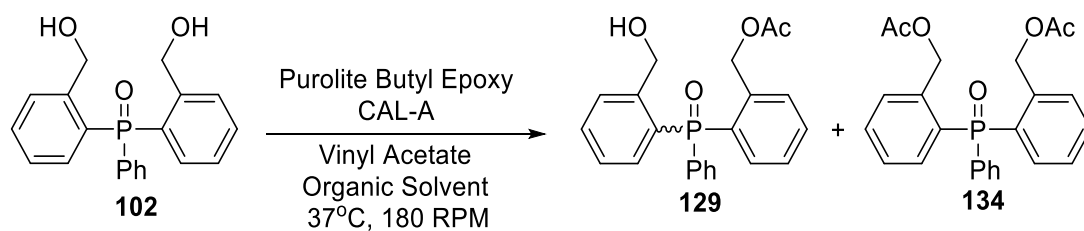


**Table 11** – Solvent screening for the Purolite BE immobilized CAL-A catalysed desymmetrization of **102**.

Solvent	Acetate Donor	Conversion to <b>129</b>	e.e. ( <b>129</b> )
EA	VA	9%	23%
DCM	VA	0%	N/A
Toluene	VA	0%	N/A
Et <sub>2</sub> O	VA	7%	15%
THF	VA	0%	N/A
VA	VA	65%	94%

Reaction Conditions: Incubated at 37°C at 180 RPM. Total volume 1 mL, organic solvent to volume, 25 mM substrate, 75 mM vinyl acetate/isopropenyl acetate, 15 mg Purolite BE CAL-A. HPLC Conditions: Daicel AD column, 1.2 mL/min, 83% Hexane/IPA at 210 nm.

Although the 3.4 mg/mL degree of immobilization of CAL-A onto the Purolite BE resin in pH 7, 0.1 M potassium phosphate buffer gave very favourable results in the desymmetrization of **95**, we attempted to load a greater amount of enzyme to see if this increased the rate of conversion and the e.e. of the reaction. Increased buffer concentration has been known to influence the amount of enzyme loaded onto the support due to the increase in ionic strength of the solution. The loading was attempted again increasing the concentration of the phosphate buffer from 0.1 M to 1 M. This led to a significantly improved loading of CAL-A at 21 mg/mL onto the Purolite BE

support. We then attempted another time course reaction over 24 hours to gauge how the increased loading of the enzyme would affect the reaction.

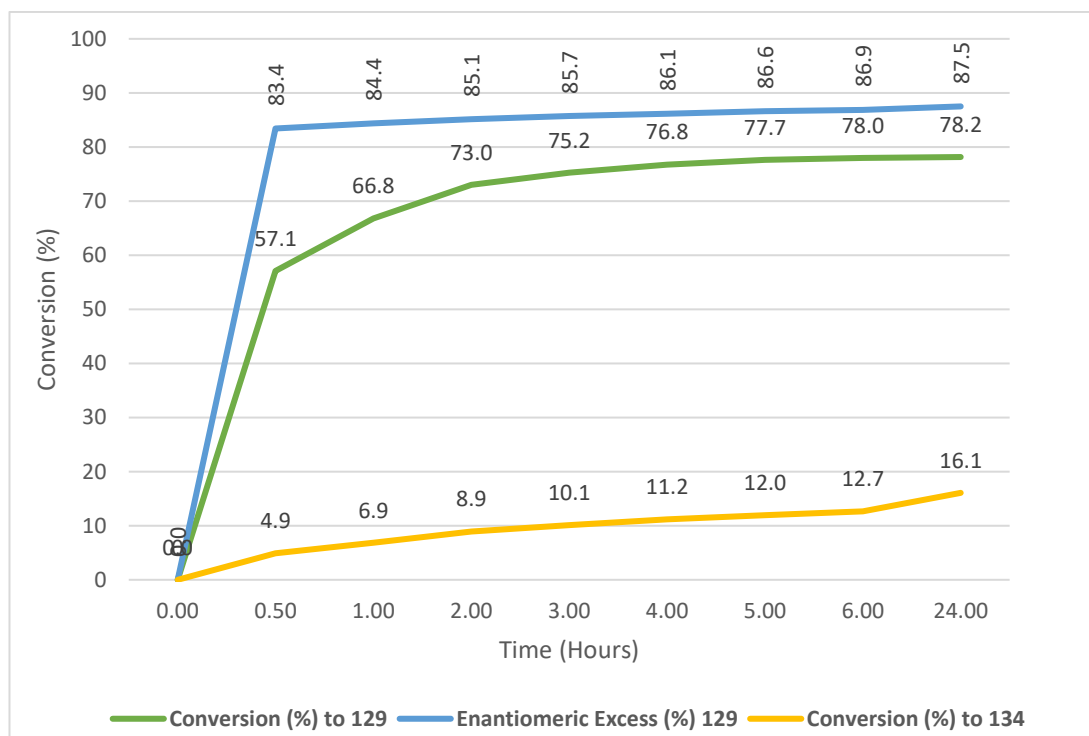


**Figure 14** – 24-hour time plot of the Purolite CAL-A immobilized lipase catalysed acetylation of **102**, with the increased degree of enzyme loading at 21 mg/mL. Reaction Conditions: Incubated at 37°C at 180 RPM for 24 hours. Total volume 1 mL, 25 mM substrate, vinyl acetate as solvent, 15 mg of Purolite BE CAL-A (21 mg/mL), 75 mM pyridine. HPLC Conditions: Daicel AD column, 1.2 mL/min, 83% Hexane/IPA at 210 nm.

As shown in **Figure 14**, the increased loading of CAL-A led to a higher rate of conversion with 60% conversion after only 0.5 hours compared to only 31.5% conversion of the lower loaded (3.4 mg/mL) enzyme support. However, the increased loading of CAL-A had a negative impact on the e.e. of the product, starting at 83% with a slow increase to the final e.e. of 87% whereas the lower

loaded support led to an e.e. of 87% which rose to a final value of just under 93%.

**Table 12** – 24-Hour time plots for the 21 mg/mL and the 3.4 mg/mL Purolite BE immobilized CAL-A catalysed acetylation of **102**.

Time (Hours)	21 mg/mL		3.4 mg/mL	
	Conversion to 129	e.e. (129)	Conversion to 129	e.e. (129)
0.5	60%	83.4%	35%	87.7%
1	72%	84.4%	42%	87.3%
2	80%	85.1%	53%	87.6%
3	84%	85.7%	61%	87.9%
4	86%	86.1%	69%	89.5%
5	88%	86.6%	75%	90.2%
6	89%	86.9%	81%	90.5%
24	93%	87.5%	93%	92.7%

Reaction Conditions: Incubated at 37°C at 180 RPM. Total volume 1 mL, 25 mM substrate, vinyl acetate to volume (1 mL), 15 mg Purolite BE CAL-A (21/3.4 mg/mL). HPLC Conditions: Daicel AD column, 1.2 mL/min, 83% Hexane/IPA at 210 nm.

### 3.2.3 – Substrate concentration with Purolite BE CAL-A

We also probed how substrate concentration affected the conversion and e.e. so, this was varied over the range of 10 mM to 100 mM. At the higher substrate concentration of 100 mM, solubility was an issue, however at all other concentrations the substrate was soluble in vinyl acetate. The reactions were

shaken at 37°C for 18 hours and analysed by chiral HPLC, the results of which are shown in **Table 13**.

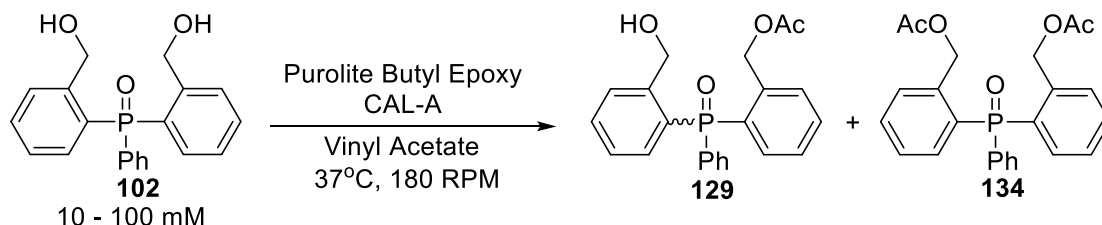


**Table 13** – Effect of substrate concentration on the Purolite BE immobilized CAL-A catalysed desymmetrization of **102**.

Concentration of Substrate ( <b>102</b> )	Conversion to <b>129</b>	Conversion to <b>134</b>	e.e. ( <b>129</b> )
10 mM	86%	11%	85%
25 mM	79%	16%	88%
50 mM	82%	11%	87%
100 mM	75%	4%	81%

Reaction Conditions: Incubated at 37°C at 180 RPM. Total volume 1 mL, 10-100 mM substrate, vinyl acetate to volume, 15 mg Purolite BE CAL-A. HPLC Conditions: Daicel AD column, 1.2 mL/min, 83% Hexane/IPA at 210 nm.

Whilst 25 mM substrate concentration did not give the greatest conversion to **108**, it gave the best e.e. by a small margin. However, it seems that substrate concentration does not have a great effect on either the activity or the enantioselectivity of the enzyme.

### 3.2.4 – Water concentration screen with Purolite BE CAL-A

At this point in the project, a larger batch of CAL-A was purchased to allow for scaling up of the reaction. Unfortunately, this batch showed slightly less

enantioselectivity than that of the previous batch. When the reaction was attempted with the new batch using the same conditions previously tested, this led to a lower e.e. of 90%, instead of the previously obtained e.e. of 95%.

We attempted to remedy the loss of selectivity through the controlled addition of water to the enzyme support as previously published work<sup>[123]</sup> within the group and elsewhere has also shown that the degree of water still present within the enzyme support can have a remarkable effect on the activity and selectivity.<sup>[125-128]</sup> The residual water is bound to the enzyme allowing it to maintain its essential surface water tension and active conformation which is key for the retention of activity. In order to ensure that no water was present in the Purolite BE immobilized CAL-A, it was dried under vacuum until it was a free-flowing solid. Varying concentrations of water from 25 mM to 125 mM was then added back into the reaction, plus one reaction where the support was saturated with water and one reaction where it was fully dried. The reaction was attempted under previous conditions with 25 mM substrate and vinyl acetate as both the acyl donor and solvent. Due to the addition of water to the reaction, hydrolysis of vinyl acetate to release acetic acid could potentially be an issue and therefore to mitigate this risk, 25 mM sodium bicarbonate was added, as opposed to pyridine which was previously used, due to it being less damaging to the protein. The reactions were left to stir at 37°C for 24 hours after which an aliquot was taken from each and analysed by chiral HPLC (**Table 14**). Interestingly, on the 1 mL scale reactions only a small percentage (<5%) of the spirophosphorane was observed meaning that the sodium bicarbonate was neutralizing any acid product.



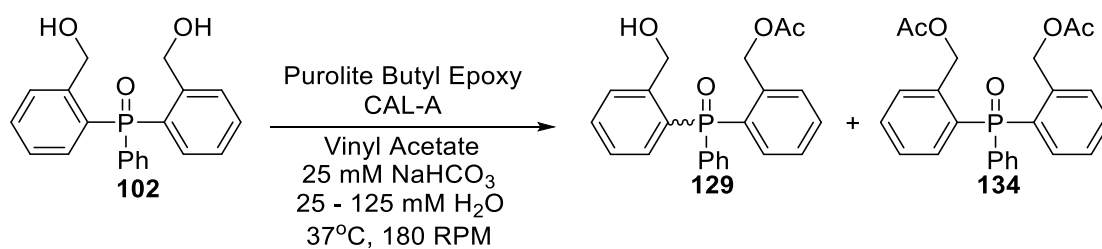


**Table 14** – Effect of water concentration in the Purolite BE immobilized CAL-A catalysed desymmetrization of **102**.

Concentration of water	Solvent	Conversion to <b>129</b>	Conversion to <b>134</b>	e.e. ( <b>129</b> )
25 mM	VA	46%	6%	81%
50 mM	VA	66%	11%	84%
75 mM	VA	75%	11%	84%
100 mM	VA	71%	16%	87%
125 mM	VA	73%	14%	86%
Saturated	VA	17%	3%	54%
Dried	VA	52%	3%	76%

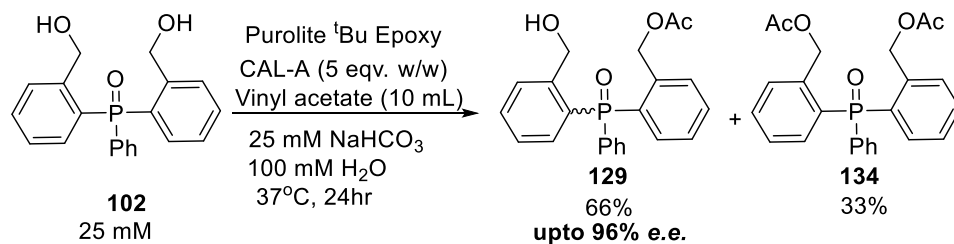
Reaction Conditions: Incubated at 37°C at 180 RPM. Total volume 1 mL, 25 mM substrate, vinyl acetate to volume, 25 – 125 mM H<sub>2</sub>O, 15 mg Purolite BE CAL-A, 25 mM NaHCO<sub>3</sub>. HPLC Conditions: Daicel AD column, 1.2 mL/min, 83% Hexane/IPA at 210 nm.

It was shown that between 50 mM and 125 mM of water the outcome of the reaction was largely similar. However, the use of the saturated support drastically reduced the conversion and e.e. of the reaction which is most likely due to the repulsion of the lipophilic substrate. Although the addition of 100 mM of water seemed to improve the reaction outcome slightly, we found the large loss in enantioselectivity could be remedied through the addition of three times as much immobilized CAL-A than used previously. These conditions

when combined on a small scale, 1 mL reaction again gave high conversion and an e.e. of just under 96%. Fortunately, the immobilized enzyme could be reused in multiple reactions before a loss in activity is observed meaning that the increased addition of immobilized enzyme was not detrimental to the throughput of the chiral material.

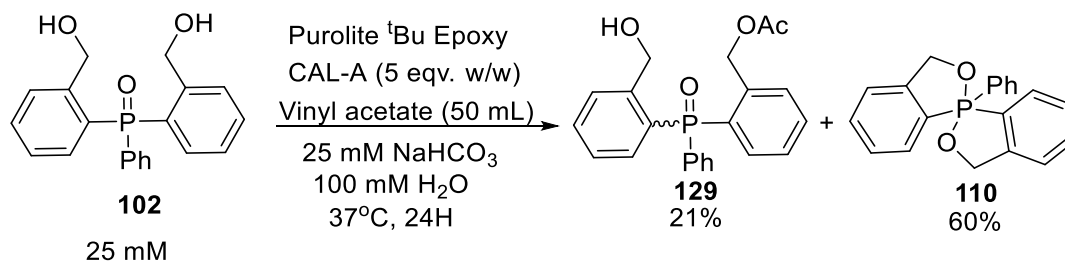
### **3.2.5 – Purolite CAL-A scale up reaction**

We then attempted to scale up to a 10 mL reaction volume (**Scheme 56**), using all of the combined conditions which gave the best results which included 25 mM substrate, 25 mM sodium carbonate, 100 mM water, 5 equivalents w/w of Purolite BE immobilized CAL-A compared to the substrate, with vinyl acetate as solvent. The 10 mL reaction was shaken at 37°C for 24 hours after which an aliquot was taken for chiral HPLC analysis which showed that all starting material had been consumed and that the mono-acetate and bis-acetate were present in a 2:1 ratio and that the e.e. of the mono-acetate was at 95%. The reaction was worked up, the mono-acetate and bis-acetate were columned as a single spot due to their identical R.F. and analysed by <sup>1</sup>H NMR and <sup>31</sup>P NMR both of which confirmed the presence of the mono-acetate and bis-acetate in a 2:1 ratio which validated our previous HPLC analysis.



**Scheme 56** – 10 mL scale reaction for the Purolite immobilized CAL-A catalysed desymmetrization of **102**.

We then attempted to increase the scale of the reaction again, up to 50 mL, which led to a very different outcome compared to the smaller scale reactions. The 50 mL reaction gave the spirophosphorane **110** was present in 60% conversion after 24 hours with only 21% of **129** (**Scheme 57**). The addition of water on the larger scale may have caused a greater amount of hydrolysis of the vinyl acetate which in turn would release a larger amount of acetic acid which the 25 mM of sodium bicarbonate could not negate.



**Scheme 57** – 50 mL scale purolite immobilized CAL-A catalysed desymmetrization which led to a large amount of **110** due to the acidic promoted cyclization of **102**.

We then attempted the reaction on this scale again but increased the concentration of sodium bicarbonate to 125 mM so that it was in excess of the

100 mM water which may cause the hydrolysis. The reaction was then left to stir at 37°C for 24 hours and an aliquot was taken which was then analysed by chiral HPLC. Even with excess sodium bicarbonate (125 mM), the reaction had still largely formed the spirophosphorane **110** due to the release of acetic acid. In order to find conditions which would prevent the cyclisation of **102** on the 50 mL scale reactions, we screened several different organic and inorganic bases, alongside 25 mM of substrate **95** and 100 mM of water in vinyl acetate as the solvent. These bases included pyridine (which had been used prior but not on a large scale), triethylamine, sodium carbonate, sodium acetate and di-basic potassium phosphate buffer. We also included a control reaction which contained no base and another reaction in which water was omitted from the reaction. The reactions were shaken at 37°C for 18 hours and an aliquot taken from each reaction and analysed by chiral HPLC (**Table 15**).

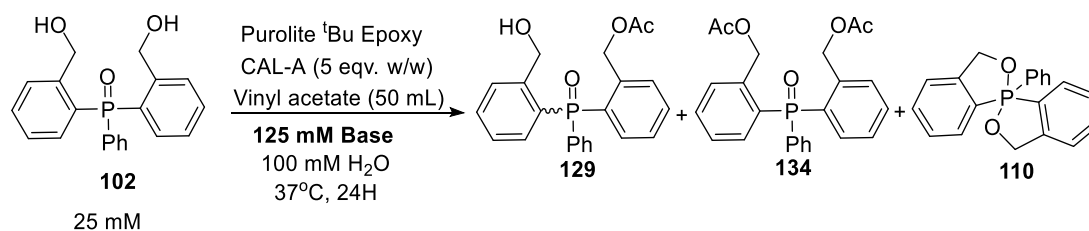


**Table 15** – Base screen for the prevention of spirophosphorane formation.

Base	Conversion to 129	Conversion to 134	Conversion to 110	e.e. (129)
Pyridine	43%	0%	44%	80%
Triethyl amine	60%	4%	16%	81%
Sodium Carbonate	66%	5%	2%	80%
Sodium Acetate	41%	0%	32%	67%
No base	35%	0%	66%	80%

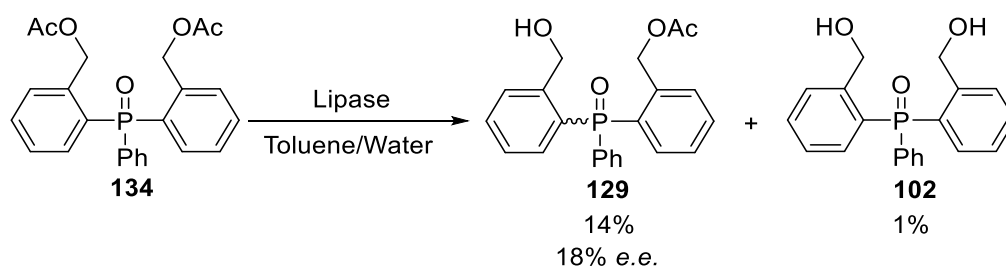
Reaction Conditions: Incubated at 37°C at 180 RPM. Total volume 50 mL, 25 mM substrate, vinyl acetate to volume, 100 mM H<sub>2</sub>O, 2.5 g enzyme support. HPLC Conditions: Daicel AD column, 1.2 mL/min, 83% Hexane/IPA at 210 nm.

Most of the bases did not prevent the formation of the spirophosphorane **110** on the larger-scale reactions however, sodium carbonate did seem to give the lowest levels of **110** whilst retaining reasonable activity. We hypothesised that a lower concentration of water would be needed to retain activity and lessen the formation of the spirophosphorane on these larger scale reactions. As shown by **Table 14**, 50 mM of water gave similar results to 75 mM, and therefore a 50 mM concentration of water would give better results on the larger scale reaction and so these conditions were used to produce any chiral material on a larger scale. Unfortunately, using these conditions on larger-scale reactions, the e.e. was shown to be slightly lower than the smaller scale

reactions (10 mL) which could most likely be attributed to the poor mixing ability of a shaker compared to other mixing methods. This could be remedied using some other mixing techniques such as a spin reactor which allows for the increased mixing of solutions without the destruction of the enzyme support.

### **3.3 – Lipase-catalysed hydrolytic desymmetrization reactions**

To access the opposite enantiomer to that of the esterification, we also attempted the reverse, hydrolysis reaction as the singular hydrolysis of the corresponding bis acetate should allow us to produce the opposite enantiomer of **129**. We synthesised **134** using 2 equivalents of acetyl chloride in DCM with the base, triethylamine and set up several conditions which have been shown in the literature to be used for the lipase catalysed hydrolysis of esters.<sup>[114, 129-131]</sup> These conditions usually require a solvent which can be saturated with water or the use of biphasic systems which circumvent any issues of solubility which may arise with the inclusion of water, which could prove problematic due to the lipophilicity of our phosphine oxide. Initially we employed a biphasic system with toluene as the organic layer in which the substrate would be soluble and then a water layer to allow for hydrolysis to occur. The reaction was stirred vigorously to allow a mixture of the two layers and was left for 24 hours at 37°C using the lipase, Immobead 150 CAL-A, and was followed by chiral HPLC.



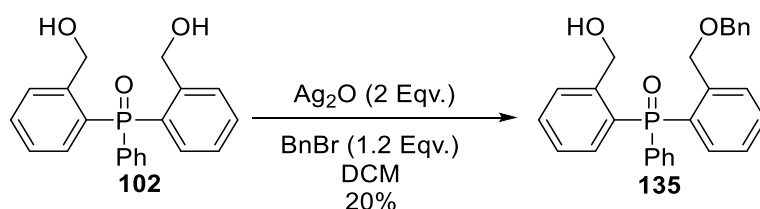
**Scheme 58** – Lipase catalysed hydrolysis of **134**, with a biphasic toluene/water solvent system.

The enzymatic hydrolysis (**Scheme 58**) showed some activity towards the bis-acetate **134** albeit low, with only 14% conversion to **129** over 24 hours with an e.e. of 18%, the double hydrolysed product diol **102** was also present in 1%. Although the ability to access the opposite enantiomer by means of hydrolysis would be useful, our synthetic approach (explained later), meant that this was not the only means by which we could access the opposite enantiomer and so the hydrolytic desymmetrization was not pursued further.

### 3.4 – Kinetic resolution of derivatives of **102**

In addition to the desymmetrization reactions, we hypothesised that the kinetic resolution of a related benzyl containing compound could be beneficial as this would give us both enantiomers in the form of the resulting acetate and the unreacted enantiomeric alcohol. Kinetic resolutions are often employed in synthesis, usually favoured over desymmetrization reactions due to the difficulty in preparing pro-chiral substrates. We knew that the benzyl ether group would be stable to any enzymatic conditions but would also provide a large amount of steric bulk which may aid in the enzymatic kinetic resolution.

Therefore, benzyl bromide was added to **95** in 1.2 equivalents along with 2 equivalents of silver oxide in DCM (**Scheme 59**). The reaction was monitored by TLC to show the formation of the mono-benzylated product. Only small amounts would be needed for screening, so we stopped the reaction after 5 hours and purified the mono-benzylated product **135** in 20% yield.



**Scheme 59** – Synthesis of racemic **135** which can be used for the lipase catalysed kinetic resolution.

For the kinetic resolution reaction of **135**, we used the Purolite BE immobilized CAL-A which gave us the most favourable reactivity for the previous desymmetrization reactions. The substrate **135** was used at 25 mM concentration along with 1.5 equivalents of vinyl acetate (37.5 mM) as the acetate donor. The reaction was then made up to 1 mL with 5 different organic solvents, shown in **Table 16**, and then shaken at 37°C and monitored by chiral HPLC.



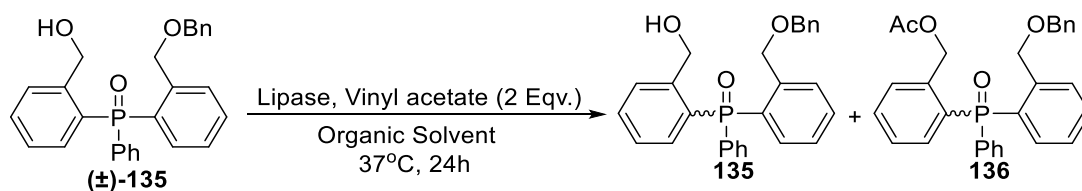


**Table 16** – CAL-A catalysed kinetic resolution of **135** in different organic solvents.

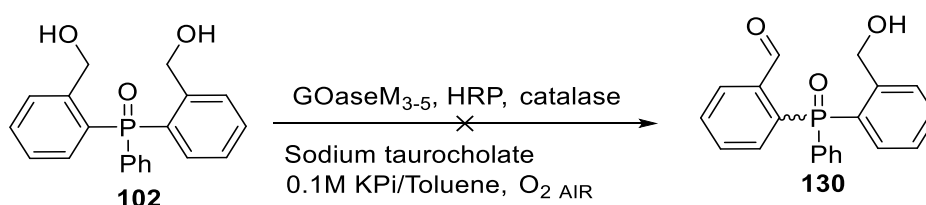
Solvent	Yield of <b>135</b>	e.e. of <b>135</b>	Yield of <b>136</b>	e.e. of <b>136</b>
VA	76%	28%	23%	88%
DCM	100%	0%	0%	0%
Et <sub>2</sub> O	56%	32%	23%	43%
THF	100%	0%	0%	0%
EA	96%	2%	4%	88%
Toluene	95%	5%	4%	86%

Reaction Conditions: Incubated at 37°C at 180 RPM. Total volume 1 mL, 25 mM substrate, vinyl acetate 37.5 mM, 20 mg Purolite BE CAL-A, organic solvent to volume. HPLC Conditions: Daicel AD column, 1.2 mL/min, 83% Hexane/IPA at 210 nm.

Only significant activity was seen in either VA or Et<sub>2</sub>O but in both the cases the selectivity was not as high as the desymmetrization reactions. Only small amounts of product (<5%) was seen in both ethyl acetate and toluene after 24 hours and no activity was observed in THF and DCM. Although it would be beneficial to have access to both enantiomers via this method, the lower e.e. observed and the poor activity means this enzymatic reaction was not implemented to produce chiral material.

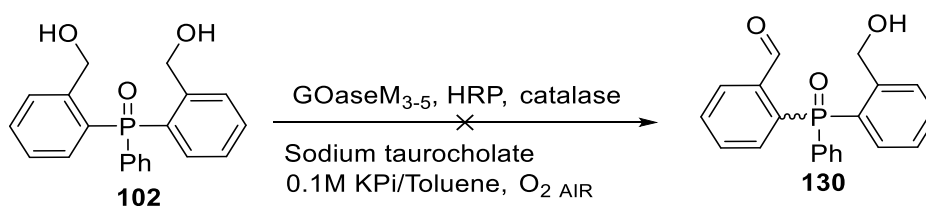
### 3.5 – Alcohol oxidase catalysed desymmetrization and kinetic resolution reactions

Together with the lipase-catalysed reactions, the pro-chiral phosphine oxide **102** could potentially be a substrate for an alcohol oxidase which would give rise to an aldehyde derivative **123** (**Scheme 59**). One alcohol oxidase which has been used extensively in these types in transformation is a mutant of Galactose oxidase, GOaseM<sub>3-5</sub>. GOaseM<sub>3-5</sub> is a copper-based enzyme which uses molecular oxygen to catalyse the oxidation of alcohols. This enzyme has been used to catalyse the oxidation of alcohols in aqueous conditions or in combination with either DMSO or CH<sub>3</sub>CN (up to 30%, as a co-solvent) to aid in solubilising lipophilic substrates.<sup>[132-134]</sup> Initial attempts at the oxidation of **102** involved GOaseM<sub>3-5</sub> in 0.1 M potassium phosphate buffer with the 30% DMSO co-solvent along with the enzyme catalase (**Scheme 60**), which catalyses the breakdown of any hydrogen peroxide formed as a by-product from the oxidation. Even with the 30% DMSO co-solvent, **102** still showed poor solubility in these conditions and so even after 24 hours of reaction, no aldehyde product was observed by <sup>1</sup>H NMR.



**Scheme 60** – Failed attempt at the GOase<sub>m3-5</sub> catalysed desymmetrization of **102**.

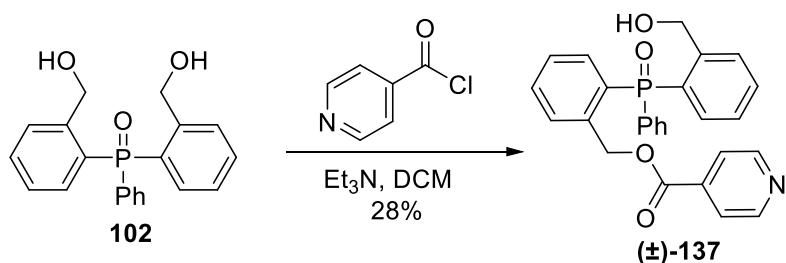
To circumvent the issue of insolubility of the substrate in the aqueous system, the enzymatic reaction was attempted using an organic-aqueous, bi-phasic system, a method often utilized in enzymatic catalysis to avoid solubility issues.<sup>[135,136]</sup> Diol **102** was then dissolved in toluene and added to the reaction along with sodium taurocholate to aid formation of an emulsion to give sufficient mixing between the organic and aqueous phase.<sup>[137]</sup> The reaction, shown in **Scheme 61**, was then shaken at 37°C for 24 hours after which the toluene was removed and the residue analysed by <sup>1</sup>H NMR to see if an aldehyde peak was present. However, no product was seen under these conditions.



**Scheme 61** – Failed GOase oxidation of **102** to give **130** in a biphasic toluene/buffer solvent system.

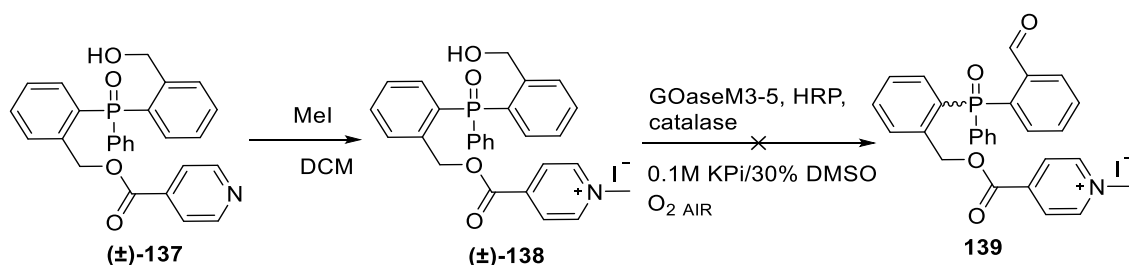
With this in mind, we hypothesised that the addition of a solubilizing group on one of the -OH groups would allow us to increase the solubility whilst still retaining the ability to undergo an enantioselective transformation albeit to a kinetic resolution. The addition of a nicotinic acid group would give us the ability to synthesise a quaternary salt which would drastically improve the solubility of the phosphine oxide in the aqueous media needed for the reaction. To achieve this, the diol was reacted with 1 equivalent of isonicotinoyl chloride, which was chosen so that the nitrogen was *-para* to into the ring, and this

proceeded in 28% yield (**Scheme 62**). The modest yield was expected due to the formation of both the bis-ester and the monoester with only 1 equivalent of the acid chloride.



**Scheme 62** – Addition of the isonicotinamide ester to **95** to give the isonicotinamide derivative ( $\pm$ )-**137**.

To form the quaternary salt, **137** was then reacted with 1 equivalent of methyl iodide in DCM, which caused the iodide salt to crash out of solution which could be filtered off from the reaction.  $^1\text{H}$  NMR showed slight degradation of the product and so it was subjected to the GOaseM<sub>3-5</sub> reaction immediately to minimise loss of product. However, even after 24 hours, no aldehyde peak was seen by  $^1\text{H}$  NMR analysis (**Scheme 63**).



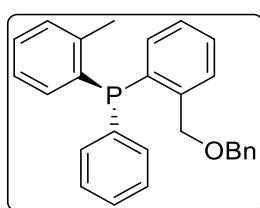
**Scheme 63** – Failed GOase<sub>m3-5</sub> catalysed oxidation of ( $\pm$ )-**138**.

### 3.6 – Conclusion

In summary, the formation of P-chiral phosphine oxides was best achieved through the desymmetrization of **102**, catalysed by Purolite BE immobilized CAL-A (5 eqv. w/w) at 37°C, with 25 mM substrate, 50 mM water, 125 mM sodium carbonate and vinyl acetate as solvent. Although this reaction could be scaled to a volume of 50 mL, this led to a slight decrease in e.e. of the mono-acetate product **129** due to the poor mixing of the larger reaction volume and the immobilized enzyme. However, smaller scale 10 mL reactions gave high selectivity (upto 96% e.e.) whilst retaining good conversion to **129** with minimal spirophosphorane **110** formation. In addition, the kinetic resolution of derivatives of **102** gave good selectivity for the acetate ester **134** (upto 88%) however, conversion to the acylated products was poor (<25%). Both the lipase-catalysed hydrolysis reactions and GOaseM<sub>3-5</sub> reactions which required aqueous conditions proved to be difficult due to the solubility of the lipophilic substrates, which not even the use of biphasic systems or co-solvents could remedy. Future work could be done to improve both the desymmetrization and kinetic resolution selectivity and conversion.

## 4 – Synthetic route to ‘ligand’ Structures

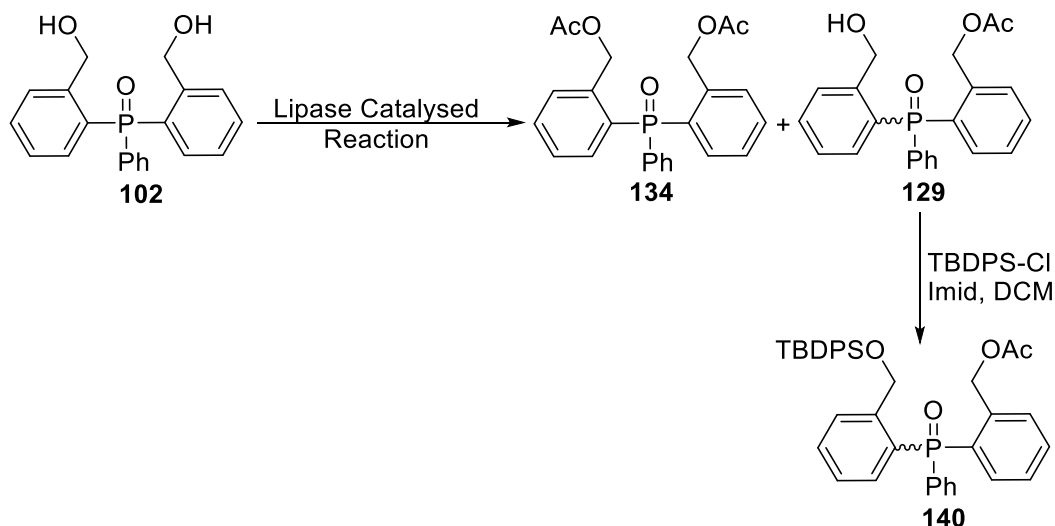
Now that we had an established chemo-enzymatic route to the chiral phosphine oxide **129** with an *e.e.* upwards of 95% we began the synthetic route to target compounds which resembled a ligand like structure. We hypothesised that a suitable ligand structure would resemble the structure shown in **Figure 15**.



Potential Ligand Structure

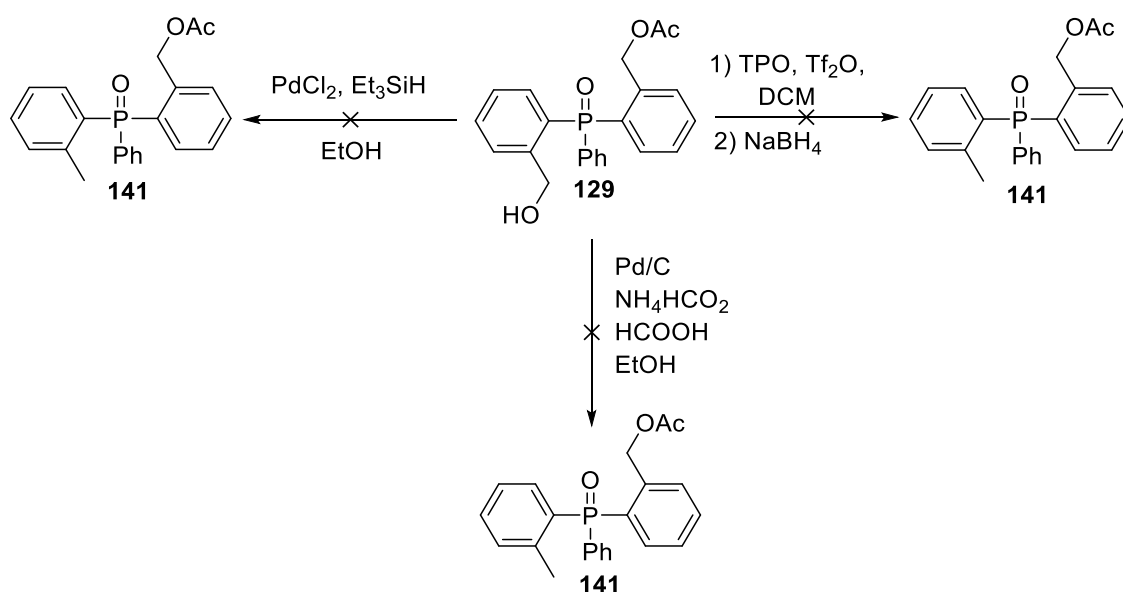
**Figure 15** – *Potential ligand structure for the copper-catalysed asymmetric 1,6-boration reactions*

Separation of **129** from the by-products of the enzymatic reactions was particularly difficult due to the oddly similar R.F. of the bis-acetate **134** as well as any unreacted starting material. Therefore, to facilitate separation by TLC and column chromatography, the reaction mixture was silyl protected *in-situ* to give mono-acetate **140** (**Scheme 64**), which now could be separated from the by-products due to its vastly different polarity.



**Scheme 64** – Silylation of **129** to give **140** which facilitated separation of the products by column chromatography.

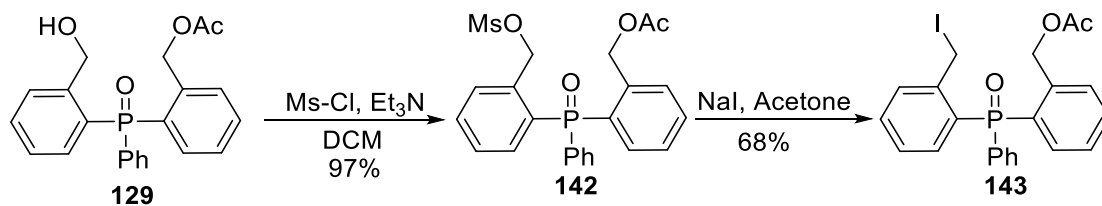
Elaboration of phosphine oxide **140** would require deoxygenation of one of the benzylic alcohol groups to form a tolyl substituent followed by formation of a benzyl ether from the remaining benzyl alcohol. As the product of enzymatic desymmetrization was the mono-acetate, the deoxygenation of the free benzylic alcohol was attempted using several different methods. The deoxygenation of the benzylic alcohol has been completed on similar structures in the literature but required 3 steps overall and caused considerable loss of yield.<sup>[102]</sup> With this in mind, we attempted the deoxygenation in a single step which has also been demonstrated previously on a variety of structures containing benzylic alcohols. Three different reactions were attempted, all of which are shown in **Scheme 65**. These included the formation of an activated phosphoether bond which would be subsequently cleaved by  $\text{NaBH}_4$  and two different palladium catalysed reactions which used either triethyl silane or formic acid as the hydride source. However, all three reactions were unsuccessful.



**Scheme 65** – Attempted one-pot reactions for the reductive cleavage of the hydroxyl group from **129** to yield an ortho-tolyl group.

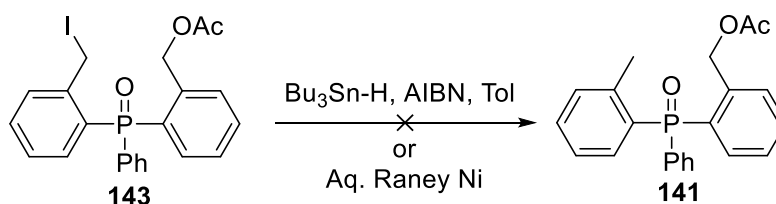
Due to the lack of deoxygenation in a single reaction, the 3 step route mentioned above and described by Kaczmarczyk *et al.*<sup>[102]</sup> was attempted in which the alcohol **129** was mesylated prior to the iodination and reductive halogenation. The reaction proceeded in almost complete conversion to give product **142**, with only minor chlorinated product and this was used without purification as it showed large amounts of degradation when purified by column chromatography. Displacement of the mesylate with iodide was accomplished using sodium iodide in acetone in a Finkelstein-type reaction and proceeded in 68% yield to give the benzylic iodide **143** as a yellow solid (**Scheme 66**).<sup>[138,139]</sup>





**Scheme 66** – Formation of the benzylic iodide **143**.

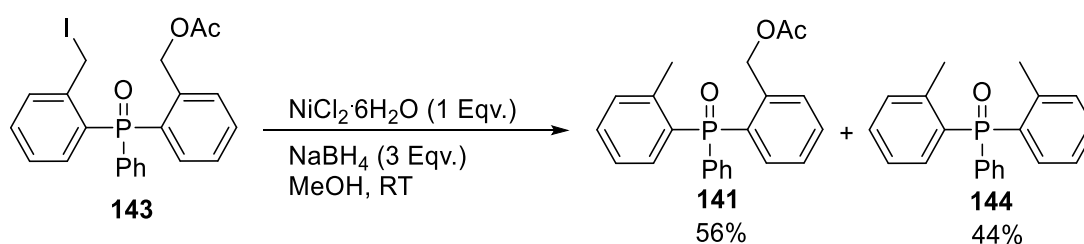
The benzylic iodide was then reacted with tributyltin hydride with AIBN for the reductive cleavage (**scheme 67**).<sup>[140]</sup> The reaction was left to reflux for 24 hours in anhydrous toluene after which TLC indicated that all starting material had been consumed. Crude analysis by  $^1\text{H}$  NMR showed several new peaks. However, none of these equated to the formation of a  $-\text{CH}_3$  group. The lack of success may be due to the AIBN being wet.



**Scheme 67** – The failed, radical reduction and reductive cleavage of the benzylic iodide derivative **143**.

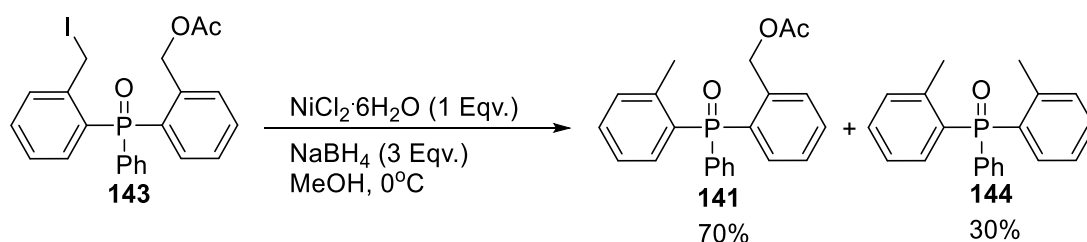
Nickel-based reductants have also been used for the reductive cleavage of benzylic halides, and specifically to displace benzylic iodides.<sup>[106-108]</sup> Both aqueous Raney Ni and nickel borohydride, which was synthesised *in-situ* from nickel (II) chloride hexahydrate and sodium borohydride, have shown efficacy for this transformation.<sup>[141-143]</sup> Both reagents were therefore tested and gave very different reactivities towards the phosphine oxide **143**. Unfortunately, Raney nickel showed no reactivity towards the C-I bond and only starting

material was recovered (**Scheme 67**). The use of nickel (II) chloride and sodium borohydride gave two products, the first of which was the product **141**, which stemmed from the expected cleavage of the C-I bond and was present in 56% yield. The second product, **144**, showed the cleavage of the benzylic iodide but also cleavage of the benzylic acetate ester leading to the bis-tolyl phenyl phosphine oxide (**Scheme 68**). This reactivity towards the benzylic ester was surprising, however. Previous literature has shown that these conditions have been applied to the cleavage of benzyl acetates previously and had good selectivity towards benzyl acetate esters.<sup>[143]</sup>



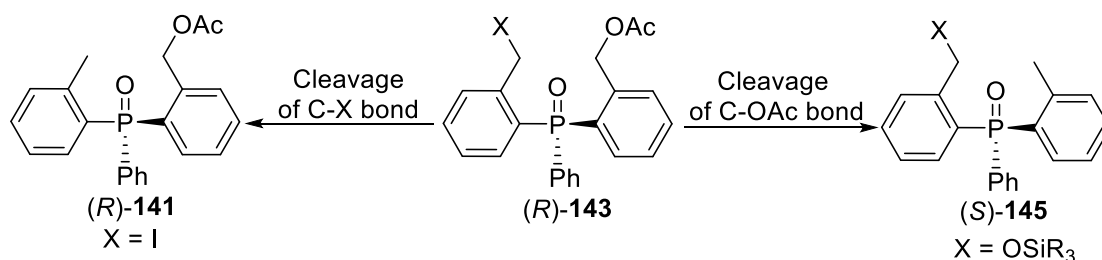
**Scheme 68** – Cleavage of the benzylic iodide and acetate ester through the addition of nickel chloride and sodium borohydride at room temperature.

The percentage of the acetate ester cleavage could be suppressed further through a reduction in temperature. When the reaction was attempted at  $0^\circ\text{C}$ , improved selectivity was obtained with compound **141** obtained in 70% yield (**Scheme 69**).



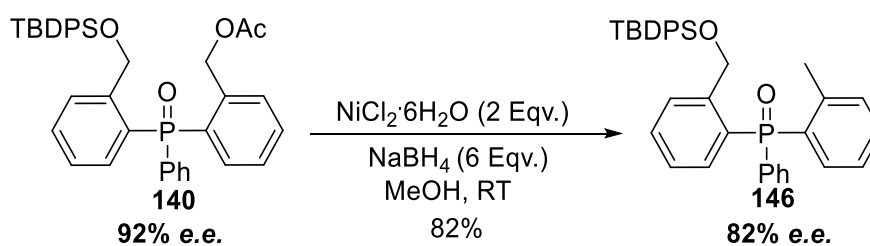
**Scheme 69** - Cleavage of the benzylic iodide and acetate ester of **143** through the addition of nickel chloride and sodium borohydride at  $0^\circ\text{C}$ .

Due to the reactivity towards the benzylic ester using nickel boride, we hypothesised that we could achieve the same reductive cleavage on the acetate ester without the requirement of the formation of the benzylic iodide. As described previously, the product of the enzymatic reaction needed the addition of the -TBDPS group to aid in separation by column chromatography, we hypothesised that this silyl protected product would be better suited to the deoxygenation and would not require the 2 steps needed to form the benzylic iodide. This would decrease the steps needed and the loss in yield to form the benzylic iodide, this route would also give us access to the opposite enantiomer the approach shown in **Scheme 70**.



**Scheme 70** – Potential synthetic approach for the formation of both the (S)- and (R)- configured ligands **(R)-141** and **(S)-145**.

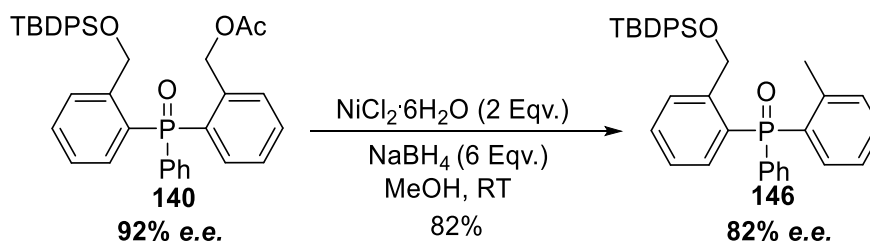
The nickel boride reaction on **140** was attempted under identical conditions to before and followed by TLC which indicated that the reaction went smoothly to one product (**Scheme 71**). However, multiple aliquots of NaBH<sub>4</sub> were needed throughout the reaction which could be due to the lower reactivity of the benzylic ester cleavage compared to the benzylic iodide. However, the product was still formed in 82% yield. The slight loss in yield seemed to be due to poor mass recovery during the working up. The reaction was filtered through a pad of celite and despite multiple organic washes, the yield did not seem to improve beyond that described. The product was characterised through <sup>31</sup>P NMR, <sup>1</sup>H NMR and <sup>13</sup>C NMR showing a singular phosphorus shift at δ 33.28, a relatively simple <sup>1</sup>H NMR with the 9 protons of the silyl –<sup>t</sup>Butyl group, the –CH<sub>3</sub> of the newly formed methyl group at δ 2.4, which is in agreement with similar phosphine oxide tolyl shifts, and finally the diastereotopic –CH<sub>2</sub> adjacent to the silyl ether at δ 4.99 with the 23 aromatic protons .



**Scheme 71** – Cleavage of the acetate ester through the addition of nickel chloride and sodium borohydride which led to a slight loss in e.e.

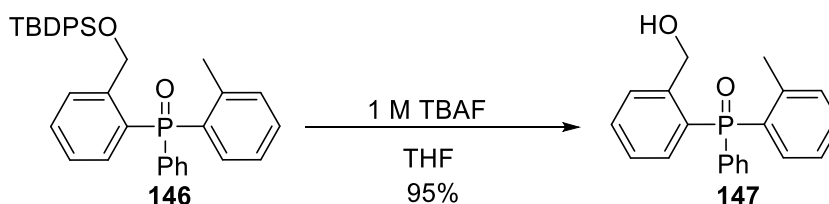
Unfortunately, the cleavage of the benzylic ester also led to a slight reduction of e.e. (approximately 10%) which is most likely due to the possible stereo-mutation of the phosphine oxide which could occur through the reduction of the phosphine oxide and subsequent oxidation of the phosphorus centre.

Therefore, to limit any potential reduction and loss of e.e. the reaction was attempted at two lower temperatures of 0°C (**Scheme 72**) and -20°C. Both conditions showed no loss of e.e. when compound **146** was analysed by chiral HPLC. This 0°C was the preferred reaction temperature.



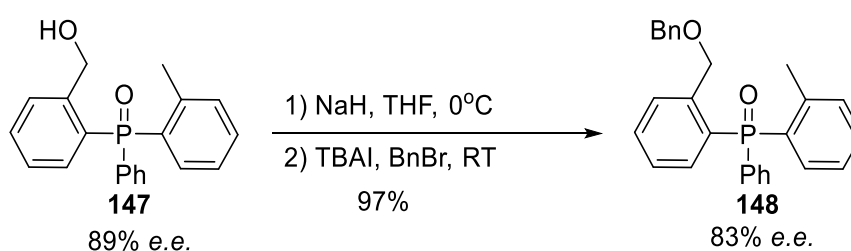
**Scheme 72** – Cleavage of the acetate ester through the addition of nickel chloride and sodium borohydride at 0°C which showed no observable loss in e.e.

The silyl group was then removed by tetrabutylammonium fluoride (TBAF) in THF to give the alcohol **147** in high yield (**Scheme 73**), which could potentially be used as a ligand once reduced to the corresponding phosphine. We hypothesised that a benzyl ether would provide increased steric bulk at the *ortho*- position but may also prevent the possible binding and reduce the reactivity of the ligand structure.



**Scheme 73** – Removal of the TBDPS- ether using 1.5 equivalents of tetrabutylammonium fluoride in THF.

The alcohol **147** was also one of the few chiral molecules during the synthesis of the chiral ligand which was crystalline. We thought this product would be a suitable candidate for recrystallisation to increase the e.e. and to potentially obtain crystal structure so that the absolute configuration of the phosphorus centre could be assigned. Several different solvent combinations were tested to recrystallize **147**, with a mixture of diethyl ether and hexane initially giving crystals of low quality. These first attempts did slightly increase the e.e. (+2-3% e.e.) of the phosphine oxide but as we had yet to reduce the phosphine oxide to the phosphine it seemed wasteful to lose any potential yield to purification prior to the reduction which would most likely cause a further loss in the e.e. of the chiral material. The protection of the hydroxyl was achieved through the formation of the benzyl ether. The hydroxyl was deprotonated with sodium hydride at 0°C and then a slight excess of benzyl bromide was added along with a catalytic amount of tetrabutylammonium iodide (TBAI) which forms the more active benzyl iodide, *in-situ*.<sup>[144]</sup>



**Scheme 74** – Benzylation of **147** using sodium hydride, TBAI and benzyl bromide in THF.

The reaction proceeded smoothly to the benzylated product in 97% yield but did lead to the loss of 6% of the e.e. of the phosphine oxide, which was unexpected (**Scheme 74**). The benzyl ether product was characterised

through NMR in which the  $^1\text{H}$  NMR showed the  $-\text{CH}_3$  at  $\delta$  2.49, two benzyl  $-\text{CH}_2$  groups at  $\delta$  4.39 and 4.97 and then 18 aromatic protons (**Figure 16**).

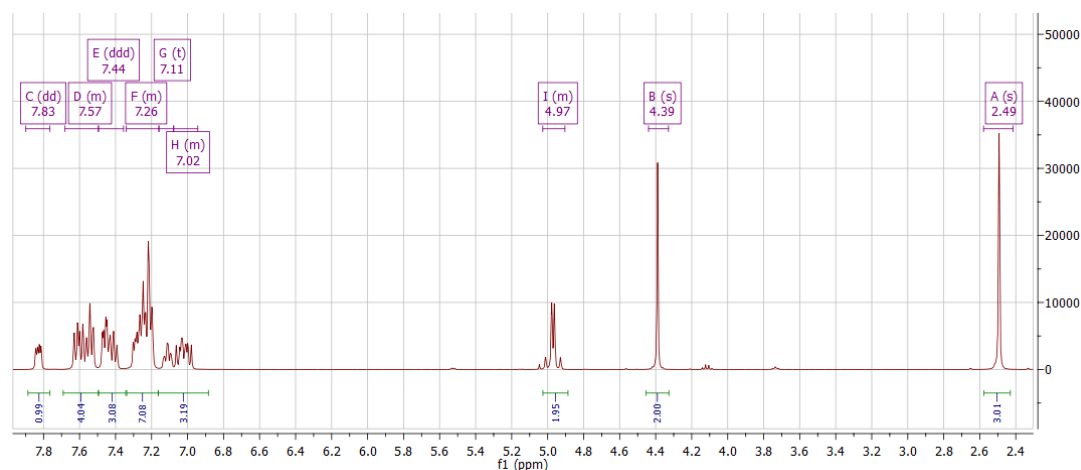
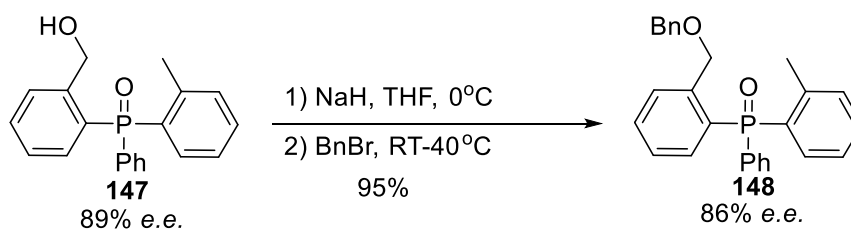


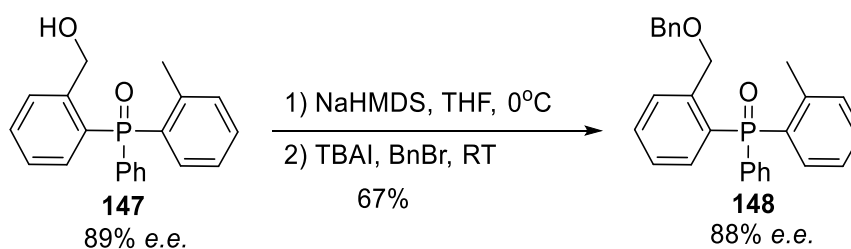
**Figure 16** –  $^1\text{H}$  NMR of benzyl ether **148**.

A literature search revealed that the addition of sodium hydride alongside a source of iodine can lead to the de-arylation of phosphine oxides which could explain the potential loss of *e.e.* using this method of benzylation. The loss of *e.e.* was decreased to only 3% when TBAI was omitted from the reaction (**Scheme 75**), highlighting the possible dearylation mechanism described by Tejo *et al.* as a potential pathway for the *e.e.* decreasing under these conditions.<sup>[145]</sup> However, the omission of TBAI also had a drastic effect on the rate of the reaction although this could be rescued through an increase in the temperature of the reaction.



**Scheme 75** – Benzylation of **147** using sodium hydride and benzyl bromide without TBAI, in THF.

The reaction was then attempted with the base, NaHMDS, which was added at -78°C to a solution of the phosphine oxide and was left to stir for 1 hour, after which benzyl bromide and TBAI was added and subsequently left overnight which led to the product in 67% yield, with only a minute drop (< 1%) in the e.e. of the product (**Scheme 76**) which was by far a more important factor in the synthesis of the final compounds.

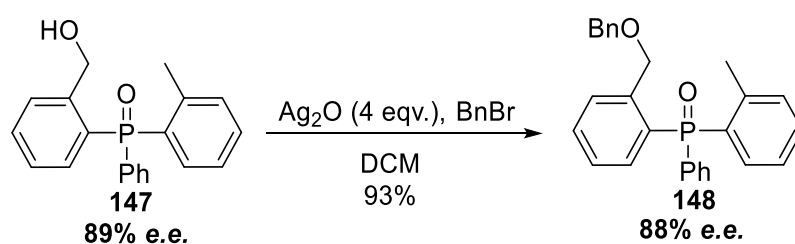


**Scheme 76** – Benzylation of **147** using NaHMDS, TBAI and benzyl bromide in THF.

Although the large loss of e.e. had been remedied using NaHMDS as the base, the lower yield of 67% was unfortunate and could be improved upon. As different bases had only been tried so far, a different approach was taken in which the benzylating agent was activated further through the addition of silver(I) oxide which increases the electrophilicity of the benzyl halide through co-ordination to the halogen.<sup>[146]</sup> Silver(I) oxide was added in slight excess (1.5



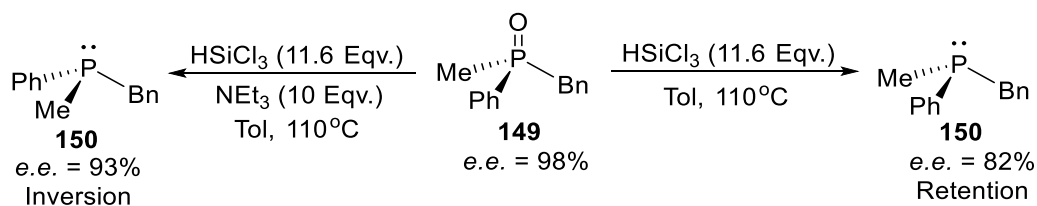
eqv.) to **147** in DCM and the reaction left to stir for 18 hours after which the reaction had not gone to completion, but had gone cleanly to the benzylated derivative, which was encouraging. The reaction was attempted again with a larger amount of silver oxide (1.5 equivalents increased to 4 equivalents), which pushed the reaction to completion after 18 hours with minimal loss in e.e. (**Scheme 77**).



**Scheme 77** – Benzylation of **147** with silver oxide and benzyl bromide to give the benzyl ether product **148**.

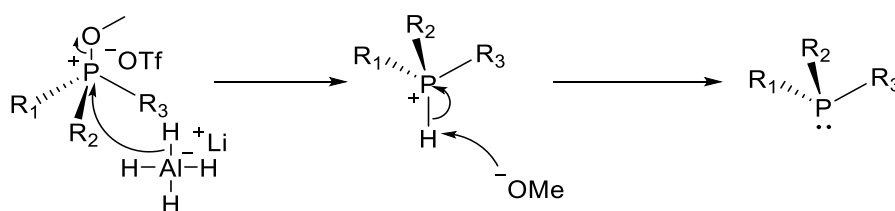
## 5 – Stereoselective reduction of phosphine oxides

Now that we had arrived at a structure which could potentially be used as a ligand for asymmetric catalysis, we then embarked upon the final step of the synthesis, the stereoselective reduction of the chiral phosphine oxide to yield the chiral phosphine **152**. Over the course of the project, multiple methods of reduction had been attempted on various intermediates often to test whether the reduction could be accomplished without eroding *e.e.* Whilst multiple methods exist for the stereospecific reduction these are often only applicable for certain structures as the stability to both oxidation and reduction varies greatly with the substituents attached to the phosphorus atom.<sup>[147,148]</sup> Furthermore, very few of these stereoselective methods proceed without any loss in chirality and usually lead to a decrease in *e.e.* which would be detrimental during the last step to form the phosphine. The most common method of reduction includes the use of silanes such as trichlorosilane which, depending on the presence of base, can cause either inversion or retention of the phosphorus atom chirality (**Scheme 78**).<sup>[149,150]</sup> However, in both cases the use of trichlorosilane has been reported to decrease the *e.e.* in the range of 5-25% which we deemed too much of a loss to be a viable method for our synthetic route. In order to maintain chirality, the conditions needed to be relatively mild and not exceed temperatures which can allow inversion to occur due to surpassing the inversion energy barrier of the resulting phosphine.



**Scheme 78** – Trichlorosilane reduction of **149** which can proceed with inversion or retention of the chirality depending on addition of triethyl amine.

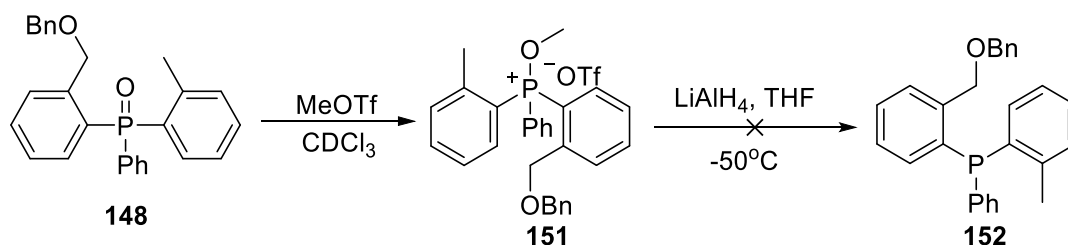
The first method of reduction attempted involved the use of the reducing agent lithium aluminium hydride at low temperatures of  $-60^\circ\text{C}$  which would limit the chance of inversion of the resulting phosphine and has been shown to retain chirality.<sup>[151]</sup> This method requires the formation of a methoxyphosphonium salt followed by displacement of the methoxy group with hydride. This method was demonstrated on several compounds retaining the e.e. of the phosphorus atom; however, it does cause inversion of the centre due to the attack of the hydride from the back of the molecule (**Scheme 79**).<sup>[151]</sup>



**Scheme 79** – Reductive cleavage of the methoxy phosphonium salt by lithium aluminium hydride leading to inversion of the phosphorus atom.

In order to ensure that the methoxyphosphonium salt had been formed, we attempted the reaction stepwise and so methyl triflate was added to the phosphine oxide **148** in deuterated chloroform so that the formation of the product could be measured by NMR. The reaction was left for 24 hours and

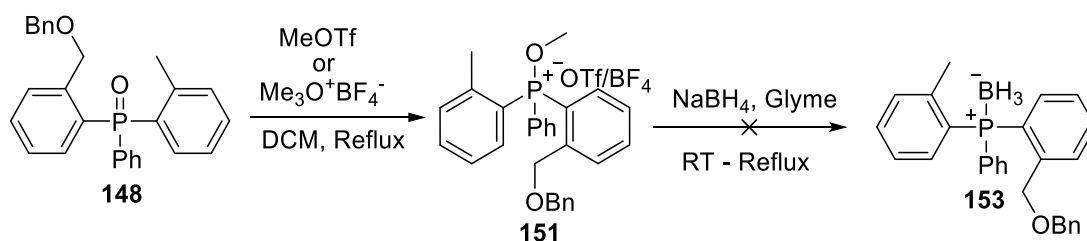
analysed by  $^{31}\text{P}$  NMR in which two major peaks were present. The first peak had a shift of  $\delta$  68.9 which most likely due to the desired methoxyphosphonium salt product as similar compounds have been reported in the literature<sup>[152]</sup> with a  $^{31}\text{P}$  NMR shift of  $\delta$  74.5. A second broad peak with a shift of  $\delta$  44.7 was also present in the reaction which belonged to an unknown product in a similar abundance. However, due to the products being phosphonium salts, purification by column chromatography of the methoxy phosphonium intermediate would be difficult and so lithium aluminium hydride was added to the reaction at  $-60^\circ\text{C}$  and left for 5 hours (**Scheme 80**). The reaction was then stopped and the crude material analysed by NMR which showed heavy degradation of the two products, most likely due to P-C bond cleavage, which has been shown to occur on similar triaryl phosphine oxides when lithium aluminium hydride is added in THF.<sup>[153]</sup>



**Scheme 80** – Failed reaction for the formation of the methoxyphosphonium salt and then subsequent displacement by lithium aluminium hydride.

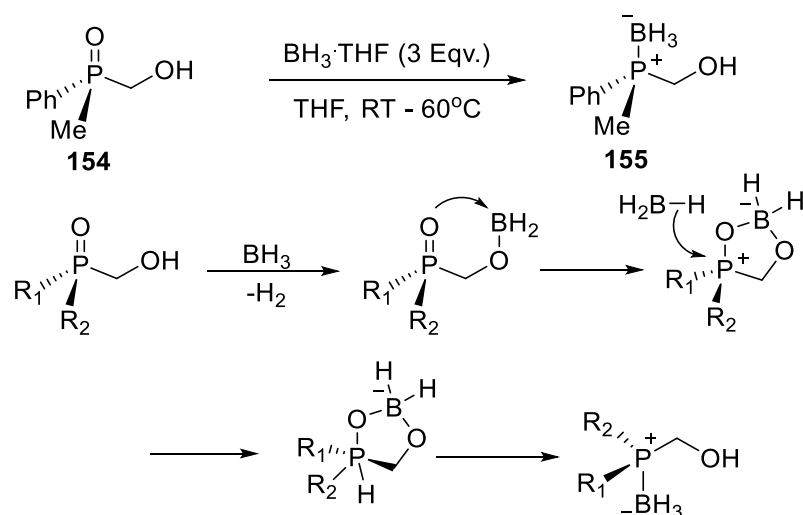
Due to the harsh nature of lithium aluminium hydride and the degradation shown, we attempted the reaction again using the less reactive, sodium borohydride, which has also been shown to reduce phosphine oxides with virtually no erosion of e.e. to give the corresponding phosphine-borane.<sup>[154]</sup>

The phosphine oxide **148** was reacted separately with two different methylating agents, trimethoxyoxonium tetrafluoroborate and methyl triflate, in DCM at reflux to ensure that the methoxyphosphonium salt was formed and then the reaction cooled to room temperature and NaBH<sub>4</sub>, dissolved in glyme, was added to the reaction and subsequently refluxed. After 24 hours at reflux, the reaction was worked up and both reactions were analysed by <sup>31</sup>P NMR and unfortunately no phosphine product was observed from either attempt at the reaction (**Scheme 81**).



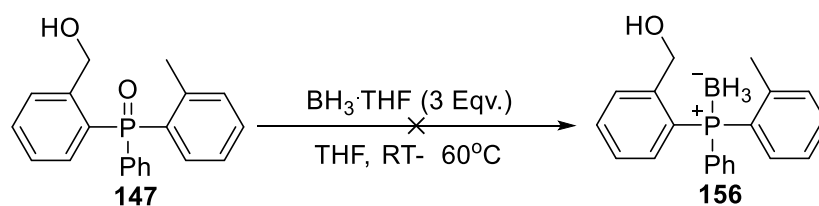
**Scheme 81** – Failed reduction of the phosphine oxide **141** from the formation of the methoxy phosphonium salt and the addition of sodium borohydride.

Following on from the attempted use of sodium borohydride to reduce **151** to give the phosphine-borane, it was noted that borane complexes, such as borane-THF and borane-SMe<sub>2</sub>, have also been shown to reduce phosphine oxides which have a proximal hydroxyl group to yield the phosphine borane, through the mechanism shown in **Scheme 82**.<sup>[155-157]</sup>



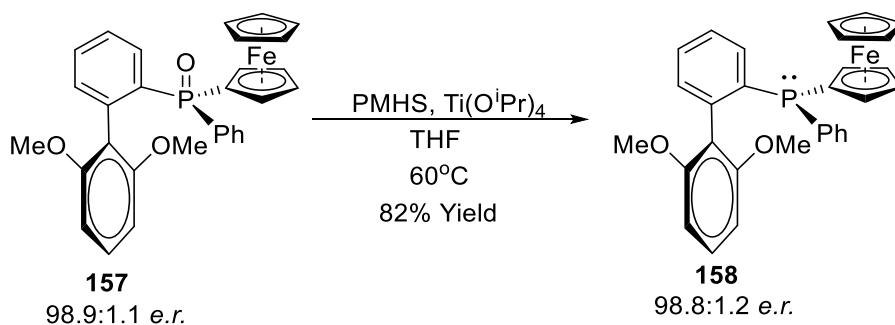
**Scheme 82** – Literature reaction and mechanism of the  $\text{BH}_3$  mediated reduction of phosphine oxides with a proximal hydroxyl group.

Stankevic *et al.* developed this reaction on phosphine oxides which contained a hydroxyl group up to 2 carbons distant from the phosphorus centre <sup>[154,157]</sup> and although **147** contains its hydroxyl group 3 carbons away we hypothesized this reaction could show the same reactivity due to the ability of the hydroxyl to add into the phosphine oxide during the formation of the spirophosphorane product **110** (**Scheme 35**). The phosphine borane product of the reaction would also be stable to both oxidation and inversion and therefore would be ideal to store straight after the reaction and would only require a small addition of an amine such as DABCO to release the phosphine prior to use.<sup>[158]</sup> Three equivalents of borane-THF was added to **147** in THF, at the lower literature temperature of  $0^\circ\text{C}$  to test whether this would reduce the phosphine oxide (**Scheme 83**). Unfortunately, no activity was seen at this lower temperature and so the temperature was increased to  $60^\circ\text{C}$ .<sup>[157]</sup> However, even after 24 hours at  $60^\circ\text{C}$  no characteristic phosphine-borane peak could be seen in the  $^{31}\text{P}$  NMR analysis of the reaction.



**Scheme 83** – Failed formation of the phosphine-borane **156** with the use of borane THF in THF at either room temperature or 60°C.

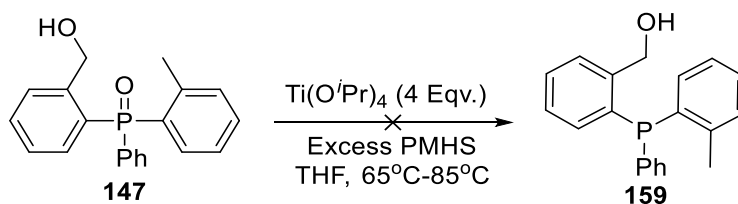
Another method which included both a relatively mild hydride source and lower temperatures was that described by Han *et al.* Polymethyl hydrogen siloxane (PMHS) was used as a hydride source in excess alongside a super stoichiometric amount of titanium isopropoxide.<sup>[159]</sup> This method has been used to reduce the bulky phosphine oxide **157** with only a minor decline in *e.e.* (0.1%), as shown in **Scheme 84**.



**Scheme 84** – Reduction of **157** with PMHS and titanium isopropoxide in THF leading to a loss of only 0.1% *e.e.*

An excess of PMHS was added to the **147**, in THF followed by 4 equivalents of Ti(OiPr)<sub>4</sub> and the reaction was stirred at 65°C for 18 hours after which no

reaction was observed and only the phosphine oxide was recovered (**Scheme 85**). The reaction was then repeated at a higher temperature (85°C) and again no reduction was observed and again, only starting material was recovered from the reaction. We hypothesised that the lack of reduction could be due to the free hydroxyl binding to the titanium species, preventing co-ordination to the phosphine oxide; we hypothesised the benzyl ether **148** would therefore be better suited to this reduction.

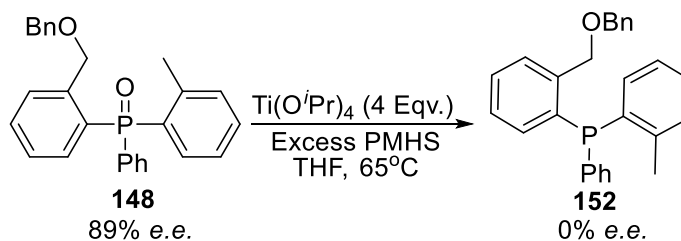


**Scheme 85** – Failed reduction of the phosphine oxide **147** with titanium isopropoxide and polymethyl hydrogen siloxane.

The reaction was then attempted again on the benzyl ether protected **148** under identical conditions which led to a reduction of the phosphine oxide to the phosphine **152** in 98% yield (**Scheme 86**), which was pleasing after the previous failed attempts and also suggests that the free -OH was likely to be interfering with the reaction and possibly co-ordinating to the titanium species. The pure phosphine showed a vastly different  $^{31}\text{P}$  NMR shift at  $\delta$  -23.15 compared to the phosphine oxide at  $\delta$  34.4 and fortunately showed only slight oxidation (<0.1%) due to atmospheric oxygen. This observed change in oxidative stability was a much-needed property as it would allow the use of the ligand under a variety of conditions and would not require an oxygen-free



environment for storage and use, increasing the potential application of the ligand.



**Scheme 86** – Successful reduction of the benzyl ether protected phosphine oxide with titanium isopropoxide and polymethyl hydrogen siloxane to give in racemised phosphine.

With a view to measure any potential e.e. degradation which may have occurred in the reduction, the phosphine was analysed by chiral HPLC, but no separation of enantiomers could be obtained by the chiral column (Daicel chiralpak-AD hexane:isopropanol, 83:17) due to the highly lipophilic nature of the phosphine. Therefore, the phosphine was oxidised back to the phosphine oxide using excess hydrogen peroxide in a DCM/water mixture and the phosphine oxide was analysed by chiral HPLC against the same sample of the phosphine oxide which had not been exposed to reductive conditions. Unfortunately, after the reduction and re-oxidation, the sample had racemised almost completely as shown by the chromatogram in **Figure 17**, which was unexpected due to the method being successfully applied to other chiral phosphine oxides which retained their chirality even after re-oxidation.<sup>[160]</sup>

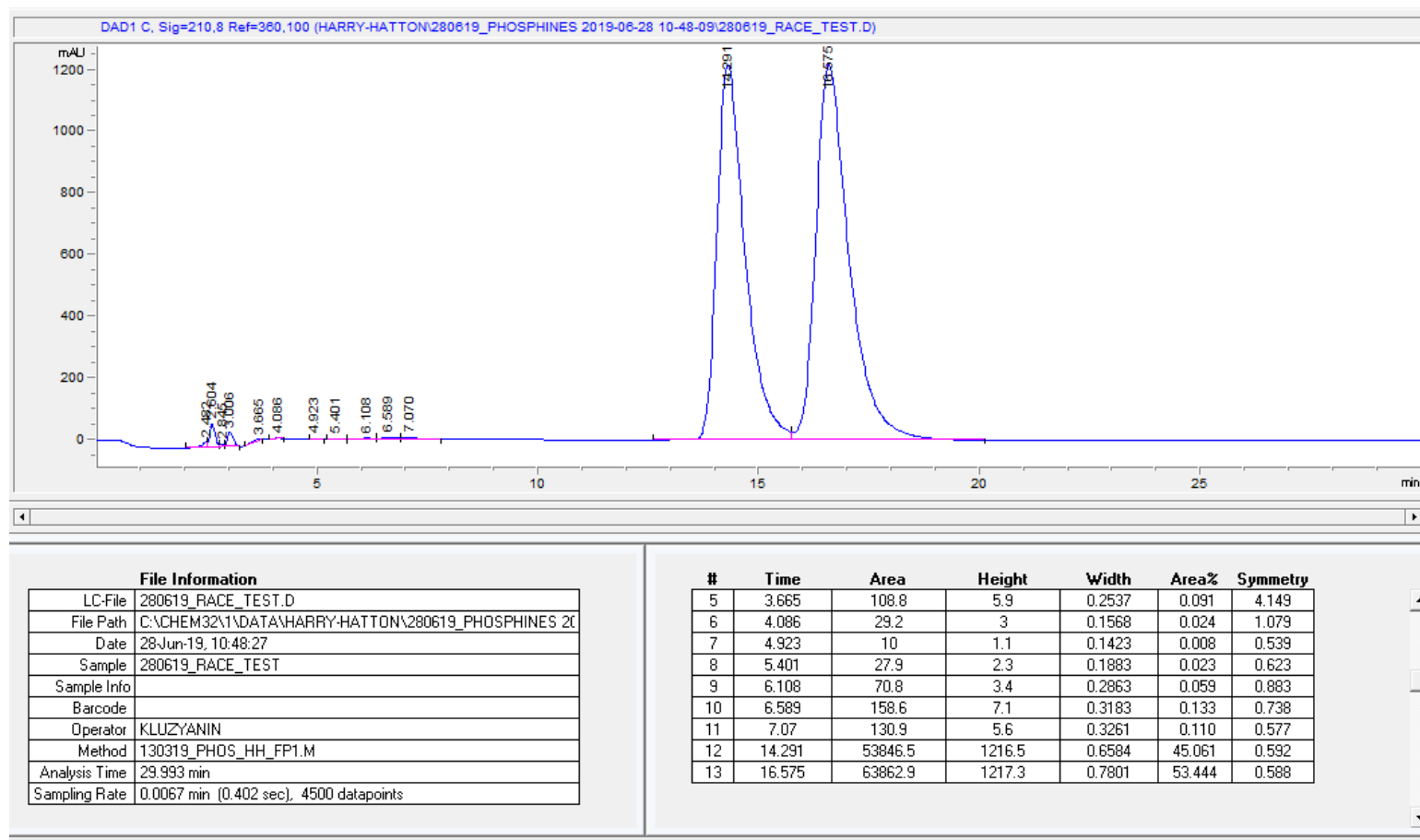
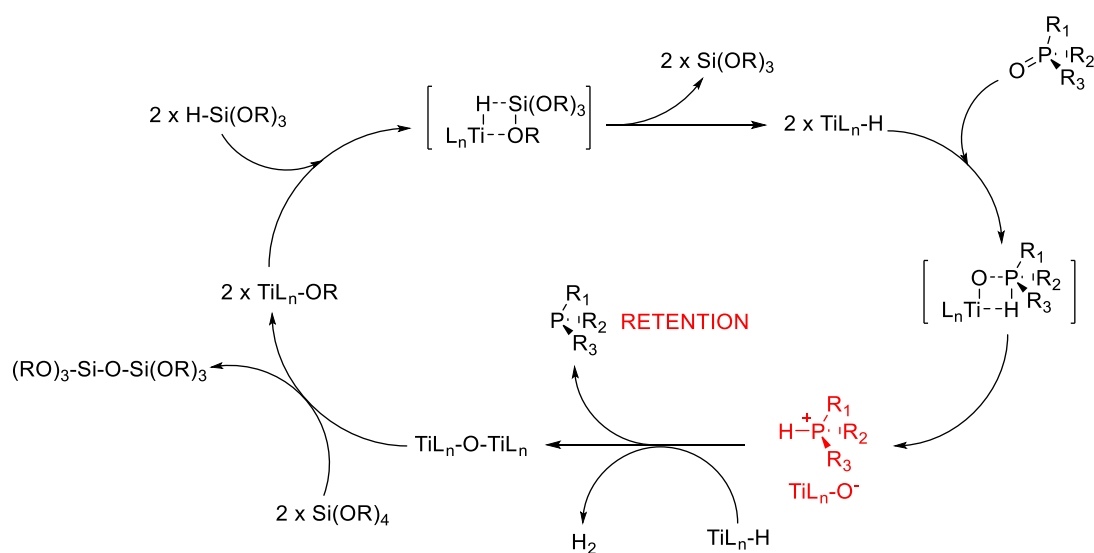


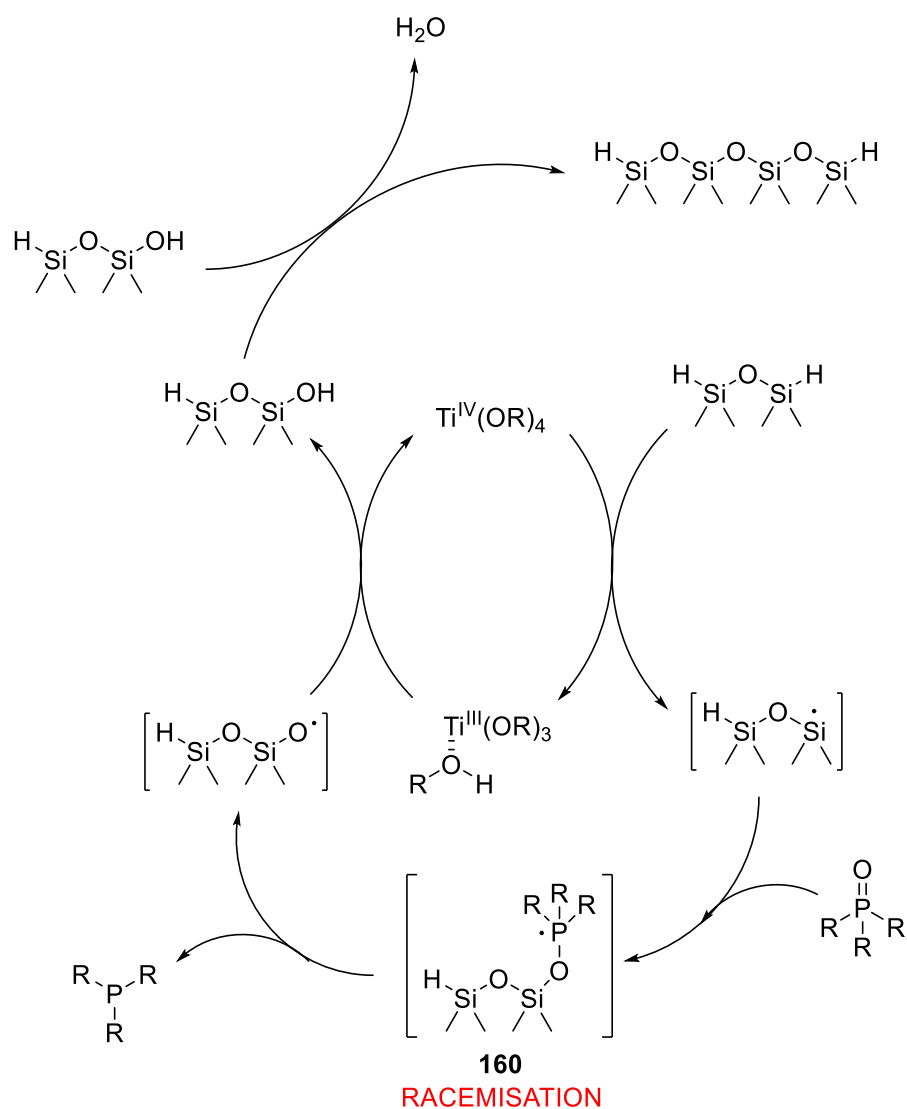
**Figure 17** – Chiral HPLC analysis of **152** (14.2 and 16.5 min) after reduction using titanium isopropoxide at 65°C and reoxidation to the phosphine oxide **148**. (Daicel Chiralpak-AD, hexane:isopropanol, 91:9)

The unexpected racemisation observed may have been due to three possible reasons. The simplest explanation is due to the temperature (65°C) causing inversion of the phosphorus atom in the phosphine which is entirely possible for our triaryl phosphine **152**. This temperature dependent inversion could also be occurring on one of the intermediates in the mechanism of the reduction, such as the phosphonium species highlight in red in **Scheme 87**.<sup>[161]</sup>



**Scheme 87** – Possible mechanism for the reduction of phosphine oxides with  $Ti(O^iPr)_4$  and a silane hydride source via the formation of the reactive titanium hydride species.

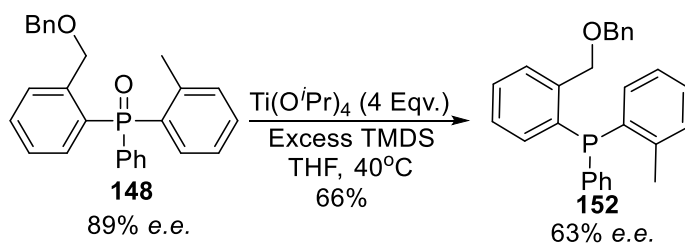
Another explanation could be due to a second reported mechanism where titanium isopropoxide is used as there is also a radical pathway which is plausible. This secondary radical pathway has been shown to be prominent when titanium isopropoxide is used in catalytic amounts and progresses through the mechanism shown **Scheme 88**, in which pseudorotation of the radical intermediate **160** can occur causing the loss of chirality.<sup>[162,163]</sup>



**Scheme 88** – Possible radical mechanism for the reduction of phosphine oxides with  $Ti(OiPr)_4$  and TMS which can lead to racemisation of the intermediate **160**.

The second method of racemisation could be due to the elevated temperature causing pyramidal inversion of the phosphorus atom in the resulting phosphine product. However, it is unknown at what temperature the energy barrier is reached. Although the suppression of a possible radical pathway is difficult, the reaction was attempted using lower temperatures of 40°C (**Scheme 89**), 20°C and 0°C and a different source of silane to see if the reduction was still

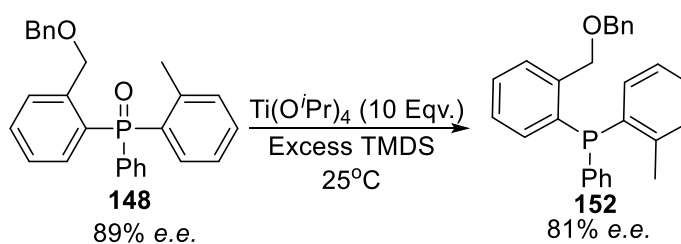
possible and if any erosion of *e.e.* was still observed at these varying temperatures. The change of silane was due to the extensive, high-temperature workup needed to degrade and remove the PMHS from the reaction. TMDS has also been applied to the reduction of phosphine oxides alongside titanium isopropoxide. At 0°C no reduction was observed after 24 hours so the temperature was increased to 20°C. This led to a very small amount of phosphine after a further 24 hours. The reaction at 40°C led to reduction of the phosphine oxide in 66% yield after 24 hours. This was oxidised for chiral analysis which showed that the *e.e.* had decreased by 26% but was still enantioenriched, which was a promising step forward. Furthermore, the reduction has proceeded with overall retention of the chiral centre which highlights that the reduction is most likely proceeding through the mechanism described in **Scheme 87**.



**Scheme 89** – Reduction of the phosphine oxide with titanium isopropoxide and excess TMDS at 40°C leading to conversion to the phosphine with a 26% decrease in *e.e.*

The reaction was attempted again at 25°C, but the equivalents of both the silane and titanium isopropoxide were increased 2.5-fold to 25 equivalents and 10 equivalents respectively (**Scheme 90**) and were added neat without any THF solvent. The increase in these reagents would hopefully increase the

formation of titanium hydride and an improved yield of the phosphine. The reaction was stirred for 18 hours under nitrogen, worked up and the crude material was analysed by  $^{31}\text{P}$  NMR which showed that the phosphine oxide had been reduced in 92.5% yield. This was encouraging as only a small percentage of phosphine was present at  $25^\circ\text{C}$  when lower equivalents of reagents were used. The phosphine was purified, oxidized using hydrogen peroxide and the resulting phosphine oxide analyzed by chiral HPLC which showed only an 8% loss in e.e. which again was a forward step towards minimizing the loss of e.e. through reduction.



**Scheme 90** – Reduction of the phosphine oxide at  $25^\circ\text{C}$  with increased equivalents of both titanium isopropoxide and TMDS leading to the phosphine with an 8% decrease in e.e.

Due to the decreasing loss in e.e. with relation to temperature, we attempted the same reduction at  $15^\circ\text{C}$  with several different silanes. We anticipated at this lower temperature the reaction would not be as facile and therefore attempting the reaction with several different silanes would give us a greater chance of seeing the reduction of the phosphine oxide. PMHS, TMDS and triethyl silane were all added in 25 equivalents to the reaction alongside 10 equivalents of  $\text{Ti}(\text{O}^i\text{Pr})_4$  and left to stir at  $15^\circ\text{C}$  for 24 hours. After this time, no reaction was seen with triethyl silane, TMDS showed partial reduction and

PMHS gave complete reduction of the phosphine oxide. The product from the PMHS containing reaction was purified, oxidized, and chiral HPLC analysis of the resulting phosphine oxide showed only a 4% loss in e.e. at this temperature which again was a promising step forward. Finally, we attempted the reaction at 5°C with the same equivalents of PMHS and  $\text{Ti}(\text{O}^i\text{Pr})_4$ , as described above, added neat to the phosphine oxide and the reaction was shaken for 48 hours instead of 24 hours as we anticipated at this temperature the reaction would be much slower. Purification, oxidation and analysis by chiral HPLC showed the phosphine oxide had been reduced in 72% conversion and that there was only a ~2% loss in e.e. which we anticipated was probably best we could achieve. However, this small loss in e.e. was very impressive in the area of stereoselective phosphine oxide reduction. The results and optimisation of the silane reductions are summarised in **Table 16**.

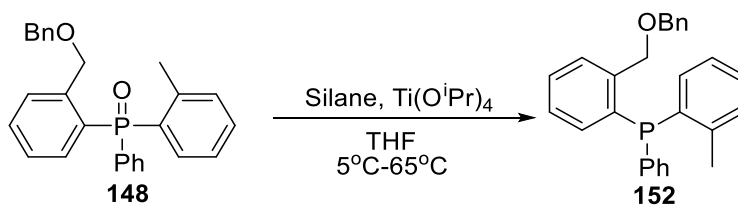


**Table 16** – Reduction of **148** with titanium isopropoxide and silanes at different temperatures and its effect on e.e. and conversion.

Temperature	Silane	Time (hr)	Eqv. Of Silane	Eqv. Of Ti(O <sup>i</sup> Pr) <sub>4</sub>	Δ e.e.	Conversion
65°C	PMHS	24	Excess	4	Racemised	97%
40°C	TMDS	24	10	4	-26%	66%
25°C	TMDS	24	10	4	NR	NR
25°C	TMDS	24	25	10	-8%	92%
15°C	TMDS	24	25	10	-5%	63%
15°C	Et <sub>3</sub> SiH	24	25	10	NR	NR
15°C	PMHS	24	Excess	10	-4%	95%
5°C	PMHS	48	Excess	10	-2%	72%

HPLC Conditions: Daicel AD column, 1.2 mL/min, 91% Hexane/IPA at 210 nm.

In order to clarify whether the phosphine was stable at the elevated temperature, we then refluxed the phosphine (85% e.e.) in THF at 65°C for 24 hours as this was the same temperature used for the reduction, shown in **Scheme 86**, which gave us full racemisation. The sample was then oxidised to the phosphine oxide for analysis by chiral HPLC which showed that the phosphine had fully racemised at 65°C and was not stable to inversion at this temperature. Although this instability was disappointing, the intended asymmetric 1,6-boration reaction takes place at room temperature (**Scheme 25**) and so we attempted a stability test of the phosphine at room temperature in solution (25°C ambient temperature). The phosphine (84% e.e.) was split into 3 aliquots and oxidised at different time points back to the phosphine oxide



for analysis by chiral HPLC. The first sample was analysed shortly after reduction which showed that the phosphine was at 84% e.e. after reduction, after 24 hours another aliquot was oxidised and analysed which showed that the e.e. had fallen to 78% showing a decrease of 6%. The next aliquot was oxidised after 72 hours and analysed which showed a decrease in e.e. of 19% from the starting e.e. of 84% down to 65% (**Figure 18**). Due to the inversion of the phosphines at room temperature, this tells us that temperature-dependent inversion barrier is around the 20°C-25°C range.

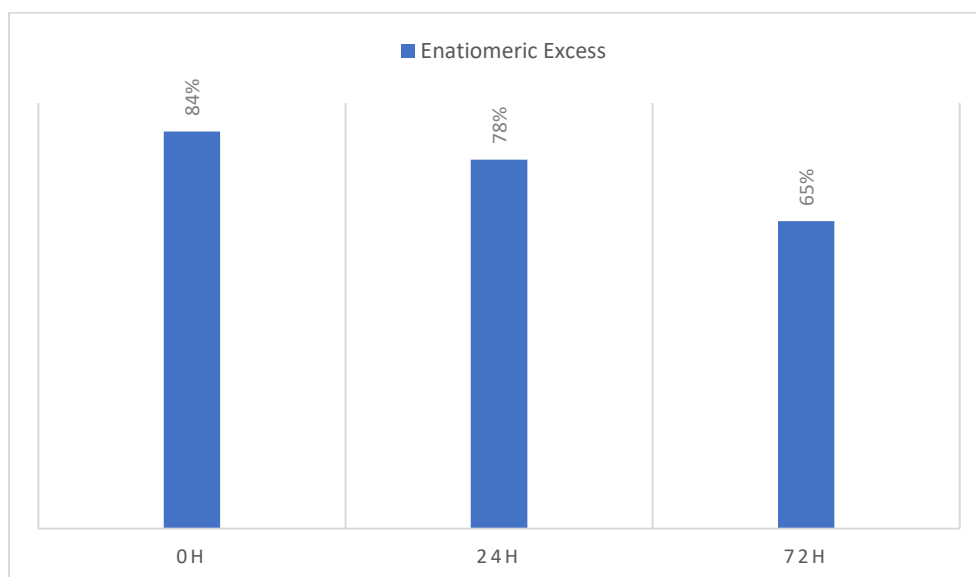
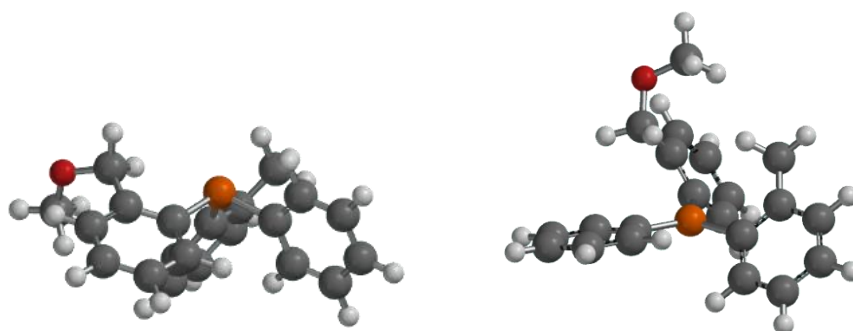


**Figure 18** – Loss of e.e. of **152** at room temperature in DCM over 72 hours.

Although this shows that the phosphine is not stable to inversion at room temperature in solution, the addition of the metal catalyst could prevent this inversion as the phosphine lone pair would bind to the metal centre. However, the loss of any e.e. of the phosphine during a reaction would be difficult to analyse during a reaction time as the ligand would be coordinated to the metal centre.

## 6 – DFT Modelling of the inversion barrier of tertiary phosphines

Due to the configurational instability of **152**, we hypothesised that the use of molecular modelling would expedite the process of finding more stable triaryl phosphines through DFT calculations of the inversion barrier of several different related phosphines. This would allow us to test numerous phosphines for inversion stability without having to synthesise them. As reported by Holz *et al.*, the Gibbs free energy of both the trigonal pyramidal geometry and the trigonal planar transition state can be calculated using DFT, where the difference equates to the inversion energy barrier.<sup>[24]</sup>

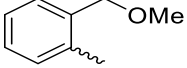
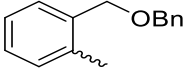
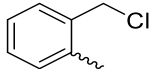
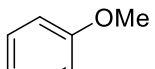
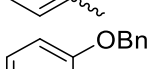
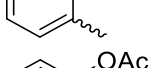
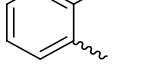
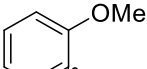
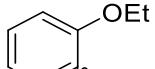
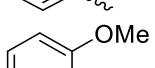
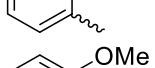
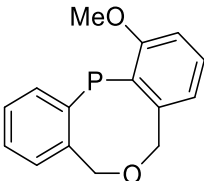
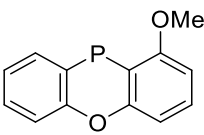


**Figure 19** – DFT modelling of A) the trigonal pyramidal ground state and B) the trigonal planar transition state of **161**.

Previous stability studies reported in the literature have shown that lowering the steric demands of the three substituents attached to the phosphorus atoms gives large increases to the inversion barrier energy.<sup>[23,24]</sup> Furthermore, changes in the electronic effects of the substituents can also lead to increases

in the inversion barrier, as electron-donating groups in the *-ortho* or *-para* position of the phenyl rings destabilise the planar transition state.<sup>[42,45,57]</sup> Therefore, a range of different tertiary phosphine structures (**Table 17**), which contained phenyl rings with varying substituents were submitted for DFT calculations. We also included a bridged structure which could potentially inhibit the inversion mechanism of the phosphine. Two different diphenyl alkyl phosphines were also calculated to gauge how the inversion energy changed when moving to diaryl alkyl phosphines. Although it would be impossible to calculate the absolute temperature at which the inversion would occur from these calculations, we could formulate a trend within our calculated structures to gauge which phosphines would give increased stability. We could also use the work by Holz *et al.* to also give an estimate at a potential half-life through comparison of their Gibbs free energy values compared to ours.<sup>[24]</sup>

**Table 17 – Phosphine structures submitted for DFT calculation.**

Compound	PR <sub>1</sub> R <sub>2</sub> R <sub>3</sub>		
	R <sub>1</sub>	R <sub>2</sub>	R <sub>3</sub>
161	Ph	<i>o</i> -tolyl	
152	Ph	<i>o</i> -tolyl	
162	Ph	<i>o</i> -tolyl	
163	Ph	<i>o</i> -tolyl	
164	Ph	<i>o</i> -tolyl	
165	Ph	<i>o</i> -tolyl	
166	Ph	<i>o</i> -tolyl	
167	Ph		
168	Me	<i>o</i> -tolyl	
169	<sup>t</sup> Bu	<i>o</i> -tolyl	
170	<i>o</i> -tolyl		
171 <sup>a</sup>	<i>o</i> -tolyl		
172 <sup>a</sup>	Ph	Me	<i>p</i> -tolyl
173 <sup>a</sup>	Ph	Me	<i>o</i> -anisyl

a – Validation structures for which the literature experimental inversion barrier was available.

For the trigonal pyramidal configuration, a conformer search was undertaken using molecular mechanics which identified several energy minimum structures. Higher-level calculations were then conducted on the lowest

energy conformer, giving us a more accurate representation of the ground state of the trigonal pyramidal configuration. The lowest energy conformer was then optimised to find the geometry equilibrium using a higher level,  $\omega$ B97X-D density functional method with the 6-31G\* dataset with Van-der Waals dispersions (which should account for the large aromatic rings in the phosphine structures). From the optimised geometry equilibrium calculation, we gained the phosphines ground state energy, which was confirmed through the lack of imaginary frequencies in the phosphines calculated IR.

We estimated the transition state to be the trigonal planar structure where the sum of the internal phosphine C-P-C bonds equalled  $360^\circ$ . The equilibrium geometry of this structure was then optimized to find the lowest energy conformation of the transition state. From the optimised trigonal planar geometry, the transition state geometry was then calculated using the same DFT,  $\omega$ B97X-D computation method with the 6-31G\* dataset, from which we gained a single imaginary frequency which corresponded to the inversion pathway (umbrella inversion) of the central phosphorus atom. The difference between the Gibbs free energy of both configurations (trigonal pyramidal and trigonal planar) was then estimated to be the inversion energy barrier. In order to validate our calculations, we also included two structures which were similar to our proposed structures and for which the experimental inversion barrier was available for comparison. Furthermore, we also included the measurement of the sum of the internal angles (C-P-C angles) surrounding the phosphorus in the trigonal pyramidal structure which would also give an insight into the stability of the molecule to inversion as shown in previous

work.<sup>[24]</sup> A higher the sum of the internal C-P-C angles would indicate increased planarity of the molecule which would lie closer to the planar transition state and therefore would require less energy for inversion to occur.

**Table 18** – *Calculated C-P-C internal angle and  $\Delta G$  at 25°C and 50°C.*

<b>Compound</b>	<b>C-P-C Angle</b>	<b>Calculated <math>\Delta G</math> 25°C</b>	<b>Calculated <math>\Delta G</math> 50°C</b>	<b>Type of Compound</b>
<b>170</b>	318.4	91.21 kJ/mol	90.92 kJ/mol	Cyclic
<b>161</b>	306.5	118.09 kJ/mol	117.64 kJ/mol	Benzylic
<b>169</b>	309.5	122.74 kJ/mol	122.53 kJ/mol	tButyl Alkyl
<b>162</b>	305.6	124.08 kJ/mol	124.34 kJ/mol	Benzylic
<b>163</b>	304.2	125.97 kJ/mol	125.49 kJ/mol	Phenolic
<b>152</b>	304.7	129.62 kJ/mol	128.72 kJ/mol	Benzylic
<b>166</b>	303.6	133.61 kJ/mol	134.45 kJ/mol	Amine
<b>164</b>	303.9	134.79 kJ/mol	135.0 kJ/mol	Phenolic
<b>167</b>	301.9	139.59 kJ/mol	140.49 kJ/mol	Phenolic
<b>171</b>	299.1	146.26 kJ/mol	146.63 kJ/mol	Cyclic
<b>172</b>	301.6	147.22 kJ/mol	148.74 kJ/mol	Methyl Alkyl
<b>173</b>	301.8	151.63 kJ/mol	152.49 kJ/mol	Methyl Alkyl
<b>165</b>	305.4	155.35 kJ/mol	155.95 kJ/mol	Phenolic
<b>168</b>	303.5	167.94 kJ/mol	168.31 kJ/mol	Methyl Alkyl

As mentioned previously, we included two structures to act as validations for our computational method and in both cases, our calculated inversion barrier value was overestimated, by 11% and 13%, respectively. Our calculated inversion barriers for compounds **172** and **173**, as shown in **Table 18**, are

147.2 kJ/mol and 151.6 kJ/mol, compared to their experimental inversion barriers of 126.8 kJ/mol and 128.9 kJ/mol (**Figure 20**).

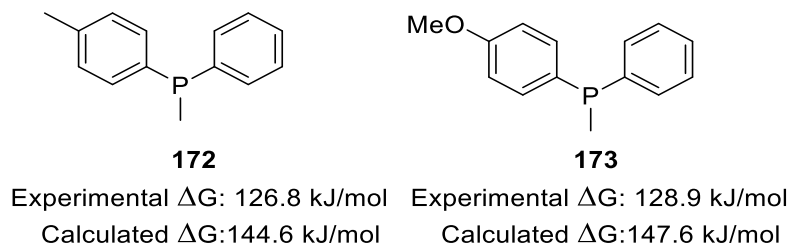


**Figure 20** – Calculated  $\Delta G$  for two phosphines for which the literature experimental value was available for comparison.

Higher-level theory calculations would undoubtedly close the gap between the calculated and experimental values, as shown by Holz *et al.* who employed the B3PW91 level of theory with a more accurate data set and the calculated values were within 3% of the experimental values.<sup>[24]</sup> However, these methods would have been too expensive to run on the systems we had available. This meant that we could not fully relate our calculated values to literature values, but we could gain a useful trend within our own compounds. Starting with the acyclic tertiary phosphines, there was a clear trend within our results with the benzylic structures, showing inversion barriers lower than the phenolic derivatives, apart from our synthesised compound **152**, which showed an unexpectedly high inversion barrier compared to the other benzylic compounds. As we have found from our experimental results, even with the increased calculated inversion barrier for **152**, compared to the other benzylic compounds, the phosphine **152** still exhibits inversion at room temperature. This suggests that the use of other similar benzylic structures as P-chiral phosphine ligands could be limited. However, the inversion barrier does

increase as we move to the phenolic structures in our series. Although compound **164** has a calculated inversion barrier lower than that of **152**, it would be difficult to see this being reflected in an actual experimental value as the series shows that the increasing number of electron-donating groups increases the inversion barrier. This is shown by the structure **167**, which contains two phenolic groups and displays a higher inversion barrier indicative that delocalisation of the phenolic oxygens into the aromatic ring destabilize the trigonal planar transition state for inversion (**Figure 21**).

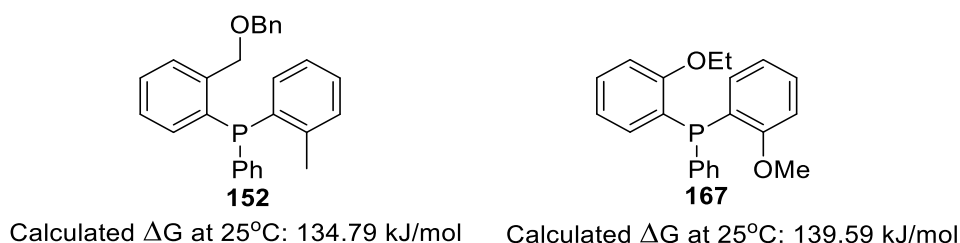


**Figure 21** – Calculated  $\Delta G$  Gibbs for benzylic phosphine **152** and phenolic phosphine **167**.

Interestingly, even the compound **165**, which contains an electron-withdrawing group in the *-ortho* position, in the form of a phenolic acetate ester, showed a very high inversion barrier of 150.96 kJ/mol. In order to gauge our triaryl phosphines stability compared to related P-chiral phosphines such as (R)-PAMP, we also included two diaryl alkyl phosphines compounds, one containing a methyl group and the second containing a 'butyl group (**Figure 20**). We anticipated that the methyl would give a greater inversion barrier as the literature suggests and this was reflected in our calculation which gave an inversion barrier of 168.3 kJ/mol and a low C-P-C angle sum of only 303.5°. However, although the inversion stability of the diaryl alkyl phosphines is very



favourable, this is often offset by their oxidative stability where the lower steric demands often cause the phosphine to oxidize rapidly on exposure to air. When moving to the <sup>t</sup>butyl containing phosphine, the inversion barrier actually falls below that of the majority of triaryl containing phosphines, at 122.74 kJ/mol (**Figure 22**), which can be attributed to large steric bulk which is reflected in the molecule's C-P-C angles sum of 309.5° which was the second-highest C-P-C angle sum in our series.

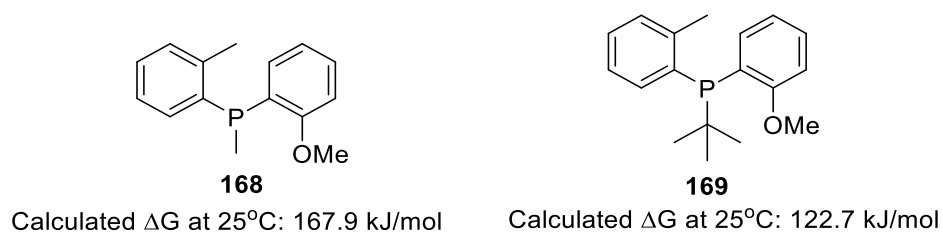


**Figure 22** – Calculated  $\Delta G$  for the two-alkyl containing phosphine **168** and **169**.

Cyclic structures, which link two of the substituents of the phosphines, have also been shown to drastically increase the inversion barrier of phosphines due to inability of the phosphine to undergo the inversion process. We included two different cyclic structures, **170** and **171**, linked through groups in the *-ortho* position which included, a dimethylene ether linkage and a phenolic linkage. The calculated inversion barrier of the larger linked structure, **170**, showed an extremely poor inversion barrier of only 91.2 kJ/mol, which was the lowest in our series by a large margin, this is most likely attributed to the steric demands of the molecule as the sum of the internal angles was extremely large at 318.4°. The phenolic linked molecule **171** showed a much higher inversion barrier of 146.2 kJ/mol, which was more in line with what we expected (**Figure**

23). However, synthesis of this type of chiral phosphine would be difficult due to the lack of available starting materials.

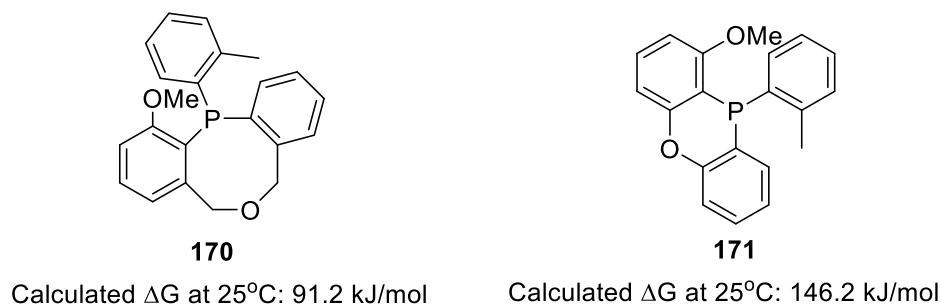


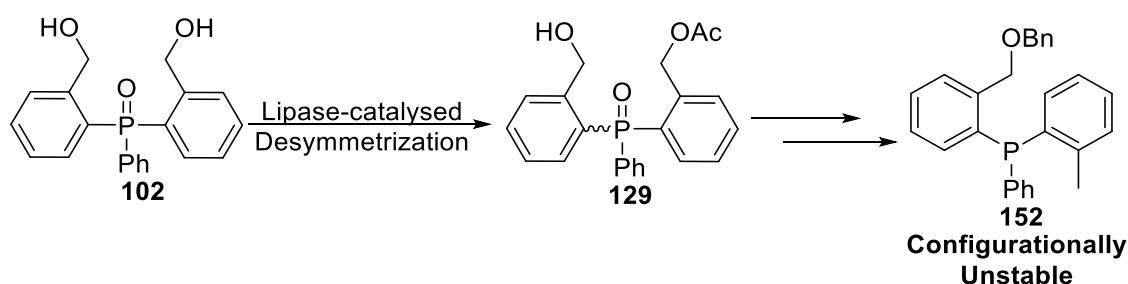
**Figure 23** - Calculated  $\Delta G$  for the cyclic phosphines **170** and **171**.

In conclusion, the calculations show that the move towards phenolic structures would provide phosphines of greater inversion stability. Although it is difficult to estimate the absolute temperature at which inversion would occur, phenolic structures could provide ligand stability at room temperature which would make them suitable for their intended use in asymmetric 1,6-boration reactions.<sup>[97-99]</sup>

## 7 – Synthesis of phenolic derivatives

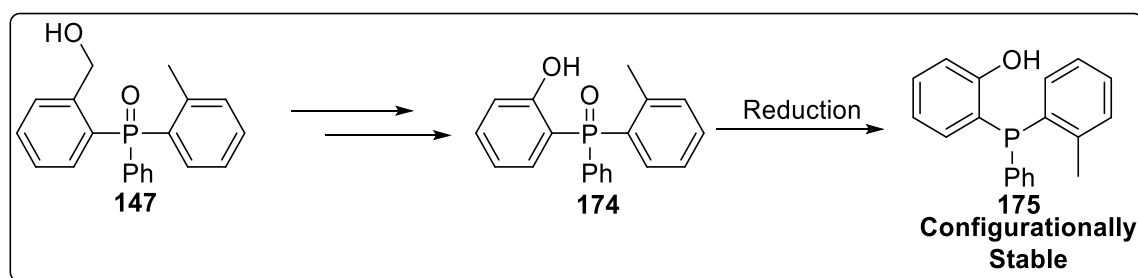
### 7.1 – Synthesis of phenolic derivatives from benzylic compound **129**

Due to the unexpected instability of the phosphine **152** (**Scheme 91**), we sought alterations to the structure. Given that we had established a synthetic route and efficient enzymatic desymmetrization of **102**, we attempted to modify intermediates derived from the biotransformation product **102**.



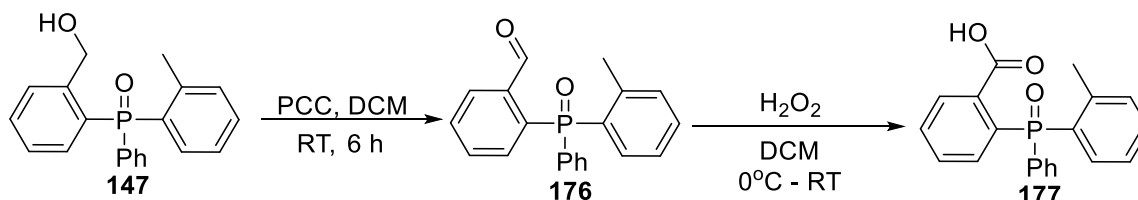
**Scheme 91** – Chemo-enzymatic route to the configurationally unstable phosphine **152** from diol **102**.

As shown by several literature inversion studies and our own DFT calculations<sup>[22-25]</sup>, the inclusion of phenolic substituents which can prevent delocalisation of the phosphorus atoms lone pair, can increase the inversion energy barrier quite substantially. With this in mind, we attempted the synthesis of a phenolic derivative from the benzyl alcohol **147** (**Scheme 92**). We hypothesised that Baeyer-Villiger oxidation of either the corresponding aldehyde or ketone would allow access to the phenolic derivative through the insertion of an oxygen atom adjacent to the phenyl ring.



**Scheme 92** – Potential synthesis of configurationally stable phenolic phosphine **175** from the benzylic compound **147**.

To achieve this, the phosphine oxide **147** hydroxyl group was oxidised to the aldehyde using pyridinium chlorochromate (PCC), in DCM at room temperature which went in high yield (**Scheme 93**) and was easily characterizable due to the aldehyde peak at  $\delta$  10.8 in the <sup>1</sup>H NMR.<sup>[164]</sup>

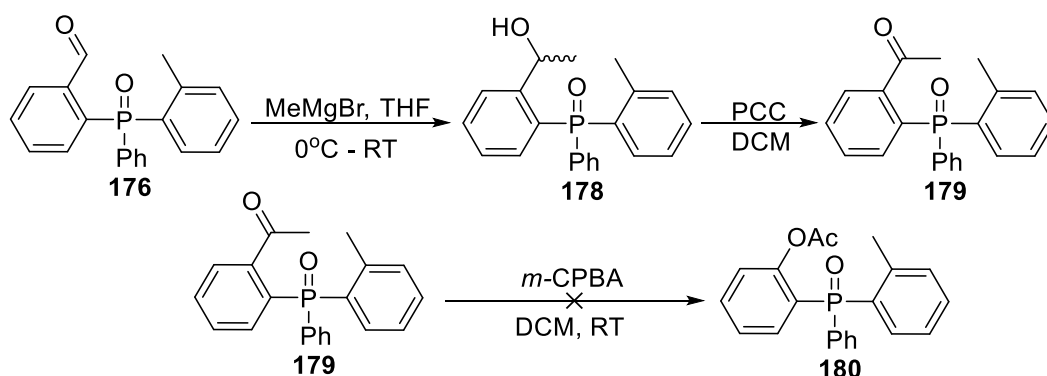


**Scheme 93** – Oxidation of **147** with PCC to yield the aldehyde derivative **176** and attempted Baeyer-Villiger leading to the acid derivative **177**.

At this point, we could also use the aldehyde product as a potential reactant for the Baeyer-Villiger oxidation as well as the precursor for the synthesis of the ketone derivative. We, therefore, attempted the Baeyer-Villiger oxidation on **177** through the addition of a slight excess hydrogen peroxide, in DCM and the reaction was stirred vigorously.<sup>[165]</sup> After consumption of the starting material the reaction was worked up and analysed by <sup>1</sup>H NMR which showed

that the aldehyde peak was no longer present but unfortunately, the aldehyde had been oxidised to the corresponding carboxylic acid.

The aldehyde derivative **176** was then dissolved in THF and cooled to 0°C, after which methyl magnesium bromide was added slowly to reaction and left to warm up to room temperature. The reaction was then quenched with sat. ammonium chloride to yield the secondary alcohol shown in **Scheme 94**. Analysis of the alcohol showed the appearance of the two diastereomers in both the <sup>1</sup>H and <sup>31</sup>P NMR in a ratio of 63:37.



**Scheme 94** – Synthesis of ketone derivative **179** and attempted Baeyer-Villiger oxidation with *m*-CPBA.

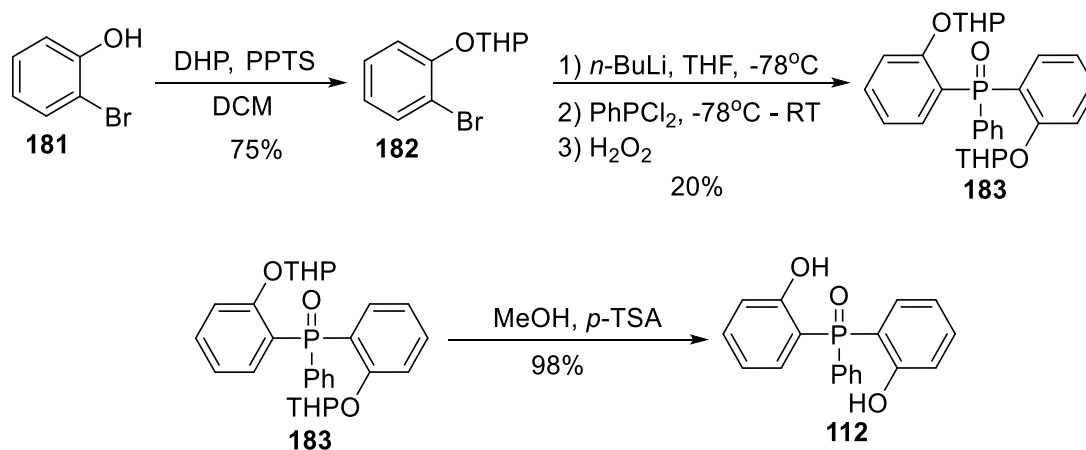
The secondary alcohol was then oxidised to the ketone with PCC which proceeded in high yield (**Scheme 94**) which was characterised through the appearance of a peak in the <sup>13</sup>C NMR at  $\delta$  202.0 corresponding to the deshielded ketone carbonyl. The Baeyer-Villiger oxidation was then attempted on the corresponding ketone, which should give a better chance of forming the acetate ester due to the migration of the phenyl ring being more favourable. A slight excess of *meta*-chloroperoxybenzoic acid (*m*-CPBA) was added to **179**

in DCM at room temperature and the reaction monitored by TLC (**Scheme 94**). After 2 hours, TLC indicated that only starting material was present and so the temperature was increased to 50°C and the reaction stirred for 24 hours. The reaction was worked up which showed that there was almost complete consumption of the starting material through  $^{31}\text{P}$  NMR analysis. However, in addition to the possible product, there was a large amount of degradation where the degradation products showed phosphine-like shifts. As a result, the synthesis of phenolic derivatives from the benzylic derivatives was not attempted further.

## 7.2 – Direct synthesis of phenolic derivatives

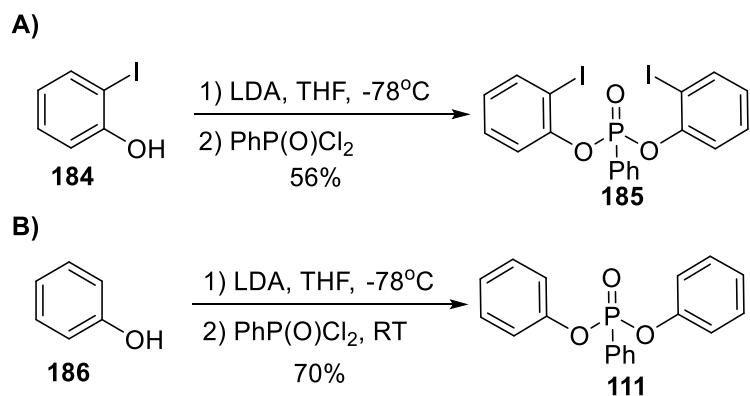
DFT Modelling had suggested that phenolic containing compounds would give the best chance of producing inversion stable ligands. The conjugation of the oxygen into the aromatic ring could limit the conjugation of the phosphorus lone pair into the aromatic ring, which would destabilize the planar pyramidal transition state and raise the inversion barrier energy. As the synthesis of phenolic groups from the benzylic compounds was extremely long and ultimately led to degradation, we hypothesised that synthesis of phenolic compounds as direct substrates for the enzymatic reactions would expedite this process. We had previously synthesised a phenolic derivative through the protection of 2-bromophenol (**181**) with DHP and catalytic *p*-TSA in DCM and then lithium-halogen exchange with *n*-BuLi to form the nucleophilic lithiated species followed by addition of dichlorophosphine and oxidation to the

phosphine oxide **183**. The THP group was then removed in acidic methanol to give the phosphine oxide **112** in 15% yield over the 4 steps (**Scheme 95**).



**Scheme 95** – Synthesis of the phosphine oxide **112** from **181**.

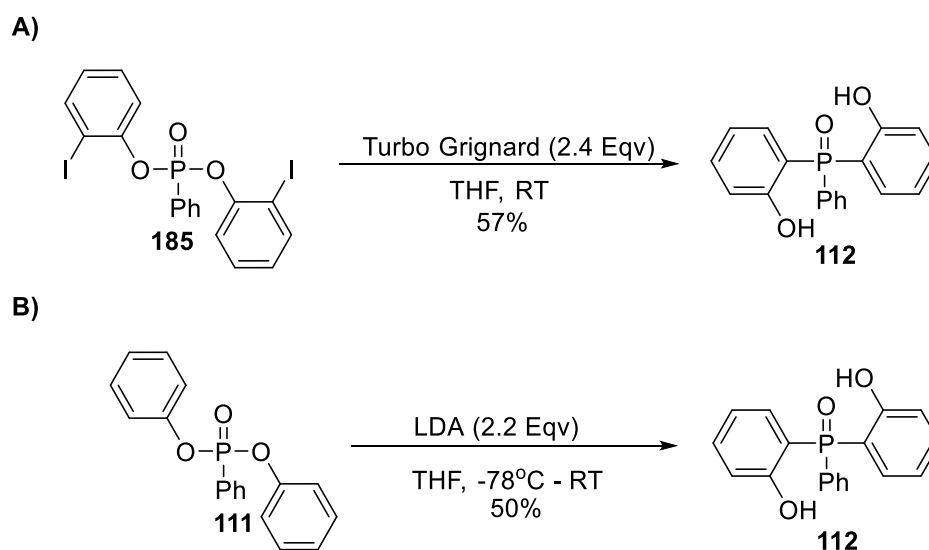
However, as the idea for the two-step synthesis of **102** had been adapted from the literature method for the synthesis of **112**, we already had an alternative two-step route in place to access the phenolic derivative **112** in good quantities for the screening of the enzymatic conditions. To compare our halogen-exchange rearrangement with the literature method, two different phosphonates **185** and **111** were synthesised (**Scheme 96**).



**Scheme 96** – Synthesis of the two phenolic phosphonates, **185** and **111** from 2-iodophenol and phenol, respectively.

The synthesis of the phosphonate from 2-iodophenol went in lower yield than that of the phenol derivative (56% against 70%), which is most likely due to the increased amount of lithium halogen exchange due to the *-ortho* directing effect of the oxygen. However, both phosphonates were synthesised in moderately high yields and were straightforward to purify by column chromatography. Rearrangement reactions were then attempted on the two different phosphonates which should give the same phosphine oxide product **112**. Turbo Grignard (2.4 eqv.) was added to the phosphonate **185** in THF at room temperature, which was analogous to the reaction conditions used for the benzyl alcohol derivatives described previously. Following the literature method for the rearrangement of **111**, LDA (2.2 eqv.) was added in THF at -78°C which was then slowly allowed to warm to room temperature and left to stir for 18 hours (**Scheme 97**). Both reactions were worked up identically and the resulting phosphine oxide was purified by column chromatography.



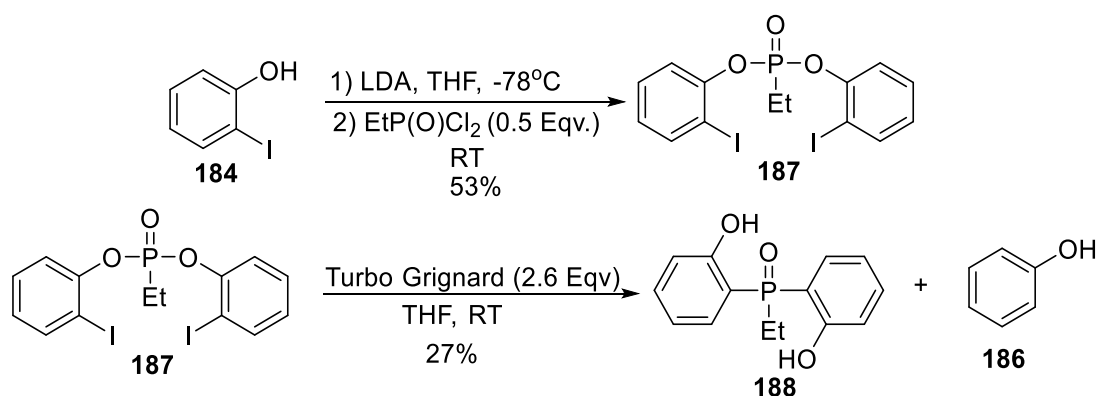


**Scheme 97** – A) Turbo Grignard mediated rearrangement of the 2-iodophenolic phosphonate **185** leading to **112**. B) LDA mediated rearrangement of the phenolic phosphonate **111** to **112**.

The rearrangement of **185** with Turbo Grignard went in 57% yield compared to the LDA mediated rearrangement which went in a slightly lower yield of 50% suggesting that the lithium halogen exchange is more favourable than the corresponding deprotonation of **111**. Further optimisation of the halogen exchange reaction could be done to increase the yields.

In addition, we also attempted the rearrangement of the ethyl phenolic derivative **187** as an expansion of the 1,3-rearrangement reaction. We hoped that the increased *-ortho* directing effect of the phenolic derivative, compared to a benzylic derivative which was also attempted (**Scheme 45**), may allow the rearrangement to occur more readily. Furthermore, the resulting ethyl containing phosphine could be advantageous due to the extra inversion

stability owed to alkyl derivatives. The phosphonate was synthesised as shown below in 53% yield and then the phosphonate was added to a solution of Turbo Grignard (2.6 Eqv.) in THF and left to stir for 24 hours. TLC analysis of the reaction showed 2 major spots which when purified were shown to be the expected rearrangement product **188** in 27% yield and a large amount of phenol which must have been displaced from the phosphonate (**Scheme 98**).

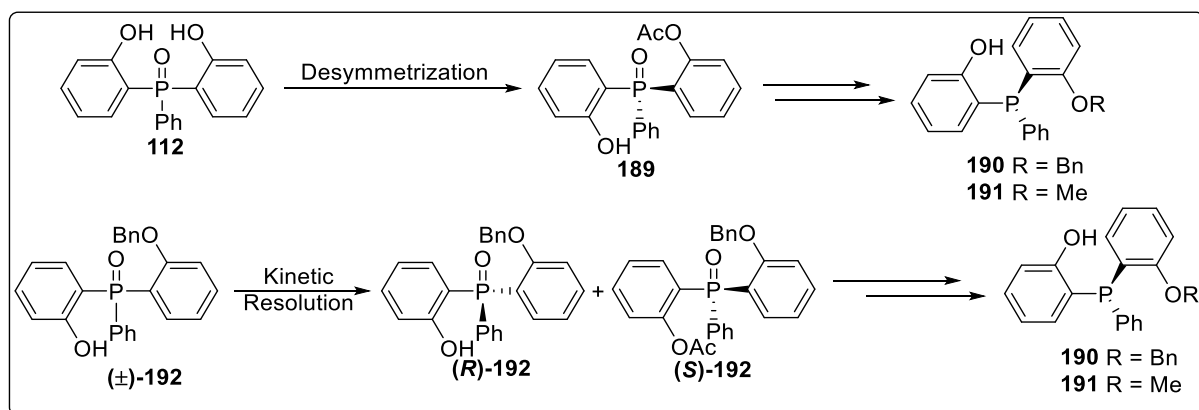


**Scheme 98** – Synthesis of the ethyl containing phosphonate **187** and its subsequent Turbo Grignard initiated rearrangement to give **188**.

## 8 – Enzymatic desymmetrization and kinetic resolutions of phenolic containing phosphine oxide derivatives

### 8.1 – Desymmetrization reactions

Now that we had synthesised the pro-chiral phosphine oxide **112**, we attempted to apply the enzymatic conditions which had been used to desymmetrize **102** previously, as these conditions were shown to give good conversion and high enantioselectivity (**Scheme 99**).



**Scheme 99** – Approaches to the enzymatic transformation of phenolic phosphine oxide **112** or racemic ( $\pm$ )-**192**.

The substrate **112** was screened against CAL-A immobilized on Purolite 'butyl epoxy resin, CAL-B and CAL-A immobead 150 from Sigma Aldrich using both acetate donors, VA and ISPA. The reactions contained 25 mM substrate and were shaken at 37°C for 18 hours after which an aliquot was taken and analysed by chiral HPLC using the corresponding racemic mono-acetate **189** standard. The enantiomers of **189** would not separate under the same HPLC conditions as the benzyl derivative **129** and so different chiral columns (AD-H and OJ) and HPLC methods were tested to try and separate the enantiomers. However, no baseline separation was possible but an estimation of the *e.e.* could be obtained from the analysis. We could then apply a modification to the structure which would allow us to separate and determine the exact *e.e.* of the modified structure.

The reactions using VA as the solvent showed no activity under any conditions, which is most likely due to the poor solubility of **112** in VA.

However, varying degree of conversion were observed when using ISPA and each of the three different enzymes (**Table 19**). CAL-A showed 34% conversion to the monoacetate product **189**. Increased product formation was seen with CAL-B and the purolite BE immobilized CAL-A showed almost complete conversion of the substrate to the mono-acetate and a large amount of the bis-acetate **193**. However, all reactions gave a low e.e. for **189** which was disappointing, given the success with the benzyl alcohol derivative **102** under these conditions. The e.e. could have increased slightly as the conversion to **189** increased but due to the poor selectivity over 18 hours, the reactions were not measured further. The poor enantioselectivity may be attributed to the lower steric bulk of the phenol derivative.

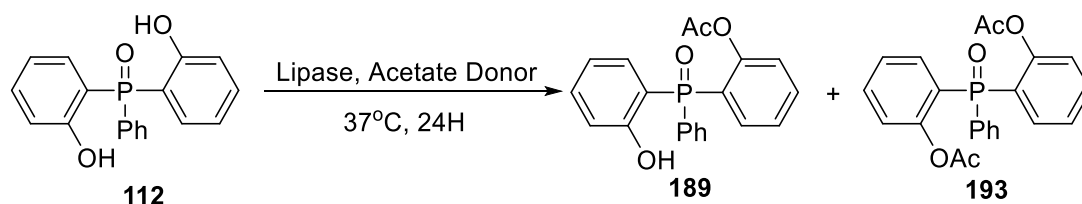
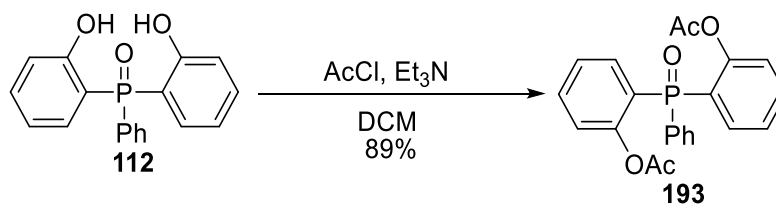


**Table 19** – Lipase-catalysed desymmetrization of **112**.

Enzyme	Acetate Donor	Conversion to <b>189</b>	Conversion to <b>193</b>	e.e. ( <b>189</b> )
CAL-B	ISPA	52%	6%	32%
CAL-A	ISPA	34%	5%	25%
Purolite BE	ISPA	45%	53%	27%
CAL-A				

Reaction Conditions: Incubated at 37°C at 180 RPM. Total volume 1 mL, 25 mM substrate, vinyl acetate to volume, 30 mg immobilized enzyme. HPLC Conditions: Daicel AD column, 1.2 mL/min, 80% Hexane/IPA at 210 nm.

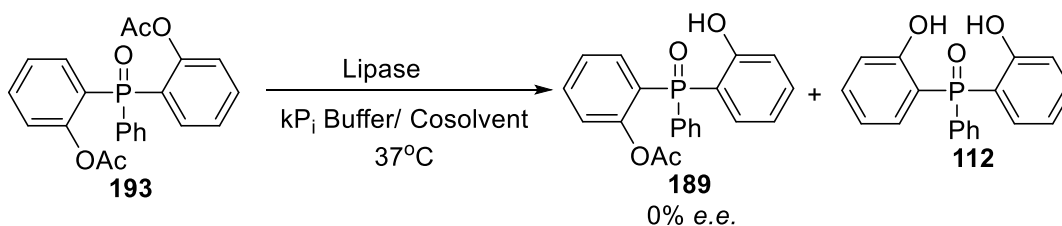
With this in mind, we hypothesised that the lipase-catalysed hydrolysis of the bulkier, bis-acetate **193**, may show improved selectivity due to greater steric demands in the enzyme active site. The bis-acetate was synthesised using AcCl and Et<sub>3</sub>N in DCM to give the product in high yield (89%) (**Scheme 100**).



**Scheme 100** – Synthesis of the phenolic bis-acetate **193** from the addition of Acetyl chloride and triethyl amine in DCM.

As shown previously in the lipase-catalysed hydrolysis reactions of **135**, the solubility of the triaryl phosphine oxide substrate in aqueous conditions was poor due to its lipophilicity. However, use of different co-solvents has been reported to increase the solubility of substrates in aqueous conditions whilst maintaining enzymatic hydrolytic activity. Four solvents which have shown success in lipase enantioselective hydrolysis reactions are acetone, THF, DMSO and *tert*-butanol<sup>[166-168]</sup>. Our substrate showed good solubility in DMSO and THF and poor solubility in both acetone and *tert*-butanol and so conditions for hydrolytic desymmetrisation of **193** were initially tested using mixtures of DMSO and buffer and THF and buffer. A range of different lipases was used including Immobead 150 CAL-A and CAL-B, Purolite immobilized CAL-A, *Humicola* sp., Novazyme 435 and PPL, alongside a control reaction which contained no enzyme to gauge background hydrolysis. The reactions were attempted on a 1 mL scale with 25 mM substrate with a 50:50 mix of the co-

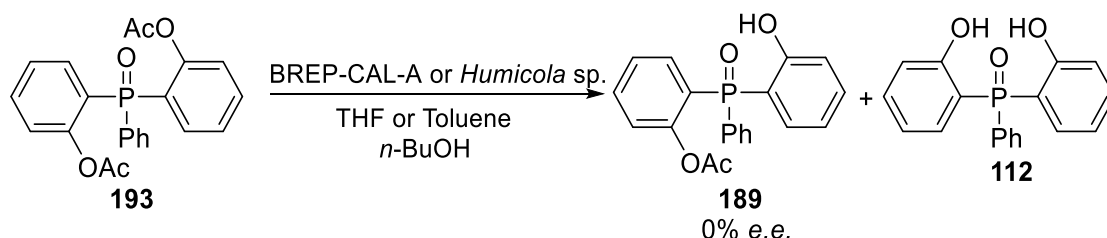
solvent (THF or DMSO) to buffer, which would hopefully ensure solubility of the substrate (**Scheme 101**). The reactions were shaken for 18 hours and an aliquot was taken after 2 hours and at the end of the 18-hour reaction for analysis by chiral HPLC. The control which contained no enzyme showed a large amount of background hydrolysis (up to 70%) giving both the mono-acetate **189** and **112**. This was seen across the whole series of reactions with no e.e. observed with any of the different lipases and conditions. This was most likely due to the instability of the phenolic acetate ester under aqueous conditions. Therefore, moving forward, we knew that the lipase-catalysed hydrolysis in aqueous conditions would not be useful for phenolic derivatives.



**Scheme 101** – The lipase catalysed hydrolytic desymmetrization of **193** which led to the formation of **189** and **112** in 0% e.e. due to background hydrolysis of the acetate ester.

Moving on from the aqueous hydrolysis, we hoped that the transesterification of the bis-acetate **193** with a suitable alcohol would be more promising as this would not require aqueous conditions and therefore would limit any background hydrolysis. Previous work within the group has shown that the use of a butanol rinsed enzyme preparation (BREP) of the lipase, *Humicola* sp., for the transesterification of enol acetate esters gave chiral molecules in high selectivity<sup>[168]</sup>. The BREPs were prepared through the addition of a solution of

the lipase enzyme, CAL-A or *Humicola* sp., to silica followed by a series of washes of the lipase-silica mixture with both *n*-butanol, and the reaction solvent of choice. For our reactions, we chose THF and toluene to act as the reaction solvent as our bis-acetate showed good solubility in both solvents and lipases also show high stability in these solvents. DMSO was no longer used for this reaction due to the difficulty in removing any residual DMSO prior to analysis by chiral HPLC as DMSO is detrimental to the column supports. The silica adsorbed CAL-A (150 mg) was added to the bis-acetate substrate (25 mM) in either THF or toluene (1 mL) as the reaction solvent and *n*-butanol was then added, in 3 equivalents with respect to the substrate, to start the transesterification (**Scheme 102**). The reactions were run alongside a control reaction in which the added silica was prepared through the series of solvent washes but in lieu of the addition of a lipase.



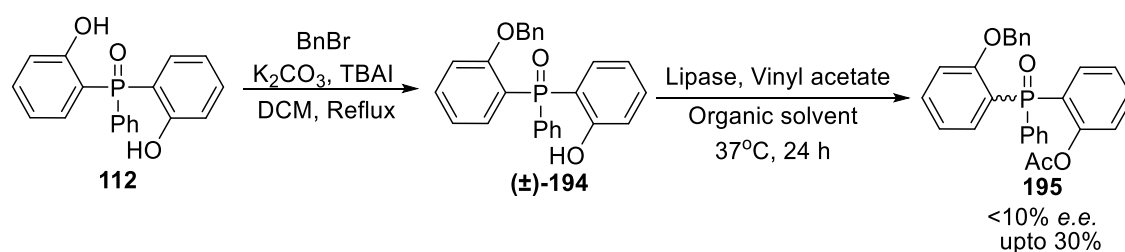
**Scheme 102** – Transesterification of **193** with BREP-CAL-A and BREP-*Humicola* sp.

The reactions were left to shake at 25°C and then an aliquot of the reaction was analysed by chiral HPLC to measure conversion and selectivity. The use of both enzymes with THF and toluene showed some transesterification activity as the monoacetate was present in all reactions ranging from 5% to 36% compared to the control reaction which showed no activity. The *Humicola*

sp. enzyme in THF showed the greatest amount of mono-acetate but unfortunately none of the reactions displayed any e.e.

## 8.2 - Kinetic resolution reactions

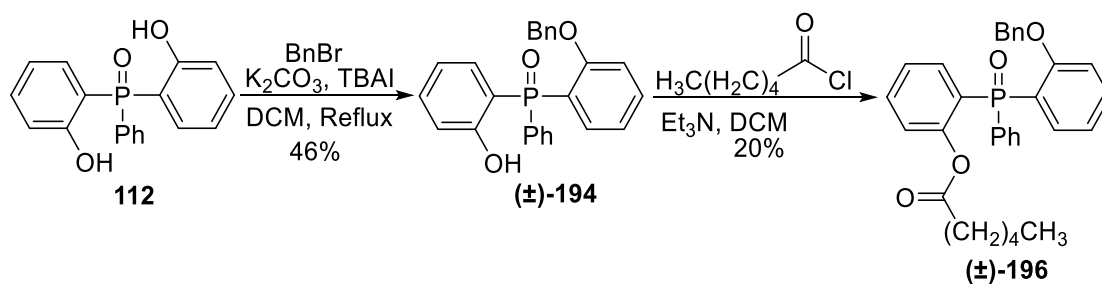
Due to the lack of any enzyme activity seen in the desymmetrization reactions, we attempted the kinetic resolution of several different compounds in hope that this would lead to enantioselectivity. We therefore synthesised the mono-benzylated phenolic derivative ( $\pm$ )-**194** (**Scheme 103**) and subjected the racemic mixture of ( $\pm$ )-**194** to the same conditions as those used in previously attempted kinetic resolutions but whilst conversion was modest (upto 30%), unfortunately a very low e.e. was observed.



**Scheme 103** – Lipase catalysed kinetic resolution of ( $\pm$ )-**194**.

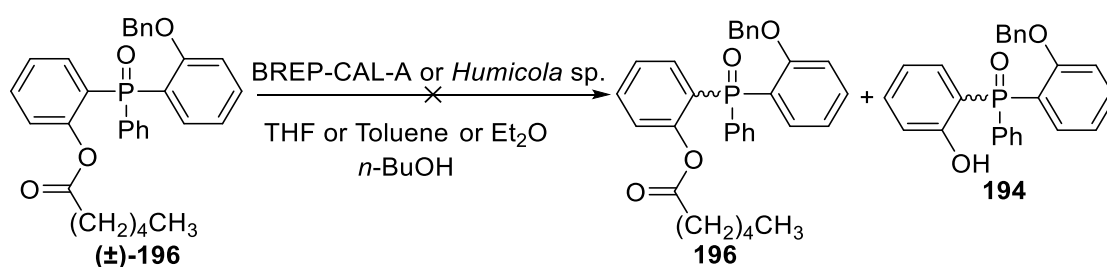
We hypothesised that moving to a bulkier ester, instead of the acetate ester, for the transesterification might give better results for a kinetic resolution and would be easier to analyse by chiral HPLC. Thus, we synthesised the phosphine oxide ( $\pm$ )-**196**, which contained the hexanoate ester and the benzyl ether (**Scheme 104**). This could increase the enantioselectivity in the formation of the acyl-enzyme complex.





**Scheme 104** – Synthesis of the mono-benzylated compound (±)-194 and the hexanoic ester derivative (±)-196.

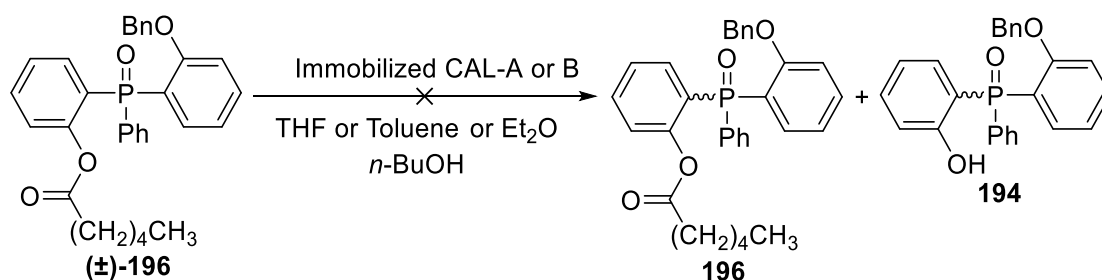
The hexanoate ester product (±)-196 was formed through the addition of thionyl chloride to hexanoic acid to form the hexanoyl chloride after which any excess thionyl chloride was removed, and then triethylamine and the phosphine oxide (±)-194 in DCM was added, to give the desired product (±)-196. The CAL-A and *Humicola* sp. BREP reactions were then attempted on this bulkier substrate with the inclusion of diethyl ether as a solvent as well as the previously utilised toluene and THF (**Scheme 105**).



**Scheme 105** – BREP-CAL-A/*Humicola* sp. transesterification of racemic (±)-196.

The reactions were attempted on the same scale as the previous BREP reactions and left to shake at 37°C for 24 hours after which an aliquot was analysed by chiral HPLC, which showed no activity in any of the reactions. We

then increased the concentration of BREP from 100 mg to 300 mg per 1 mL and the concentration of *n*-butanol from 75 mM to 150 mM and again left the reaction for another 24 hours at 37°C. After these increases in amounts of enzyme and *n*-butanol, the only substantial activity was only seen with diethyl ether with CAL-A, albeit extremely poor (<10%). In addition to these BREP reactions, the transesterification reaction was also attempted in parallel with the immobilized CAL-A and CAL-B with the three different solvents (**Scheme 106**) but as with the BREP reactions, no activity was seen in any case. This lack of activity could be due to the substrate molecule now being too large to fit into the active site of the enzyme.

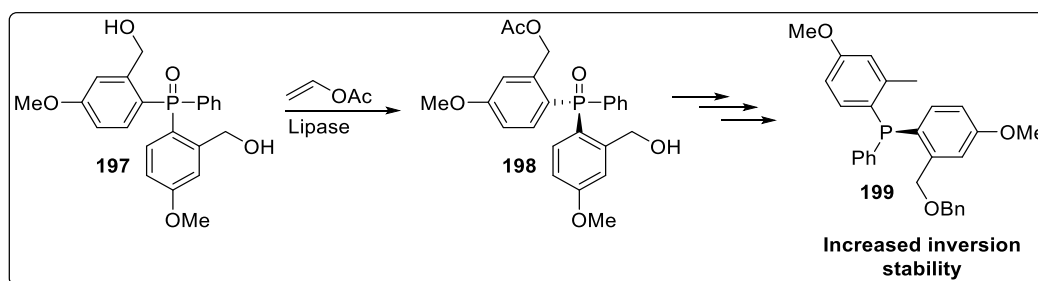


**Scheme 106** –CAL-A/B catalyzed transesterification of racemic (±)-**189**.

## 9 - Conclusion

We have successfully developed a chemo-enzymatic route to benzylic triaryl chiral phosphine oxides and phosphines which utilizes the enantioselectivity of enzymes in a lipase-catalysed desymmetrization. The use of Purolite BE immobilized CAL-A alongside vinyl acetate in optimized conditions gave the phosphine oxide **129** in yields of up to 70% with a e.e. of up to 96% (**Scheme**

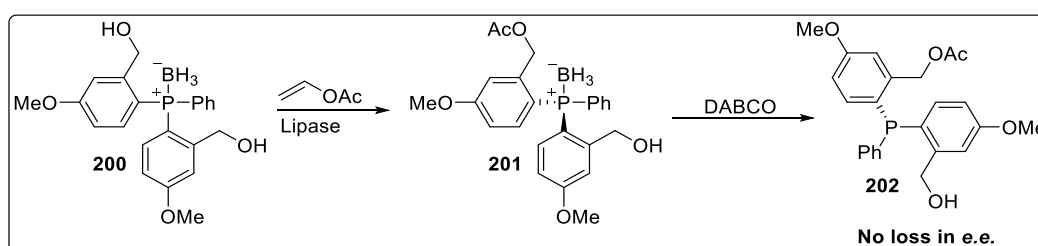
56). This enzymatic methodology could potentially be applied to several different benzylic triaryl phosphine oxide structures, with only minor adjustments to the synthetic route to the prochiral precursor. We then arrived at the 'ligand like' structure **148** through the cleavage of the acetate ester using nickel borohydride and the addition of a benzyl ether group on the remaining alcohol for stability and steric bulk. A modified method for the reduction of the phosphine oxide **148** was used utilizing titanium isopropoxide and either TMS or PMHS which yielded the chiral phosphine **152** with only small losses in *e.e.* (<4%) (**Table 16**). Although the phosphine **152** displayed poor stability to inversion, even at room temperature, further modifications to the structure with the inclusion of electron donating groups on the aromatic substituents (**197-199**) would destabilise the transition state for inversion, increasing stability (**Scheme 107**).



**Scheme 107** – Potential phosphine oxide and phosphine structures for increased inversion stability.

Future work should be focused around creating analogues of the benzylic phosphines and phosphine oxides which would display increased stability to inversion whilst retaining a 'ligand like' structure which would be applicable to copper-catalysed asymmetric 1,6-boration reactions. Furthermore, if the enzymatic kinetic resolution or desymmetrization of the phenolic analogues

could be achieved this would provide a quicker route to more stable phosphines. However, further work is needed to establish conditions which give both high conversion and enantioselectivity for the phenolic phosphine oxides. In addition, once a stable phosphine structure has been established the use of phosphine-boranes (**200** & **202**) could expedite the synthetic route, without the need for the difficult phosphine oxide reduction which leads to a slight loss in e.e. (**Scheme 108**).



**Scheme 108** – Use of phosphine-boranes to bypass the loss of e.e. which occurs during reduction of **152**.

## 10 - Experimental

### 10.1 - General experimental

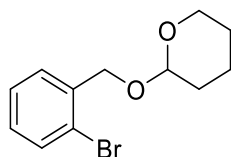
Analytical methods: Analytical thin layer chromatography (TLC) was performed on Whatman F254 precoated silica gel plates (250  $\mu\text{m}$  thickness). Visualization was accomplished with a UV light and/or a  $\text{KMnO}_4$  solution. Flash column chromatography (FCC) was performed using Whatman Silica Gel60 $\text{\AA}$  (230-400 mesh). Normal and reverse phase HPLC was performed on an Agilent system (Santa Clara, CA, USA) equipped with a G1379A degasser, G1312A binary pump, a G1329 well plate autosampler unit, a G1315B diode array detector and a G1316A temperature-controlled column compartment. The University of Liverpool Analytical Services Department provided mass spectrometry performed on a HR-ESI-MS TOF spectrometer (MicroMass). Solvents were of analytical or HPLC grade and were purchased or dried over molecular sieves where necessary. Potassium phosphate buffers were prepared using dibasic and monobasic potassium phosphate and pH adjusted to achieve the desired pH. Crude CAL-A solutions were purchased from STREM. Immobead CAL-A/B, PPL and *Humicola* sp. were purchased from Sigma Aldrich.  $^1\text{H}$  NMR and  $^{13}\text{C}$  NMR were recorded on Bruker AV 500 MHz & Bruker DPX 400 MHz NMR spectrometers in the indicated deuterated solvents. For  $^1\text{H}$  NMR  $\text{CDCl}_3$  was set to 7.26 ppm ( $\text{CDCl}_3$  singlet) and for  $^{13}\text{C}$  NMR to 77.66 ppm ( $\text{CDCl}_3$ , centre of triplet). All values for  $^1\text{H}$  NMR and  $^{13}\text{C}$  NMR chemical shifts for deuterated solvents were obtained from Cambridge Isotope Labs. Data are reported in the following order: chemical shift in ppm

( $\delta$ ), integration, (multiplicity, which are indicated by br (broadened), s (singlet), d (doublet), t (triplet), q (quartet), m (multiplet)) and coupling constants ( $J$ , Hz).

## 10.2 - Chapter 2 synthesis of phosphines and phosphine oxides

### experimental

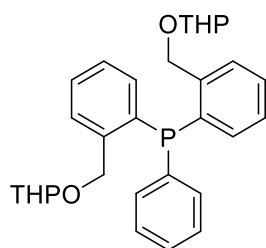
Synthesis of 2-((2-bromobenzyl)oxy)tetrahydro-2H-pyran (**97**)<sup>[170]</sup>



2-Bromobenzyl alcohol (**96**) (0.93 g, 5 mmol) was dissolved in DCM (50 mL) and DHP (0.5 mL, 5.5 mmol, 1.2 eqv.) was added followed by *p*-TSA (95 mg, 0.5 mmol). The reaction was left to stir at room temperature and monitored by TLC. When the reaction was deemed complete, the reaction was washed with sodium bicarbonate (10 mL), water (10 mL) and brine (10 mL) and the organic layer dried over  $MgSO_4$ , filtered and the solvent removed *in vacuo*. The crude product was purified by column chromatography (eluent: hexane:ethyl acetate; 33:1) to give the title compound (1.02g, 76%) as a clear liquid.  $^1H$  NMR ( $CDCl_3$ , 400MHz)  $\delta$  1.48-1.92 (6H, m), 3.54 (1H, m) 3.90 (1H, m) 4.55 (1H, d,  $J$ = 13.5 Hz), 4.75 (1H, t,  $J$  = 3.4 Hz), 4.81 (1H, d,  $J$  = 13.3 Hz, - $CH_2$ ), 7.09 (1H, td,  $J$  = 7.8, 1.6 Hz ), 7.27 (1H, td,  $J$  = 7.3 Hz, 3.6 Hz), 7.50 (2H, d,  $J$  = 7.9 Hz);  $^{13}C$  NMR ( $CDCl_3$ , 100 MHz)  $\delta$  19.3, 25.5, 30.5, 62.0, 68.5, 98.3, 122.7, 127.3,

128.7, 129, 132.4, 137.9. HRMS: (ESI<sup>+</sup>) Calculated for C<sub>12</sub>H<sub>15</sub>BrO<sub>2</sub>Na: 293.0148 Found [M+Na]<sup>+</sup>: 293.0138 (3.28 ppm), 295.0143 (3.44 ppm).

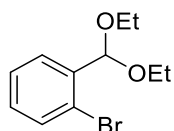
Synthesis of Phenylbis(2-(((tetrahydro-2H-pyran-2-yl)oxy)methyl)phenyl)phosphane (**99**)



To a solution of **90** (0.59 g, 2.1 mmol) in THF (20mL), 1.6 M *n*-BuLi (1.49 mL, 1.1 eqv.) was added dropwise at -78°C and the reaction left to stir for an hour. P,P-dichlorophenyl phosphine (0.14 mL, 1.08 mmol) was then added dropwise over 5 minutes and the reaction was allowed to warm to room temperature and was left for 24 hours. Water (10 mL) was then cautiously added to reaction and allowed to stir for ten minutes. The organic and aqueous layer were then separated and washed with water and ethyl acetate, respectively. The organic layer was then dried over MgSO<sub>4</sub>, filtered and the solvent removed *in vacuo* and the crude residue purified by column chromatography (eluent: hexane:ethyl acetate; 9:1) to leave the title compound (210 mg, 40%) as a viscous clear oil. <sup>1</sup>H NMR (CDCl<sub>3</sub>, 400 MHz) δ 1.18-1.69 (12H, m), 3.45 (2H, m), 3.81 (2H, m), 4.58 (2H, m) 4.71 (2H, m) 4.92 (2H, m), 6.85 (2H, dd, *J* = 7.2, 3.8 Hz), 7.15 – 7.24 (4H, m), 7.29 (3H, m), 7.33 (2H, m), 7.53 (2H, m).

HRMS: (ESI<sup>+</sup>) Calculated for C<sub>30</sub>H<sub>36</sub>O<sub>4</sub>P: 491.2346 Found [M+H]<sup>+</sup>: 491.2328 (3.59 ppm).

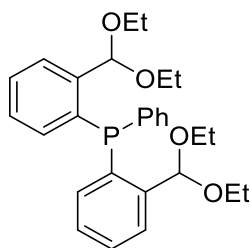
Synthesis of 1-bromo-2-(diethoxymethyl)benzene (**104**)<sup>[171]</sup>



To a solution of 2-bromobenzaldehyde (**103**) (1.26 mL, 10.8 mmol) in EtOH (15 mL), triethyl orthoformate (5.4 mL, 32.4 mmol) was added followed by a catalytic amount of conc. HCl. The reaction was left to stir at 50°C and was monitored by TLC. When complete, the volume of the reaction was reduced, and DCM (30 mL) was added followed by sodium bicarbonate (10 mL). The organic layer and aqueous layers were separated, and the organic layer washed with water (15 mL), brine (15 mL) and then dried over MgSO<sub>4</sub> and the solvent removed *in-vacuo*. The product was purified by column chromatography to leave the title compound (2.36 g, 84%) as a clear liquid. <sup>1</sup>H NMR (CDCl<sub>3</sub>, 400 MHz) δ 1.25 (6H, t, *J* = 7.1 Hz), 3.59 (2H, dq, *J* = 9.3, 7.0 Hz), 3.69 (2H, dq, *J* = 9.3, 7.0 Hz), 5.68 (1H, s), 7.15 (1H, dd, *J* = 7.9, 1.7 Hz), 7.32 (1H, dd, *J* = 11.1, 3.9 Hz), 7.53 (1H, dd, *J* = 8.0, 0.7 Hz), 7.68 (1H, dd, *J* = 8.0, 0.7 Hz). <sup>13</sup>C NMR (CDCl<sub>3</sub>, 100 MHz) δ 15.23, 62.37, 101.29, 122.99, 127.23, 128.31, 129.88, 137.97. HRMS: (ESI<sup>+</sup>) Calculated for C<sub>11</sub>H<sub>15</sub>O<sub>2</sub>BrNa : 281.0148 Found [M+Na]<sup>+</sup>: 281.0147 (0.17 ppm), 283.0133 (0.35 ppm).

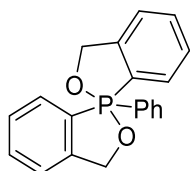


## Synthesis of bis(2-(diethoxymethyl)phenyl)(phenyl)phosphane (**105**)



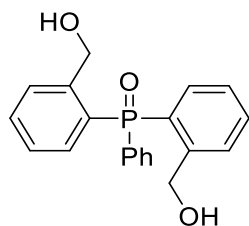
To a solution of **104** (1.82 g, 7.0 mmol) in anhydrous THF (50 mL) at  $-78^{\circ}\text{C}$ , was added 1.6 M *n*-BuLi (4.8 mL, 7.75 mmol) dropwise and the reaction left to stir for an hour. Dichlorophenyl phosphine (0.48 mL, 3.5 mmol) was then added dropwise over 5 minutes, the reaction was allowed to warm to room temperature and was left for 24 hours. Water (25 mL) was then cautiously added to reaction and allowed to stir for ten minutes. The organic and aqueous layer were then separated and washed with water and ethyl acetate, respectively. The organic layer was then dried over  $\text{MgSO}_4$ , filtered and the solvent removed *in vacuo* and the crude residue was purified by column chromatography (eluent: hexane:ethyl acetate; 19:1) to give the title compound (449 mg, 27%) as a yellow solid.  $^1\text{H}$  NMR ( $\text{CDCl}_3$ , 400 MHz)  $\delta$  0.95 (3H, t,  $J = 9.1$  Hz), 0.99 (3H, t,  $J = 9.1$  Hz), 3.39 (2H, m), 3.50 (2H, m), 6.11 (1H, s), 6.13 (1H, s), 6.95 (1H, dd,  $J = 4.4, 1.0$  Hz), 6.96 (1H, dd,  $J = 4.4, 1.0$  Hz), 7.25 (4H, m), 7.32 (3H, m), 7.30 (2H, td,  $J = 7.5, 1.1$  Hz), 7.76 (1H, dd,  $J = 4.2, 1.3$  Hz), 7.77 (1H, dd,  $J = 4.2, 1.3$  Hz).  $^{31}\text{P}$  NMR ( $\text{CDCl}_3$ , 162 MHz)  $\delta$  -28. HRMS: (ESI<sup>+</sup>) Calculated for  $\text{C}_{28}\text{H}_{35}\text{O}_5\text{PNa}$ : 505.2114 Found  $[\text{M}+\text{Na}]^+$ : 505.2115 (-0.09 ppm). Phosphine showed oxidation under analysis.

Synthesis of 1-phenyl-1,3,3'-trihydro-1H-1,1'-spiro[benzo[c][1,2]oxaphosphole] (**110**)<sup>[75,76]</sup>



To a solution of **102** (100 mg, 0.3 mmol) in THF (5 mL) was added 1 M HCl (0.3 mL, 0.3 mmol) and the reaction left to stir for 12 hours at 60°C. Once complete, the reaction was neutralized with sodium bicarbonate and the aqueous layer extracted with ethyl acetate (3 x 5 mL). The organic layer was then dried over magnesium sulphate, filtered and the solvent removed *in vacuo*. The residue was then purified by column chromatography (eluent: hexane:ethyl acetate; 95:5) to give the title compound (84 mg, 87%) as a white solid. <sup>1</sup>H NMR (CDCl<sub>3</sub>, 400 MHz) δ 4.93 (2H, dd, *J* = 14.2, 2.2 Hz), 5.11 (2H, dd, *J* = 14.2, 5.7 Hz), 7.32 (5H, m), 7.45 (2H, m), 7.52 (2H, m), 7.62 (2H, m), 8.39 (2H, m). <sup>13</sup>C NMR (CDCl<sub>3</sub>, 100 MHz) δ 65.7, 122.4 (d, *J* = 16.3 Hz), 127.7 (d, *J* = 13.3 Hz), 127.9 (d, 15.3 Hz), 129.1 (d, *J* = 3.3 Hz), 129.6-131.3 (d, *J* = 168.6 Hz), 130.4 (d, *J* = 11.5 Hz), 131.8 (d, *J* = 3.3 Hz), 140.1 (d, *J* = 165.1 Hz), 148.4 (d, *J* = 27.0 Hz). <sup>31</sup>P NMR (CDCl<sub>3</sub>, 162 MHz) δ -36.4. HRMS: (ESI<sup>+</sup>) Calculated for C<sub>20</sub>H<sub>18</sub>O<sub>2</sub>P: 321.1039 Found [M+H]<sup>+</sup>: 321.1043 (-1.41 ppm).

Synthesis of bis(2-(hydroxymethyl)phenyl)(phenyl)phosphine oxide (**102**)<sup>[73]</sup>



*Method A*

To a solution of **97** (1.5 g, 5.56 mmol) in anhydrous THF (80 mL) at  $-78^{\circ}\text{C}$ , was added 1.6 M *n*-BuLi (3.82 mL, 6.11 mmol) dropwise and the reaction left to stir for an hour. P,P-dichlorophenylphosphine (0.37 mL, 2.78 mmol) was then added dropwise over 5 minutes, the reaction was allowed to warm to room temperature and was left for 24 hours. Water (30 mL) was then cautiously added to reaction and allowed to stir for ten minutes. The organic and aqueous layer were then separated and washed with water and ethyl acetate, respectively. The organic layer was then dried over  $\text{MgSO}_4$ , filtered and the solvent removed *in vacuo* and the crude residue was dissolved in 2:1 solution of DCM (30 mL) and  $\text{H}_2\text{O}$  (15 mL) and  $\text{H}_2\text{O}_2$  (0.63 mL, 5.56 mmol) was added and the reaction was left to stir for 2 hours. The organic and aqueous layer were then separated and washed with  $\text{H}_2\text{O}$  and DCM, respectively. The organic layer was then dried over  $\text{MgSO}_4$ , filtered and the solvent removed to leave a crude residue which was dissolved in MeOH (10 mL) and *p*-TSA (53 mg, 0.27 mmol) and left to stir for 5 hours after which the reaction was washed with sat. sodium bicarbonate solution (10 mL). The organic layer and aqueous layer were separated and the organic layer dried over  $\text{MgSO}_4$ , filtered and the solvent removed after which the crude residue was purified by column

chromatography (eluent: ethyl acetate:hexane; 3:2) to give the title compound (210 mg, 23%) as a white solid.  $^1\text{H}$  NMR ( $\text{CDCl}_3$ , 400 MHz)  $\delta$  4.58 (2H, d,  $J = 12.9$  Hz), 4.67 (2H, d,  $J = 12.9$  Hz), 5.22 (2H, br, -OH), 6.92 (2H, dd,  $J = 14.4$ , 7.6 Hz), 7.27 (2H, m), 7.56 (9H, m).  $^{13}\text{C}$  NMR ( $\text{CDCl}_3$ , 400 MHz)  $\delta$  64.5 (d,  $J = 5.0$  Hz), 127.4 (d,  $J = 13.2$  Hz), 128.7 (d,  $J = 33.0$  Hz), 129.83, 130.4, 130.8, 131.5, 131.8 (d,  $J = 10.1$  Hz), 132.1 (d,  $J = 10.1$  Hz), 132.7 (d,  $J = 2.8$  Hz), 133.2 (d,  $J = 2.7$  Hz), 133.5 (d,  $J = 133$ .Hz), 146.5 (d,  $J = 7.7$  Hz).  $^{31}\text{P}$  NMR ( $\text{CDCl}_3$ , 162 MHz)  $\delta$  40.49. HRMS: (ESI $^+$ ) Calculated for  $\text{C}_{20}\text{H}_{19}\text{O}_3\text{PNa}$ : 361.0964 Found  $[\text{M}+\text{Na}]^+$ : 361.0971 (-1.86 ppm). HPLC separation (DAICEL AD, hexane/isopropanol 83:17, 1.2 mL/min, UV = 254, 210 nm;  $t_R = 19.4$  min.

#### *Method B*

Hydrolysis of spirophosphorane **110** to give bis(2-(hydroxymethyl)phenyl)(phenyl)phosphine oxide (**102**)

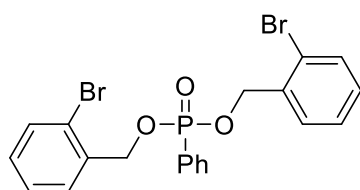
Spirophosphorane **110** (0.65 g, 1.29 mmol) was dissolved in a 2:1 solution of ethanol (10 mL) and water (5 mL). Conc. HCl (0.5 mL) was then added dropwise and the reaction was stirred at 50°C and monitored by TLC. After 24 hours, no starting material or spirophosphorane remained and the reaction volume was reduced and then neutralized by the addition of sat. sodium bicarbonate solution. The product was then extracted with DCM (20 mL x 3), and the organic layer dried over  $\text{MgSO}_4$ , filtered and the solvent removed *in vacuo*. The product was then purified by column chromatography (eluent: ethyl

acetate:hexane; 3:2) to give the title compound (406 mg, 93%) as a white solid.

Data identical to method A.

### 10.3 - Chapter 2.3 phosphonate synthesis and rearrangement experimental

Synthesis of bis((2-bromophenoxy)methyl)(phenyl)phosphine oxide (**114**)



#### *Method A*

To a solution of **106** (0.93 g, 8.92 mmol) in THF (60 mL) was added, DMAP (31 mg, 0.44 mmol), triethyl amine (1.2 mL, 21.6 mmol) followed by dichlorophenyl phosphine (0.34 mL, 4.46 mmol) and the reaction was left to stir at room temperature for 4 hours. After this time, H<sub>2</sub>O (30 mL) was added and the aqueous and organic layers were separated and washed with ethyl acetate and water, respectively. The organic layer was then dried over MgSO<sub>4</sub>, filtered and the solvent removed. The residue was then dissolved in a 2:1 solution of DCM and H<sub>2</sub>O and 30% H<sub>2</sub>O<sub>2</sub> (0.56 mL, 8.92 mmol) was added and the reaction stirred for 2 hours. The organic and aqueous layer were then separated and washed with H<sub>2</sub>O and DCM, respectively. The organic layer

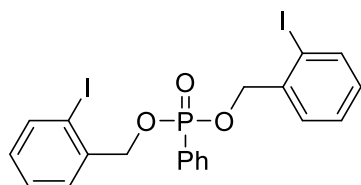
was then dried over MgSO<sub>4</sub>, filtered and the solvent removed to leave a crude residue which was purified by column chromatography (eluent: hexane:ethyl acetate; 75:25) to give the title compound (0.71 g, 32%) as a clear oil. <sup>1</sup>H NMR (CDCl<sub>3</sub>, 400 MHz) δ 5.10 (2H, dd, *J* = 12.7, 7.2 Hz), 5.18 (2H, dd, *J* = 12.7 Hz, 7.2 Hz), 7.12 (2H, t, *J* = 7.6 Hz), 7.26 (2H, t, *J* = 7.5 Hz), 7.40 – 7.58 (7H, m), 7.86 (1H, d, *J* = 8.0 Hz), 7.89 (1H, d, *J* = 7.2 Hz). <sup>13</sup>C NMR (CDCl<sub>3</sub>, 400 MHz) δ 67.0 (d, *J* = 4.9 Hz), 122.6, 127.5, 128.5 (d, *J* = 15.3 Hz), 129.3, 129.7, 131.8 (d, *J* = 10.1 Hz), 132.6, 132.8 (d, *J* = 3.1 Hz), 135.4 (d, *J* = 7.5 Hz). <sup>31</sup>P NMR (CDCl<sub>3</sub>, 162 MHz) δ 19.79. HRMS: (ESI<sup>+</sup>) Calculated for C<sub>20</sub>H<sub>17</sub>Br<sub>2</sub>O<sub>3</sub>PNa: 519.9174 Found [M+Na]<sup>+</sup>: 516.9179 (-0.02 ppm), 517.9213 (-0.01 ppm), 518.9159 (0.01 ppm), 519.9174 (-0.01 ppm), 520.9139 (-0.02 ppm), 521.9172 (0.02 ppm).

#### Method B

To a solution of diisopropyl amine (1.69 mL, 12 mmol) in THF (40 mL) at -78°C was added 1.6 M *n*-BuLi (6.87 mL, 11 mmol) and the reaction stirred for 10 minutes. After this, 2-bromobenzyl alcohol (1.87 g, 10 mmol) was added and stirred for a further 30 minutes after which, phenyl phosphinic dichloride (0.786 mL, 5 mmol) was added and the reaction allowed to warm to room temperature and was left for 16 hours. Water (20 mL) was then added to the reaction and the organic and aqueous layers were separated and washed with water and ethyl acetate, respectively. The organic layer was then dried over MgSO<sub>4</sub>, filtered, the solvent removed *in vacuo* and the crude material purified by

column chromatography (eluent: hexane:ethyl acetate; 75:25 to give the title compound (1.85 g, 75%) as a clear oil. Data identical to method A.

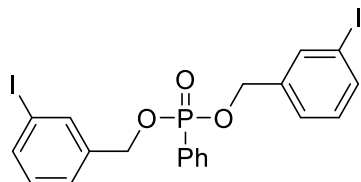
#### Synthesis of bis(2-iodobenzyl) phenylphosphonate (**118**)



To a solution of diisopropyl amine (1.97 mL, 14 mmol) in THF (80 mL) at  $-78^{\circ}\text{C}$  was added 1.6 M n-BuLi (7.5 mL, 12 mmol) and the reaction stirred for 10 minutes. After this, 2-iodobenzyl alcohol (2.34 g, 10 mmol) was added and stirred for a further 30 minutes after which, phenyl phosphinic dichloride (0.74 mL, 5 mmol) was added and the reaction allowed to warm to room temperature and was left for 16 hours. Water (40 mL) was then added to the reaction and the organic and aqueous layers were separated and washed with water and ethyl acetate, respectively. The organic layer was then dried over  $\text{MgSO}_4$ , filtered, the solvent removed *in vacuo* and the crude material purified by column chromatography (eluent: hexane:ethyl acetate; 75:25) to give the title compound (2.2 g, 75%) as a clear oil.  $^1\text{H}$  NMR ( $\text{CDCl}_3$ , 400 MHz)  $\delta$  5.09 (2H, dd,  $J = 12.7, 7.4$  Hz), 5.13 (2H, dd,  $J = 12.7, 7.4$  Hz), 6.97 (2H, t,  $J = 7.6$  Hz), 7.30 (2H, t,  $J = 7.5$  Hz), 7.42 (2H, d,  $J = 7.7$  Hz), 7.45 (2H, m), 7.55 (1H, t,  $J = 7.4$  Hz), 7.78 (2H, d,  $J = 7.9$  Hz), 7.8 (2H, dd,  $J = 13.6, 7.8$  Hz).  $^{13}\text{C}$  NMR ( $\text{CDCl}_3$ , 400 MHz)  $\delta$  71.39 (d,  $J = 5.0$  Hz), 128.4, 128.5, 128.6, 129.0, 129.9, 131.9 (d,  $J = 10.2$  Hz), 132.8 (d,  $J = 3.1$  Hz), 138.4 (d,  $J = 7.5$  Hz), 139.3.  $^{31}\text{P}$

NMR (CDCl<sub>3</sub>, 162 MHz)  $\delta$  19.52. HRMS: (ESI<sup>+</sup>) Calculated for C<sub>20</sub>H<sub>17</sub>I<sub>2</sub>O<sub>3</sub>PNa: 612.8897 Found [M+Na]<sup>+</sup>: 612.8904 (1.16 ppm).

Synthesis of bis(3-iodobenzyl) phenylphosphonate (**127**)

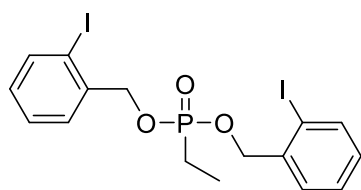


To a solution of diisopropyl amine (1.97 mL, 14 mmol) in THF (80 mL) at -78°C was added 1.6 M *n*-BuLi (7.5 mL, 12 mmol) and the reaction stirred for 10 minutes. After this, 3-iodobenzyl alcohol (1 g, 4.2 mmol) was added and stirred for a further 30 minutes after which, phenyl phosphinic dichloride (0.74 mL, 5 mmol) was added and the reaction allowed to warm to room temperature and was left for 16 hours. Water (15 mL) was then added to the reaction and the organic and aqueous layers were separated and washed with water and ethyl acetate, respectively. The organic layer was then dried over MgSO<sub>4</sub>, filtered, the solvent removed *in vacuo* and the crude material purified by column chromatography (eluent: hexane:ethyl acetate; 75:25) to give the title compound (2.6 g, 89%) as a clear oil. <sup>1</sup>H NMR (CDCl<sub>3</sub>, 400 MHz)  $\delta$  4.97 (2H, dd, *J* = 12.1, 8.0 Hz), 5.05 (2H, dd, *J* = 12.1, 8.0 Hz), 7.05 (2H, t, *J* = 7.8 Hz), 7.27 (2H, d, *J* = 7.8 Hz), 7.46 (2H, m), 7.56 (1H, t, *J* = 7.4 Hz), 7.68 – 7.59 (4H, m), 7.78 (1H, d, *J* = 7.7 Hz), 7.81 (1H, d, *J* = 7.8 Hz). <sup>13</sup>C NMR (CDCl<sub>3</sub>, 100 MHz)  $\delta$  <sup>13</sup>C NMR (101 MHz, CDCl<sub>3</sub>)  $\delta$  66.57 (d, *J* = 5.3 Hz), 94.3, 126.4, 127.0, 128.2, 128.6 (d, *J* = 15.3 Hz), 130.3, 131.8 (d, *J* = 10.2 Hz), 132.9 (d, *J* = 3.1



Hz), 136.6, 137.4, 138.2 (d,  $J = 6.6$  Hz).  $^{31}\text{P}$  ( $\text{CDCl}_3$ , 162 MHz)  $\delta$  20.07. HRMS: (ESI $^+$ ) Calculated for  $\text{C}_{20}\text{H}_{17}\text{I}_2\text{O}_3\text{PNa}$ : 612.8896 Found  $[\text{M}+\text{Na}]^+$ : 612.8912 (2.46 ppm).

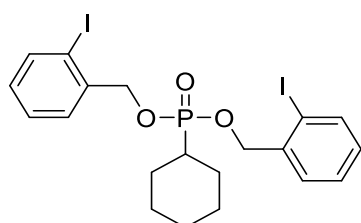
#### Synthesis of bis(2-iodobenzyl) ethylphosphonate (**119**)



To a solution of diisopropyl amine (1.97 mL, 14 mmol) in THF (60 mL) at  $-78^\circ\text{C}$  was added 1.6 M *n*-BuLi (7.5 mL, 12 mmol) and the resulting mixture was stirred for 10 minutes. 2-Iodobenzyl alcohol (2.46 g, 10 mmol) was added and the reaction was warmed to room temperature and stir for 30 minutes. Ethyl phosphinic dichloride (0.51 mL, 5 mmol) was then added dropwise and the reaction was left to stir for 24 hours after which sat. ammonium chloride (40 mL) was added and aqueous layer was extracted with ethyl acetate (3 x 25 mL). The organic layer was then dried over  $\text{MgSO}_4$ , filtered and the solvent removed *in-vacuo* and the crude material purified by column chromatography (eluent: hexane:ethyl acetate; 3:2) to give the title compound (1.5 g, 56%) as a clear oil.  $^1\text{H}$  NMR ( $\text{CDCl}_3$ , 400 MHz)  $\delta$  1.21 (3H, dt,  $J = 20.5, 7.7$  Hz), 1.88 (2H, dq,  $J = 18.3, 7.7$  Hz), 5.02 (2H, dd,  $J = 11.3, 5.9$  Hz), 5.04 (2H, dd,  $J = 11.3, 5.9$  Hz), 7.00 (2H, td,  $J = 7.8, 1.7$  Hz), 7.34 (2H, td,  $J = 7.6, 1.0$  Hz), 7.43 (2H, dd,  $J = 7.7, 1.4$  Hz), 7.81 (2H, dd,  $J = 7.9, 0.9$  Hz).  $^{13}\text{C}$  NMR ( $\text{CDCl}_3$ , 100 MHz) 6.6 (d,  $J = 6.9$  Hz), 18.4, 19.8, 70.9 (d,  $J = 6.0$  Hz), 97.48, 128.4, 128.9,

129.8, 138.7 (d,  $J = 6.7$  Hz), 139.3.  $^{31}\text{P}$  NMR ( $\text{CDCl}_3$ , 162 MHz)  $\delta$  34.73.  
HRMS: (ESI $^+$ ) Calculated for  $\text{C}_{16}\text{H}_{17}\text{O}_3\text{PI}_2\text{Na}$ : 565.8902 Found  $[\text{M}+\text{Na}]^+$ :  
565.8911 (1.14 ppm).

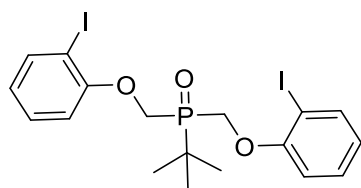
### Synthesis of the bis(2-iodobenzyl) cyclohexylphosphonate (**121**)



To a solution of diisopropyl amine (1.41 mL, 10 mmol), in THF (60 mL) at  $-78^\circ\text{C}$  was added 1.6 M *n*-BuLi (5.4 mL, 8 mmol) and the resulting mixture stirred for 10 minutes. 2-Iodobenzyl alcohol (1.76 g, 7.2 mmol) was added and the reaction was warmed to room temperature and stir for 30 minutes. Dichlorocyclohexyl phosphine (0.66 g, 3.6 mmol) was then added dropwise and the reaction was left to stir for 24 hours after which sat. ammonium chloride (40 mL) was added and aqueous layer was extracted with ethyl acetate (3 x 25 mL). The organic layer was then dried over  $\text{MgSO}_4$ , filtered and then dissolved in a 2:1 solution of DCM to water, then 30 % hydrogen peroxide (1 mL, 2 eqv.) was added and left to stir for 2 hours. Water (10 mL) was then added to the reaction and the organic layer separated and the aqueous layer was washed with DCM (10 mL). The organic layers were then combined, dried over  $\text{MgSO}_4$ , filtered and solvent removed *in-vacuo* and the crude material purified by column chromatography (eluent: hexane:ethyl

acetate; 85:15) to give the title compound (0.9 g, 42%) as a white solid.  $^1\text{H}$  NMR ( $\text{CDCl}_3$ , 400 MHz)  $\delta$  1.15-2.09 (11H, m), 5.02 (2H, dd,  $J = 11.5, 7.5$  Hz), 5.06 (2H, dd,  $J = 11.5, 7.5$  Hz), 6.97 (2H, td,  $J = 7.7, 1.5$  Hz), 7.32 (2H, td,  $J = 7.7, 1.1$  Hz), 7.42 (2H, dd,  $J = 7.6, 1.2$  Hz), 7.78 (2H, dd,  $J = 7.9, 0.9$  Hz).  $^{13}\text{C}$  NMR ( $\text{CDCl}_3$ , 100 MHz) 25.77 (d,  $J = 1.4$  Hz), 25.8 (d,  $J = 4.6$  Hz), 26.0 (d,  $J = 16.5$  Hz), 35.9 (d,  $J = 141.43$  Hz), 70.8 (d,  $J = 6.4$  Hz), 97.5, 128.4, 128.9, 129.7, 138.9 (d,  $J = 6.6$  Hz), 139.3.  $^{31}\text{P}$  NMR ( $\text{CDCl}_3$ , 162 MHz)  $\delta$  33.86. HRMS: (ESI $^+$ ) Calculated for  $\text{C}_{20}\text{H}_{23}\text{O}_3\text{P}_2\text{Na}$ : 618.9366 Found  $[\text{M}+\text{Na}]^+$ : 618.9369 (-0.35 ppm).

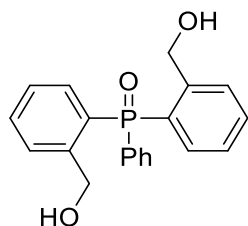
#### Synthesis of *tert*-butylbis((2-iodophenoxy)methyl)phosphine oxide (**124**)



To a solution of diisopropyl amine (2 mL, 114 mmol), in THF (60 mL) at  $-78^\circ\text{C}$  was added 1.6 M *n*-BuLi (7.5 mL, 12 mmol) and the resulting mixture stirred for 10 minutes. 2-Iodobenzyl alcohol (2.34 g, 10 mmol) was added and the reaction was warmed to room temperature and stir for 30 minutes. Dichloro *t*-butyl phosphine (0.8 g, 5 mmol) was then added dropwise and the reaction was left to stir for 24 hours. After which sat. ammonium chloride (40 mL) was added and aqueous layer was extracted with ethyl acetate (3 x 25 mL). The organic layer was then dried over  $\text{MgSO}_4$ , filtered, and then dissolved in a 2:1 solution of DCM to water, then hydrogen peroxide (1 mL, 2 eqv.) was added

and left to stir for 2 hours. Water (10 mL) was then added to the reaction and the organic layer separated and the aqueous layer was washed with DCM (10 mL). The organic layers were then combined, dried over MgSO<sub>4</sub>, filtered and solvent removed *in-vacuo* and the crude material purified by column chromatography (eluent: hexane:ethyl acetate; 80:20) to give the title compound (1.15 g, 41%) as a white solid. <sup>1</sup>H NMR (CDCl<sub>3</sub>, 400 MHz) δ 1.26 (9H, d, *J* = 17.1 Hz), 4.98 (2H, dd, *J* = 12.1, 7.6 Hz), 5.04 (2H, dd, *J* = 12.1, 7.6 Hz), 6.97 (2H, td, *J* = 7.7, 1.7 Hz), 7.32 (2H, td, *J* = 7.6, 1.0 Hz), 7.42 (2H, dd, *J* = 7.7, 1.5 Hz), 7.78 (2H, dd, *J* = 7.9, 1.0 Hz). <sup>13</sup>C NMR (CDCl<sub>3</sub>, 100 MHz) δ 24.8 (d, *J* = 2.3 Hz), 31.8 (d, *J* = 141.5 Hz), 71.1 (d, *J* = 6.9 Hz), 97.5 (d, *J* = 13.2 Hz), 128.4, 128.8, 129.7, 139.0 (d, *J* = 6.2 Hz), 139.3. <sup>31</sup>P NMR (CDCl<sub>3</sub>, 162 MHz) δ 38.16. HRMS: (ESI<sup>+</sup>) Calculated for C<sub>18</sub>H<sub>21</sub>I<sub>2</sub>O<sub>3</sub>PNa: 592.921 Found [M+Na]<sup>+</sup>: 592.9208 (0.25 ppm).

Synthesis of **102** by 1,4-rearrangement of bis(2-iodobenzyl) phenylphosphonate (**118**)



#### Method A

To a solution of bis(2-iodobenzyl) phenylphosphonate **118** (0.675 g, 1.14 mmol) in THF (20 mL) at -78°C was added 1.6 M *n*-BuLi (1.57 mL, 2.51 mmol)

and the reaction left to warm up to room temperature over 24 hours. After this, water (10 mL) was added and the organic and aqueous layer separated and washed with water and ethyl acetate, respectively. The organic layer was then dried over  $\text{MgSO}_4$ , filtered and the solvent removed *in vacuo* to leave a crude oil which was purified by column chromatography (eluent: chloroform:acetone; 9:1) to give the title compound (0.14 g, 37%) as a white solid.  $^1\text{H}$  NMR ( $\text{CDCl}_3$ , 400 MHz)  $\delta$  4.58 (2H, d,  $J = 12.9$  Hz), 4.67 (2H, d,  $J = 12.9$  Hz), 5.22 (2H, br, -OH), 6.92 (2H, dd,  $J = 14.4, 7.6$  Hz), 7.27 (2H, m), 7.56 (9H, m).  $^{13}\text{C}$  NMR ( $\text{CDCl}_3$ , 400 MHz)  $\delta$  64.5 (d,  $J = 5.0$  Hz), 127.4 (d,  $J = 13.2$  Hz), 128.7 (d,  $J = 33.0$  Hz), 129.83, 130.4, 130.8, 131.5, 131.8 (d,  $J = 10.1$  Hz), 132.1 (d,  $J = 10.1$  Hz), 132.7 (d,  $J = 2.8$  Hz), 133.2 (d,  $J = 2.7$  Hz), 133.5 (d,  $J = 133$ .Hz), 146.5 (d,  $J = 7.7$  Hz).  $^{31}\text{P}$  NMR ( $\text{CDCl}_3$ , 162 MHz)  $\delta$  40.49. HRMS: (ESI<sup>+</sup>) Calculated for  $\text{C}_{20}\text{H}_{19}\text{O}_3\text{PNa}$ : 361.0964 Found  $[\text{M}+\text{Na}]^+$ : 361.0971 (-1.86 ppm). HPLC separation (DAICEL AD, hexane/isopropanol 83:17, 1.2 mL/min, UV = 254, 210 nm; tR = 19.4 min.

## Method B

To a solution of bis(2-iodobenzyl) phenylphosphonate (1.79 g, 3 mmol) in THF (30 mL) was added 1.3 M  $(\text{CH}_3)_2\text{CHMgCl} \cdot \text{LiCl}$  (5.63 mL, 7.2 mmol) and the reaction left to stir at room temperature for 24 hours. After this, the reaction was washed with sat. ammonium chloride solution (15 mL). The organic and aqueous layers were then separated and washed with water and ethyl acetate, respectively. The organic layer was then dried over  $\text{MgSO}_4$ , filtered and the solvent removed *in vacuo* to leave a crude oil which was purified by

recrystallization from 3:2 ethyl acetate to hexane to give the title compound (0.66 g, 65%) as a white solid. Data identical to method A.

#### **10.4 - Chapter 3 enzymatic desymmetrization and kinetic resolution reactions experimental**

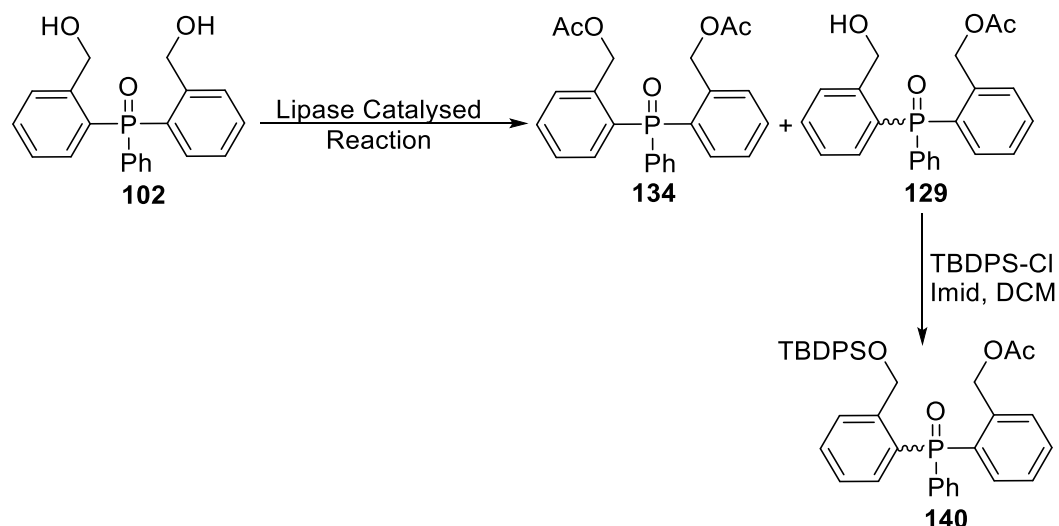
##### Enzyme Condition screening HPLC

HPLC analysis was undertaken on an Agilent Infinity 1260 HPLC, using a DAICEL Chiralpak-AD column (Daicel, 5  $\mu$ m particle size, 250 mm x 4.6 mm). The mobile phase comprised of (A) IPA: (B) Hexane with an isocratic system of 17% (A) to 83% (B) with a flow rate of 1.2 mL/min, an injection volume of 5  $\mu$ L and a column temperature of 30°C. Signals were recorded at 200 nm, 210 nm, 220 nm, 254 nm.

##### Lipase Enzyme Assay

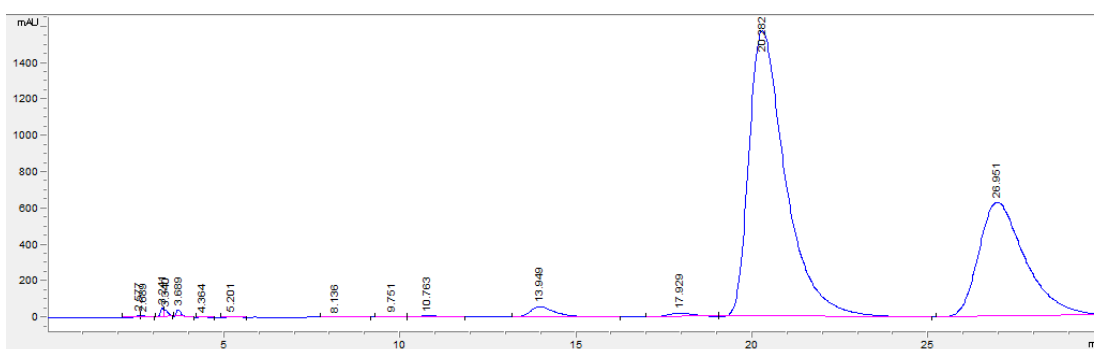
The diol **102** (8.4 mg, 25 mM), lipase enzyme (5 mg), base (25 mM), acyl donor (75 mM, 3 eqv.) and an appropriate solvent (1 mL) were left to shake for a specified amount of time at a specified temperature. An aliquot was then taken, the solvent removed, and the crude material resuspended in the HPLC mobile phase to be analysed by chiral HPLC. If needed, the reaction was purified by column chromatography (eluent: ethyl acetate:hexane; 60:40) to give the product as an oil.

Scaled up Lipase Catalysed desymmetrisation of diol **102** to give **129** and subsequent TBDPS protection



The diol **102** (85 mg, 25 mM), Purolite immobilized CAL-A (5 eqv. w/w), sodium carbonate (132 mg, 125 mM) and water (9  $\mu$ L, 50 mM) were all added to vinyl acetate (10 mL) and shaken at 37°C for 24 hours and monitored by chiral HPLC (<95% e.e.) after which the reaction was neutralized with sat. sodium bicarbonate solution (5 mL). The vinyl acetate was then removed *in-vacuo* and the aqueous layer extracted with ethyl acetate (5 mL x 3), dried over MgSO<sub>4</sub>, filtered and the solvent removed to leave the crude material. The crude residue was then dissolved in DCM (5 mL) and TBDPS-Cl (0.2 mL, 0.75 mmol) and imidazole (100 mg, 1.5 mmol) was added and refluxed for 15 hours after which the reaction was washed with 1 M HCl (5 mL), 1 M NaOH (5 mL) and sat. brine (5 mL) and the organic layer dried over MgSO<sub>4</sub>, filtered and the solvent removed *in-vacuo*. The product was then purified by column chromatography (eluent: hexane:ethyl acetate; 70:30) to give the title compound **140** (103 mg, 66%) as a clear oil. <sup>1</sup>H NMR (CDCl<sub>3</sub>, 400 MHz)  $\delta$  1.01 (9H, s), 1.68 (3H, s),

5.01 (2H, m), 5.39 (2H, q,  $J = 13.2$  Hz), 7.04 (3H, m), 7.24 (5H, m), 7.35 (4H, m), 7.49 (9H, m), 7.59 (1H, t,  $J = 7.6$  Hz), 8.05 (1H, dd,  $J = 7.4, 3.8$  Hz).  $^{13}\text{C}$  NMR ( $\text{CDCl}_3$ , 100 MHz)  $\delta$  19.3, 20.4, 26.9, 63.8 (m), 64.4 (d,  $J = 3.9$  Hz), 126.2 (d,  $J = 12.7$  Hz), 127.1 (d,  $J = 10.0$  Hz), 127.5, 127.6 (d,  $J = 2.1$  Hz), 128.5 (d,  $J = 12.2$  Hz), 128.8 (d,  $J = 101.4$  Hz), 129.5 (d,  $J = 2.4$  Hz), 130.0, 130.6 (d,  $J = 89.3$  Hz), 131.9 (m), 132.0 (m), 132.3 (d,  $J = 2.5$  Hz), 132.5 (d,  $J = 12.0$  Hz), 132.9 (d,  $J = 12.4$  Hz), 133.3 (d,  $J = 4.0$  Hz), 135.4 (d,  $J = 1.0$  Hz), 141.0 (d,  $J = 6.9$  Hz), 146.2 (d,  $J = 7.6$  Hz), 170.2.  $^{31}\text{P}$  NMR ( $\text{CDCl}_3$ , 162 MHz)  $\delta$  33.3. HRMS: (ESI<sup>+</sup>) Calculated for  $\text{C}_{38}\text{H}_{39}\text{O}_4\text{PSiNa}$ : 641.2247 Found  $[\text{M}+\text{Na}]^+$ : 641.2249 (-0.23 ppm).



Peak	Area	Percentage by Area	e.e.
13.9 (129)	2729.9	1.5%	
17.9 (102)	1062	<1%	N/A
20.2 (129)	113858.5	65%	95%
26.9 (134)	57231.2	33%	N/A

GOase-catalysed oxidation of **102**



To a solution of diol **102** (10 mg, 25 mM) in DMSO (300  $\mu$ L) was added 0.1 M  $\text{KPi}$  buffer (0.52 mL), catalase (80  $\mu$ L, 3 mg/mL pH 7.6), sat. copper sulphate solution (80  $\mu$ L) and GOase (20  $\mu$ L, 3 mg/mL). The reaction was then shaken at 25°C for 24 hours, extracted with ethyl acetate, dried over  $\text{MgSO}_4$ , filtered and the solvent removed *in-vacuo*. The crude residue was then analysed by  $^1\text{H}$  NMR which showed no oxidation had occurred.

Lipase screen for the catalysed hydrolytic desymmetrization of diacetate **134**

To a solution of diacetate **134** (9 mg, 25 mM) in toluene (1 mL) was added Lipase (25 mg),  $\text{KPi}$  Buffer (1 mL) and the reaction was stirred vigorously for 24 hours at 37°C. An aliquot was then taken, and the toluene removed *in-vacuo*, the residue was resuspended in the mobile phase of the HPLC and analysed by chiral HPLC.

Kinetic Resolution screen of ( $\pm$ )-alcohol **135** by lipase catalysed acylation

To a solution of the ( $\pm$ )-alcohol **135** (8.4 mg, 25 mM) in organic solvent (1 mL) was added lipase (20 mg) and an acetate donor (4.6  $\mu$ L, 50 mM) and the reaction was shaken for 24 hours at 37°C after which an aliquot was taken and analysed by chiral HPLC.

**Immobilization of CAL-A**

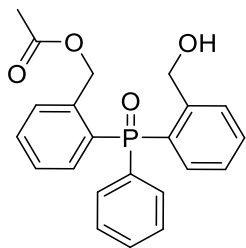
## Eurpergit Resin

Crude CAL-A (5 mL, 6000 U/g, STREM) was dissolved in 0.1 M KPi buffer pH 7 (5 mL). The concentration before immobilisation was recorded (7 – 21 mg/mL). Eurpergit CM (10 g) was added and left in a shaking incubator on 150 rpm at 25°C for 24 hours. The amount of enzyme absorbed onto the resin (2.0 mg/mL) was determined by UV spectroscopy (428nm). Blocking buffer (3M Glycine in 0.1M KPi pH 7) was added and left to shake for 30 minutes. The immobilised enzyme was filtered off and washed with KPi buffer pH 7 and then KPi buffer pH 7 with 1 M NaCl and then dried.

## Purolite Resins

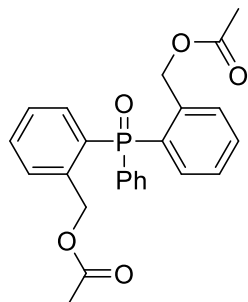
Crude CAL-A (5 mL, 6000 U/g, STREM) was dissolved in 0.1 M KPi buffer pH 7 (5 mL). The concentration before immobilisation was recorded (7 – 25 mg/mL). Purolite resin (10 g) was added and left in a shaking incubator on 150 rpm at 25°C for 24 hours. The amount of enzyme absorbed onto the resin (2.4 – 21 mg/mL) was determined by UV spectroscopy (428nm). The immobilised enzyme was filtered off and washed with KPi buffer pH 7 and dried.

Synthesis of 2-((2-(hydroxymethyl)phenyl)(phenyl)phosphoryl)benzyl acetate ((±)-**129**)



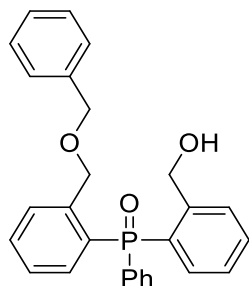
Phosphine oxide **102** (80 mg, 0.32 mmol) was dissolved in dry DCM (5 mL). Triethyl amine (86  $\mu$ L, 0.61 mmol) followed by acetyl chloride (40.3  $\mu$ L, 0.56 mmol) were added and the reaction left to stir for 2 hours. The organic layer was then washed with 1 M HCl (2.5 mL), H<sub>2</sub>O (2.5 mL), brine (2.5 mL) and dried over MgSO<sub>4</sub>, filtered and the solvent removed. The crude residue was then purified by column chromatography (eluent: hexane:ethyl acetate; 70:30) to give the title compound (90 mg, 89%) as a white solid. <sup>1</sup>H NMR (CDCl<sub>3</sub>, 400 MHz)  $\delta$  1.70 (3H, s), 4.58 (2H, dd, AB,  $J$  = 12.7 Hz), 5.49 (2H, dd, AB,  $J$  = 13.1 Hz), 5.69 (1H, br, -OH), 7.00 (2H, m), 7.29 (2H, m), 7.46-7.64 (9H, m). <sup>13</sup>C NMR (CDCl<sub>3</sub>, 100 MHz)  $\delta$  20.3, 64.5 (d,  $J$  = 4.0 Hz), 64.7 (d,  $J$  = 5.0 Hz), 127.3 (d,  $J$  = 13.1 Hz), 127.6 (d,  $J$  = 12.9 Hz), 128.7 (d,  $J$  = 12.4 Hz), 129.7 (d,  $J$  = 101.1 Hz), 130.5 (d,  $J$  = 10.0 Hz), 131.1 (d,  $J$  = 18.0 Hz), 131.7 (d,  $J$  = 10.1 Hz), 132.1 (d,  $J$  = 10.0 Hz), 132.4 (d,  $J$  = 2.8 Hz), 132.6 (d,  $J$  = 2.6 Hz), 132.8 (d,  $J$  = 2.7 Hz), 133.4 (d,  $J$  = 1.4 Hz), 141.3 (d,  $J$  = 6.9 Hz), 146.4 (d,  $J$  = 7.8 Hz), 170.3. <sup>31</sup>P NMR (CDCl<sub>3</sub>, 162 MHz)  $\delta$  37.96. HRMS: (ESI<sup>+</sup>) Calculated for C<sub>22</sub>H<sub>21</sub>O<sub>4</sub>PNa: 403.107 Found [M+Na]<sup>+</sup>: 403.1075 (-1.29 ppm). HPLC separation (DAICEL AD, hexane/isopropanol 83:17, 1.2 mL/min, UV = 210 nm; tR (A) = 14.8 min, tR (B) = 21.6 min), e.e = 0%.

Synthesis of ((phenylphosphoryl)bis(2,1-phenylene))bis(methylene) diacetate  
**(134)**



Phosphine oxide **102** (58 mg, 0.17 mmol) was dissolved in dry DCM (5 mL). Triethyl amine (60  $\mu$ L, 0.41 mmol) followed by acetyl chloride (27  $\mu$ L, 0.37 mmol) was added and the reaction left to stir for 2 hours. The organic layer was then washed with 1 M HCl (2.5 mL), H<sub>2</sub>O (2.5 mL), brine (2.5 mL) and dried over MgSO<sub>4</sub>, filtered and the solvent removed. The crude residue was then purified by column chromatography (eluent: hexane:ethyl acetate; 3:2) to give the title compound (41 mg, 55%) as a clear oil. <sup>1</sup>H NMR (CDCl<sub>3</sub>, 400 MHz)  $\delta$  1.85 (6H, s), 5.40, (2H, m) 5.51 (2H, m), 7.04 (2H, m), 7.29 (2H, m), 7.49 (2H, m) 7.53-7.64 (7H, m). <sup>13</sup>C NMR (CDCl<sub>3</sub>, 100 MHz)  $\delta$  20.4, 64.4 (d, *J* = 4.1 Hz), 127.4 (d, *J* = 12.7 Hz), 128.6 (d, *J* = 12.3 Hz), 130.1 (d, *J* = 9.9 Hz), 130.3, 131.3, 132.0 (d, *J* = 2.9 Hz), 132.2 (d, *J* = 7.5 Hz), 132.2, 133.4 (d, *J* = 12.2 Hz), 141.1 (d, *J* = 7.0 Hz), 170.3. <sup>31</sup>P NMR (CDCl<sub>3</sub>, 162 MHz)  $\delta$  34.41. HPLC separation (DAICEL AD-H, hexane/isopropanol 83:17, 1.2 mL/min, UV = 254, 210 nm; t<sub>R</sub> = 26.9 min.

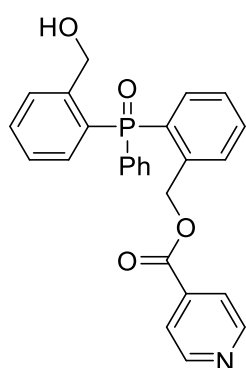
Synthesis of (2-((benzyloxy)methyl)phenyl)(2-(hydroxymethyl)phenyl)(phenyl) phosphine oxide ((±)-**135**)



To a solution of **102** (0.66 g, 2 mmol) in DCM (15 mL) was added silver (I) oxide (1.8 g, 8 mmol) and benzyl bromide (0.285 mL, 2.4 mmol) and the reaction was monitored by TLC for the appearance of the benzylated product. After 5 hours, reaction was filtered and the solution washed with water (3 x 5 mL) and the organic layer dried over MgSO<sub>4</sub>, filtered and the solvent removed *in-vacuo* to leave the crude residue. The product was purified by column chromatography (eluent: hexane:ethyl acetate; 50:50) to give the title compound (159 mg, 20%) as a clear oil. <sup>1</sup>H NMR (CDCl<sub>3</sub>, 400 MHz) δ 4.36 (2H, s), 4.59 (2H, m), 4.91 (2H, s), 5.78 (1H, t, *J* = 7.38 Hz), 6.96 (2H, m), 7.24 (7H, m), 7.49 (4H, m), 7.57 (4H, m), 7.81 (1H, dd, *J* = 7.6, 3.9 Hz). <sup>13</sup>C NMR (CDCl<sub>3</sub>, 100 MHz) δ 64.7 (d, *J* = 4.9 Hz), 70.0 (d, *J* = 4.7 Hz), 72.8, 126.8 (d, *J* = 13.0 Hz), 127.3 (d, *J* = 13.0 Hz), 127.5, 127.9 (d, *J* = 57.5 Hz), 128.7 (d, *J* = 12.3 Hz), 128.8 (d, *J* = 102.5 Hz), 129.0 (d, *J* = 10.1 Hz), 131.0 (d, *J* = 6.9 Hz), 131.7 (d, *J* = 10.0 Hz), 131.9, 132.1 (d, *J* = 10.0 Hz), 132.3 (d, *J* = 2.8 Hz), 132.7 (d, *J* = 2.6 Hz), 132.9 (d, *J* = 12.9 Hz), 133.3 (d, *J* = 13.0 Hz), 138.0, 144.2 (d, *J* = 7.3 Hz), 146.4 (d, *J* = 7.7 Hz). <sup>31</sup>P NMR (CDCl<sub>3</sub>, 161 MHz) δ 38.0 (s). HRMS: (ESI<sup>+</sup>) Calculated for C<sub>27</sub>H<sub>25</sub>O<sub>3</sub>PNa: 451.1434 Found [M+Na]<sup>+</sup>:

451.1439 (-1.21 ppm). HPLC separation (DAICEL AD, hexane/isopropanol 83:17, 1.2 mL/min, UV = 254, 210 nm; tR (A) = 14.0 min, tR (B) = 17.4 min, e.e. = 0%.

Synthesis of 2-((2-(2-(hydroxymethyl)phenyl)(phenyl)phosphoryl)benzyl)isonicotinate ((±)-**137**)



To a solution of **102** (0.25 g, 0.75 mmol) in DCM (8 mL) was added isonicotinoyl chloride hydrochloride (0.13 g, 0.75 mmol), followed by triethyl amine (0.21 mL, 1.51 mmol) and the reaction left to stir at room temperature for 24 hours. After this time, the reaction was stopped, washed with water ( 3 x 5 mL) and the organic layer was dried over MgSO<sub>4</sub>, filtered and the solvent removed *in vacuo* to leave a residue which was purified by column chromatography (eluent: hexane:ethyl acetate; 4:1) to give the title compound (95.3 mg, 28%) as a clear oil. <sup>1</sup>H NMR (CDCl<sub>3</sub>, 400 MHz) δ 4.69 (2H, d, *J* = 6.7 Hz), 5.70 (1H, t, *J* = 7.3 Hz), 5.86 (2H, m), 6.90 (1H, dd, *J* = 14.3, 7.6 Hz), 7.04 (1H, dd, *J* = 14.3, 7.6 Hz), 7.34 (1H, t, *J* = 7.1 Hz), 7.47 (6H, m), 7.58 (4H, m), 7.69 (1H, m), 8.59 (2H, d, *J* = 5.3 Hz). <sup>13</sup>C NMR (CDCl<sub>3</sub>, 100 MHz) δ 64.6 (d, *J* = 5.0 Hz), 65.6 (d, *J* = 3.8 Hz), 122.8, 127.3 (d, *J* = 13.1 Hz), 128.1 (d, *J*

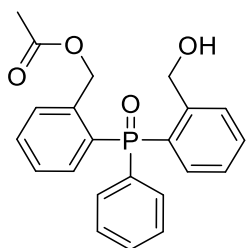
= 12.9 Hz), 128.8 (d,  $J = 12.4$  Hz), 129.5, 131.0, 130.5, 131.5 (d,  $J = 10.0$  Hz), 131.7 (d,  $J = 10.1$  Hz), 132.0 (d,  $J = 10.0$  Hz), 132.5 (d,  $J = 2.8$  Hz), 132.7 (d,  $J = 2.6$  Hz), 132.9 (d,  $J = 2.6$  Hz), 133.3 (d,  $J = 13.0$  Hz), 133.7 (d,  $J = 12.6$  Hz), 136.8, 140.5 (d,  $J = 6.8$  Hz), 146.3 (d,  $J = 7.8$  Hz), 150.2, 164.6.  $^{31}\text{P}$  NMR ( $\text{CDCl}_3$ , 162.8 MHz)  $\delta$  38.11. HRMS: (ESI $^+$ ) Calculated for  $\text{C}_{26}\text{H}_{23}\text{NO}_4\text{P}$ : 444.1359 Found  $[\text{M}+\text{H}]^+$ : 444.1365 (-1.22 ppm).

## 10.5 - Chapter 4 synthesis of ligand structures experimental

### HPLC analysis

HPLC analysis was undertaken on an Agilent Infinity 1260 HPLC, using a DAICEL Chiralpak-AD column (Daicel, 5  $\mu\text{m}$  particle size, 250 mm x 4.6 mm). The mobile phase comprised of (A) IPA: (B) Hexane with an isocratic system of 9% (A) to 91% (B) with a flow rate of 1.2 mL/min, an injection volume of 5  $\mu\text{L}$  and a column temperature of 30°C. Signals were recorded at 200 nm, 210 nm, 220 nm, 254 nm.

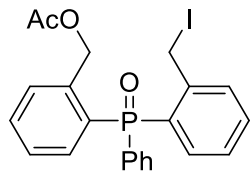
Removal of the Silyl-group from **140** to give **129**



To a solution of **140** (0.23 g, 0.37 mmol) in THF (10 mL) was added 1 M TBAF (0.56 mL, 0.56 mmol) dropwise. The reaction was then allowed to stir at room temperature for 24 hours, after which the reaction was washed with sat. ammonium chloride solution (10 mL) and the aqueous layer extracted with ethyl acetate (10 mL). The organic layer was then dried over MgSO<sub>4</sub>, filtered and the solvent removed. The residue was then purified by column chromatography (eluent: hexane:ethyl acetate; 3:2) to give the title compound (133 mg, 94%) as a clear oil. <sup>1</sup>H NMR (CDCl<sub>3</sub>, 400 MHz) δ 1.70 (3H, s), 4.58 (2H, d, AB, *J* = 12.7 Hz), 5.49 (2H, d, AB, *J* = 13.1 Hz), 5.69 (1H, br, -OH), 7.00 (2H, m), 7.29 (2H, m), 7.46-7.64 (9H, m). <sup>13</sup>C NMR (CDCl<sub>3</sub>, 100 MHz) δ 20.3, 64.5 (d, *J* = 4.0 Hz), 64.7 (d, *J* = 5.0 Hz), 127.3 (d, *J* = 13.1 Hz), 127.6 (d, *J* = 12.9 Hz), 128.7 (d, *J* = 12.4 Hz), 129.7 (d, *J* = 101.1 Hz), 130.5 (d, *J* = 10.0 Hz), 131.1 (d, *J* = 18.0 Hz), 131.7 (d, *J* = 10.1 Hz), 132.1 (d, *J* = 10.0 Hz), 132.4 (d, *J* = 2.8 Hz), 132.6 (d, *J* = 2.6 Hz), 132.8 (d, *J* = 2.7 Hz), 133.4 (d, *J* = 1.4 Hz), 141.3 (d, *J* = 6.9 Hz), 146.4 (d, *J* = 7.8 Hz), 170.3. <sup>31</sup>P NMR (CDCl<sub>3</sub>, 162 MHz) δ 37.96. HRMS: (ESI<sup>+</sup>) Calculated for C<sub>22</sub>H<sub>21</sub>O<sub>4</sub>PNa: 403.107 Found [M+Na]<sup>+</sup>: 403.1075 (-1.29 ppm). HPLC separation (DAICEL AD, hexane/isopropanol 83:17, 1.2 mL/min, UV = 254, 210 nm; tR (A) = 14.8 min, tR (B) = 21.6 min), e.e. = 96%.



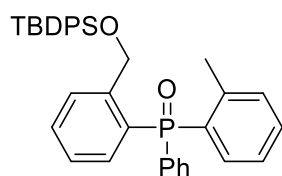
Synthesis of 2-((2-(iodomethyl)phenyl)(phenyl)phosphoryl)benzyl acetate  
(143)



To monoacetate **129** (133 mg, 0.35 mmol) in DCM (5 mL) was added triethylamine (60  $\mu$ L, 0.45 mmol) followed by mesyl chloride (30  $\mu$ L, 0.39 mmol) and the reaction stirred for 5 hours at room temperature. The reaction was then washed with sat. sodium bicarbonate (5 mL), 1 M HCl (5 mL) and brine (5 mL). The organic layer was then dried over  $\text{MgSO}_4$ , filtered and the solvent removed and the mesylated compound used without purification. To mesylated material **142** (152 mg, 0.33) was added sodium iodide (149 mg, 1 mmol) and acetone (5 mL). The reaction was then left 12 hours and the solvent removed *in-vacuo*, the residue was then dissolved in ethyl acetate (10 mL) and washed with sat.  $\text{Na}_2\text{S}_2\text{O}_3$  solution. The organic layer was then dried over  $\text{MgSO}_4$ , filtered and the solvent removed. The residue was then purified by column chromatography (eluent: hexane:ethyl acetate; 1:1) to give the title compound (110 mg, 68%) as a cream solid.  $^1\text{H}$  NMR ( $\text{CDCl}_3$ , 400 MHz)  $\delta$  1.76 (3H, s), 5.04 (2H, dd,  $J = 14.0, 9.9$  Hz), 5.51 (2H, m), 6.94 (1H, dd,  $J = 14.0, 7.7$  Hz), 7.10 (1H, dd,  $J = 14.2, 7.5$  Hz), 7.19 (1H, m), 7.30 (1H, m), 7.51 (3H, m), 7.60 (6H, m).  $^{13}\text{C}$  NMR ( $\text{CDCl}_3$ , 100 MHz)  $\delta$  3.56 (d,  $J = 4.4$  Hz), 20.5, 64.4 (d,  $J = 4.1$  Hz), 127.0 (d,  $J = 12.6$  Hz), 127.6 (d,  $J = 12.7$  Hz), 128.6 (d,  $J = 12.3$  Hz), 129.8 (d,  $J = 16.0$  Hz), 130.2 (d,  $J = 15.9$  Hz), 130.8 (d,  $J = 15.9$  Hz),

131.3, 132.2 (d,  $J = 2.8$  Hz), 132.3, 132.4, 132.4, 132.5 (d,  $J = 2.5$  Hz), 133.3 (d,  $J = 12.5$  Hz), 133.5 (d,  $J = 6.3$  Hz), 133.6 (d,  $J = 3.6$  Hz), 141.1 (d,  $J = 7.0$  Hz), 144.5 (d,  $J = 6.9$  Hz), 170.3.  $^{31}\text{P}$  NMR ( $\text{CDCl}_3$ , 162 MHz)  $\delta$  34.7. HRMS: (ESI $^+$ ) Calculated for  $\text{C}_{22}\text{H}_{20}\text{O}_3\text{PNa}$ : 513.0087 Found  $[\text{M}+\text{Na}]^+$ : 513.0092 (-0.89 ppm).

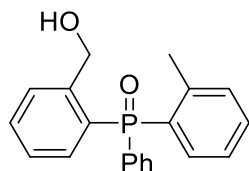
Synthesis of (2-(((tert-butyldiphenylsilyl)oxy)methyl)phenyl)(phenyl)(o-tolyl)phosphine oxide (**146**)



To a solution of **140** (254 mg, 0.43 mmol) in MeOH (10 mL), was added  $\text{NiCl}_2 \cdot 6\text{H}_2\text{O}$  (50 mg, 0.43 mmol) followed by  $\text{NaBH}_4$  (51 mg, 1.39 mmol) after which the solution turned black and became effervescent. The reaction was then stirred at  $0^\circ\text{C}$  and followed by TLC with  $\text{NaBH}_4$  (5 mg) being added at regular intervals. Once complete, the reaction was quenched with excess MeOH (10 mL) and filtered through a pad of celite, which was washed with both ethyl acetate and DCM. The filtrate was then concentrated and washed with water and the aqueous layer re-extracted with ethyl acetate. The organic layers were then combined, dried over  $\text{MgSO}_4$ , filtered and the solvent removed *in-vacuo*. The residue was then purified by column chromatography (eluent: hexane:ethyl acetate; 50:50) to give the title compound (202 mg, 83%) as a clear oil.  $^1\text{H}$  NMR ( $\text{CDCl}_3$ , 400 MHz)  $\delta$  1.03 (9H, s), 2.40 (3H, s), 4.94 (1H,

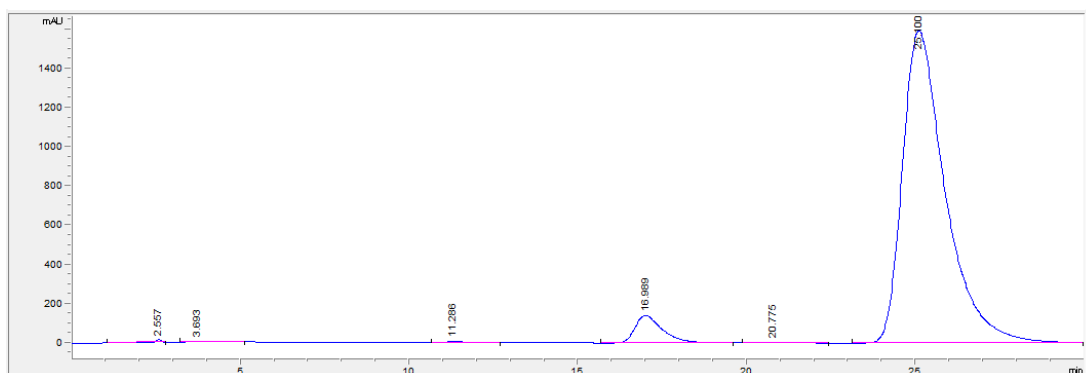
d,  $J = 15.3$  Hz), 5.04 (1H, d,  $J = 15.3$  Hz), 6.96 (2H, m), 7.16 (1H, m), 7.2-7.28 (6H, m), 7.35 (5H, m), 7.49 (7H, m), 7.59 (1H, t,  $J = 7.6$  Hz), 8.04 (1H, dd,  $J = 7.6, 4.0$  Hz).  $^{13}\text{C}$  NMR ( $\text{CDCl}_3$ , 100 MHz)  $\delta$  19.3, 21.7 (d,  $J = 4.4$  Hz), 26.94, 63.8 (d,  $J = 4.6$  Hz), 125.3 (d,  $J = 12.9$  Hz), 126.3 (d,  $J = 12.5$  Hz), 127.6 (d,  $J = 2.7$  Hz), 128.4 (d,  $J = 12.0$  Hz), 128.6 (d,  $J = 100.2$  Hz), 129.5 (d,  $J = 1.2$  Hz), 130.5 (d,  $J = 102.2$  Hz), 131.7 (d,  $J = 2.7$  Hz), 131.8 (m, overlapping peaks), 132.1 (d,  $J = 9.8$  Hz), 132.3 (d,  $J = 11.7$  Hz), 132.7 (d,  $J = 13.0$  Hz), 133.4 (d,  $J = 4.3$  Hz), 135.4, 143.3 (d,  $J = 7.9$  Hz), 146.2 (d,  $J = 7.5$  Hz).  $^{31}\text{P}$  NMR ( $\text{CDCl}_3$ , 400 MHz)  $\delta$  33.2 (s). HRMS: (ESI<sup>+</sup>) Calculated for  $\text{C}_{36}\text{H}_{37}\text{O}_2\text{PSiNa}$ : 583.2193 Found  $[\text{M}+\text{Na}]^+$ : 583.2197 (-0.74 ppm).

Synthesis of (2-(hydroxymethyl)phenyl)(phenyl)(o-tolyl)phosphine oxide (**147**)



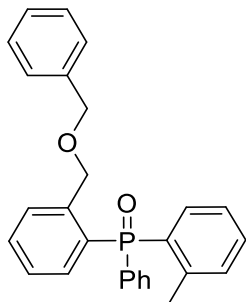
To a solution of **139** (202 mg, 0.36 mmol) in THF (5 mL) was added 1 M TBAF (0.54 ml, 0.54 mmol) and the reaction stirred at room temperature for 2 Hours. The reaction was then stopped by the addition of sat. ammonium chloride (5 mL) and the aqueous layer was then extracted with ethyl acetate (5 mL x 3), the organic layers were combined, dried over  $\text{MgSO}_4$ , filtered and then the solvent removed *in-vacuo*. The crude material was then purified by column chromatography (eluent: hexane:ethyl acetate; 50:50) to give the title compound (110 mg, 95%) as a white solid.  $^1\text{H}$  NMR ( $\text{CDCl}_3$ , 400 MHz)  $\delta$  2.50

(3H, s), 4.61 (2H, d,  $J = 7.2$  Hz), 5.91 (1H, t, 7.2 Hz, -OH), 6.92 (1H, dd,  $J = 14.7, 7.9$  Hz) 6.99 (1H, dd,  $J = 14.5, 8$  Hz), 7.13 (1H, t,  $J = 6.8$  Hz), 7.26 (1H, m), 7.33 (1H, m), 7.49 (5H, m), 7.60 (3H, m).  $^{13}\text{C}$  NMR ( $\text{CDCl}_3$ , 100 MHz)  $\delta$  21.8 (d,  $J = 4.6$  Hz), 64.8 (d,  $J = 4.7$  Hz), 125.4 (d,  $J = 13.2$  Hz), 127.3 (d,  $J = 13.0$  Hz), 128.7 (d,  $J = 12.2$  Hz), 129.9 (d,  $J = 104.2$  Hz), 130.9 (d,  $J = 5.6$  Hz), 131.7 (d,  $J = 9.9$  Hz), 132.0 (d,  $J = 10.3$  Hz), 132.1 (m), 132.2 (m), 132.4 (d,  $J = 2.5$  Hz), 132.7 (d,  $J = 2.6$  Hz), 133.1 (d,  $J = 13.2$  Hz), 143.5 (d,  $J = 7.8$  Hz), 146.6 (d,  $J = 7.6$  Hz).  $^{31}\text{P}$  NMR ( $\text{CDCl}_3$ , 162 MHz)  $\delta$  38.02 (s). HRMS: (ESI<sup>+</sup>) Calculated for  $\text{C}_{20}\text{H}_{19}\text{O}_2\text{PNa}$ : 345.1015 Found  $[\text{M}+\text{Na}]^+$ : 345.102 (-1.58 ppm). HPLC separation (DAICEL AD, hexane/isopropanol 91:9, 1.2 mL/min, UV = 254, 210 nm; tR (A) = 16.9 min, tR (B) = 25.1 min), e.e = 92%. Purity = 99%



Peak	Area
16.9	7897.3
25.1	140288.8

Synthesis of (2-((benzyloxy)methyl)phenyl)(phenyl)(o-tolyl)phosphine oxide  
(148)

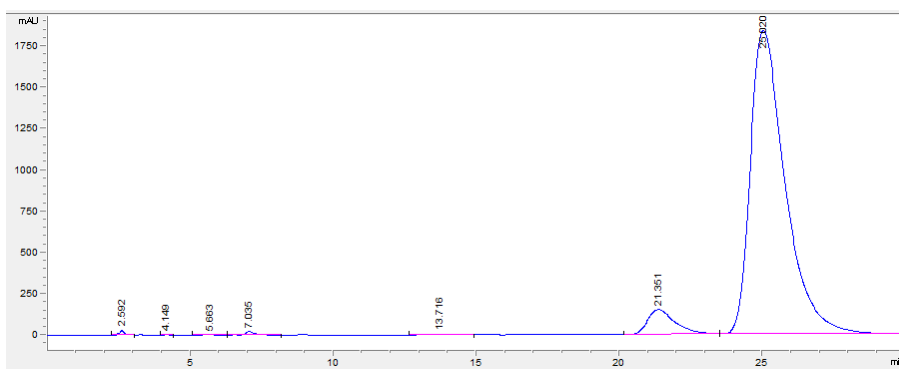


To a solution of **140** (110 mg, 0.33 mmol) in THF (5 mL) at 0°C was added NaH (17.28 mg, 0.36 mmol) after which the reaction allowed to warm up to room temperature. TBAI (11 mg, 0.03 mmol) and benzyl bromide (42.7  $\mu$ L, 0.36 mmol) were added and the reaction monitored by TLC. After all starting material had been consumed, the reaction was quenched with water (5 mL). The organic layer was separated, washed with sat. ammonium chloride solution, sat. brine and dried over magnesium sulphate. The product was purified by column chromatography (eluent: hexane:ethyl acetate; 50:50) to give the title compound (103 mg, 97%) as a clear oil.  $^1\text{H}$  NMR ( $\text{CDCl}_3$ , 400 MHz)  $\delta$  2.49 (s, 3H), 4.40 (s, 2H), 4.94 (1H, d,  $J = 13.7$  Hz), 5.01 (1H, d,  $J = 13.7$  Hz), 7.05 (3H, m), 7.24 (7H, m), 7.42 (3H, m), 7.43 (2H, t,  $J = 7.5$  Hz), 7.60 (2H, m), 7.83 (1H, dd,  $J = 7.7, 3.8$  Hz).  $^{13}\text{C}$  NMR ( $\text{CDCl}_3$ , 100 MHz)  $\delta$  21.8 (d,  $J = 4.4$  Hz), 70.1 (d,  $J = 4.3$  Hz), 72.7, 125.3 (d,  $J = 12.9$  Hz), 126.7 (d,  $J = 12.7$  Hz), 127.4, 127.6, 128.2, 128.5 (d,  $J = 12.1$  Hz), 128.7 (d,  $J = 10.1$  Hz), 129.7 (d,  $J = 100.6$  Hz), 130.9 (d,  $J = 102.7$  Hz), 131.8 (m), 132.1 (m), 132.6 (d,  $J = 12.5$  Hz), 133.0 (d,  $J = 13.0$  Hz), 133.1, 138.3, 143.3 (d,  $J = 7.8$  Hz),

144.1 (d,  $J = 7.2$  Hz).  $^{31}\text{P}$  NMR ( $\text{CDCl}_3$ , 162 MHz)  $\delta$  34.7. HRMS: (ESI<sup>+</sup>)  
Calculated for  $\text{C}_{27}\text{H}_{25}\text{O}_2\text{PNa}$ : 435.1484 Found  $[\text{M}+\text{Na}]^+$ : 435.1488 (-0.91 ppm).  
HPLC separation (DAICEL AD, hexane/isopropanol 91:9, 1 mL/min, UV = 210  
nm; tR (A) = 21.4 min, tR (B) = 25.2 min), e.e = 83%.

#### Method B

To a solution of **147** (322 mg, 1 mmol) in DCM (10 mL) was added Silver (I)  
Oxide (926 mg, 4 mmol) and the reaction stirred at 40°C and followed by TLC.  
Once all starting material had been consumed, the reaction was cooled to  
room temperature and washed with water (10 mL). The organic layer was dried  
over  $\text{MgSO}_4$ , filtered and the solvent removed *in-vacuo* to leave the crude  
residue which was purified by column chromatography (eluent: hexane:ethyl  
acetate; 50:50) to give the title compound (383 mg, 93%) as a clear oil. Data  
identical to method A. HPLC separation (DAICEL AD, hexane/isopropanol  
91:9, 1 mL/min, UV = 254 nm; tR (A) = 21.3 min, tR (B) = 25.8 min), e.e = 88%.



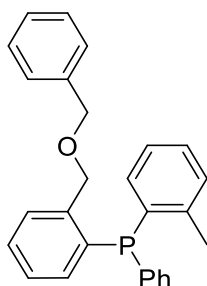
Peak	Area
21.3	9896.6
25.8	155152.4

## 10.6 – Chapter 5 phosphine oxide reduction experimental

### HPLC analysis

HPLC analysis was undertaken on an Agilent Infinity 1260 HPLC, using a DAICEL Chiralpak-AD column (Daicel, 5  $\mu\text{m}$  particle size, 250 mm x 4.6 mm). The mobile phase comprised of (A) IPA: (B) Hexane with an isocratic system of 9% (A) to 91% (B) with a flow rate of 1.2 mL/min, an injection volume of 5  $\mu\text{L}$  and a column temperature of 30°C. Signals were recorded at 200 nm, 210 nm, 220 nm, 254 nm.

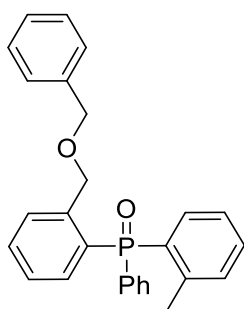
### Synthesis of (2-((benzyloxy)methyl)phenyl)(phenyl)(o-tolyl)phosphane (**152**)



To a solution of phosphine oxide **148** (20 mg, 48  $\mu\text{mol}$ ) in THF (2 mL) under argon was added PMHS (1 mL) followed by titanium isopropoxide (60  $\mu\text{L}$ , 194  $\mu\text{mol}$ , 10 equiv). The mixture was heated at 65°C for 18 hours to complete the reaction. The mixture was cooled to ambient temperature. Then the solvent was removed under reduced pressure and residue was cooled to 0°C and 1M NaOH (15 mL) was added slowly. The mixture was extracted with ethyl acetate, dried over  $\text{MgSO}_4$ , filtered and the solvent removed *in-vacuo* and the

residue purified by column chromatography (eluent: hexane:ethyl acetate; 97:3) to give the title compound (17.7 mg, 94%) as a white solid.  $^1\text{H}$  NMR ( $\text{CDCl}_3$ , 400 MHz)  $\delta$  2.24 (3H, s), 4.69 (2H, m), 6.64 (1H, m), 6.76 (1H, m), 6.97 (1H, t,  $J = 7.3$  Hz), 7.05-7.30 (15H, m), 7.49 (1H, dd,  $J = 7.0, 4.3$  Hz).  $^{13}\text{C}$  NMR ( $\text{CDCl}_3$ , 100 MHz)  $\delta$  20.1 (d,  $J = 21.2$  Hz), 69.4 (d,  $J = 24.4$  Hz), 71.3, 125.0, 126.3, 126.7, 126.9 (d,  $J = 57.1$  Hz), 127.0 (d,  $J = 5.5$  Hz), 127.5 (d,  $J = 7.2$  Hz), 127.6, 127.8 (d,  $J = 24.7$  Hz), 129.0 (d,  $J = 4.7$  Hz), 132.2 (d,  $J = 61.2$  Hz), 133.1 (d,  $J = 20.1$  Hz), 134.4 (d,  $J = 10.9$  Hz), 134.6 (d,  $J = 9.4$  Hz), 141.12 (d,  $J = 25.9$  Hz), 141.7 (d,  $J = 23.8$  Hz).  $^{31}\text{P}$  NMR ( $\text{CDCl}_3$ , 162 MHz)  $\delta$  -23.75. HRMS: (ESI $^+$ ) Calculated for  $\text{C}_{27}\text{H}_{26}\text{OP}$ : 397.1716 Found  $[\text{M}+\text{H}]^+$ : 397.1716 (-0.11 ppm).

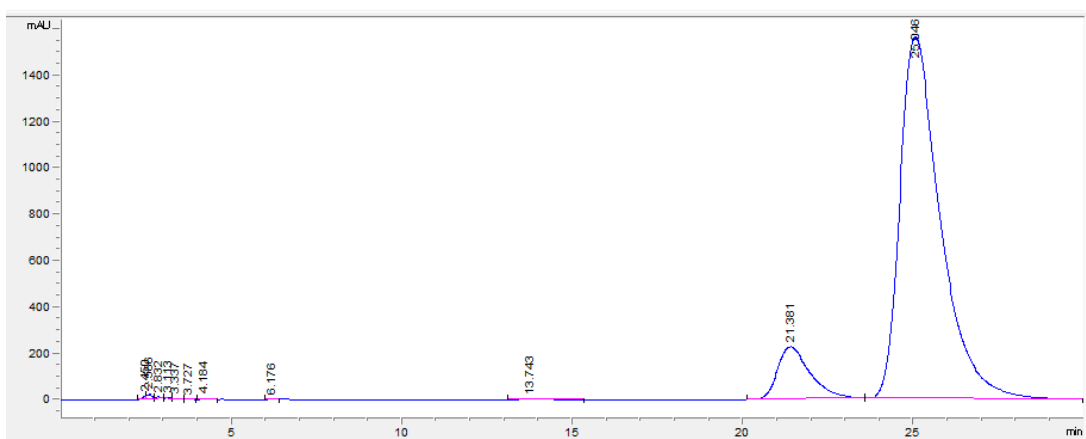
Oxidation of phosphine bis(2-(hydroxymethyl)phenyl)(phenyl)phosphine oxide) **152** to give phosphine oxide **148**



Phosphine **152** (17.7 mg, 45  $\mu\text{mol}$ ) was dissolved in a 2:1 solution of DCM to water (1 mL), then 30 % hydrogen peroxide (0.1 mL) was added and left to stir for 2 hours. Water (1 mL) was then added to the reaction and the organic layer separated and the aqueous layer was washed with DCM (2 mL). The organic layers were then combined, dried over  $\text{MgSO}_4$ , filtered and solvent removed



*in-vacuo* and the crude material purified by column chromatography (eluent: hexane:ethyl acetate; 50:50) to give the title compound (19 mg, 99%) as a clear oil.  $^1\text{H}$  NMR ( $\text{CDCl}_3$ , 400 MHz)  $\delta$  2.49 (s, 3H), 4.40 (s, 2H), 4.94 (1H, d,  $J = 13.7$  Hz), 5.02 (1H, d,  $J = 13.7$  Hz), 7.05 (3H, m), 7.24 (7H, m), 7.42 (3H, m), 7.43 (2H, t,  $J = 7.5$  Hz), 7.60 (2H, m), 7.83 (1H, dd,  $J = 7.7, 3.8$  Hz).  $^{13}\text{C}$  NMR ( $\text{CDCl}_3$ , 100 MHz)  $\delta$  21.8 (d,  $J = 4.4$  Hz), 70.1 (d,  $J = 4.3$  Hz), 72.7, 125.3 (d,  $J = 12.9$  Hz), 126.7 (d,  $J = 12.7$  Hz), 127.4, 127.6, 128.2, 128.5 (d,  $J = 12.1$  Hz), 128.7 (d,  $J = 10.1$  Hz), 129.7 (d,  $J = 100.6$  Hz), 130.9 (d,  $J = 102.7$  Hz), 131.8 (m), 132.1 (m), 132.6 (d,  $J = 12.5$  Hz), 133.0 (d,  $J = 13.0$  Hz), 133.1, 138.3, 143.3 (d,  $J = 7.8$  Hz), 144.1 (d,  $J = 7.2$  Hz).  $^{31}\text{P}$  NMR ( $\text{CDCl}_3$ , 162 MHz)  $\delta$  34.7. HRMS: (ESI $^+$ ) Calculated for  $\text{C}_{27}\text{H}_{25}\text{O}_2\text{PNa}$ : 435.1484 Found  $[\text{M}+\text{Na}]^+$ : 435.1488 (-0.91 ppm). HPLC separation (DAICEL AD, hexane/isopropanol 91:9, 1 mL/min, UV = 254 nm; tR (A) = 21.3 min, tR (B) = 25.0 min, e.e = 84%.



Peak	Area
21.3	13077.4
25.0	148330.9

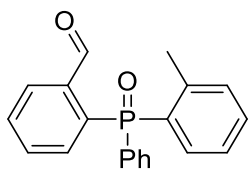
## 10.7 – Chapter 6 inversion barrier calculation experimental (DFT)

### DFT Inversion Studies of Phosphines **152, 161-173**

Structure optimizations have been carried out at the CCB97X-D density functional level of theory with the 6-31G\* dataset using the SPARTAN 18 program. The optimized geometries were characterized as energy minimums at the potential energy surface from frequency calculations at the same level of theory; i.e., the energy minimum structure has only real frequencies or authentic transition state have only one imaginary vibration mode, which connects the reactant and product. The Gibbs free energies that were calculated in au were then scaled to the designated temperature and converted to kJ/mol and the difference between the two conformations energies taken as the inversion barrier.

## 10.8 - Chapter 7 synthesis of phenolic structures from **147** experimental

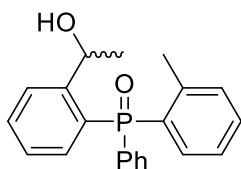
### Synthesis of 2-(phenyl(o-tolyl)phosphoryl)benzaldehyde (**176**)



To a solution of **147** (100 mg, 0.31 mmol) in DCM (5 mL) was added pyridinium chlorochromate (85 mg, 0.37 mmol) and the reaction stirred at room temperature for 5 hours after which an excess of diethyl ether was added, and

the reaction filtered. The solvent was then removed *in-vacuo* and the residue purified by column chromatography (eluent: hexane:ethyl acetate; 50:50) to give the title compound (70 mg, 71%) as a white solid.  $^1\text{H}$  NMR ( $\text{CDCl}_3$ , 400 MHz)  $\delta$  2.52 (3H, s), 7.00 (2H, dd,  $J = 14.4, 7.5$  Hz), 7.17 (2H, m), 7.34 (1H, dd,  $J = 7.5, 4.3$  Hz), 7.42-7.72 (8H, m), 8.19 (1H, dd,  $J = 4.0, 0.8$  Hz), 10.84 (1H, s).  $^{13}\text{C}$  NMR ( $\text{CDCl}_3$ , 100 MHz)  $\delta$  21.8, 125.5 (d,  $J = 13.2$  Hz), 128.8 (d,  $J = 12.3$  Hz), 129.0 (d,  $J = 8.8$  Hz), 130.5 (d,  $J = 104.1$  Hz), 131.66, 132.1-132.22 (m, overlapping signals), 132.2 (d,  $J = 2.8$  Hz), 132.3 (d,  $J = 2.8$  Hz), 132.5 (d,  $J = 2.7$  Hz), 132.7 (d,  $J = 3.7$  Hz), 132.9 (d,  $J = 11.0$  Hz), 133.0, 133.2, 135.4 (d,  $J = 95.3$  Hz), 139.9 (d,  $J = 6.4$  Hz), 143.3 (d,  $J = 8.0$  Hz), 191.6 (d,  $J = 5.2$  Hz).  $^{31}\text{P}$  NMR ( $\text{CDCl}_3$ , 161 MHz)  $\delta$  34.17. HRMS: (ESI $^+$ ) Calculated for  $\text{C}_{20}\text{H}_{17}\text{O}_2\text{PNa}$  : 343.0858 Found  $[\text{M}+\text{Na}]^+$ : 343.0863 (-1.39 ppm).

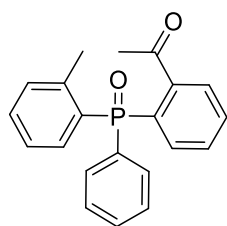
Synthesis of (2-(1-hydroxyethyl)phenyl)(phenyl)(o-tolyl)phosphine oxide (**178**)



To a solution of **176** (35 mg, 0.1 mmol) in THF (2 mL) at 0°C, was added 3 M MeMgBr (46.5  $\mu\text{L}$ , 0.14 mmol) and the reaction warmed up to room temperature and left to stir for 5 hours after which the reaction was quenched through the addition of sat. ammonium chloride solution (2 mL). The organic layer and aqueous layer were then separated, and the aqueous layer extracted with ethyl acetate (3 x 1 mL) and the organic layers combined, dried over

MgSO<sub>4</sub>, filtered and the solvent removed *in-vacuo*. The crude residue was then purified by column chromatography (eluent: hexane:ethyl acetate; 50:50) to give the title compound (25 mg, 74%) as a white solid. <sup>1</sup>H NMR (CDCl<sub>3</sub>, 400 MHz) δ 1.53 (3H, d, *J* = 6.6 Hz), 2.47 (3H, s), 5.24 (1H, m), 6.85-7.05 (2H, m), 7.10-7.25 (2H, m), 7.33 (1H, dd, *J* = 11.1, 6.7 Hz), 7.42-7.72 (8H, m). <sup>13</sup>C NMR (CDCl<sub>3</sub>, 100 MHz) δ 20.8, 21.6 (d, *J* = 4.6 Hz), 66.9 (d, *J* = 5.2 Hz), 125.3 (d, *J* = 13.2 Hz), 126.9 (d, *J* = 13.2 Hz), 127.2 (d, *J* = 10.0 Hz), 128.7 (d, *J* = 12.2 Hz), 130.0, 132.1-132.3 (m, overlapping peaks), 132.4 (d, *J* = 2.6 Hz), 132.6 (d, *J* = 2.6 Hz), 132.9 (d, *J* = 13.4 Hz), 133.5 (d, *J* = 13.2 Hz), 143.3 (d, *J* = 8.0 Hz), 150.4 (d, *J* = 7.3 Hz). <sup>31</sup>P NMR (CDCl<sub>3</sub>, 161 MHz) δ 38.7. HRMS: (ESI<sup>+</sup>) Calculated for C<sub>21</sub>H<sub>21</sub>O<sub>2</sub>PNa : 359.1171 Found [M+Na]<sup>+</sup>: 359.1178 (-1.85 ppm).

#### Synthesis of 1-(2-(phenyl(o-tolyl)phosphoryl)phenyl)ethan-1-one (**179**)

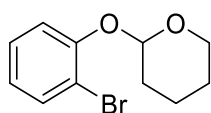


To a solution of **178** (2-(1-hydroxyethyl)phenyl)(phenyl)(o-tolyl)phosphine oxide (25 mg, 0.075 mmol) in DCM (5 mL) was added pyridinium chlorochromate (20 mg, 0.089 mmol) and the reaction stirred at room temperature for 5 hours after which an excess of diethyl ether was added, and the reaction filtered. The solvent was then removed *in-vacuo* and the residue purified by column chromatography (eluent: hexane:ethyl acetate; 70:30) to

give the title compound (21 mg, 84%) as a colourless residue.  $^1\text{H}$  NMR ( $\text{CDCl}_3$ , 400 MHz)  $\delta$  2.41 (3H, s), 2.44 (3H, s), 7.05-7.17 (2H, m), 7.26 (1H, m), 7.41 (1H, t,  $J = 7.4$  Hz), 7.47 (4H, m), 7.54 (1H, m), 7.55-7.67 (4H, m).  $^{13}\text{C}$  NMR ( $\text{CDCl}_3$ , 100 MHz)  $\delta$  21.5 (d,  $J = 4.7$  Hz), 22.6, 125.0 (d,  $J = 13.4$  Hz), 127.6 (d,  $J = 9.3$  Hz), 128.4 (d,  $J = 12.3$  Hz), 129.89 (d,  $J = 11.9$  Hz), 130.6 (d,  $J = 17.8$  Hz), 131.6-131.8 (m, overlapping peaks), 131.9 (d,  $J = 2.7$  Hz), 132.1 (d,  $J = 9.8$  Hz), 132.9 (d,  $J = 105.9$  Hz), 133.7 (d,  $J = 13.2$  Hz), 134.0 (d,  $J = 10.7$  Hz), 142.6 (d,  $J = 8.3$  Hz), 145.2 (d,  $J = 7.1$  Hz), 202.3.  $^{31}\text{P}$  NMR ( $\text{CDCl}_3$ , 161 MHz)  $\delta$  34.30. HRMS: (ESI<sup>+</sup>) Calculated for  $\text{C}_{21}\text{H}_{19}\text{O}_2\text{PNa}$ : 357.1015 Found  $[\text{M}+\text{Na}]^+$ : 357.1023 (-2.2 ppm).

### 10.8.1 – Chapter 8.2 direct synthesis of phenolic phosphine oxides experimental

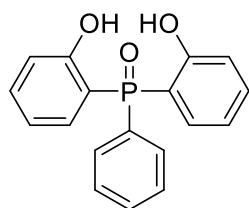
Synthesis of 2-(2-bromophenoxy)tetrahydro-2H-pyran (**182**)



2-Bromophenol (**181**) (1.23 mL, 11.6 mmol) was dissolved in DCM (50 mL) and DHP (1.26 mL, 13.9 mmol) was added followed by *PPTS* (0.27 g, 1.1 mmol). The reaction was left to stir at room temperature for 24 hours. After the allotted time, the reaction was washed with sodium bicarbonate (25 ml), water (25 mL) and brine (25 mL) and the organic layer dried with  $\text{MgSO}_4$ , filtered and the solvent removed *in-vacuo*. The crude product was purified by column

chromatography (eluent: hexane:ethyl acetate; 33:1) to give the title compound (2.24 g, 75%) as a clear oil.  $^1\text{H}$  NMR ( $\text{CDCl}_3$ , 400MHz)  $\delta$  1.51 – 2.17 (6H, m), 3.56 (1H, m), 3.87 (1H, td,  $J = 11.0, 2.8$  Hz), 5.47 (1H, s), 6.81 (1H, t,  $J = 7.6$  Hz), 7.12 (1H, d,  $J = 8.2$  Hz), 7.19 (1H, t,  $J = 7.8$  Hz), 7.50 (1H, d,  $J = 8.2$  Hz).  $^{13}\text{C}$  NMR ( $\text{CDCl}_3$ , 100 MHz)  $\delta$  18.3, 25.3, 30.2, 61.7, 96.6, 113.15, 122.77, 128.3, 133.2, 153.4. HRMS: (ESI $^+$ ) Calculated for  $\text{C}_{11}\text{H}_{13}\text{BrNaO}_2$ : 280.0148 Found  $[\text{M}+\text{Na}]^+$ : 280.0138 (3.28 ppm).

### Synthesis of bis(2-hydroxyphenyl)(phenyl)phosphine oxide (**112**)

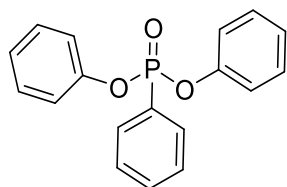


To a solution of **182** (01.94 g, 7.57 mmol) in anhydrous THF (50 mL), 1.6 M *n*-BuLi (5.2 mL, 8.33 mmol) was added dropwise at  $-78^\circ\text{C}$  and the reaction left to stir for an hour. P,P-dichlorophenylphosphine (0.51 mL, 3.78 mmol) was then added dropwise over 5 minutes, the reaction was allowed to warm to room temperature and was left to stir for 24 hours. Water (25 mL) was then cautiously added to reaction and allowed to stir for ten minutes. The organic and aqueous layer were then separated and washed with water and ethyl acetate, respectively. The organic layer was then dried over  $\text{MgSO}_4$ , filtered and the solvent removed *in vacuo* and the crude residue was dissolved in 2:1 solution of DCM (10 mL) and  $\text{H}_2\text{O}$  (5 mL) and  $\text{H}_2\text{O}_2$  (0.85 mL, 7.5 mmol) was added and the reaction was left to stir for 2 hours. The organic and aqueous

layer were then separated and washed with H<sub>2</sub>O and DCM, respectively. The organic layer was then dried over MgSO<sub>4</sub>, filtered and the solvent removed to leave a crude residue which was used in the next step without purification.

The residue was dissolved in methanol (30 mL) and *p*TSA (150 mg, 0.75 mmol) was added and the reaction was left to stir at room temperature for 24 hours. After this time, the volume of the reaction was reduced and DCM (25 mL) was added. The organic layer was then washed with sat. sodium bicarbonate (15 mL), water (15 mL), brine (15 mL) and dried over MgSO<sub>4</sub>, filtered and the solvent removed *in vacuo*. The resulting solid was purified by column chromatography (eluent: hexane:ethyl acetate; 70:30) to give the title compound (483 mg, 20%) as a white solid. <sup>1</sup>H NMR (400 MHz, CDCl<sub>3</sub>) δ 6.90 (4H, m), 7.39 – 7.72 (9H, m), 10.83 (2H, s). <sup>13</sup>C (CDCl<sub>3</sub>, 100 MHz) δ 115.1, 116.2, 117.1 (d, *J* = 7.2 Hz), 119.4 (d, *J* = 12.1 Hz), 128.8 (d, *J* = 9.9 Hz), 131.3 (d, *J* = 10.7 Hz), 132.2 (d, *J* = 2.7 Hz), 133.4 (d, *J* = 9.0 Hz), 134.7 (d, *J* = 1.8 Hz), 161.2 (d, *J* = 3.4 Hz) <sup>31</sup>P NMR (CDCl<sub>3</sub>, 162 MHz) δ 34.0. HRMS: (ESI<sup>+</sup>) Calculated for C<sub>18</sub>H<sub>15</sub>O<sub>3</sub>PNa: Found [M+Na]<sup>+</sup>: 333.0653 (-0.68 ppm).

## Synthesis of diphenyl phenyl phosphonate (**111**)



### Method A

To a solution of phenol (**186**) (0.84 g, 8.92 mmol) in THF (60 mL) was added, DMAP (54 mg, 0.44 mmol), triethyl amine (3 mL, 21.6 mmol) followed by dichlorophenyl phosphine (0.6 mL, 4.46 mmol) and the reaction was left to stir at room temperature for 4 hours. After this time, sat. ammonium chloride solution (30 mL) was added and the aqueous and organic layers were separated and washed with ethyl acetate and water, respectively. The organic layer was then dried over  $\text{MgSO}_4$ , filtered and the solvent removed. The residue was then dissolved in a 2:1 solution of DCM and  $\text{H}_2\text{O}$  and 30%  $\text{H}_2\text{O}_2$  (1 mL, 8.92 mmol) was added and the reaction stirred for 2 hours. The organic and aqueous layer were then separated and washed with  $\text{H}_2\text{O}$  and DCM, respectively. The organic layer was then dried over  $\text{MgSO}_4$ , filtered and the solvent removed to leave a crude residue which was purified by column chromatography (eluent: hexane:ethyl acetate; 90:10) to give the title compound (0.95 g, 69%) as a white solid.  $^1\text{H}$  NMR ( $\text{CDCl}_3$ , 400 MHz)  $\delta$  7.12 (2H, t,  $J = 7.0$  Hz), 7.26 (8H, m), 7.46 (2H, dd,  $J = 12.1, 7.3$  Hz), 7.55 (1H, t,  $J = 7.4$  Hz), 7.98 (1H, d,  $J = 8.1$  Hz), 8.02 (1H, d,  $J = 8.1$  Hz).  $^{13}\text{C}$  NMR ( $\text{CDCl}_3$ , 100 MHz)  $\delta$  120.6 (d,  $J = 4.5$  Hz), 125.2 (d,  $J = 0.6$  Hz), 128.7 (d,  $J = 15.8$  Hz),

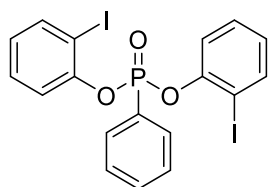


129.7, 132.2 (d,  $J = 10.4$  Hz), 133.2 (d,  $J = 3.1$  Hz), 150.4 (d,  $J = 7.6$  Hz).  $^{31}\text{P}$  NMR ( $\text{CDCl}_3$ , 162 MHz)  $\delta$  11.81. HRMS: (ESI $^+$ ) Calculated for  $\text{C}_{18}\text{H}_{15}\text{O}_3\text{PNa}$  : 333.0651 Found  $[\text{M}+\text{Na}]^+$ : 333.0658 (-1.96 ppm).

#### Method B

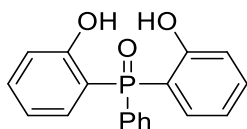
To a solution of diisopropyl amine (2 mL, 14 mmol), in THF (60 mL) was added 1.6 M *n*-BuLi (7.5 mL, 12 mmol) at  $-78^\circ\text{C}$  and stirred for 10 minutes after which phenol (0.94 g, 10 mmol) and the reaction was allowed to warm to room temperature and stir for 30 minutes. Phenyl phosphinic dichloride (0.75 mL, 5 mmol) was then added dropwise and the reaction was left to stir for 24 hours after which sat. ammonium chloride (40 mL) was added and aqueous layer was extracted with ethyl acetate (3 x 25 mL). The organic layer was then dried over  $\text{MgSO}_4$ , filtered and then dissolved in a 2:1 solution of DCM to water, then hydrogen peroxide (1 mL, 2 eqv.) was added and left to stir for 2 hours. Water (10 mL) was then added to the reaction and the organic layer separated and the aqueous layer was with DCM (10 mL). The organic layers were then combined, dried over  $\text{MgSO}_4$ , filtered and solvent removed *in-vacuo* and the crude material purified by column chromatography (eluent: hexane:ethyl acetate; 85:15) to give the title compound (1.07 g, 70%) as a white solid. Data identical to method A.

## Synthesis of bis(2-iodophenyl) phenylphosphonate (**185**)



To a solution of diisopropyl amine (1.98 mL, 14 mmol) in THF (40 mL) at  $-78^{\circ}\text{C}$  was added 1.6 M n-BuLi (7.5 mL, 12 mmol) and the reaction stirred for 10 minutes. After this, 2-iodophenol (2.2 g, 10 mmol) was added and stirred for a further 30 minutes after which, phenyl phosphinic dichloride (0.786 mL, 5 mmol) was added and the reaction allowed to warm to room temperature and was left for 16 hours. Sat. ammonium chloride solution (20 mL) was then added to the reaction and the organic and aqueous layers were separated and washed with water and ethyl acetate, respectively. The organic layer was then dried over  $\text{MgSO}_4$ , filtered, the solvent removed *in vacuo* and the crude material purified by column chromatography (eluent: hexane:ethyl acetate; 90:10) to give the title compound (1.58 g, 56%) as a clear oil.  $^1\text{H}$  NMR ( $\text{CDCl}_3$ , 400 MHz)  $\delta$  6.85 (2H, t,  $J = 7.6$  Hz), 7.24 (2H, td,  $J = 7.8, 1.4$  Hz), 7.46 (2H, dt,  $J = 8.2, 1.3$  Hz), 7.51 (2H, m), 7.61 (1H, td,  $J = 7.3, 1.3$ ), 7.75 (2H, d,  $J = 7.9$  Hz), 8.19 (2H, m).  $^{13}\text{C}$  NMR ( $\text{CDCl}_3$ , 400 MHz)  $\delta$  88.9 (d,  $J = 7.8$  Hz), 120.89 (d,  $J = 2.7$  Hz), 126.2 (d,  $J = 195.1$  Hz), 126.6 (d,  $J = 0.6$  Hz), 128.6 (d,  $J = 16.2$  Hz), 129.6 (d,  $J = 1.0$  Hz), 132.8 (d,  $J = 11.0$  Hz), 133.7 (d,  $J = 3.2$  Hz), 139.3, 150.6 (d,  $J = 7.2$  Hz).  $^{31}\text{P}$  NMR ( $\text{CDCl}_3$ , 161 MHz)  $\delta$  12.49. HRMS: (ESI $^+$ ) Calculated for  $\text{C}_{18}\text{H}_{15}\text{I}_2\text{O}_3\text{PNa}$ : 584.8584 Found  $[\text{M}+\text{Na}]^+$ : 584.858 (0.62ppm).

## Synthesis of bis(2-hydroxyphenyl)(phenyl)phosphine oxide (**112**)<sup>[77]</sup>



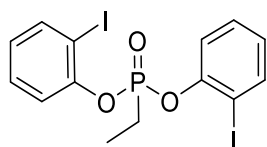
### Method A

To a solution of **185** (1.5 g, 2.67 mmol) in THF (25 mL), was added 1.3 M Turbo Grignard (4.9 mL, 6.4 mmol) and the reaction was stirred at room temperature of 24 hours. After this, the reaction was washed with sat. ammonium chloride solution (15 mL). The aqueous layer was then acidified with 1 M HCl and then washed with ethyl acetate (3 x 10 mL). The organic fractions were then combined, dried over MgSO<sub>4</sub>, filtered and the solvent removed *in vacuo* to leave a crude oil which was purified by column chromatography (eluent: hexane:ethyl acetate; 70:30) to give the title compound (440 mg, 57%) as a white solid. <sup>1</sup>H NMR (400 MHz, CDCl<sub>3</sub>) δ 6.90 (4H, m), 7.39 – 7.72 (9H, m), 10.83 (2H, s). <sup>13</sup>C (CDCl<sub>3</sub>, 100 MHz) δ 115.1, 116.2, 117.1 (d, *J* = 7.2 Hz), 119.4 (d, *J* = 12.1 Hz), 128.8 (d, *J* = 9.9 Hz), 131.3 (d, *J* = 10.7 Hz), 132.2 (d, *J* = 2.7 Hz), 133.4 (d, *J* = 9.0 Hz), 134.7 (d, *J* = 1.8 Hz), 161.2 (d, *J* = 3.4 Hz) <sup>31</sup>P NMR (CDCl<sub>3</sub>, 162 MHz) δ 34.0. HRMS: (ESI<sup>+</sup>) Calculated for C<sub>18</sub>H<sub>15</sub>O<sub>3</sub>PNa: Found [M+Na]<sup>+</sup>: 333.0653 (-0.68 ppm). HPLC separation (DAICEL AD, hexane/isopropanol 80:20, 1.2 mL/min, UV = 210, 254 nm; t<sub>R</sub> = 13.1 min

### Method B

To a solution of diisopropyl amine (1.98 mL, 14 mmol) in THF (40 mL) at -78°C was added 1.6 M *n*-BuLi (7.5 mL, 12 mmol) and the reaction stirred for 10 minutes. After this, **90** (1.07 g, 3.45 mmol) was added and the reaction allowed to warm to room temperature and was left for 16 hours. Sat. ammonium chloride solution (20 mL) was then added to the reaction and the organic and aqueous layers were separated and washed with water and ethyl acetate, respectively. The organic layer was then dried over MgSO<sub>4</sub>, filtered, the solvent removed *in vacuo* and the crude material purified by column chromatography (eluent: hexane:ethyl acetate; 75:25) to give the title compound (0.38 g, 35%) as a clear oil. Data identical to method A.

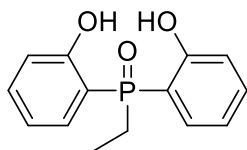
#### Synthesis of bis(2-iodophenyl) ethylphosphonate (**187**)



To a solution of diisopropyl amine (2 mL, 14 mmol), in THF (60 mL) was added 1.6 M *n*-BuLi (7.5 mL, 12 mmol) at -78°C and stirred for 10 minutes after which 2-iodophenol (2.20 g, 10 mmol) and the reaction was allowed to warm to room temperature and stir for 30 minutes. Ethyl phosphinic dichloride (0.53 mL, 5 mmol) was then added dropwise and the reaction was left to stir for 24 hours after which sat. ammonium chloride (40 mL) was added and aqueous layer was extracted with ethyl acetate (3 x 25 mL). The organic layer was then dried over MgSO<sub>4</sub>, filtered and the solvent removed *in-vacuo* and the crude material

purified by column chromatography (eluent: hexane:ethyl acetate; 85:15) to give the title compound (1.32 g, 52%) as a white solid.  $^1\text{H}$  NMR ( $\text{CDCl}_3$ , 400 MHz)  $\delta$  1.47 (3H, dt,  $J = 22.0, 7.7$  Hz), 2.28 (2H, dq,  $J = 18.5, 7.7$  Hz), 6.88 (2H, t,  $J = 7.6$  Hz), 7.26 (2H, td,  $J = 7.6, 1.6$  Hz), 7.37 (2H, dt,  $J = 8.2, 1.3$  Hz), 7.79 (2H, d,  $J = 7.9$  Hz).  $^{13}\text{C}$  NMR ( $\text{CDCl}_3$ , 100 MHz)  $\delta$  24.8 (d,  $J = 2.3$  Hz), 31.8 (d,  $J = 141.5$  Hz), 71.1 (d,  $J = 6.9$  Hz), 97.5 (d,  $J = 13.2$  Hz), 128.4, 128.8, 129.7, 139.0 (d,  $J = 6.2$  Hz), 139.3.  $^{31}\text{P}$  NMR ( $\text{CDCl}_3$ , 162 MHz)  $\delta$  38.16. HRMS: (ESI $^+$ ) Calculated for  $\text{C}_{14}\text{H}_{13}\text{I}_2\text{O}_3\text{PNa}$ : 536.8584 Found  $[\text{M}+\text{Na}]^+$ : 536.8582 (0.39 ppm).

#### Synthesis of ethylbis(2-hydroxyphenyl)phosphine oxide (**188**)



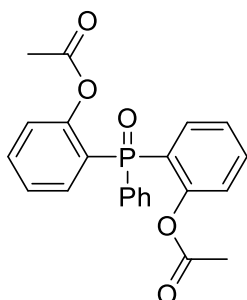
To a solution of **187** (1.2 g, 2.37 mmol) in THF (20 mL) was added 1.3 M Turbo Grignard (4.4 mL, 5.7 mmol) at room temperature and left to stir for 18 hours. The reaction was then quenched with the addition of sat. ammonium chloride solution (15 mL) and the aqueous layer extracted with ethyl acetate (3 x 10 mL) and the organic layers combined, dried over  $\text{MgSO}_4$ , filtered and the solvent removed. The crude residue was then purified by column chromatography (eluent: hexane:ethyl acetate; 60:40) to give the title compound (166 mg, 27%) as a clear oil.  $^1\text{H}$  NMR (DMSO, 400 MHz)  $\delta$  1.04 (3H, dt,  $J = 18.7, 7.6$  Hz), 2.5 (2H, m), 6.90 (4H, m), 7.38 (2H, m), 7.61 (2H, ddd,  $J = 13.0, 7.7, 1.6$  Hz), 11.04 (2H, s).  $^{13}\text{C}$  NMR (DMSO, 100 MHz)  $\delta$  5.59

(d,  $J = 5.4$  Hz), 22.69 (d,  $J = 72.9$  Hz), 116.0 (d,  $J = 97.3$  Hz), 116.9 (d,  $J = 7.1$  Hz), 119.4 (d,  $J = 11.4$  Hz), 132.5 (d,  $J = 8.2$  Hz), 134.2, 160.8 (d,  $J = 3.8$  Hz).  $^{31}\text{P}$  NMR (DMSO, 161 MHz)  $\delta$  44.99. HRMS: (ESI<sup>+</sup>) Calculated for C<sub>14</sub>H<sub>16</sub>O<sub>3</sub>P: Found [M+H]<sup>+</sup>: 263.0834 (-0.9 ppm).

### 10.9 - Chapter 8 phenolic phosphine oxide desymmetrization and kinetic resolution experimental

HPLC analysis was undertaken on an Agilent Infinity 1260 HPLC, using a DAICEL Chiralpak-AD column (Daicel, 5  $\mu\text{m}$  particle size, 250 mm x 4.6 mm). The mobile phase comprised of (A) IPA: (B) Hexane with an isocratic system of 20% (A) to 80% (B) with a flow rate of 1.2 mL/min, an injection volume of 5  $\mu\text{L}$  and a column temperature of 30°C. Signals were recorded at 200 nm, 210 nm, 220 nm, 254 nm.

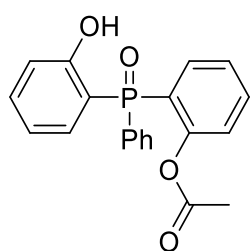
#### Synthesis of (phenylphosphoryl)bis(2,1-phenylene) diacetate (**193**)



Phosphine oxide **112** (80 mg, 0.32 mmol) was dissolved in dry DCM (5 mL) and triethyl amine (86  $\mu\text{L}$ , 0.61 mmol) followed by acetyl chloride (40.3  $\mu\text{L}$ , 0.56 mmol) was added and the reaction left to stir for 2 hours. After this the

organic layer was then washed with 1 M HCl (2.5 mL), H<sub>2</sub>O (2.5 mL), brine (2.5 mL) and dried over MgSO<sub>4</sub>, filtered and the solvent removed. The crude residue was then purified by column chromatography (eluent: hexane:ethyl acetate; 70:30) to give the title compound (90 mg, 89%) as a white solid. <sup>1</sup>H NMR (CDCl<sub>3</sub>, 400 MHz) δ 1.85 (6H, s), 7.28 (4H, m), 7.48 (4H, m), 7.57 (3H, m), 7.77 (2H, m). <sup>13</sup>C NMR (CDCl<sub>3</sub>, 100 MHz) δ 20.5, 123.9 (d, *J* = 6.3 Hz), 124.3, 125.3, 125.7 (d, *J* = 11.9 Hz), 128.5 (d, *J* = 12.3 Hz), 131.6 (d, *J* = 10.3 Hz), 132.0 (d, *J* = 2.8 Hz), 133.4 (d, *J* = 2.0 Hz), 133.5 (d, *J* = 8.5 Hz), 152.5 (d, *J* = 1.6 Hz), 168.5. <sup>31</sup>P NMR (CDCl<sub>3</sub>, 162 MHz) δ 33.57. HRMS: (ESI<sup>+</sup>) Calculated for C<sub>22</sub>H<sub>19</sub>O<sub>5</sub>PNa: 417.0862 Found [M+Na]<sup>+</sup>: 417.0866 (-0.97 ppm). HPLC separation (DAICEL AD, hexane/isopropanol 80:20, 1.2 mL/min, UV = 210, 254 nm; t<sub>R</sub> = 24.8 min

Synthesis of 2-((2-hydroxyphenyl)(phenyl)phosphoryl)phenyl acetate ((±)-**189**)



Phosphine oxide **112** (61 mg, 0.19 mmol) was dissolved in dry DCM (5 mL) and triethyl amine (30 μL, 0.21 mmol) followed by acetyl chloride (14.1 μL, 0.19 mmol) was added and the reaction left to stir for 2 hours. After this the organic layer was then washed with 1 M HCl (2.5 mL), H<sub>2</sub>O (2.5 mL), brine

(2.5 mL) and dried over MgSO<sub>4</sub>, filtered and the solvent removed. The crude residue was then purified by column chromatography (eluent: hexane:ethyl acetate; 3:1) to give the title compound (60 mg, 86%) as a white solid. <sup>1</sup>H NMR (CDCl<sub>3</sub>, 400 MHz) δ 1.83 (3H, s), 6.84 (1H, td, *J* = 7.1, 1.8 Hz), 6.99 (1H, m), 7.05 (1H, m), 7.28 (2H, m), 7.41 (2H, m), 7.51 (2H, m), 7.61 (2H, m), 7.75 (2H, m), 11.20 (1H, s). <sup>13</sup>C NMR (CDCl<sub>3</sub>, 100 MHz) δ 20.3, 110.6 (d, *J* = 106.9 Hz), 118.6 (d, *J* = 7.8 Hz), 119.1 (d, *J* = 12.7 Hz), 124.2 (d, *J* = 103.4 Hz), 124.3 (d, *J* = 6.2 Hz), 125.8 (d, *J* = 12.0 Hz), 128.8 (d, *J* = 12.7 Hz), 131.3 (d, *J* = 10.5 Hz), 131.4 (d, *J* = 108.5 Hz), 131.5 (d, *J* = 10.2 Hz), 134.0 (d, *J* = 9.2 Hz), 134.2 (d, *J* = 2.0 Hz), 134.4 (d, *J* = 2.2 Hz), 152.8 (d, *J* = 1.8 Hz), 163.8 (d, *J* = 3.1 Hz), 168.3. <sup>31</sup>P NMR (CDCl<sub>3</sub>, 161 MHz) δ 36.9. Calculated for C<sub>20</sub>H<sub>17</sub>O<sub>4</sub>PNa: 375.0757 Found [M+Na]<sup>+</sup>: 375.0762 (-1.4 ppm). HPLC separation (DAICEL AD, hexane/isopropanol 80:20, 1.2 mL/min, UV = 210, 254 nm; tR (A) = 18.4 min, tR (B) = 19.0, e.e. = 0%.

#### Butanol Rinsed Enzyme Preparation (BREP)

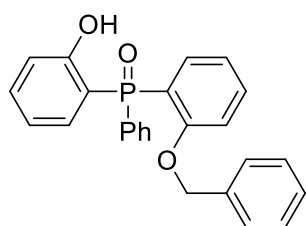
To an aqueous enzyme solution (2.5 mL Crude CAL-A, 6000 U/g) in pH 7 KPi buffer (2.5 mL) was added silica (0.5 g) and the resulting solution was left to shake at room temperature for 2 hours. The buffer was decanted off and the remaining silica was washed with *n*-butanol (3 x 5 mL) and then washed again with the reaction solvent of choice (3 x 5 mL).

#### BREP Reaction



To a solution of the substrate (10.6 mg, 25  $\mu$ mol) in the desired solvent (1 mL) was added the BREP (150 mg), followed by n-butanol (6.7  $\mu$ L, 75  $\mu$ mol) and the reaction was shaken at 37°C and monitored by chiral HPLC.

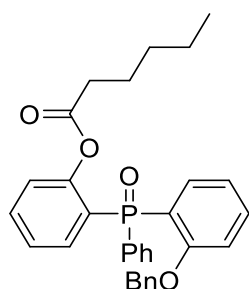
Synthesis of (2-(benzyloxy)phenyl)(2-hydroxyphenyl)(phenyl)phosphine oxide  
**((±)-194)**



To a solution of **112** (155 mg, 0.5 mmol) in DCM (5 mL), was added potassium carbonate (100 mg, 0.7 mmol), TBAI (32 mg, 0.05 mmol) and benzyl bromide (72  $\mu$ L, 0.6 mmol) and the reaction was refluxed until TLC showed complete conversion of the starting material. The reaction was then cooled to room temperature and washed with water (2.5 mL x 3) and brine (2.5 mL) and the organic layer dried over MgSO<sub>4</sub>, filtered and the solvent removed *in-vacuo* to leave a colourless solid which was purified by column chromatography (eluent: hexane:ethyl acetate; 60:40) to give the title compound (91 mg, 46%) as a white solid. <sup>1</sup>H NMR (CDCl<sub>3</sub>, 400 MHz)  $\delta$  4.91 (2H, s), 6.62 (1H, m), 6.86 (2H, d, *J* = 6.7 Hz), 6.90 (1H, dd, *J* = 8.1, 5.0 Hz), 6.95-7.10 (3H, m), 7.16-7.26 (3H, m), 7.32 (1H, ddd, *J* = 8.5, 2.6, 1.3 Hz), 7.42 (2H, td, *J* = 7.6, 3.1 Hz), 7.54 (2H, m), 7.64 (2H, m), 7.75 (1H, ddd, *J* = 14.0, 7.6, 1.7 Hz), 11.38 (1H, s, -OH). <sup>13</sup>C NMR (CDCl<sub>3</sub>, 100 MHz)  $\delta$  70.3, 111.2 (d, *J* = 106.8 Hz), 118.3 (d, *J* = 7.7 Hz), 118.5 (d, *J* = 12.8 Hz), 119.4 (d, *J* = 104.6 Hz), 121.0 (d, *J* = 12.1 Hz), 127.9

(d,  $J = 90.1$  Hz), 128.0, 128.5 (d,  $J = 12.9$  Hz), 131.2 (d,  $J = 10.9$  Hz), 132.06, 132.03, 132.5 (d,  $J = 10.5$  Hz), 133.1, 133.9 (d,  $J = 2.2$  Hz), 134.8 (d,  $J = 2.0$  Hz), 135.0 (d,  $J = 7.9$  Hz), 135.4, 160.0 (d,  $J = 3.2$  Hz), 164.0 (d,  $J = 3.2$  Hz).  $^{31}\text{P}$  NMR ( $\text{CDCl}_3$ , 162 MHz)  $\delta$  38.15. HRMS: (ESI $^+$ ) Calculated for  $\text{C}_{25}\text{H}_{21}\text{O}_3\text{PNa}$  : 423.1121 Found  $[\text{M}+\text{Na}]^+$ : 423.1116 (1.19 ppm) HPLC separation (DAICEL AD, hexane/isopropanol 80:20, 1.2 mL/min, UV = 210, 254 nm; tR (A) = 16.0 min, tR (B) = 16.2, e.e. = 0%.

Synthesis of 2-((2-(benzyloxy)phenyl)(phenyl)phosphoryl)phenyl hexanoate (( $\pm$ )-**196**)

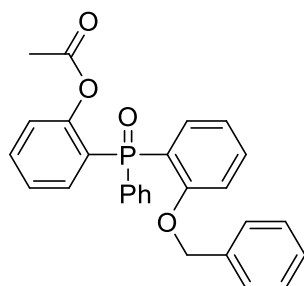


To a solution of hexanoic acid (0.125 mL, 1 mmol) in DCM (10 mL) was added thionyl chloride (87  $\mu\text{L}$ , 1.2 mmol) dropwise at 0°C followed by a catalytic amount of DMF. The reaction was left to stir for 3 hours at room temperature after which the solvent and excess thionyl chloride was removed *in-vacuo*. The crude residue was then dissolved in DCM (10 mL) and **179** (320 mg, 0.8 mmol) was added followed by triethyl amine (0.2 mL, 1.4 mmol) and the reaction was left to stir at room temperature 5 hours. The reaction was then washed with 1 M HCl sol. (5 mL), 1 M NaOH sol. (5 mL) and brine (5 mL) and the organic layer dried over  $\text{MgSO}_4$ , filtered and the solvent removed *in-vacuo* to leave a clear oil which was purified by column chromatography (eluent: hexane:ethyl

acetate; 60:40) to give the title compound (100 mg, 20%) as a clear oil.  $^1\text{H}$  NMR ( $\text{CDCl}_3$ , 400 MHz)  $\delta$  0.86 (3H, t,  $J = 7.1$  Hz), 1.20 (4H, m), 1.37 (2H, m), 1.83 (2H, td,  $J = 7.3, 1.5$  Hz), 4.81 (2H, m), 6.92 (3H, m), 7.08 (2H, m), 7.20 (4H, m), 7.33 (3H, m), 7.46 (3H, m), 7.80 (2H, m), 7.95 (1H, ddd,  $J = 13.8, 7.6, 1.6$  Hz).  $^{13}\text{C}$  NMR ( $\text{CDCl}_3$ , 100 MHz)  $\delta$  13.9, 22.2, 23.8, 31.1, 33.2, 70.2, 111.7 (d,  $J = 6.6$  Hz), 120.9 (d,  $J = 106$  Hz), 121.1 (d,  $J = 11.8$  Hz), 123.5 (d,  $J = 6.4$  Hz), 125.3 (d,  $J = 12.1$  Hz), 125.7 (d,  $J = 106.5$  Hz), 127.9 (overlapping peaks), 128.0 (d,  $J = 12.6$  Hz), 127.8-128.3 (d,  $J = 48.3$  Hz), 131.4 (d,  $J = 2.8$  Hz), 132.0 (d,  $J = 10.3$  Hz), 132.4 (d,  $J = 109.7$  Hz), 132.4 (d,  $J = 2.1$  Hz), 133.6 (d,  $J = 8.9$  Hz), 133.9 (d,  $J = 2.0$  Hz), 134.4 (d,  $J = 6.9$  Hz), 135.5, 153.3 (d,  $J = 1.8$  Hz), 159.4 (d,  $J = 3.4$  Hz), 171.4.  $^{31}\text{P}$  NMR ( $\text{CDCl}_3$ , 161 MHz)  $\delta$  22.68 (s). HRMS: (ESI $^+$ ) Calculated for  $\text{C}_{31}\text{H}_{31}\text{O}_4\text{PNa}$ : 521.1852 Found  $[\text{M}+\text{Na}]^+$ : 521.1857 (-1 ppm). HPLC separation (DAICEL AD, hexane/isopropanol 80:20, 1.2 mL/min, UV = 210, 254 nm;  $t_R$  (A) = 31.0 min,  $t_R$  (B) = 39.6, e.e. = 0%.

Synthesis of 2-((2-(benzyloxy)phenyl)(phenyl)phosphoryl)phenyl acetate

(195)



To a solution **194** (21 mg, 0.053 mmol) in DCM (1 mL), was added triethyl amine (10.4  $\mu\text{L}$ , 0.074 mmol) and AcCl (4.6  $\mu\text{L}$ , 0.064 mmol) and the reaction was stirred at room temperature for 5 hours. The reaction was then washed

with 1 M HCl sol. (1 mL), 1 M NaOH sol. (1 mL) and brine (1 mL) and the organic layer dried over MgSO<sub>4</sub>, filtered and the solvent removed *in-vacuo* to give the title compound (21 mg, 97%) as a white solid. <sup>1</sup>H NMR (CDCl<sub>3</sub>, 400 MHz) δ 1.64 (3H, s), 4.82 (2H, AB, *J* = 11.1 Hz), 6.92 (3H, m), 7.05-7.23 (6H, m), 7.34 (3H, m), 7.47 (3H, m), 7.81 (2H, m), 7.97 (1H, ddd, *J* = 13.7, 7.6, 1.6 Hz). <sup>13</sup>C NMR (CDCl<sub>3</sub>, 100 MHz) δ 20.2, 70.2, 111.8 (d, *J* = 6.7 Hz), 120.8 (d, *J* = 106.1 Hz), 121.1 (d, *J* = 11.8 Hz), 123.5 (d, *J* = 6.3 Hz), 125.4 (d, *J* = 12.1 Hz), 125.7 (d, *J* = 106.4 Hz), 127.1, 127.6, 128.9, 129.0 (d, *J* = 6.4 Hz), 131.3 (d, *J* = 4.3 Hz), 132.1 (d, *J* = 2.3 Hz), 132.3 (d, *J* = 6.3 Hz), 132.7 (d, *J* = 2.2 Hz), 135.3 (d, *J* = 4.5 Hz) 133.8 (d, *J* = 106.2 Hz), 134.2 (d, *J* = 1.3 Hz), 136.7, 154.2 (d, *J* = 3.4 Hz), 160.0 (d, *J* = 3.2 Hz), 169.0 (d, *J* = 3.2 Hz). <sup>31</sup>P NMR (CDCl<sub>3</sub>, 161 MHz) δ 22.69. HRMS: (ESI<sup>+</sup>) Calculated for C<sub>27</sub>H<sub>23</sub>O<sub>4</sub>PNa: 465.1226 Found [M+Na]<sup>+</sup>: 465.1232 (-1.25 ppm). HPLC separation (DAICEL AD, hexane/isopropanol 80:20, 1.2 mL/min, UV = 210, 254 nm; tR (A) = 29.1 min, tR (B) = 32.5 min, e.e. = 0%.

## 11 – References

- 1 J. F. Teichert and B. L. Feringa, *Angew. Chemie - Int. Ed.*, 2010, **49**, 2486–2528.
- 2 P. W. N. M. Van Leeuwen, P. C. J. Kamer, C. Claver, O. Pàmies and M. Diéguez, *Chem. Rev.*, 2011, **111**, 2077–2118.
- 3 H. Fernández-Pérez, P. Etayo, A. Panossian and A. Vidal-Ferran, *Chem. Rev.*, 2011, **111**, 2119–2176.
- 4 W. Li and X. Zhang, *Phosphorus(III) Ligands Homog. Catal. Des. Synth.*, 2012, 27–80.
- 5 E. I. Musina, A. S. Balueva and A. A. Karasik, *Phosphines: Preparation, reactivity and applications*, 2019, vol. 2019- January.
- 6 W. S. Knowles and M. J. Sabacky, *Chem. Commun.*, 1968, 1445–1446.
- 7 W. S. Knowles, M. J. Sabacky and B. D. Vineyard, *Ann. N. Y. Acad. Sci.*, 1973, **214**, 119–124.
- 8 W. S. Knowles, M. J. Sabacky, B. D. Vineyard and D. J. Weinkauff, *J. Am. Chem. Soc.*, 1975, **97**, 2567–2568.
- 9 L. C. Cross and W. Klyne, *Rules Nomencl. Org. Chem.*, 1976, **67**, 13–
- 10 A. G. Orpen and N. G. Connelly, *Organometallics*, 1990, **9**, 1206–1210.
- 11 W. A. Henderson and S. A. Buckler, *J. Am. Chem. Soc.*, 1960, **82**, 5794–5800.
- 12 C. A. Tolman, *Chem. Rev.*, 1977, **77**, 313–348.
- 13 R. H. Crabtree, *The Organometallic Chemistry of the Transition Metals, Fourth Edition*, **2005**.

- 14 C. A. Tolman, *J. Am. Chem. Soc.*, 1970, **92**, 2956–2965.
- 15 K. A. Bunten, L. Chen, A. L. Fernandez and A. J. Poë, *Coord. Chem. Rev.*, 2002, **233**, 41–51.
- 16 H. Clavier and S. P. Nolan, *Chem. Commun.*, 2010, **46**, 841–861
- 17 C. Koelmel, C. Ochsenfeld and R. Ahlrichs, *Theor. chim. acta*, 1992, **82**, 271.
- 18 A. Rauk, L. C. Allen and K. Mislow, *Angew. Chemie Int. Ed. English*, 1970, **9**, 400–414.
- 19 M. S. Gordon and S. Yabushita, *Chem. Phys. Lett.*, 1985, **117**, 321–325.
- 20 K. Mislow, *Trans. N. Y. Acad. Sci.*, 1973, **35**, 227–242.
- 21 A. Schmiedekamp, S. Skaarup, P. Pulay and J. E. Boggs, *J. Chem. Phys.*, 1977, **66**, 5769–5776.
- 22 S. Creve and M. T. Nguyen, *J. Phys. Chem. A*, 1998, **102**, 6549–6557.
- 23 A. J. Arduengo, D. A. Dixon and D. C. Roe, *J. Am. Chem. Soc.*, 1986, **108**, 6821–6823.
- 24 J. Holz, H. Jiao, M. Gandelman and A. Börner, *European J. Org. Chem.*, 2018, **23**, 2984–2994.
- 25 C. D. Montgomery, *J. Chem. Educ.*, 2013, **90**, 661–664.
- 26 R. D. Baechler and K. Mislow, *J. Am. Chem. Soc.*, 1970, **92**, 3090–3093.
- 27 T. E. Barder and S. L. Buchwald, *J. Am. Chem. Soc.*, 2007, **129**, 5096–5101.

- 28 B. Stewart, A. Harriman and L. J. Higham, *Organometallics*, 2011, **30**, 5338–5343.
- 29 E. Brulé, Y. Pei, F. Lake, F. Rahm and C. Moberg, *Mendeleev Commun.*, 2004, **14**, 276–277.
- 30 J. K. Whitesell, *Chem. Rev.*, 1989, **89**, 1581–1590.
- 31 A. Miyashita, A. Yasuda, H. Takaya, K. Toriumi, T. Ito, T. Souchi and R. Noyori, *J. Am. Chem. Soc.*, 1980, **102**, 7932–7934.
- 32 F. Guo, M. A. McGilvary, M. C. Jeffries, B. N. Graves, S. A. Graham and Y. Wu, *Molecules*, 2017, **22**, 1–10.
- 33 M. Kitamura, M. Tsukamoto, Y. Bessho, M. Yoshimura, U. Kobs, M. Widhalm and R. Noyori, *J. Am. Chem. Soc.*, 2002, **124**, 6649–6667.
- 34 C. A. Sandoval, T. Ohkuma, K. Muñiz and R. Noyori, *J. Am. Chem. Soc.*, 2003, **125**, 13490–13503.
- 35 T. Ohkuma, H. Takeno, Y. Honda and R. Noyori, *Adv. Synth. Catal.*, 2001, **343**, 369–375.
- 36 V. V. Thakur, M. D. Nikalje and A. Sudalai, *Tetrahedron Asymmetry*, 2003, **14**, 581–586.
- 37 M. Yoshimura, S. Tanaka and M. Kitamura, *Tetrahedron Lett.*, 2014, **55**, 3635–3640.
- 38 K. Mashima, K. hei Kusano, N. Sato, Y. ichi Matsumura, K. Nozaki, H. Kumobayashi, N. Sayo, Y. Hori, T. Ishizaki, S. Akutagawa and H. Takaya, *J. Org. Chem.*, 1994, **59**, 3064–3076.
- 39 R. Noyori, *Angew. Chemie - Int. Ed.*, 2002, **41**, 2008–2022.
- 40 T. Imamoto, K. Sugita and K. Yoshida, *J. Am. Chem. Soc.*, 2005, **127**, 11934–11935.

- 41 G. Makado, T. Morimoto, Y. Sugimoto, K. Tsutsumi, N. Kagawa and K. Kakiuchi, *Adv. Synth. Catal.*, 2010, **352**, 299–304.
- 42 I. D. Gridnev, M. Yasutake, N. Higashi and T. Imamoto, *J. Am. Chem. Soc.*, 2001, **123**, 5268–5276.
- 43 Z. Cao, K. Du, J. Liu and W. Tang, *Tetrahedron*, 2016, **72**, 1782–1786.
- 44 X. Wei, B. Qu, X. Zeng, J. Savoie, K. R. Fandrick, *et al.* *J. Am. Chem. Soc.*, 2016, **138**, 15473–15481.
- 45 O. Korpiun and K. Mislow, *J. Am. Chem. Soc.*, 1967, **89**, 4784–4786.
- 46 O. Korpiun, R. A. Lewis, J. Chickos and K. Mislow, *J. Am. Chem. Soc.*, 1968, **90**, 4842–4846.
- 47 B. D. Vineyard, W. S. Knowles, M. J. Sabacky, G. L. Bachman and D. J. Weinkauff, *J. Am. Chem. Soc.*, 1977, **99**, 5946–5952.
- 48 S. Juge, M. Stephan, S. Achi and J. P. Genet, *Phosphorus. Sulfur. Silicon Relat. Elem.*, 1990, **49–50**, 267–270.
- 49 S. Jugé, *Phosphorus, Sulfur Silicon Relat. Elem.*, 2008, **183**, 233–248.
- 50 R. A. Meyers, P. T. Anastas and J. B. Zimmerman, *Green Chemistry and Chemical Engineering, Introduction*, 2012.
- 51 C. J. Li and B. M. Trost, *Proc. Natl. Acad. Sci. U. S. A.*, 2008, **105**, 13197–13202.
- 52 U. T. Bornscheuer, G. W. Huisman, R. J. Kazlauskas, S. Lutz, J. C. Moore and K. Robins, *Nature*, 2012, **485**, 185–194.
- 53 R. A. Sheldon, *Green Chem.*, 2014, **16**, 950–963.
- 54 R. S. Varma, *Green Chem.*, 2014, **16**, 2027–2041.



- 55 P. T. Anastas and J. C. Warner, *Green Chemistry: Theory and Practice*, Oxford University Press, 1998.
- 56 P. Anastas and N. Eghbali, *Chem. Soc. Rev.*, 2010, **39**, 301–312.
- 57 M. L. Burnett, *Environ. Manage.*, 1998, **22**, 213–224.
- 58 R. A. Sheldon, *Green Chem.*, 2007, **9**, 1273–1283.
- 59 Pasteur, L. *C. R. Acad. Sci.*, **1858** 46, 615
- 60 J. Gal, *Chirality*, 2008, **20**, 5–19.
- 61 L. D. Kohn and W. B. Jakoby, *J. Biol. Chem.*, 1968, **243**, 2465–2471.
- 62 K. Faber, *Biotransformations in Organic Chemistry*, Springer Science & Business Media, Berlin, Heidelberg, **2012**.
- 63 K. Plasch, V. Resch, J. Hitce, J. Popłoński, K. Faber and S. M. Glueck, *Adv. Synth. Catal.*, 2017, **359**, 959–965.
- 64 A. Baba and T. Yoshioka, *J. Org. Chem.*, 2007, **72**, 9541–9549.
- 65 D. Zhu, Y. Yang and L. Hua, *J. Org. Chem.*, 2006, **71**, 4202–4205.
- 66 D. L. Nelson, M. M. Cox, *Lehninger Principles of Biochemistry*, **2013**.
- 67 D. Whitford, *Proteins: structure and function*, John Wiley & Sons, **2013**.
- 68 R. Wolfenden and M. J. Snider, *Acc. Chem. Res.*, 2001, **34**, 938–945.
- 69 G. M. Whitesides and C.-H. Wong, *Angew. Chem. Int. Ed. Engl.*, 1985, **24**, 617–718.
- 70 E. Fischer, *Ber. Dtsch. Chem. Ges.*, 1894, **27**, 1–4.
- 71 D. E. Koshland, *Proc. Natl. Acad. Sci. U.S.A.*, 1958, **44**, 98–104.
- 72 D. E. Koshland, *J. Cell. Comp. Physiol.*, 1959, **54**, 245–258.
- 73 J. M. Yon, D. Perahia and C. Ghélis, *Biochimie*, 1998, **80**, 33–42.

- 74 K. Nakamura and T. Matsuda, in *Enantiomer Separation: Fundamentals and Practical Methods*, ed. F. Toda, Springer Netherlands, Dordrecht, 2004, pp. 231–266.
- 75 H. Pellissier, *Chirality from Dynamic Kinetic Resolution*, The Royal Society of Chemistry, 2011.
- 76 B. Martín-Matute and J. E. Bäckvall, *Curr. Opin. Chem. Biol.*, 2007, **11**, 226–232.
- 77 A. M. Evans, *Eur. J. Clin. Pharmacol.*, 1992, **42**, 237–256.
- 78 M. Pérez-Venegas, A. M. Rodríguez-Treviño and E. Juaristi, *ChemCatChem*, 2020, **12**, 1782–1788.
- 79 F. Rebolledo, J. Gonzalez-Sabin and V. Gotor, in *Stereoselective Synthesis of Drugs and Natural Products, 2V Set, First Edition*, John Wiley & Sons, First Edit., 2013, vol. 4, pp. 1683–1711.
- 80 P. M. Dinh, J. A. Howarth, A. R. Hudnott, J. M. J. Williams and W. Harris, *Tetrahedron Lett.*, 1996, **37**, 7623–7626.
- 81 N. Jana, T. Mahapatra and S. Nanda, *Tetrahedron Asymmetry*, 2009, **20**, 2622–2628.
- 82 J. W. Cornforth, *Science*, 1976, **193**, 121–125.
- 83 R. Bentley, *Nature*, 1978, **276**, 673–676.
- 84 A. G. Ogston, *Nature*, 1948, **162**, 963.
- 85 F. E. Chen, X. X. Chen, H. F. Dai, Y. Y. Kuang, B. Xie and J. F. Zhao, *Adv. Synth. Catal.*, 2005, **347**, 549–554.
- 86 K. Shioji, Y. Kurauchi and K. Okuma, *Bull. Chem. Soc. Jpn.*, 2003, **76**, 833–834.

- 87 P. Kiełbasiński, J. Omelańczuk and M. Mikołajczyk, *Tetrahedron Asymmetry*, 1998, **9**, 3283–3287.
- 88 D. Wiktelius, M. J. Johansson, K. Luthman and N. Kann, *Org. Lett.*, 2005, **7**, 4991–4994.
- 89 A. N. Serreqi and R. J. Kazlauskas, *J. Org. Chem.*, 1994, **59**, 7609–7615.
- 90 P. Kiełbasiński, R. Zurawiński, M. Albrycht and M. Mikołajczyk, *Tetrahedron Asymmetry*, 2003, **14**, 3379–3384.
- 91 O. I. Kolodiaznyi, *Russ. Chem. Rev.*, 2011, **80**, 883–910.
- 92 D. F. Xiang, A. N. Bigley, E. Desormeaux, T. Narindoshvili and F. M. Raushel, *Biochemistry*, 2019, **58**, 3204–3211.
- 93 H. Chea, H.-S. Sim and J. Yun, *Adv. Synth. Catal.*, 2009, **351**, 855–858.
- 94 H.-Y. Jung, X. Feng, H. Kim and J. Yun, *Tetrahedron*, 2012, **68**, 3444–3449.
- 95 H. Kima and J. Yuna, *Adv. Synth. Catal.*, 2010, **352**, 1881–1885.
- 96 S. Kobayashi, P. Xu, T. Endo, M. Ueno and T. Kitanosono, *Angew. Chemie - Int. Ed.*, 2012, **51**, 12763–12766.
- 97 Y. Luo, I. D. Roy, A. G. E. Madec and H. W. Lam, *Angew. Chemie - Int. Ed.*, 2014, **53**, 4186–4190.
- 98 Y. Luo, S. M. Wales, S. E. Korkis, I. D. Roy, W. Lewis and H. W. Lam, *Chem. - A Eur. J.*, 2018, **24**, 8315–8319.
- 99 J. I. Martínez, J. J. Smith, H. B. Hepburn and H. W. Lam, *Angew. Chemie - Int. Ed.*, 2016, **55**, 1108–1112.

- 100 Professor Yunfei Luo, Anhui Province Key Laboratory of Advanced Catalytic Materials and Reaction Engineering, School of Chemistry and Chemical Engineering, Hefei University of Technology, Hefei, 230009, China.
- 101 T. W. Green and P. G. M. Wuts, *Protective Groups in Organic Synthesis*, Wiley-Interscience, New York, 49th–54th edn., **1999**.
- 102 S. Kaczmarczyk, M. Kwiatkowska, L. Madalińska, A. Barbachowska, M. Rachwalski, J. Błaszczak, L. Sieroń and P. Kiełbasiński, *Adv. Synth. Catal.*, 2011, **353**, 2446–2454.
- 103 R. Ramachandran, G. Prakash, S. Selvamurugan, P. Viswanathamurthi, J. G. Malecki, W. Linert and A. Gusev, *RSC Adv.*, 2015, **5**, 11405–11422.
- 104 E. F. Landvatter and T. B. Rauchfuss, *J. Chem. Soc. Chem. Commun.*, 1982, 1170–1171.
- 105 D. Hellwinkel and W. Krapp, *Chem. Ber.*, 1978, **111**, 13–41.
- 106 B. Dhawan and D. Redmore, *ChemInform*, 1990, **21**, 1990.
- 107 B. Dhawan and D. Redmore, *Synth. Commun.*, 1987, **17**, 465–468.
- 108 H. Duddeck and R. Lecht, *Phosphorus and Sulfur*, 1987, **29**, 169–178.
- 109 A. J. Kendall, C. A. Salazar, P. F. Martino and D. R. Tyler, *Organometallics*, 2014, **33**, 6171–6178.
- 110 F. Plénat, S. Ibrahim and H.-J. Cristau, *Synthesis (Stuttg.)*, 1988, 912–913.
- 111 M. Kim, F. Sanda and T. Endo, *Macromolecules*, 2000, **33**, 2359–2363.
- 112 A. Krasovskiy and P. Knochel, *Angew. Chemie - Int. Ed.*, 2004, **43**, 3333–3336.

- 113 A. Krasovskiy, B. F. Straub and P. Knochel, *Angew. Chemie - Int. Ed.*, 2005, **45**, 159–162.
- 114 A. Kumar, K. Dhar, S. S. Kanwar and P. K. Arora, *Biol. Proced. Online*, 2016, **18**, 1–11.
- 115 A. Kundys, E. Białecka-Florjańczyk, A. Fabiszewska and J. Małajowicz, *J. Polym. Environ.*, 2018, **26**, 396–407.
- 116 R. N. Lima, C. S. dos Anjos, E. V. M. Orozco and A. L. M. Porto, *Mol. Catal.*, 2019, **466**, 75–105.
- 117 P. M. Dinh, J. A. Howarth, A. R. Hudnott, J. M. J. Williams and W. Harris, *Tetrahedron Lett.*, 1996, **37**, 7623–7626.
- 118 A. M. Klibanov, *Nature*, 2001, **409**, 241–246.
- 119 P. A. Fitzpatrick and A. M. Klibanov, *J. Am. Chem. Soc.*, 1991, **113**, 3166–3171.
- 120 A. M. Klibanov, *Ann. N. Y. Acad. Sci.*, 1987, **501**, 129–129.
- 121 K. S. Siddiqui and R. Cavicchioli, *Extremophiles*, 2005, **9**, 471–476.
- 122 S. H. Ha, S. H. Lee, D. T. Dang, M. S. Kwon, W. J. Chang, Y. J. Yu, I. S. Byun and Y. M. Koo, *Korean J. Chem. Eng.*, 2008, **25**, 291–294.
- 123 Y. Luo and A. J. Carnell, *J. Org. Chem.*, 2010, **75**, 2057–2060.
- 124 R. C. Rodrigues, C. Ortiz, Á. Berenguer-Murcia, R. Torres and R. Fernández-Lafuente, *Chem. Soc. Rev.*, 2013, **42**, 6290–6307.
- 125 D. K. Oladepo, P. J. Hauling and V. F. Larsen, *Biocatal. Biotransformation*, 1994, **8**, 283–287.
- 126 P. Adlercreutz, *Eur. J. Biochem.*, 1991, **614**, 609–614.
- 127 M. Arroyo, J. M. Sánchez-Montero and J. V. Sinisterra, *Enzyme Microb. Technol.*, 1999, **24**, 3–12.

- 128 K. Rezaei, E. Jenab and F. Temelli, *Crit. Rev. Biotechnol.*, 2007, **27**, 183–195.
- 129 S. H. Schöfer, N. Kaftzik, P. Wasserscheid and U. Kragl, *Chem. Commun.*, 2001, 425–426.
- 130 N. Öhrner, C. Orrenius, A. Mattson, T. Norin and K. Hult, *Enzyme Microb. Technol.*, 1996, **19**, 328–331.
- 131 M. Solymár, A. Liljeblad, L. Lázár, F. Fülöp and L. T. Kanerva, *Tetrahedron Asymmetry*, 2002, **13**, 1923–1928.
- 132 F. Escalettes and N. J. Turner, *ChemBioChem*, 2008, **9**, 857–860.
- 133 S. Herter, S. M. McKenna, A. R. Frazer, S. Leimkühler, A. J. Carnell and N. J. Turner, *ChemCatChem*, 2015, **7**, 2313–2317.
- 134 N. J. Turner, *Chem. Rev.*, 2011, **111**, 4073–4087.
- 135 P. M. Dinh, J. A. Howarth, A. R. Hudnott, J. M. J. Williams and W. Harris, *Tetrahedron Lett.*, 1996, **37**, 7623–7626.
- 136 K. Martinek, A. N. Semenov and I. V. Berezin, *BBA - Enzymol.*, 1981, **658**, 76–89.
- 137 A. Miller, L. Majauskaite and K. H. Engel, *Eur. Food Res. Technol.*, 2004, **218**, 349–354.
- 138 T. W. Baughman, J. C. Sworen, K. B. Wagener, *Tetrahedron*, 2004, **60**, 10943–10948.
- 139 D. J. Maloney and S. M. Hecht, *Org. Lett.*, 2005, **7**, 4297–4300.
- 140 L. W. Menapace and H. G. Kuivila, *J. Am. Chem. Soc.*, 1964, **86**, 3047–3051.
- 141 J. M. Khurana, S. Kumar and B. Nand, *Can. J. Chem.*, 2008, **86**, 1052–

- 142 A. J. De Koning, *Org. Prep. Proced. Int*, 1975, **7**, 31–34.
- 143 A. Gogia and J. M. Khuran, *Org. Prep. Proced. Int*, 1997, **29**, 1–32.
- 144 S. Czernecki, C. Georgoulis, C. Provelenghiou, *Tetrahedron Lett.*, 1976, **17**, 3535-3536
- 145 C. Tejo, J. H. Pang, D. Y. Ong, M. Oi, M. Uchiyama, R. Takita and S. Chiba, *Chem. Commun.*, 2018, **54**, 1782–1785.
- 146 A. Bouzide, G. Sauvé, *Tetrahedron Lett.*, 1997, **38**, 5945-5948.
- 147 E. Podyacheva, E. Kuchuk and D. Chusov, *Tetrahedron Lett.*, 2019, **60**, 575–582.
- 148 D. Hérault, D. H. Nguyen, D. Nuel and G. Buono, *Chem. Soc. Rev.*, 2015, **44**, 2508–2528.
- 149 H. Fritzsche, U. Hasserodt, F. Korte, G. Friese and K. Adrian, *Chem. Ber.*, 1965, **98**, 171–174.
- 150 L. Horner and W. D. Balzer, *Tetrahedron Lett.*, 1965, 1157–1162.
- 151 T. Imamoto, S. Kikuchi, T. Miura and Y. Wada, *Org. Lett.*, 2001, **3**, 87.
- 152 D. Gatineau, L. Giordano and G. Buono, *J. Am. Chem. Soc.*, 2011, **133**, 10728–10731.
- 153 L. J. Higham, E. F. Clarke, H. Müller-Bunz and D. G. Gilheany, *J. Organomet. Chem.*, 2005, **690**, 211–219.
- 154 M. Stankevič and K.M. Pietrusiewicz, *J. Org. Chem.*, 2007, **72**, 816–822
- 155 S. Lemouzy, D. H. Nguyen, V. Camy, M. Jean, D. Gatineau, L. Giordano, J. V. Naubron, N. Vanthuyne, D. Hérault and G. Buono, *Chem. - A Eur. J.*, 2015, **21**, 15607–15621.

- 156 M. Kwiatkowska, G. Krasieński, M. Cypryk, T. Cierpień and P. Kielbasiński, *Tetrahedron Asymmetry*, 2011, **22**, 1581–1590.
- 157 S. Sowa, M. Stankevič, A. Szmigielska, H. Małuszyńska, A. E. Koziol and K. M. Pietrusiewicz, *J. Org. Chem.*, 2015, **80**, 1672–1688.
- 159 Z. S. Han, N. Goyal, M. A. Herbage *et al.*, *J. Am. Chem. Soc.*, 2013, **135**, 2474–2477.
- 160 L. Horner, *Pure Appl. Chem.*, 1964, **9**, 225
- 161 T. Coumbe, N. J. Lawrence and F. Muhammad, *Tetrahedron Lett.*, 1994, **35**, 625–628.
- 162 C. Petit, A. Favre-Re´guillon, B. Albela, L. Bonneviot, G. Mignani and M. Lemaire, *Organometallics*, 2009, **28**, 6379–6382;
- 163 C. Petit, E. Poli, A. Favre-Re´guillon, L. Khrouz, S. Denis-Quanquin, L. Bonneviot, G. Mignani and M. Lemaire, *ACS Catal.*, 2013, 1431–1438.
- 164 E. J. Corey and J. W. Suggs, *Tetrahedron Lett.*, 1975, **16**, 2647–2650.
- 165 M. Uyanik and K. Ishihara, *ACS Catal.*, 2013, **3**, 513–520.
- 166 K. Watanabe and S. Ueji, *J. Chem. Soc. Perkin 1*, 2001, 1386–1390.
- 167 A. M. Klibanov, *Nature*, 2001, **409**, 241–246.
- 168 A. J. Carnell, S. A. Swain and J. E. Bickley, *Tetrahedron Lett.*, 1999, **40**, 8633–8636.
- 170 W. Kirmse and K. Kund, *J. Org. Chem.*, 1990, **55**, 2325–2332.
- 171 J. M. Chezal, E. Moreau, N. Desbois, Y. Blache, O. Chavignon and J. C. Teulade, *Tetrahedron Lett.*, 2004, **45**, 553–556.